Transcription factor EB-mediated neurotrophic and neuroprotective effects: relevance to Parkinson's disease

Albert Torra i Talavera

Universitat Autònoma de Barcelona

Transcription factor EB-mediated neurotrophic and neuroprotective effects: relevance to Parkinson's disease

TESI DOCTORAL

2019

Programa de Doctorat en Neurociències

Institut de Neurociències – Universitat Autònoma de Barcelona

Tesi realitzada al laboratori de Malalties Neurodegeneratives del Vall d'Hebron Institut de Recerca (VHIR)

Doctorand	Director	Director
Albert Torra i Talavera	Dr. Miquel Vila Bover	Dr. Jordi Bové Badell

Tutor

Dr. José Rodríguez Álvarez

Turn your wounds into wisdom

-Oprah Winfrey-

ACKNOWLEDGMENTS

En primer lloc voldria agrair al Miquel Vila per donar-me l'oportunitat, durant aquests més de 6 anys, d'haver format part del seu laboratori. No només he tingut la sort d'haver realitzat la tesi doctoral al teu lab, sinó també el que va començar sent el treball final de grau i el treball final de màster. Moltes gràcies per tot el que m'has ensenyat, per haver-me permès anar sempre que he volgut a qualsevol congrés a presentar els meus resultats (fins i tot a l'altra punta del món!), per haver confiat en mi durant tot aquest temps i per haver-me recolzat en les situacions més difícils. També m'agradaria agrair enormement al meu altre director durant tot aquest temps, el Jordi Bové, per haver-me guiat tots aquests anys durant el dia a dia al laboratori i sobretot per haver-me aguantat durant l'etapa estressant del review de l'article! Espero i desitjo que hagis gaudit tant com jo d'aquesta experiència tant a nivell professional com personal, i que finalment aconseguim trobar algun dia l'esperada cura del Parkinson!

També m'agradaria agrair enormement a tots els companys de laboratori, tant als membres actuals com als que he compartit algun moment de la meva estada al lab! A Annabelle, por haberme enseñado tantísimo siendo uno de sus Chiquis, por enseñarme a pronunciar correctamente algunas palabras del francés (sobretodo Ponceau), por ir a comer juntos alguna que otra vez durante la etapa final de la tesis, y por haber hecho que todos estos años hayan sido, a la vez que productivos, divertidísimos! Nada hubiera sido lo mismo sin ti, y espero que muchos más estudiantes tengan la misma suerte que tuve yo de aprender de ti! A la Thais, per haver-me ensenyat i ajudat sempre que ho he necessitat, per les llargues xerrades al passadís i per haver compartit amb mi molta de la frustració dels experiments *in vitro* de TFEB! Gràcies per haver-me recolzat sempre i pels ànims durant l'etapa final de la tesi! A Iria, por haber compartido todos estos años de despacho juntos, por el apoyo constante y, por supuesto, por enseñarme muchas técnicas del intrigante mundo de cultivos (esperemos que algún día a las LUHMES les dé finalmente por querer sobrevivir!). Espero que te vaya estupendamente en tu nueva etapa! A l'Ariadna, per compartir també tots aquests anys de despatx al meu costat i per haver-me aconsellat molt útilment sempre que ho he necessitat. També per aportar-me una font de glucosa constant amb els caramels, i per compartir el típpex, la grapadora sense grapes i el famós regle (espero que et serveixi per molts més articles!). A la Marta Martinez, per haver-me aconsellat amb alguns protocols quan ho he necessitat i per ajudar-me a trobar la solució a algun que altre maldecap amb els aïllaments de mitocondris (al final ho vam aconseguir!). To Celine, for giving me also some

useful advice on mitochondria experiments via email and Skype, even being you now on the other side of the world! A Bea, por enseñarme muchas cosas sobre todo en mi etapa inicial en el laboratorio, y por haber compartido conmigo grandes momentos no solo dentro del lab, sino también fuera de él. Gracias por unirte conmigo en la realización de muchísimas carreras (espero que las que hicimos juntos las disfrutaras tanto como yo!). Te deseo lo mejor y que te vaya todo estupendamente por Pamplona (recuerda que tengo pendiente venir a verte!). A l'Ariadna Recasens, per haver compartit els teus últims anys de tesi amb els meus primers anys al lab. Espero que estigui anant tot molt bé per Sydney! A la Sandra, per haver compartit molts moments junts durant les nostres tesis, que si la plataforma del SIA de la UAB ens borra tots els documents adjunts, que si es bloqueja i mil-i-una divertides històries més! Espero que el teu postdoc a Nova York sigui de gran profit i que no perdem mai el contacte! Al Jordi Romero, pel que va començant sent una simple col·laboració amb el nostre lab i que només ens vèiem de tant en tant pel microscopi, a lo que va acabar sent compartir tot el meu recorregut de la tesi i gairebé tots els dinars! Gràcies per tots aquests anys de diversió assegurada, per haver fet els meus moments de poyata més amens amb la happy neuron i derivats, per haver fet amb mi la cursa de la Sanitat Catalana a Can Ruti amb el seus generosos metres de desnivell (algun dia bastant llunyà farem la versió de més km's...) i per totes les pizzes cheesix i pecados carnales que ens hem cruspit (som uns grassos...)! Al Jordi Galiano, has estat un magnífic company i amic al mateix temps. Trobaré a faltar les llarguíssimes xerrades al nostre "segon despatx" al passadís, fer-te sustos (hehe), les teves caipiroskes i els entrepans de trauma de tonyina amb doble de formatge calent! Ha estat un magnífic plaer haver compartit gran part de la tesi amb tu i t'agraeixo enormement les múltiples xerrades estant "mig-tajes" (± 15%) després d'haver provat gairebé totes les cerveses artesanes d'algun que altre bar (tenim pendent de repetir algun dia aquell bar de les patates braves...!). Et desitjo molta sort per lo poquet que et queda de tesi i, per suposat, ens anirem veient! A la Núria, ha estat un plaer compartir els últims anys de despatx al teu costat, hem parlat i rigut molt amb els mítics "no pot ser...", que si els fold change, els delta CT, els delta delta CT... i, sobretot, per haver compartit els moments de gula de les 16:00h amb el pot de Nutella mano a mano (tot i que més jo, ho reconec!)! Gràcies també pels moments de desconnexió amb cerveses i espero que mantinguem el contacte per fer-ne moltes més! Molta sort i ànims pels anys que et queden de tesi! A Marta González, por resolverme algunas dudas y no darte por vencida con el tema del DOPAL (tampoco con el bote de glicina!). A la Marta Montpeyó, al Jordi Riera, a la Cris, al Joan, a l'Helena, a les noves incorporacions i també a diversos estudiants que han passat pel lab (la Anne, la Sara, la Laura, el Xavier, la Mercè, i l'Alice). Gràcies a tots per compartir un tros d'aquesta etapa amb mi!

Als veïns del laboratori de Malalties Mitocondrials, per proporcionar-me protocols i el material necessari pels experiments de DNA mitocondrial.

A la Silvia i l'Anna del laboratori de Neurologia Pediàtrica, per haver compartit alguns magnífics moments de desconnexió a l'aclamat "banquillo" de la màquina de cafè, i també per haver-me resolt alguns dubtes referents al papeleo del dipòsit de la tesi!

También me gustaría agradecer a Analía Bortolozzi, por haberme acogido durante un tiempo en su laboratorio en el IDIBAPS para realizar algunos de los experimentos, así como por sus útiles consejos. A l'Esther Ruiz, per haver-me ensenyat i compartit la majoria del temps de la meva breu estada al vostre lab i també alguns moments divertits en congressos! També a la Neus i al Rubén, per ajudar-me amb el tema de la cirurgia!

Al Joan, la Marta, les meves amigues del màster Lídia i Laura, la Neus i al Lluís. Moltes gràcies a tots per haver compartit grans moments amb mi i espero que en puguem compartir molts més!

Als meus pares, que tot i que lamentablement ja no estigueu aquí, vau ser vosaltres qui em vau motivar a realitzar una tesi doctoral. Aquesta tesi va per vosaltres! Als meus tiets i cosins, i en especial a la meva germana Anna, que m'ha recolzat en tot moment i m'ha ajudat a desconnectar quan més ho he necessitat compartint múltiples viatges arreu del món, escapades *express* i moltíssimes altres experiències junts! I les que ens queden per fer! També a la seva parella, per donar-me ànims durant els últims moments de la tesi!

Moltes gràcies a tots i totes, aquesta tesi no hagués estat el mateix sense vosaltres!

TABLE OF CONTENTS

LIST OF TABLES

LIST OF FIGURES

LIST OF ABBREVIATIONS

Only those appearing more than once in the text.

4E-BP1	eIF4E-binding protein 1
6-OHDA	6-hydroxydopamine
AAV	adeno-associated virus
AKT	protein kinase B
ALDH	aldehyde dehydrogenase
Alm	alamethicin
ALP	autophagy-lysosomal pathway
ANG1	angiogenin 1
AR	aspect ratio
ATG	autophagy-related protein
ATP	adenosine triphosphate
BAD	Bcl-2-associated death promoter
BAX	Bcl-2-associated X
BBB	blood-brain barrier
BCL-2	B-cell lymphoma 2
BCL-XL	B-cell lymphoma-extra large
BDNF	brain-derived neurotrophic factor
bHLH	basic helix-loop-helix
BIM	Bcl-2-interacting mediator of cell death
CLEAR	coordinated lysosomal expression and regulation
CMA	chaperone-mediated autophagy
CNTF	ciliary neurotrophic factor
COMT	catechol-O-methyltransferase
CTS	cathepsin

Cyt c	cytochrome c
DA	dopamine
DAT	dopamine transporter
DNA	deoxyribonucleic acid
DOPAC	3,4-dihydroxyphenylacetic acid
DOPAL	3,4-dihydroxyphenyl-3-acetaldehyde
eIF4E	eukaryotic translation initiation factor 4E
ER	endoplasmic reticulum
ERK	extracellular signal-regulated kinase
ETC	electron transport chain
GAPDH	glyceraldehyde 3-phosphate dehydrogenase
GCase	glucocerebrosidase
GDNF	glial cell line-derived neurotrophic factor
GSK3	glycogen synthase kinase 3
GWAS	genome-wide association studies
HPLC	high-performance liquid chromatography
HSP60	heat shock protein 60
HVA	homovanillic acid
i.p.	intraperitoneal
IF	immunofluorescence
IHC	immunohistochemistry
IMM	inner mitochondrial membrane
JNK	c-JUN N-terminal kinase
KO	knockout
LAMP1	lysosomal-associated membrane protein 1
LBs	Lewy bodies
LC3	light chain 3
LMP	lysosomal membrane permeabilization

LSDs	lysosomal storage disorders
MAO	monoamine oxidase
MAPK	mitogen-activated protein kinase
MFN1	mitofusin 1
MFN2	mitofusin 2
MITF	microphthalmia-associated transcription factor
MOMP	mitochondrial outer membrane permeabilization
MPP^+	1-methyl-4-phenylpyridinium iodide
MPTP	1-methyl-4-phenyl-1,2,3,6-tetrahydropyridine
mRNA	messenger RNA
mtDNA	mitochondrial DNA
mTOR	mammalian target of rapamycin
mTORC1	mammalian target of rapamycin complex 1
mTORC2	mammalian target of rapamycin complex 2
NDRG1	N-Myc downstream regulated 1 protein
NGF	nerve growth factor
NM	neuromelanin
OD	optical density
OMM	outer mitochondrial membrane
OPA1	optic atrophy 1
OXPHOS	oxidative phosphorylation
p90RSK	p90 ribosomal S6 kinase
PD	Parkinson’s disease
PERK	PRKR-like ER kinase
PGC-1a	peroxisome-proliferator-activated receptor gamma co-activator-1alpha
PI3K	phosphatidylinositol 3-kinase
Rag	Ras-related GTP-binding
Rheb	Ras homolog enriched in brain

ROS	reactive oxygen species
RPS6	ribosomal protein S6
S6K1	p70 ribosomal S6 kinase 1
shRNA	short hairpin RNA
SNpc	substantia nigra *pars compacta*
STN	subthalamic nucleus
TBK1	TANK binding protein 1
TEM	transmission electron microscopy
TFAM	mitochondrial transcription factor A
TFE3	transcription factor E3
TFEB	transcription factor EB
TFEC	transcription factor EC
TH	tyrosine hydroxylase
TIM	translocase of the mitochondrial inner membrane
TOM	translocase of the mitochondrial outer membrane
TSC	tuberous sclerosis complex
UPR	unfolded protein response
UPS	ubiquitin-proteasome system
VDAC1	voltage-dependent anion channel 1
VMAT2	vesicular monoamine transporter-2
VTA	ventral tegmental area
ZIP	leucine zipper
ZKSCAN3	KRAB and SCAN domains 3
Δψm	mitochondrial membrane potential

ABSTRACT

Abstract

The possible implication of transcription factor EB (TFEB) as a therapeutic target in Parkinson's disease (PD) has gained momentum since it was discovered that TFEB controls lysosomal biogenesis and autophagy and that its activation might counteract lysosomal impairment and protein aggregation. However, the majority of putative direct targets of TFEB described to date is linked to a range of biological processes that are not related to the autophagy-lysosomal system. In this thesis, we assessed the effect of overexpressing TFEB by means of an adeno-associated viral vector in mouse substantia nigra dopaminergic neurons and studied several molecular processes that may offer potential benefits in the context of PD. In this line, we demonstrated that TFEB overexpression drove a previously unknown *bona fide* neurotrophic effect accompanied by an enhanced dopaminergic function, activation of pro-survival signaling pathways and mitochondrial changes that altogether may contribute to render neurons less prone to cell death. To delve further into this concept, we studied the therapeutic potential of TFEB in a parkinsonian context, that induced by the neurotoxin MPTP. In this regard, we showed that TFEB overexpression was indeed able to block MPTP-induced neurodegeneration both at the cell body level as well as striatal dopaminergic terminals and restored neuronal activity/function and phenotype in the MPTP mouse model of PD. Moreover, TFEB overexpression also counteracted the deleterious events like lysosomal depletion and mitochondria-mediated cell death that are linked to MPTP neurotoxicity and PD. Besides, we unraveled that activating the autophagy-lysosomal pathway by knocking down the master repressor of autophagy ZKSCAN3 did not prevent MPTP-induced neurodegeneration or atrophy. Altogether, our results uncover new mechanisms decisive for the neuroprotective effect elicited by TFEB and highlight increasing TFEB activity as a therapeutic approach to fight neuronal death and restore neuronal function in PD and other neurodegenerative diseases.

INTRODUCTION

1. Introduction

1.1. Parkinson's disease

1.1.1. Pathophysiology

It has been over 200 years since Dr James Parkinson was first to describe a neurological syndrome called *paralysis agitans* (shaking palsy), which later would bear his name (Parkinson, 1817; Schnabel, 2010). Parkinson's disease (PD) is a chronic neurodegenerative disorder mainly characterized by progressive loss of dopaminergic neurons in the substantia nigra *pars compacta* (SNpc), which project their axons to the basal ganglia and synapse in the striatum (i.e. caudate and putamen nucleus). These neurons contain neuromelanin (NM), a dark-brown pigment that can be both seen microscopically and macroscopically. Loss of these NM-laden neurons demonstrates the marked loss of dopaminergic neurons as a principal neuropathology of PD. Another neuropathological hallmark required for a definitive diagnosis of PD is the presence of intracytoplasmic eosinophilic inclusions named Lewy bodies (LBs) (Dauer and Przedborski, 2003; Poewe *et al.*, 2017) (**Figure 1**). Although α-synuclein is the major constituent of LBs (Spillantini *et al.*, 1998), a large number of other components such as ubiquitin, lipids and chaperones, among others, have also been described (Wakabayashi *et al.*, 2007).

Degeneration of SNpc dopamine (DA)-secreting neurons leads to a depletion of this neurotransmitter in the striatum, and thus results in the characteristic cardinal motor features of PD such as resting tremor, rigidity, bradykinesia and postural instability. On this basis and given that neurodegeneration in this region starts before the onset of motor symptoms, some controversy is present about the estimates of SNpc neuron loss at disease onset. Some works state that motor symptoms appear when about 50-70% of the SNpc dopaminergic neurons are lost (Lang and Lozano, 1998; Dauer and Przedborski, 2003; Ross *et al.*, 2004). However, a more recent study suggests that the motor signs of PD start to appear when about 30% of the

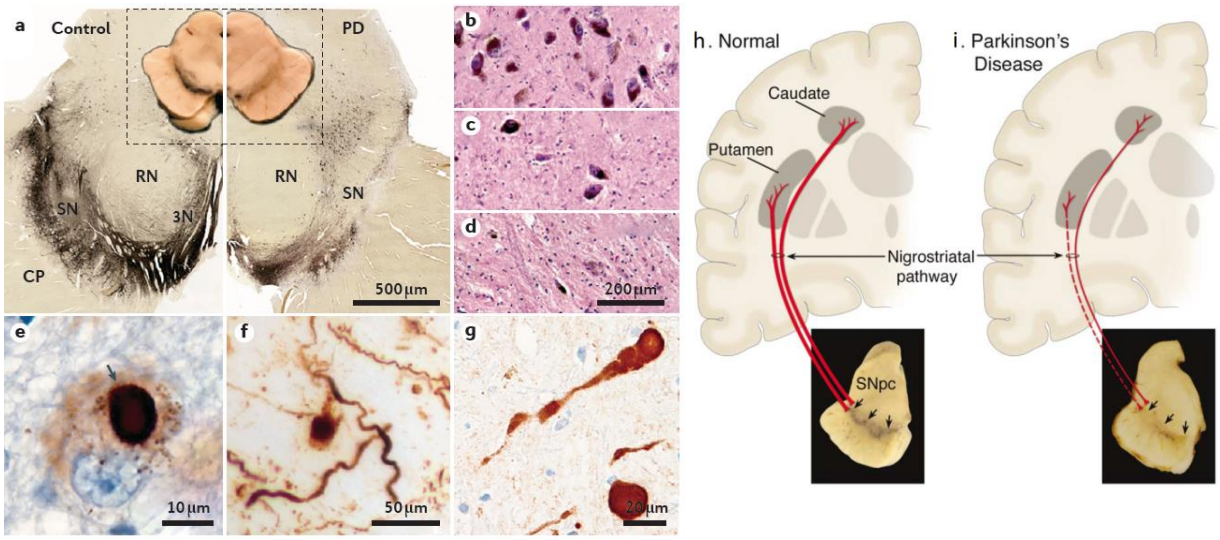

Figure 1. Neuropathology of Parkinson's disease. (**a**) Macroscopically (inset) and transverse analysis of post-mortem midbrains show the selective loss of SNpc dopaminergic neurons. (**b-d**) Hematoxylin and eosin staining of the SNpc region in (**b**) a healthy control showing a normal distribution of NM-laden neurons versus PD post-mortem patients showing a (**c**) moderate or (**d**) severe pigmented neuron loss. (**e-g**) Immunohistochemistry against α-synuclein in PD post-mortem tissue demonstrates the presence of (**e**) intracytoplasmic Lewy bodies rich in α-synuclein (arrow), (**f**) intracellular and extracellular α-synuclein deposited structures, and (**g**) α-synuclein spheroids in neuronal axons. (**h-i**) Schematic representation of (**h**) the normal nigrostriatal pathway, which is composed of dopaminergic neurons whose bodies are located in the SNpc and project their axons to the striatum, where they release dopamine, versus (**i**) degeneration of the nigrostriatal pathway due to the loss of dopaminergic neurons in PD. (Adapted from Poewe *et al.*, 2017 *Nat. Rev. Dis. Primers*; Dauer and Przedborski, 2003 *Neuron*)

dopaminergic neurons of the SNpc are lost in comparison to age-matched controls (Cheng *et al.*, 2010).

Even though PD was initially reported as a motor disorder due to cell loss is mainly concentrated in ventrolateral and caudal portions of the SNpc with sparing of the more medial and dorsal regions (Fearnley and Lees, 1991), it has long been documented that the neuropathology underlying PD involves many other brain areas that are not directly involved in motor control. These areas include: noradrenergic areas such as locus coeruleus; cholinergic areas such as the dorsal motor nucleus of vagus and the nucleus basalis of Meynert; serotonergic areas such as the raphe nuclei of the brainstem; and other regions such as the hypothalamus, the olfactory

tubercle and parts of the limbic cortex and the neocortex. Therefore, most of PD patients reveal a wide variety of non-motor signs, including autonomic dysfunction (e.g. constipation, orthostatic hypotension and urogenital dysfunction), neuropsychiatric dysfunction (e.g. anhedonia, apathy, anxiety, psychosis and dementia), sleep disorders (e.g. sleep fragmentation, insomnia and rapid eye movement sleep behavior disorder) and sensory symptoms (e.g. abnormal sensations and pain) (Braak *et al.*, 2003; Poewe, 2008). Some of these non-motor symptoms actually antedate motor disturbances by several years or even decades, and thus may have a potential diagnostic utility in early stages of PD (**Figure 2**).

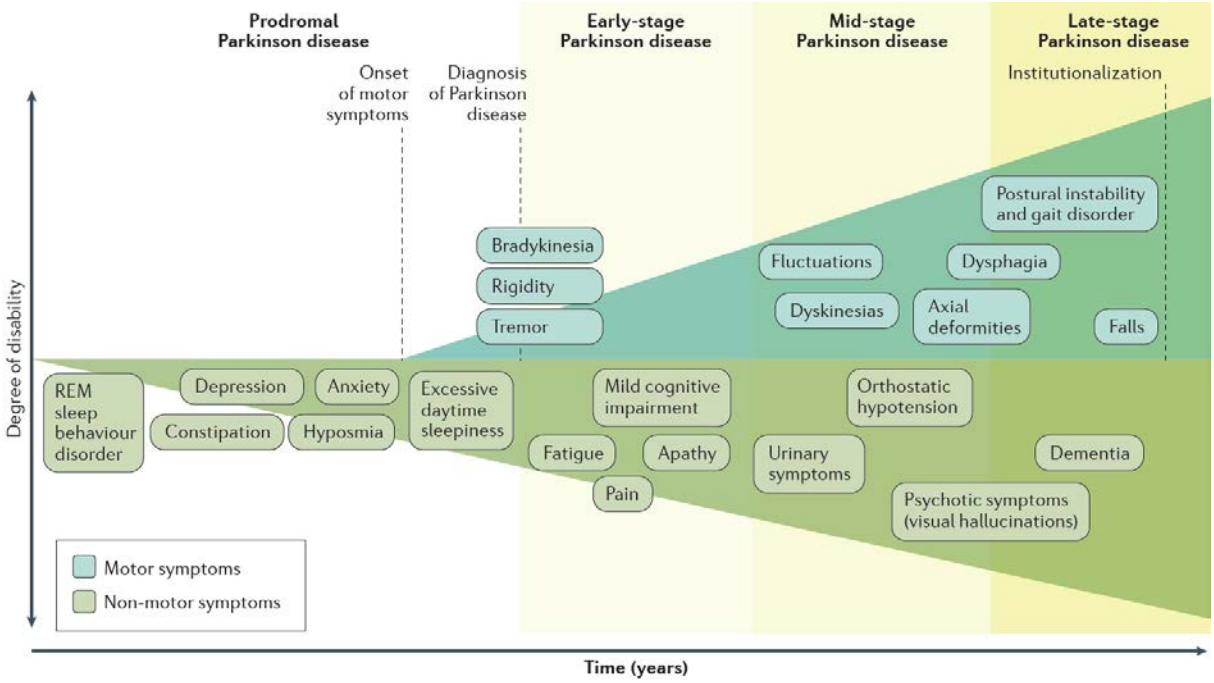

Figure 2. Clinical motor and non-motor symptoms of Parkinson's disease. Before the diagnosis based on cardinal motor features, PD is preceded by a prodromal phase based by non-motor symptoms such as sleep disorders, constipation and hyposmia. Over the course of the disease, PD is driven by both motor and non-motor symptoms, which induce progressive disability (From Poewe *et al.*, 2017 *Nat. Rev. Dis. Primers*).

1.1.2. Symptom management

As discussed above, loss of SNpc neurons leads to striatal DA depletion, which causes the major PD motor symptoms. In dopaminergic neurons, DA is synthesized through DOPA-decarboxylase enzyme from L-3,4-dihydroxyphenylalanine (L-DOPA), which is first yielded from the hydroxylation of the amino acid L-tyrosine through the rate-limiting enzyme on DA biosynthesis, tyrosine hydroxylase (TH) (Molinoff and Axelrod, 1971; Barron *et al.*, 2010).

To date, no effective strategy has been successfully developed to halt the progression of PD due to the poor understanding of the molecular mechanisms underlying the progressive neurodegeneration of the disease. However, sundry pharmaceutical strategies have been developed to alleviate PD-associated motor symptoms, such as MAO or COMT inhibitors and DA receptor agonists, which are available in different formulations the most common being the tablets. Since these treatments have plentiful side effects, all are titrated to the lowest effective dose (Buyan-Dent *et al.*, 2018).

Nevertheless, replenishment of striatal DA through the oral administration of L-DOPA, generally known as levodopa, still represents nowadays as the gold standard of PD treatment (Tambasco *et al.*, 2018). Unlike DA, levodopa can cross the blood-brain barrier (BBB) and be taken up into remaining dopaminergic neurons, where it is metabolized to DA and released into the synapse over time to stimulate striatal DA receptors (Hauser, 2009). Co-administration of levodopa with carbidopa or benserazide, which are dopa-decarboxylase inhibitors (DDCIs), reduces the peripheral conversion of levodopa to DA and thus increasing the bio-availability of levodopa and enhancing its clinical effect (Nagatsu and Sawada, 2009; Salat and Tolosa, 2013). Despite levodopa successfully improves motor symptoms in early PD stages, its long-term administration results in a decline of its effectiveness and is often associated with unbearable side effects such as dyskinesias (hyperkinetic involuntary movements), wearing-off (re-emergence of motor symptoms due to the lowing effect of levodopa) and “on-off” fluctuations (sudden changes in movement

control), among others (Poewe *et al.*, 2010; Salat and Tolosa, 2013). This fact renewed interest in neurosurgical procedures such as stimulation of the subthalamic nucleus (STN), which has been demonstrated as an effective treatment for advanced stages of PD when levodopa is no longer effective (Benabid *et al.*, 2000). High-frequency stimulation or lesions of the STN reduce the excessive activity of this region and thus alleviate PD motor symptoms (Thobois *et al.*, 2002).

Even though motor signs are the main focus of therapeutic strategies in PD, the broad spectrum of non-motor symptoms are common in PD patients and often contribute to the impairment of patients' quality of life. Some drugs already approved for another indication are available to treat each concrete symptom, albeit they are of limited efficacy, especially those related to treat wakefulness and sleep disorders (Seppi *et al.*, 2019).

1.1.3. Etiology and risk factors

Although the exact cause of PD remains elusive, research studies point to multifactorial etiology including environmental factors, genetics, or a combination of both (de Lau and Breteler, 2006). Epidemiologic studies reveal that most PD cases are idiopathic (sporadic) and only about 10% of PD patients have a familial history (Thomas and Beal, 2007).

Aging is the most irrefutable risk factor for developing PD. Meta-analyses studies demonstrate that PD has a global prevalence with age that affects 2-3% of the population above 65 years, and it is expected to increase over time due to rising aging population and the expectancy of life (Pringsheim *et al.*, 2014). Gender seems to play another key role, indicating a higher prevalence and incidence in men than in women probably due to the latter are somehow protected by increased estrogen activity (Haaxma *et al.*, 2007; Shulman, 2007).

1.1.3.1. Environmental factors

Many environmental risk factors have been proposed to contribute in sporadic PD pathogenesis, being lifelong exposure to pesticides (i.e. insecticides, herbicides and fungicides) the most proposed to increase risk of PD (Lai *et al.*, 2002; Yan *et al.*, 2018). Mitochondrial dysfunction by inhibiting complex I of the electron transport chain (ETC) has been reported as the main mechanism through these compounds can produce parkinsonism (Betarbet *et al.*, 2000; Cochemé and Murphy, 2008). In fact, decreased complex I activity has been documented in the SNpc of patients with PD (Schapira *et al.*, 1990), supporting the proposition that pesticides may play a key role in the PD pathogenesis.

Some specifics diets have also been described to contribute in the susceptibility of PD. While animal fat consumption has a positive association of PD (Anderson *et al.*, 1999), others such as coffee consumption display a strong negative association (Palacios *et al.*, 2012). In fact, caffeine showed a dose-response reduction in the risk of PD among caffeine consumers (Costa *et al.*, 2010), probably by antagonizing adenosine A2A receptors (Rivera-Oliver and Díaz-Ríos, 2014). Cigarette smoking is a well-known cause of adverse health outcomes, even though numerous studies have consistently shown that smoking is associated with a drastic reduced risk of PD (Hernán *et al.*, 2002; Thacker *et al.*, 2007). Some works support the hypothesis that nicotine can exert its neuroprotective effect through increasing DA release or inhibiting MAO-B enzyme thus preventing toxin-induced neuronal damage (Tan *et al.*, 2003; Quik, 2004; Quik *et al.*, 2008). Other factors such as physical activity may be associated with a lower risk of PD (Chen *et al.*, 2005a), although it has to be further explored.

Regarding other environmental factors such as exposure to metals, alcohol consumption, intake of antioxidant vitamins or trauma and head injury, are not very straightforward and their potential relevance in the etiology of PD remain unknown (Lai *et al.*, 2002; de Lau and Breteler, 2006).

1.1.3.2. Genetics

Large genome-wide association studies (GWAS) have shed light on the genetic basis of PD, especially identifying numerous mutations in several genes of *PARK* loci that cause familiar forms of the disease. Of those confirmed, mutations in *SNCA* (*PARK1/4*), encoding for α-synuclein, *LRRK2* (*PARK8*), *VPS35* (*PARK17*) and *CHCHD2* (*PARK22*) display an autosomal dominant mode of inheritance, while mutations in *PRKN* (*PARK2*), *PINK1* (*PARK6*), *DJ-1* (*PARK7*), *ATP13A2* (*PARK9*), *PLA2G6* (*PARK14*), *FBX07* (*PARK15*), *DNAJC6* (*PARK19*), *SYNJ1* (*PARK20*) and *VPS13C* (*PARK23*) are responsible for autosomal recessive PD forms (Lesage and Brice, 2009; Edvardson *et al.*, 2012; Klein and Westenberger, 2012; Krebs *et al.*, 2013; Lesage *et al.*, 2016). An updated review of the *PARK* genes and loci believed to cause familiar PD is listed in **Table 1**. These genes located in *PARK* loci codify for proteins that are implicated in many different processes of the cell, despite most are involved in maintenance of mitochondrial quality system. In fact, alterations in mitochondrial homeostasis have been documented to be affected in both familial and sporadic PD patients (Subramaniam and Chesselet, 2013), thus making mitochondria one of the main candidates in PD pathogenesis.

Although some familiar forms of PD are clinically indistinguishable from sporadic PD, others cause atypical clinical features (e.g. early onset). Nevertheless, GWAS have confirmed that some PARK genes are also affected in sporadic PD. Moreover, many mutations in other genes not related to *PARK* loci have also been described to increase the risk of sporadic PD, being those in *GBA1* gene the most prevalent (Poewe *et al.*, 2017). Recessive mutations in *GBA1* gene encoding for the lysosomal enzyme glucocerebrosidase (GCase) are known to cause the most common lysosomal-storage disorder, Gaucher's disease (GD). Furthermore, heterozygous *GBA1* mutations are also present in 5-25% of idiopathic PD cases, thus making *GBA1* mutations the highest genetic risk factor for PD (Schapira, 2015; O'Regan *et al.*, 2017). In this context, GCase activity was found to be decreased in PD patients carrying *GBA1* mutations (Gegg *et al.*, 2012) and even in patients with no *GBA1* affectation (Alcalay *et al.*, 2015), further supporting a role of defective lysosomal function in PD.

Table 1. PARK-designated PD loci.

Locus	Gene	Protein	Inheritance	Protein function
PARK1 / PARK4	*SNCA*	α-synuclein	AD	Synaptic protein. Major component of LB
PARK2	*PRKN*	Parkin	AR	E3 ubiquitin ligase involved in protein degradation
PARK3	*Unknown*	Unknown	AD	Unknown
PARK5	*UCHL1*	UCH-L1	AD	Processing of ubiquitin precursors
PARK6	*PINK1*	PINK1	AR	Mitochondrial kinase involved in mitochondrial quality control
PARK7	*DJ1*	DJ-1	AR	Redox-sensitive chaperone with an anti-oxidative stress function
PARK8	*LRRK2*	LRRK2 / Dardarin	AD	Multiple functions by several protein domains
PARK9	*ATP13A2*	ATPase 13A2	AR	Maintenance of lysosomal and mitochondrial cation homeostasis
PARK10	*Unknown*	Unknown	AD	Unknown
PARK11	*Unknown*	Unknown	AD	Unknown
PARK12	*Unknown*	Unknown	Unknown	Unknown
PARK13	*HTRA2*	HTRA2 / Omi	AD	Serine protease involved in caspase-dependent apoptosis
PARK14	*PLA2G6*	Phospholipase A2 Group VI	AR	Lipase involved in phospholipid metabolism
PARK15	*FBXO7*	F-box only protein 7	AR	E3 ubiquitin ligase involved in protein degradation
PARK16	*Unknown*	Unknown	Unknown	Unknown
PARK17	*VPS35*	VPS35	AD	Mitochondria-peroxisomes and endosome-trans-Golgi trafficking
PARK18	*EIF4G1*	eIF-4G1	AD	Recruitment of mRNA to the ribosome
PARK19	*DNAJC6*	HSP40 Auxilin	AR	Regulation of molecular chaperone activity
PARK20	*SYNJ1*	Synaptojanin 1	AR	Regulation of synaptic vesicle dynamics
PARK22	*CHCHD2*	CHCHD2	AD	Negative regulator of mitochondria-mediated apoptosis
PARK23	*VPS13C*	VPS13C	AR	Delivery of damaged mitochondria cargo to lysosomes

AD, autosomal dominant; AR, autosomal recessive.

1.1.4. Experimental animal models

The establishment of experimental models of PD is crucial to shed light on the pathophysiological mechanisms underlying PD neuronal cell death. Over the years, many organisms have been used to model PD from vertebrate organisms such as rodents (Vingill *et al.*, 2018), nonhuman primates (Vermilyea and Emborg, 2015) and fishes (Matsui *et al.*, 2012) to invertebrates like nematodes (Martinez *et al.*, 2017), flies (Xiong and Yu, 2018) and yeast (Menezes *et al.*, 2015).

Notwithstanding none of these models faithfully recapitulate the complexity of the human condition, tremendous strides toward contributing to a better understanding of the neurobiological basis of the disease and assessment of novel therapies have been achieved.

1.1.4.1. Genetic models

In contrast to toxin-based models, genetic models are based on targeted mutation or deletion of those genes known to cause PD in humans. On the one hand, deletion or mutation of protective genes (i.e. *PINK1*, *PRKN* and *DJ1*) should be able to recapitulate PD much in the same way that mutations on these genes cause PD in humans (Lee *et al.*, 2012). Nonetheless, individual deletion of these genes (Dawson *et al.*, 2010) or even deletion of the three at the same time (Kitada *et al.*, 2009) have absent neuronal degeneration. On the other hand, even though we currently know that genetic alterations (i.e. mutations, duplications and triplications) in *SNCA* gene cause various inheritance PD-associated forms, transgenic α-synuclein models also fail to display a consistent dopaminergic neuronal death and only subtle functional features are observed (Fernagut and Chesselet, 2004). Viral vectors are another genetic tool that has been used to induce a robust induction of a transgene in a determined region of the brain by means of stereotactic injections (Lee *et al.*, 2012). Recombinant adenoviral, adeno-associated viral (AAV), retroviral and lentiviral vectors have been widely used for gene delivery in the central nervous system, but

AAV remain the most used due their high transduction efficiency, specific cellular tropism and low immunogenicity (Schneider *et al.*, 2008; Piguet *et al.*, 2017). In this regard, many works have used AAV to drive exogenous α-synuclein in the SNpc, showing dopaminergic neurodegeneration and reproducing behavioral motor deficits in both rats and mice (Kirik *et al.*, 2002; Decressac *et al.*, 2012a; Oliveras-Salvá *et al.*, 2013). Besides, new genetic models recently emerged focusing on other PD-associated genes, such as *VPS35* (Tang *et al.*, 2015), *FBXO7* (Vingill *et al.*, 2016), *ATP13A2* (Kett *et al.*, 2015), and *GBA1* (Soria *et al.*, 2017), and albeit some of them seem to be promising genetic models, to date none of the current genetic models completely fulfills all of the key features of the human disease.

1.1.4.2. Toxic models

Neurotoxin-based models have been used over the years for testing degeneration of the nigrostriatal pathway and nowadays remain the cornerstone in simulating PD. Classically, these models are based on 6-hydroxydopamine (6-OHDA) and 1-methyl-4-phenyl-1,2,3,6-tetrahydropyridine (MPTP) administration. While both are selective catecholaminergic neurotoxins, the former has to be injected directly into the brain due to 6-OHDA barely crosses the BBB, whereas the latter can be systematically injected (Bové *et al.*, 2005; Blesa and Przedborski, 2014).

Despite 6-OHDA and MPTP neurotoxin-based animal models are the best characterized and most widely used, the more recently developed rotenone and paraquat models have emerged to increase the understanding of PD neuronal cell death (Salama and Arias-Carrión, 2011; Bové and Perier, 2012).

1.1.4.2.1. The MPTP mouse model

MPTP was identified in early 1980s, when drug addicts self-administered a street preparation of MPPP, an analog of the narcotic meperidine, contaminated with MPTP

and developed a severe and irreversible parkinsonism (Langston *et al.*, 1983). Several years later, postmortem examination of these patients confirmed moderate to severe neurodegeneration of the nigrostriatal pathway (Langston *et al.*, 1999). However, MPTP toxicity is not restricted to humans, since many species have been used to model PD such as nonhuman primates (Meissner *et al.*, 2003; Porras *et al.*, 2012), mice (Bové and Perier, 2012) and even worms (Kitamura *et al.*, 1998). Rats, though, were found to be resistant to MPTP neurotoxin (Zuddas *et al.*, 1994), since the dose required to induce dopaminergic neurodegeneration implied an extraordinary mortality rate (Giovanni *et al.*, 1994). Still, some studies succeed modeling PD in rats by stereotaxic injection of the active metabolite of MPTP, MPP^+ (Staal and Sonsalla, 2000). Nevertheless, mice and monkeys are the most common MPTP models, being the former the most popular choice given that no training and no sundry resources are needed (Bové *et al.*, 2005; Tieu, 2011), although mice gender, age and strains play a key role in variations of MPTP sensitivity (Muthane *et al.*, 1994; Smeyne *et al.*, 2005).

Many regimens of intoxication have been used in the MPTP mouse model, but the acute and sub-acute regimens are the most characterized so far (Bové and Perier, 2012). On the one hand, Jackson-Lewis and Przedborski developed the acute MPTP regimen, which consists of four intraperitoneal (i.p.) injections of 20 mg/kg MPTP with 2 hour intervals in a single day. This type of regimen leads to about 70% of SNpc dopaminergic neurons to be lost and consequently up to 90% of dopamine depletion in the striatum (Jackson-Lewis *et al.*, 1995). However, with this type of regimen dopaminergic neurons die by a non-apoptotic cell death, contrasting to human disease (Mochizuki *et al.*, 1996; Hirsch *et al.*, 1999). On the other hand, Tatton and Kish developed the sub-acute regimen consisting of one i.p. injection of 30 mg/kg MPTP daily for five consecutive days (Tatton and Kish, 1997). This regimen leads to a more progressive neurodegeneration with 30% of dopaminergic cell loss and 50% depletion of DA in the striatum. In this case, the mechanism of neuronal cell death is apoptotic and the lesion is stabilized within 21 days after the last MPTP injection (Vila *et al.*, 2001; Perier *et al.*, 2007). However, other approaches regarding MPTP

administration have been attempted in order to achieve a more progressive dopaminergic degeneration, such as those related to co-administrate MPTP with probenecid (Petroske *et al.*, 2001) to reduce MPTP metabolism, or even using osmotic pumps in order to infuse low doses of MPTP over time (Fornai *et al.*, 2005).

The mechanism of MPTP toxicity has been widely characterized (Dauer and Przedborski, 2003; Vila and Przedborski, 2003). After its administration, MPTP, as a lipophilic compound, rapidly crosses the BBB and is taken up by glial cells, where it is first converted to 1-methyl-4-phenyl-2,3-dihydropyridinium ($MPDP^+$) by MAO-B enzyme. Levels of this enzyme, only shared with serotonergic neurons, is believed to be the responsible of different sensitivity to MPTP between mice strains (Meredith and Rademacher, 2011). $MPDP^+$ is then converted to MPP^+ and released to the extracellular space, where it is taken up by dopaminergic neurons through dopamine transporter (DAT) (**Figure 3**).

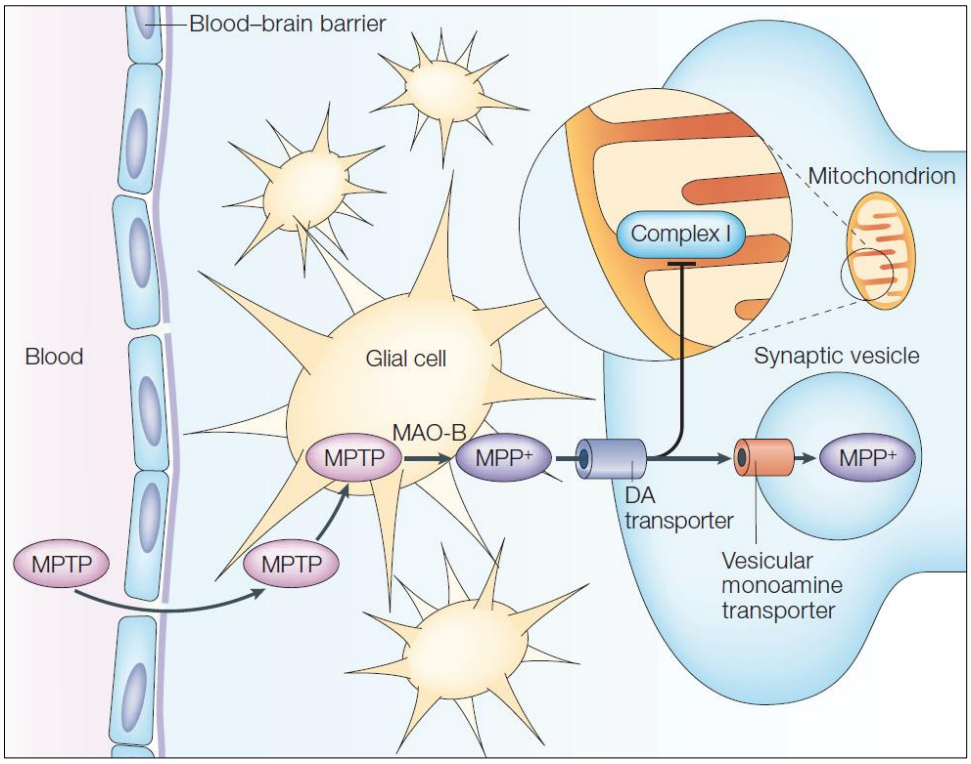

Figure 3. Metabolism and mechanism of action of MPTP. When MPTP is systemically injected, it rapidly crosses the BBB and is metabolized to the active toxic compound MPP^+ in astrocytic cells. MPP^+ has high affinity for DA transporters (DAT) and thus is taken up by dopaminergic neurons, where it mainly inhibits complex I of the ETC in mitochondria. From Vila and Przedborski, 2003 *Nat. Rev. Neurosci.*

Once inside dopaminergic neurons, MPP^+ acts at multiple levels. On one side, MPP^+ enters to the mitochondria due to the inside-negative mitochondrial membrane potential (Δψm) and inhibits complex I of the ETC, producing reactive oxygen species (ROS) and a reduction of adenosine triphosphate (ATP) levels (Dauer and Przedborski, 2003). On the other side, MPP^+ can also enter into synaptic vesicles through vesicular monoamine transporter-2 (VMAT2) and leads to a redistribution of vesicular DA to the cytosol, where, in turn, is autoxidized and generates toxic free radicals harmful to neurons (Lotharius and O'Malley, 2000). These pathological events have also been documented in PD neurons (Schapira *et al.*, 1990; Hattingen *et al.*, 2009; Burbulla *et al.*, 2017). Besides, it has also been demonstrated that MPP^+ acts as a destabilizing factor, affecting microtubule dynamics and therefore inducing synaptic dysfunction by axon fragmentation (Cappelletti *et al.*, 2005; Burke and O'Malley, 2013). The combination of all these events triggers a cascade of molecular pathways that ultimately lead to neuronal cell death.

To date, the MPTP model remains as the gold standard of PD available models because it recapitulates several features of the disease, including: (i) SNpc dopaminergic lost; (ii) sparing of VTA dopaminergic neurons; (iii) greater affectation of projections (especially those to the putamen) than nigral cell bodies; and (iv) α-synuclein post-translational modifications (Dauer and Przedborski, 2003; Bové and Perier, 2012). For all above commented, numerous studies have used the MPTP mouse model to study the mechanisms of dopaminergic neuronal death and the development of neuroprotective strategies (Vila *et al.*, 2001; Perier *et al.*, 2005, 2007; Ramonet *et al.*, 2013; Bové *et al.*, 2014; Franco-Iborra *et al.*, 2018a; Pil Yun *et al.*, 2018a).

1.1.5. Mechanisms of neuronal cell death and therapeutic targets in PD

A better understanding of the pathological mechanisms underlying PD neuronal cell death is crucial for the discovery of potential neuroprotective strategies. The most progress to date has been focused in the loss of SNpc dopaminergic neurons that

explains the motor signs of the disease (Zeng *et al.*, 2018). Albeit diverse efforts have been carried out to deepen our current knowledge of PD pathogenesis, the mechanism that ultimately leads to cell death is still unsettled.

Some insights into PD pathogenesis come from PD postmortem patients, although most actually arise from experimental models of PD, mainly those produced by neurotoxins such as MPTP. The most significant mechanisms include dysregulation of: oxidative stress and dopamine metabolism, survival and programmed cell death pathways, mitochondria, calcium, alpha-synuclein, protein handling and non-cell-autonomous mechanisms (Levy *et al.*, 2009; Fahn *et al.*, 2011; Zeng *et al.*, 2018). Modulation of these mechanisms is currently being tested as putative neuroprotective strategies in clinical trials (Athauda and Foltynie, 2015) (**Figure 4**). However, these pathways cross-interact with each other, generating an even more complex network and thus limiting the effectiveness of these neuroprotective strategies. Hence, neuroprotective approaches that act at multiple levels may increase the likelihood of developing better disease-modifying treatments for PD.

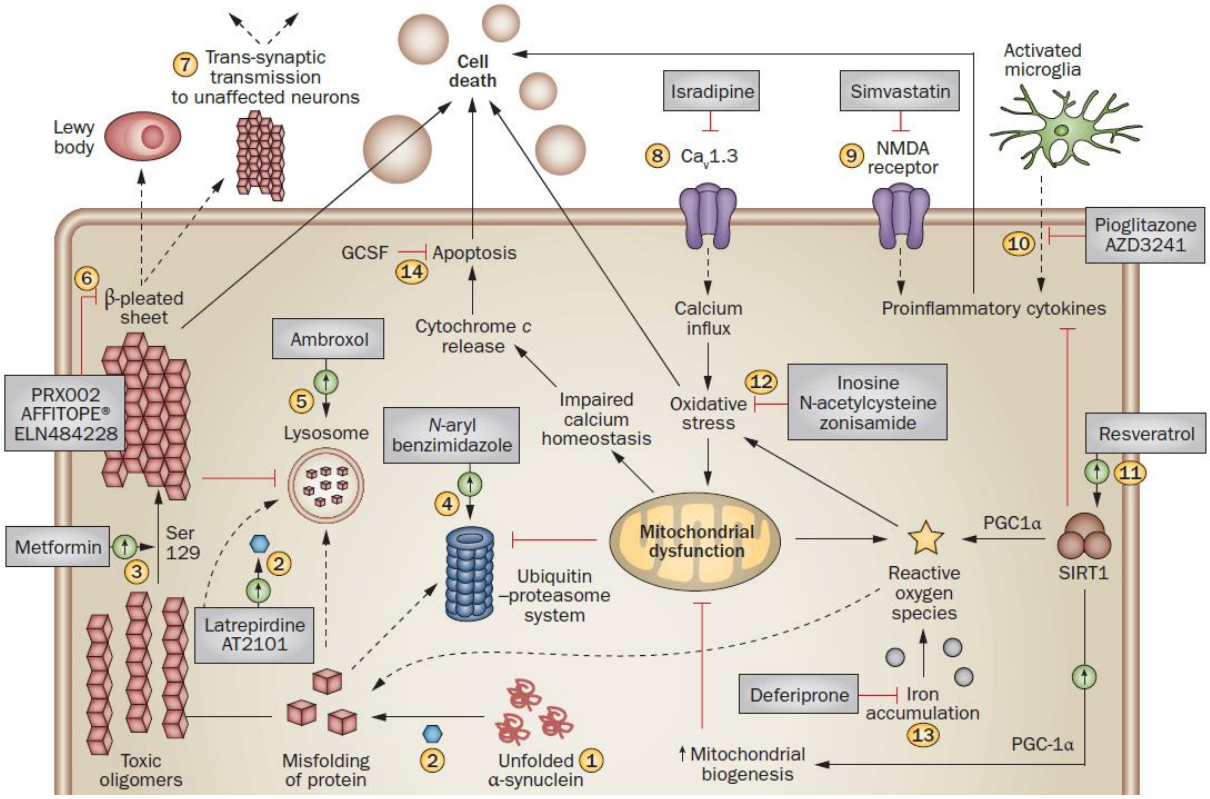

Figure 4. Pathologic mechanisms of PD and possible targets for intervention. Some drugs (grey boxes), which some of them are currently being tested in clinical trials, are aimed to target some

mechanism of PD pathogenesis such as protein misfolding, oxidative stress, apoptosis and microglial activation. From Athauda and Foltynie, 2015 *Nat. Rev. Neurol.*

1.1.5.1. Oxidative stress and dopamine metabolism

The imbalance between the generation of ROS and cellular antioxidant defenses, commonly known as oxidative stress, has long been described as a potential mechanism that leads to cell demise. The main evidence of such pathological event relies on postmortem analyses of PD patients, which confirmed an increased presence of oxidized proteins (Keeney *et al.*, 2006), DNA (Zhang *et al.*, 1999) and lipids (Bosco *et al.*, 2006) in the SNpc. In line with the above, the reduced form of glutathione (GSH) and glutathione peroxidase (GPx), which are leading antioxidants of brain cells, are however decreased in the SNpc of PD patients (Kish *et al.*, 1985; Pearce *et al.*, 1997). Contribution of ROS in neuronal cell death was described years ago by the fact that boosting ROS scavengers, such as glutathione and superoxide dismutase (SOD), have a neuroprotective effect in various PD animal models (Asanuma *et al.*, 1998; Leret *et al.*, 2002; Cheng *et al.*, 2009).

There are several sources of ROS, such as those derived from mitochondrial dysfunction and neuroinflammation, although DA metabolism is one of the major outcomes of ROS (Fahn *et al.*, 2011; Hwang, 2013). In normal conditions, DA is normally stored into synaptic vesicles through VMAT2, preventing DA oxidation due to low vesicular pH levels (Segura-Aguilar and Paris, 2014). This vesicular DA is transported to the neuronal terminal, where it is released into the synaptic space. Extracellular DA is picked up by DAT and either recycled into synaptic vesicles or metabolized by monoamine oxidase B (MAO-B) to 3,4-dihydroxyphenyl-3-acetaldehyde (DOPAL), which is then oxidized to 3,4-dihydroxyphenylacetic acid (DOPAC) by aldehyde dehydrogenase (ALDH). Around 50% of DOPAC is eliminated, while the other half is finally converted to homovanillic acid (HVA), the final metabolite of DA, through catechol-O-methyltransferase (COMT). Especially DOPAL has been reported to be an endogenous neurotoxin with high electrophilicity

able to adversely interact with proteins and producing ROS (Vanle *et al.*, 2017), and its implication in neuronal cell demise has been reported in rodents (Panneton *et al.*, 2010). Indeed, DOPAL levels are increased in postmortem PD tissue (Goldstein *et al.*, 2011).

Otherwise, cytosolic DA (pH 7.4) is highly reactive and can be easily oxidized. In fact, this may be triggered due to decreased VMAT2 density levels that actually have been observed in the SNpc of PD patients (Thibaut *et al.*, 1995). Likewise, mice expressing low VMAT2 have an increased cytosolic DA levels, DA oxidation, increased ROS levels, several damage to cellular components and exhibit a progressive loss of dopaminergic neurons (Caudle *et al.*, 2008). In line with this and as commented previously, it has been demonstrated that in the MPTP model there is a redistribution of vesicular DA to the cytosol that contributes to the generation of ROS (Lotharius and O'Malley, 2000). DA oxidation leads to quinones and semiquinones like 6-OHDA, which has been used over the years to model PD thus highlighting the vulnerability of dopaminergic neurons to oxidative stress (Schapira and Jenner, 2011). Other DA-induced adducts, such as aminochrome or soluble alpha-synuclein oligomers, have also been demonstrated to increase ROS and to be harmful for neurons (Hastings *et al.*, 1996; Burbulla *et al.*, 2017; Mor *et al.*, 2017). In contrast, lowering cytosolic DA by increasing VMAT2 levels has a neuroprotective effect in PD-related neurodegeneration (Muñoz *et al.*, 2012; Lohr *et al.*, 2014, 2016).

The final step of DA oxidation leads to NM, whose levels are increased in PD neurons (Halliday *et al.*, 2005; Carballo-Carbajal *et al.*, 2019). However, its particular role has remained quite mysterious until now. In line with this, we have recently demonstrated that NM progressive buildup interferes with normal cell function, triggering PD-like neuronal degeneration and dysfunction, and that lowering NM levels by enhancing lysosomal exocytosis confers a *bona fide* neuroprotection (Carballo-Carbajal *et al.*, 2019).

Some therapeutic strategies aimed to reduce oxidative stress, such as rasagiline and selegiline, have proven to be of limited effectiveness in clinical trials (Athauda and Foltynie, 2015). Interestingly, increasing urate levels, glutathione levels and reducing iron accumulation, however, are currently being evaluated and by the moment they seem to demonstrate more potent disease-modifying effects (Athauda and Foltynie, 2015).

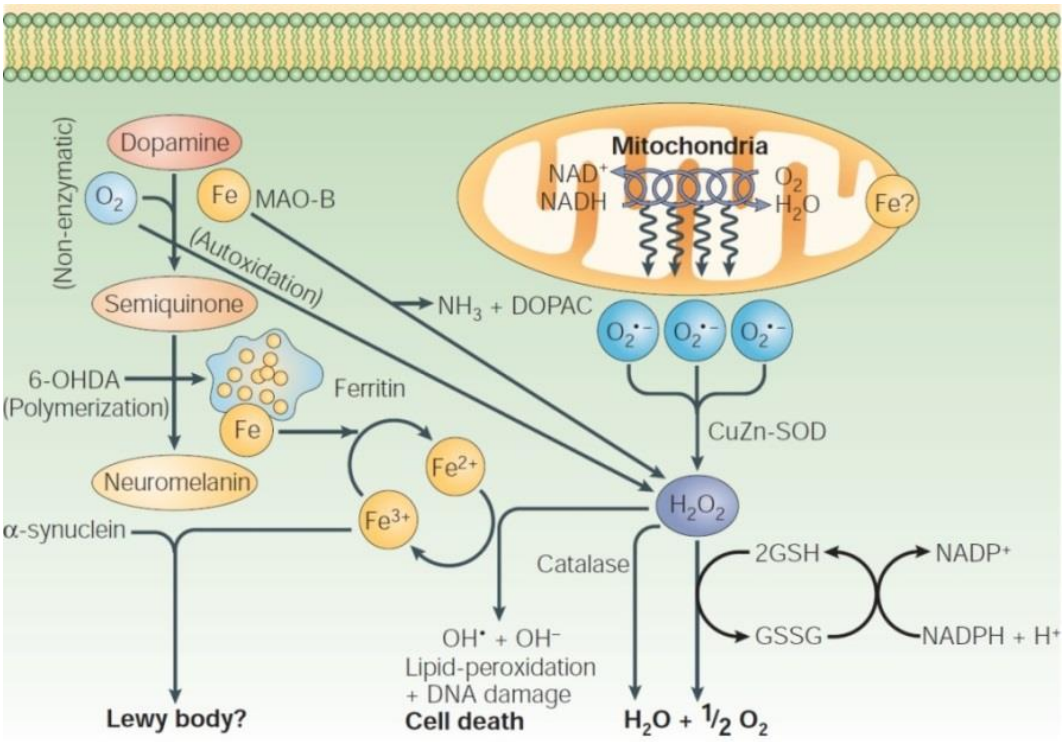

Figure 5. Oxidative stress hypothesis of PD. Increased oxidation of DA together with increased iron levels in PD patients could lead to the formation of DA-derived quinones and semiquinones, which damage cellular components such as DNA, proteins and lipids, thus inducing neuronal death. From Zecca *et al.*, 2004 *Nat. Rev. Neurosci.*

1.1.5.2. Survival and programmed cell death pathways alterations

An efficient network of signal transduction pathways is crucial for the maintenance of neuronal viability (Morrison *et al.*, 2003). In this regard, various intracellular signaling cascades, such as mitogen-activated protein kinase (MAPK) and protein kinase B (AKT)/mammalian target of rapamycin (mTOR), are critical for the fate of a neuron that can result in cell death or persistent survival (Morrison *et al.*, 2003; Kumar Jha *et*

al., 2015). Several changes in various proteins implicated in either ligand level (e.g. neurotrophic factors) or the intracellular signaling cascade have been reported in PD patients (Toulorge *et al.*, 2016), thus creating a disequilibrium that tips the balance towards neuronal death.

1.1.5.2.1. MAPK pathway

MAPK is a superfamily of serine/threonine protein kinases present in all eukaryotic cells and its signaling is characterized by a 3-tier signaling cascade by phosphorylation: MAPKKK, MAPKK and MAPK (Burke, 2007). After diverse stimuli (e.g. growth factors, oxidative stress and cytokines), the interaction of MAPKKK with a small GTP-binding protein belonging to the Ras/Rho family results in the phosphorylation and therefore activation of MAPKKK, which, in turn, phosphorylates and activates MAPKK. MAPKK, when activated, phosphorylates the threonine and tyrosine residues of the activation loop of kinase subdomain VIII of MAPK. Finally, MAPK phosphorylates in a proline-directed manner a widely number of substrates implicated in numerous processes of the cell including cell cycle control, protein biosynthesis, differentiation, survival and apoptosis, among others (Kyriakis and Avruch, 2012). Three major branches of MAPKs have been characterized: the extracellular signal-regulated kinases (ERKs), the c-JUN N-terminal kinases (JNKs) and the p38 kinases (Zhang and Liu, 2002; Dzamko *et al.*, 2014). In general, while the activation of the ERKs is normally implicated in cell survival, the JNKs and p38 kinases are often facilitating neuronal apoptosis (Morrison *et al.*, 2003) (**Figure 6**). In fact, ERK and JNK-p38 are mutually regulated in an opposed manner (Xia *et al.*, 1995; Kyriakis and Avruch, 2012). For all above commented, several research studies have been gathered to study the contribution of MAPK signaling in PD pathogenesis.

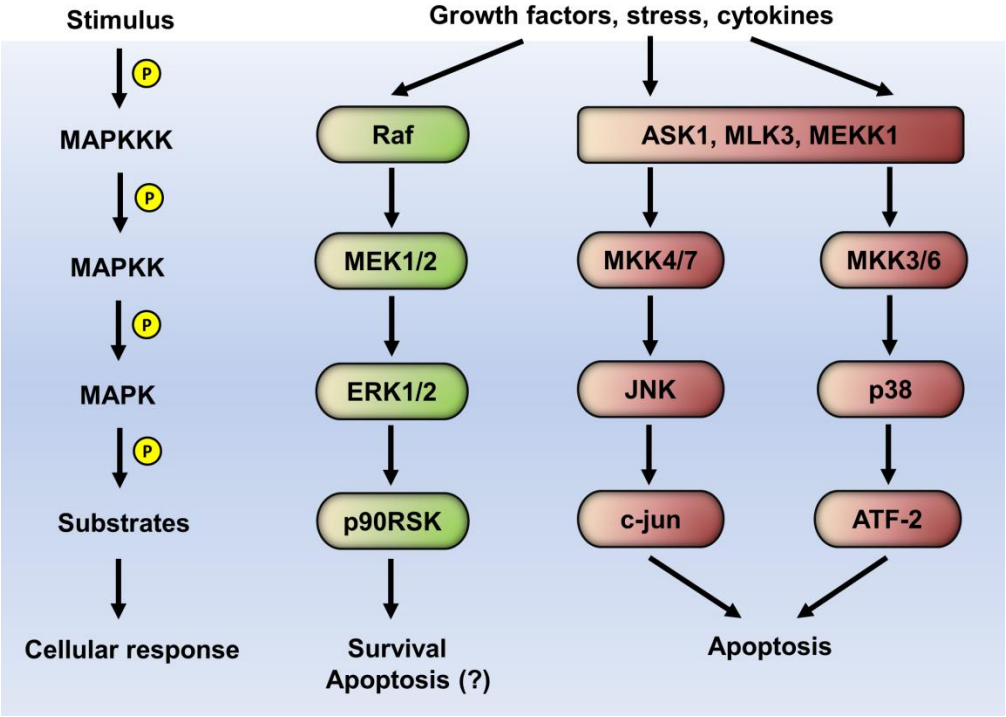

Figure 6. Simplified scheme of MAPK signaling. After diverse stimuli, a cascade of phosphorylations is initiated through the 3-tier of MAP kinases (MAPKKK, MAPKK, MAPK) that ultimately leads to phosphorylation of several substrates, generating different cellular responses.

There is accumulating evidence that JNK and p38 are robustly activated and therefore contributing to dopaminergic death in different PD models (Choi *et al.*, 1999; Saporito *et al.*, 2000; Newhouse *et al.*, 2004). Indeed, both the substrate of JNK, c-jun, and p38 have been reported to be increased in the SNpc of PD patients (Hu *et al.*, 2011). In this regard, genetic or pharmacological inhibition of JNK or p38 signaling results in a potential neuroprotection in several PD animal models (Hunot *et al.*, 2004; Chambers *et al.*, 2011, 2013; Crocker *et al.*, 2011; Choi *et al.*, 2014).

In contrast, ERK has found to be important in neuronal survival, plasticity, memory and growth (Xia *et al.*, 1995; Xue *et al.*, 2000; Sweatt, 2001; Thiels and Klann, 2001). ERK can act at multiple levels to lead an ultimately pro-survival effect (Lu and Xu, 2006). On the one hand, ERK induces a transcriptional repression or decreases the activity of pro-apoptotic molecules (e.g. caspases, BIM, BAD) and, at the same time, an upregulation of anti-apoptotic proteins (e.g. BCL-XL, CREB) via enhancement

both their transcription and activity (Lu and Xu, 2006). Some of these effects are partially mediated by p90 ribosomal S6 kinase (p90RSK), the most known substrate effector of ERK1/2 (Xing *et al.*, 1996; Carriere *et al.*, 2008). However, an increased levels of the phosphorylated form of ERK1/2 (Zhu *et al.*, 2003) and p90RSK (Zhu *et al.*, 2002) have been found in dopaminergic neurons of PD patients, although it is believed that ERK signaling is initiated as a neuroprotective compensatory mechanism to counteract death signals (Hetman *et al.*, 1999). In contrast, some studies have reported that, under some special circumstances, this pathway can act in a pro-apoptotic manner contributing to neuronal death (Kulich and Chu, 2001; Gómez-Santos *et al.*, 2002; Cheung and Slack, 2004). Therefore, further elucidation about ERK1/2 function in regulating both survival and cell death is required to understand its precise role in PD pathogenesis.

1.1.5.2.2. AKT/mTOR pathway

AKT/mTOR has been long known to be a crucial pathway for neuronal survival and growth (Burke, 2007). AKT is a serine/threonine kinase whose activation occurs when many ligands, normally growth factors, bind to their receptors on the cell surface resulting in an induction of phosphatidylinositol 3-kinase (PI3K), which activates AKT. Activated AKT has an anti-apoptotic effect at multiple levels: (i) inhibition of JNK signaling by negatively regulating the JNK pathway scaffolds JIP1 (Kim *et al.*, 2002) and POSH (Figueroa *et al.*, 2003); (ii) inhibition of fork head box-O class (FOXO) transcription factors and thus reducing the expression of pro-apoptotic molecules, such as BIM; (iii) increasing the levels of anti-apoptotic proteins, such as BCL-XL; and (iv) activation of mTOR signaling (Levy *et al.*, 2009; Winter *et al.*, 2011).

mTOR is a serine/threonine protein kinase, belonging to PI3K-related kinase family, that exists in two complexes referred to as mTOR complex 1 (mTORC1) and mTOR complex 2 (mTORC2) (Coquillard *et al.*, 2015), which regulate multitude of

intracellular signaling proteins depending of nutrient availability and cellular bioenergetics (Altomare and Khaled, 2012).

mTORC1 it is made up of three core proteins: mTOR as a catalytic subunit, regulatory-associated protein of mTOR (Raptor) and mammalian lethal with Sec13 protein 8 (mLST8); and two inhibitory subunits, DEP-domain-containing mTOR-interacting protein (Deptor) and proline-rich AKT substrate 40 kDa (PRAS40) (Laplante and Sabatini, 2009). Besides AKT, activation of mTORC1 can also be achieved through ERK pathway, which inhibits tuberous sclerosis complex 2 (TSC2/tuberin), a negative regulator of mTORC1 activity (Winter *et al.*, 2011). Inhibition of TSC2 leads to the activation of Ras homolog enriched in brain (Rheb), which, in turn, activates mTORC1 (Parmar and Tamanoi, 2010). mTORC1 is pivotal for cell growth and metabolism, and for such it regulates many processes like protein synthesis, lipid synthesis, nucleotide synthesis and autophagy (Saxton and Sabatini, 2017). In particular, mTORC1 activates protein synthesis and cell growth by phosphorylating p70 ribosomal S6 kinase 1 (S6K1) and eukaryotic translation initiation factor 4E (eIF4E)-binding protein 1 (4E-BP1). Phosphorylation of S6K1 on Thr389 by mTORC1 leads to its activation, which, in turn, phosphorylates many substrates (e.g. RPS6 and eIF4B) to promote mRNA translation (Magnuson *et al.*, 2012). It has also been demonstrated, though, that both ERK1/2 and p90RSK can also phosphorylate and activate S6K1 and RPS6, linking the ERK pathway directly to the mRNA translational machinery (Roux *et al.*, 2007). Besides, 4E-BP1 binds and sequesters eIF4E, inhibiting protein translation. When 4E-BP1 is phosphorylated by mTORC1, it releases eIF4E and allows the formation of eIF4F complex and the subsequent translation initiation (Gingras *et al.*, 1999). Moreover, mTORC1 also activates the sterol responsive element binding protein (SREBP), which is involved in lipid biosynthesis (Lewis *et al.*, 2011), and bifunctional methylenetetrahydrofolate dehydrogenase/cyclohydrolase (MTHFD2) that regulates purine biosynthesis (Ben-Sahra *et al.*, 2016). By contrast, autophagy is negatively regulated by mTORC1 through phosphorylation and thereby repression of unc-51 like kinase 1 (ULK1) and

autophagy-related protein 13 (ATG13), which are important for autophagy initiation (Ganley *et al.*, 2009; Hosokawa *et al.*, 2009).

Regarding mTORC2, it is formed by: mTOR as a catalytic subunit, rapamycin-insensitive companion of mTOR (Rictor), protein observed with Rictor-1 (Protor-1), mLST8, mammalian stress-activated protein kinase interacting protein (mSIN1); and, as in mTORC1, the inhibitory subunit Deptor (Laplante and Sabatini, 2009). In contrast to mTORC1, mTORC2 regulates other functions including: cytoskeletal remodeling by phosphorylating the protein kinase C (PKC) family (α, δ, γ and ε), paxillin, RhoA and Rac1; and cell survival by phosphorylating AKT at S473 hydrophobic domain (Laplante and Sabatini, 2009; Saxton and Sabatini, 2017) (**Figure 7**). However, AKT can also be phosphorylated on the same residue by other kinases, such as TANK binding protein 1 (TBK1) (Ou *et al.*, 2011).

The key role of AKT and mTOR activities on dopaminergic survival is strengthened by the fact that diminished levels of phosphorylated/activated AKT were found in SNpc dopaminergic neurons of PD patients (Malagelada *et al.*, 2008). This could be explained due to increased levels of RTP801/REDD1, a pro-apoptotic protein that suppresses mTOR activity through TSC complex and induces neuronal cell death (Brugarolas *et al.*, 2004; Malagelada *et al.*, 2006), were found in TH-positive neurons of PD patients (Malagelada *et al.*, 2006). Moreover, AKT activity has also been found to be reduced in different models of PD (Malagelada *et al.*, 2008; Tasaki *et al.*, 2010), whereas overexpression of AKT was shown to have neuroprotective effects in several PD models (Salinas *et al.*, 2001; Ries *et al.*, 2006; Malagelada *et al.*, 2008; Aleyasin *et al.*, 2010; Tasaki *et al.*, 2010). However, protein translation, one of the main mTORC1 downstream functions, has received little attention in PD (Taymans *et al.*, 2015). Since only few studies have linked protein translation machinery with PD pathogenesis (Tain *et al.*, 2009; Malagelada *et al.*, 2010; Garcia-Esparcia *et al.*, 2015), this fundamental cellular function and its connection with neuronal survival still needs to be further investigated.

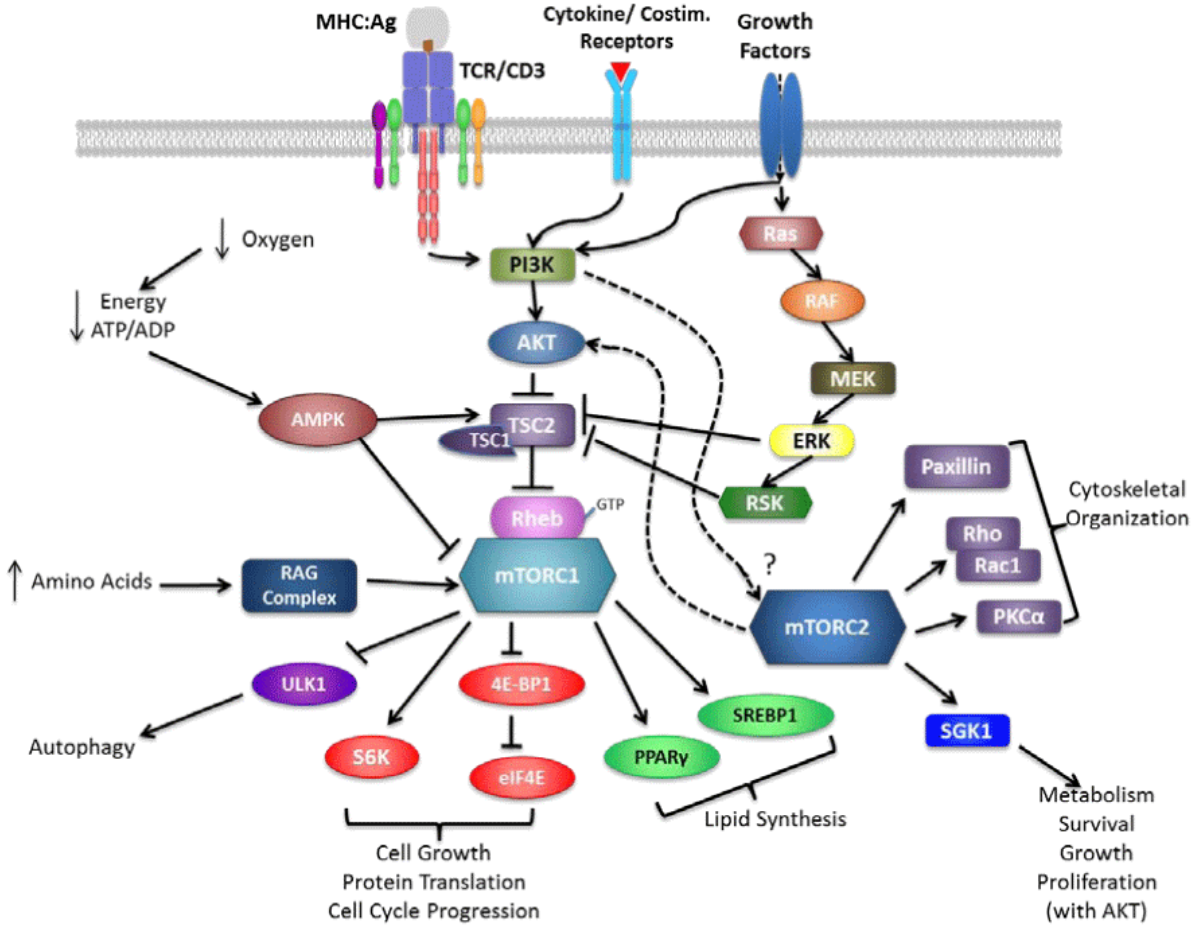

Figure 7. Scheme of mTOR signaling pathway. Binding of some ligands, such as growth factors, to their receptors initiates the AKT and ERK signaling, which increase mTORC1 activity by inhibiting the repressor of Rheb, TSC2. mTORC1, in turn, induces several cellular responses such as cell growth, protein translation, cell cycle progression, lipid synthesis and inhibition of autophagy. From Coquillard *et al.*, 2015 *SOJ Immunol.*

1.1.5.2.3. Neurotrophic factors

Neurotrophic factors such as glial cell line-derived neurotrophic factor (GDNF), brain-derived neurotrophic factor (BDNF), ciliary neurotrophic factor (CNTF) and nerve growth factor (NGF), among others, are important for the development, maintenance and survival of neurons (Bhardwaj and Deshmukh, 2018). After binding to the corresponding receptors belonging to p75 and Trk families of tyrosine kinase receptors (TKRs), neurotrophic factors activate both AKT and ERK signaling

(Patapoutian and Reichardt, 2001; Morrison *et al.*, 2003; Coquillard *et al.*, 2015). However, several studies have observed decreased levels of many neurotrophic factors in PD patients including GDNF (Chauhan *et al.*, 2001; Mogi *et al.*, 2001), BDNF (Parain *et al.*, 1999; Chauhan *et al.*, 2001), CNTF (Chauhan *et al.*, 2001), NGF (Mogi *et al.*, 1999), and some of their receptors like RET (Decressac *et al.*, 2012b), leading to AKT and ERK signaling lost. This neurotrophic signaling lost is believed to contribute to neuronal death (Decressac *et al.*, 2012b; Kang *et al.*, 2017) and may account for the neuronal dysfunction and atrophy accompanied by a loss of phenotype that involves TH downregulation in PD (Kastner *et al.*, 1993; Rudow *et al.*, 2008; Kordower *et al.*, 2013). Because of this, a large amount of interest in increasing neurotrophic factors levels to protect and repair the degenerating nigrostriatal pathway has been for years a rationale for developing therapeutic strategies for PD. To date, however, the general outcome of neurotrophic factor-based therapy in clinical trials has been unsatisfactory (Ferreira *et al.*, 2018).

1.1.5.3. Mitochondrial dysfunction

Neurons have a high metabolic rate and require a constant supply of energy to maintain the membrane excitability and to properly handle energy-intensive biological processes such as neurotransmission and plasticity. This provision of energy mainly relies on aerobic metabolism by mitochondria (Levy *et al.*, 2009). However, mitochondria also participate in other cellular processes, such as calcium homeostasis and apoptosis (Kann and Kovács, 2006). Therefore, disruption of mitochondrial homeostasis and thereby leading to mitochondrial dysfunction can be highly detrimental for neurons. In fact, mitochondrial dysfunction has repeatedly been associated with PD pathogenesis (Vila *et al.*, 2008; Fahn *et al.*, 2011; Franco-Iborra *et al.*, 2016; Zeng *et al.*, 2018).

1.1.5.3.1. OXPHOS system

Mitochondria are double membrane bound organelles including the inner mitochondrial membrane (IMM) and the outer mitochondrial membrane (OMM). The IMM is packed with multiple proteins, being those related to oxidative phosphorylation (OXPHOS) the most abundant. OXPHOS is the system designated to couple cellular respiration to the production of energy in the form of ATP. This process takes place in the IMM and involves the transfer of electrons down the respiratory chain, which is made up by five mitochondrial respiratory complexes: reduced nicotinamide adenine dinucleotide dehydrogenase-ubiquinone oxidoreductase (complex I), succinate dehydrogenase-ubiquinone oxidoreductase (complex II), ubiquinone-cytochrome c oxidoreductase (complex III), cytochrome c oxidase (complex IV) and ATP synthase (complex V) (Perier and Vila, 2012) (**Figure 8**). Several defects in OXPHOS system have been observed in PD brains, from decreased complex I activity (Schapira *et al.*, 1990) to decreased most of OXPHOS protein levels (Moisoi *et al.*, 2009; Franco-Iborra *et al.*, 2018a). Reinforcing a potential role for complex I defects in PD pathology, most of the pesticides that have linked to PD induce complex I dysfunction (Sherer *et al.*, 2002; Richardson *et al.*, 2009).

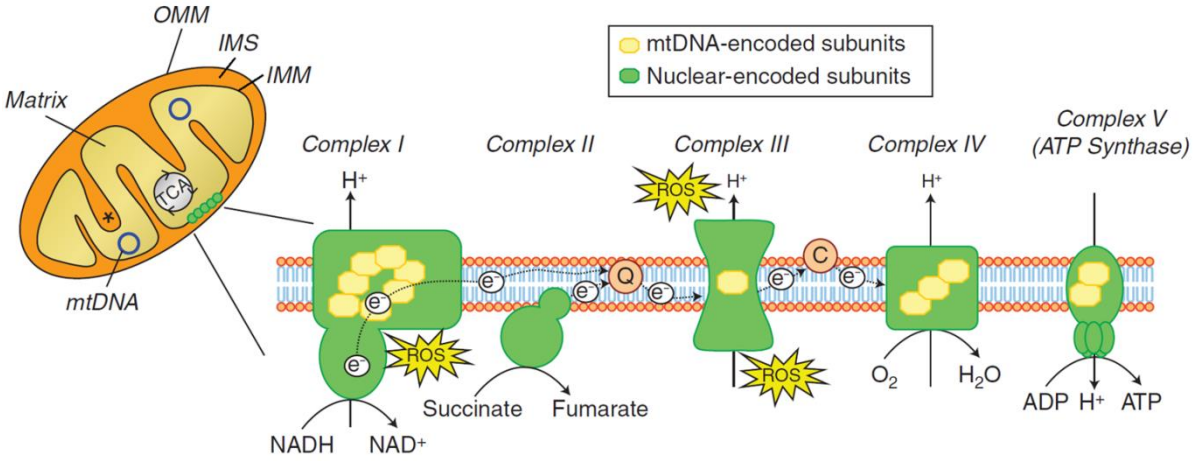

Figure 8. Schematic representation of mitochondrial compartmentalization and OXPHOS complexes. Mitochondria are composed by two membranes that enclose 4 compartments: the outer mitochondrial membrane (OMM), the intermembrane space (IMS), the inner mitochondrial membrane (IMM) and the matrix, where mitocondrial DNA (mtDNA) is located. The OXPHOS system located in the IMM is composed by 5 complexes that are formed, at the same time, by multiple subunits. Only 13 subunits are mtDNA-encoded (yellow), while the others are nuclear-encoded (green) and imported into the mitochondria. From Perier and Vila, 2012 *Cold Spring Harb. Perspect. Med.*

1.1.5.3.2. Mitochondrial protein import

However, IMM not also harbors OXPHOS system proteins but also other proteins such as TIM23 complex, which is implicated in the mitochondrial protein import machinery together with TOM20 complex that is located in the OMM (Pfanner *et al.*, 2019). Because about 99% of mitochondrial proteins are nuclear-encoded, mitochondrial protein import is essential for mitochondrial function (Wiedemann and Pfanner, 2017). In fact, a defect on mitochondrial protein import system and its possible contribution to human disease have been observed in both PD brains and PD models (Bender *et al.*, 2013; Di Maio *et al.*, 2016; Franco-Iborra *et al.*, 2018a). In this line, it has been demonstrated that α-synuclein binds to TOM20 complex, inhibiting mitochondrial protein import and, consequently, enhancing ROS production and loss of mitochondrial membrane potential (Di Maio *et al.*, 2016). In contrast, restoration of mitochondrial protein import function by overexpressing mitochondrial translocases machinery has beneficial effects (Bender *et al.*, 2013; Di Maio *et al.*, 2016; Franco-Iborra *et al.*, 2018a).

1.1.5.3.3. Mitochondrial dynamics

In order to keep a healthy mitochondrial network, dysfunctional mitochondria are degraded mainly through PINK1/Parkin-dependent mitophagy and this is balanced with *de novo* generation of mitochondria (Seo *et al.*, 2018) (**Figure 9**). This mitochondrial biogenesis relies on peroxisome-proliferator-activated receptor gamma co-activator-1alpha (PGC-1α), which activates other transcription factors like nuclear respiratory factor 1 (NRF1) and nuclear respiratory factor 2 (NRF2), among others (Scarpulla *et al.*, 2012). These transcription factors coordinate mitochondrial biogenesis through the expression of mitochondrial transcription factor A (TFAM), which functions in both mtDNA transcription and replication, and the transcription of genes implicated in multiple mitochondrial functions (Scarpulla *et al.*, 2012). It has been reported that mutations on PD-familial genes *PRKN* and *PINK1* impair

mitochondrial removal, causing mitochondrial dysfunction (Greene *et al.*, 2003; Park *et al.*, 2006). Moreover, decreased levels of PGC-1α (Shin *et al.*, 2011) and TFAM (Grünewald *et al.*, 2016) have been reported in PD patients. In fact, specific deletion of TFAM in dopaminergic neurons of mice (termed MitoPark mice) leads to a progressive parkinsonism with respiratory-chain-deficient dopaminergic neurons (Ekstrand *et al.*, 2007), whereas overexpressing TFAM counteracted MPP^+-induced mitochondrial dysfunction (Piao *et al.*, 2012).

Mitochondria are dynamic organelles capable of undergoing fusion and division (fission) events to adapt to different changes in cellular requirements and to ensure an adequate function (**Figure 9**). Mitochondrial dynamics is an important constituent of neuron quality control, considering that defects on this system have detrimental consequences that contribute to the pathogenesis of several neurodegenerative diseases (Itoh *et al.*, 2013). On the one hand, mitochondrial fusion is regulated by dynamin-like GTPases, such as mitofusin 1 (MFN1), mitofusin 2 (MFN2) and optic atrophy 1 (OPA1). MFN1 and MFN2 are located in the OMM and are required for the initial mitochondria tethering and OMM fusion, while OPA1 is anchored to the mitochondrial cristae inner membrane and is necessary for IMM fusion and cristae morphogenesis (Perier and Vila, 2012). When mitochondria fusion, mitochondrial content is mixed and it has a highly beneficial outcome by attenuating the potential deleterious effects of mutated mtDNA or misfolded proteins (Chen *et al.*, 2010; Van der Bliek *et al.*, 2013). Moreover, the reason for the formation of hyperfused mitochondrial networks is to preserve the proper mitochondrial membrane potential and allowing the OXPHOS complexes to cooperate more efficiently, maximizing ATP synthesis (Westermann, 2012). Therefore, increased mitochondrial fusion extends the mitochondrial network and is generally associated with beneficial effects and neuronal survival (Sugioka *et al.*, 2004; Neuspiel *et al.*, 2005; Chen *et al.*, 2007; Van der Bliek *et al.*, 2013). The most direct evidence of the key role of mitochondrial fusion in neuronal homeostasis relies on the fact that mutations in *MFN2* and *OPA1* genes lead to defective mitochondrial fusion and cause neurological disorders, such as Charcot-Marie-Tooth disease type 2A (Züchner *et al.*, 2004) and dominant optic

atrophy (Delettre *et al.*, 2000), respectively. Moreover, loss of MFN2 results in progressive, retrograde degeneration of dopaminergic neurons in the nigrostriatal circuit in mice (Pham *et al.*, 2012), while overexpressing OPA1 confers neuroprotection in the MPTP mouse model of PD (Ramonet *et al.*, 2013). On the other hand, mitochondrial fission implicates the mobilization of the cytosolic dynamin related protein 1 (DRP1) protein to the OMM, where it polymerizes into ring-like assemblies and constricts the membranes through GTP hydrolysis in order to facilitate mitochondrial division. Mitochondrial fission takes place to facilitate mitochondria transport through neuronal projections, or when damaged mitochondria have to be removed from a healthy network by mitophagy. However, increased mitochondrial fission has been widely associated to high levels of stress, such as those induced by neurotoxins damage (Van der Bliek *et al.*, 2013), and to participate in apoptosis (Frank *et al.*, 2001; Meuer *et al.*, 2007). In line with this, MPP^+ and 6-OHDA neurotoxins induce mitochondrial fragmentation (Gomez-Lazaro *et al.*, 2008; Chuang *et al.*, 2016), while inhibition of Drp1 prevents neuronal death (Filichia *et al.*, 2016). Therefore, enhancing mitochondrial fusion and/or decrease mitochondrial fission could be likely beneficial for PD.

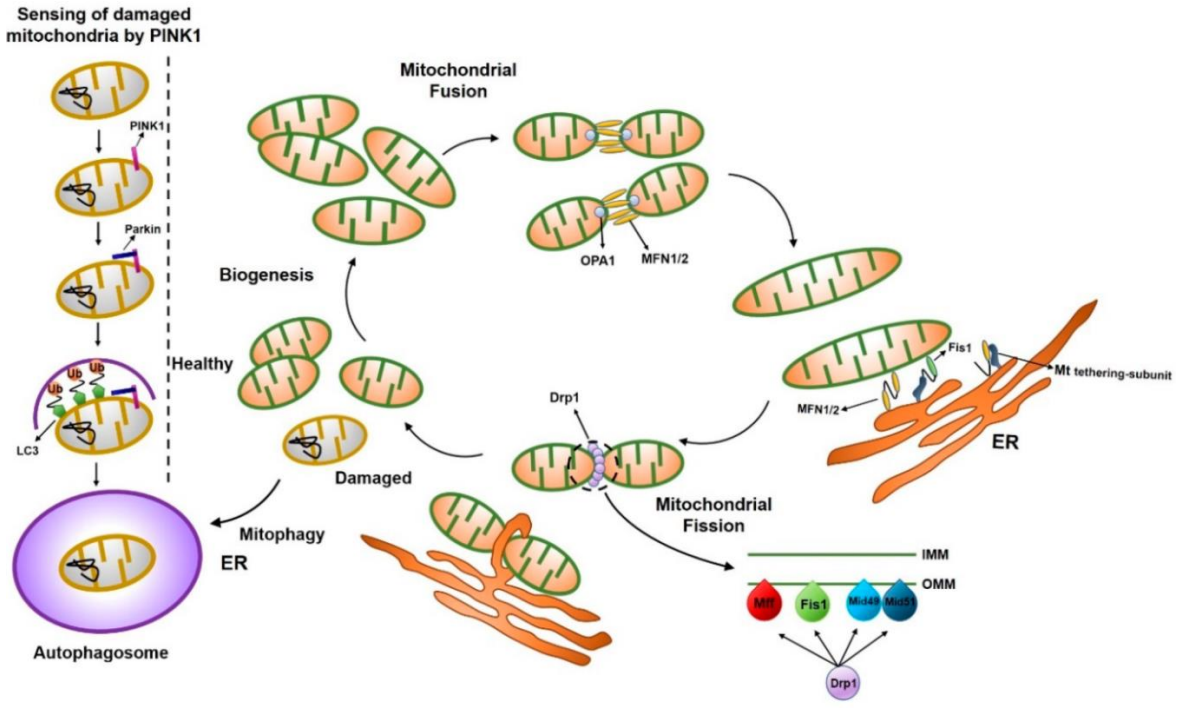

Figure 9. Representation of mitochondrial dynamics. Mitochondria are constantly undergoing fusion and fission processes in order to preserve a suitable mitochondrial homeostasis. Mitochondrial

fusion, mediated by MFN1, MFN2 and OPA1, improves mitochondrial network and occurs more often in cells that rely on OXPHOS to produce ATP, such as neurons. In contrast, mitochondrial fission is mediated by the recruitment of DRP1 to the OMM by multiple proteins including mitochondrial fission protein 1 (FIS1), mitochondrial fission factor (MFF), mitochondrial dynamics proteins of 49 (MID49) and 51 kDa (MID51). It is important to point out that endoplasmic reticulum plays an important role in mitochondrial fission by mediating constriction and defining division sites prior to DRP1 recruitment. Mitochondrial fission isolates damaged and/or dysfunctional mitochondria to be removed mainly by PINK1/Parkin mitophagy. From Seo *et al.*, 2018 *Int. J. Mol. Sci.*

1.1.5.3.4. Mitochondria and calcium homeostasis

Besides endoplasmic reticulum (ER) participates in mitochondria fission, this organelle and mitochondria also participate in calcium (Ca^{2+}) homeostasis, which has been implicated in PD pathogenesis (Perier and Vila, 2012). It is well stablished that adult dopaminergic neurons are Ca^{2+}-dependent pacemakers, a process driven by L-type Ca^{2+} channels (Chan *et al.*, 2007). Therefore, neurons must cope with high cytosolic Ca^{2+} load, although it is highly neurotoxic. For this reason, Ca^{2+} has to be buffered in intracellular components including mitochondria and ER. However, excessive cytosolic Ca^{2+} burden can propagate to the mitochondria and induce mitochondrial dysfunction by ensuing mitochondrial membrane permeabilization, triggering programmed cell death (Meredith and Rademacher, 2011; Perier and Vila, 2012). Importantly, neurotoxin-induced neurodegeneration can be attenuated by L-type Ca^{2+} channel antagonists like isradipine (Chan *et al.*, 2007), which is being tested in clinical trials, supporting a pathogenic role of Ca^{2+} in mediating mitochondria-mediated cell death in PD.

1.1.5.3.5. Mitochondria-mediated cell death

Cells have two distinct molecular pathways to trigger apoptotic cell death: the extrinsic/death receptor and the intrinsic/mitochondrial pathways. The extrinsic pathway involves the activation of cell-surface receptors termed “death receptors”, which belong to the tumor necrosis factor receptor superfamily (TNFRS), such as

tumor necrosis factor receptor 1 (TNFR1) or Fas/CD95 (Perier *et al.*, 2012). In contrast, the intrinsic pathway is activated by several cellular stressors, such as DNA damage, Ca^{2+} overload, ROS, and loss of trophic signaling (Perier *et al.*, 2012; Venderova and Park, 2012). Both pathways ultimately trigger the activation of the executioner caspase-3 that leads to apoptosis. While apoptosis is known to be a physiological process that occurs in normal cells, it can lead to neurodegeneration when it is over-activated (Vila and Przedborski, 2003). In PD, the intrinsic pathway is believed to play a greater role in triggering programmed cell death than the extrinsic pathway (Venderova and Park, 2012).

Mitochondria are important decoding stations of the apoptotic process, as they contain many molecules in the IMS like cytochrome c, which when released into the cytosol, binds to apoptotic protease-activating factor-1 (APAF-1) and forms an oligomerized structure called apoptosome. The apoptosome induces apoptotic cell death by the recruitment and activation of caspase-9, which, in turn, activates caspase-3 (Jiang and Wang, 2000). The release of these apoptotic molecules located in the IMS is mediated by mitochondrial outer membrane permeabilization (MOMP), which is considered the point-of-no-return in the intrinsic apoptotic pathway (**Figure 10**). MOMP and thereby apoptosis are governed by different proteins that belong to the Bcl-2 family, which is divided into three groups depending on their role: (i) anti-apoptotic proteins that prevent MOMP, such as B-cell lymphoma-extra large (BCL-XL) and B-cell lymphoma 2 (BCL-2); (ii) pro-apoptotic proteins that promote MOMP by a pore-form activity, such as Bcl-2-associated X (BAX) and Bcl-2 homologous antagonist killer (BAK); and (iii) BH3-only proteins that are mainly up-regulated by JNK signaling (Donovan *et al.*, 2002; Lei and Davis, 2003; Lu and Xu, 2006), such as Bcl-2-interacting mediator of cell death (BIM), BH3-interacting domain (BID) and Bcl-2-associated death promoter (BAD), which induce apoptosis by activating pro-apoptotic proteins (e.g. BAX) or by inactivating anti-apoptotic proteins (e.g. BCL-XL) (Perier *et al.*, 2012; Kale *et al.*, 2018).

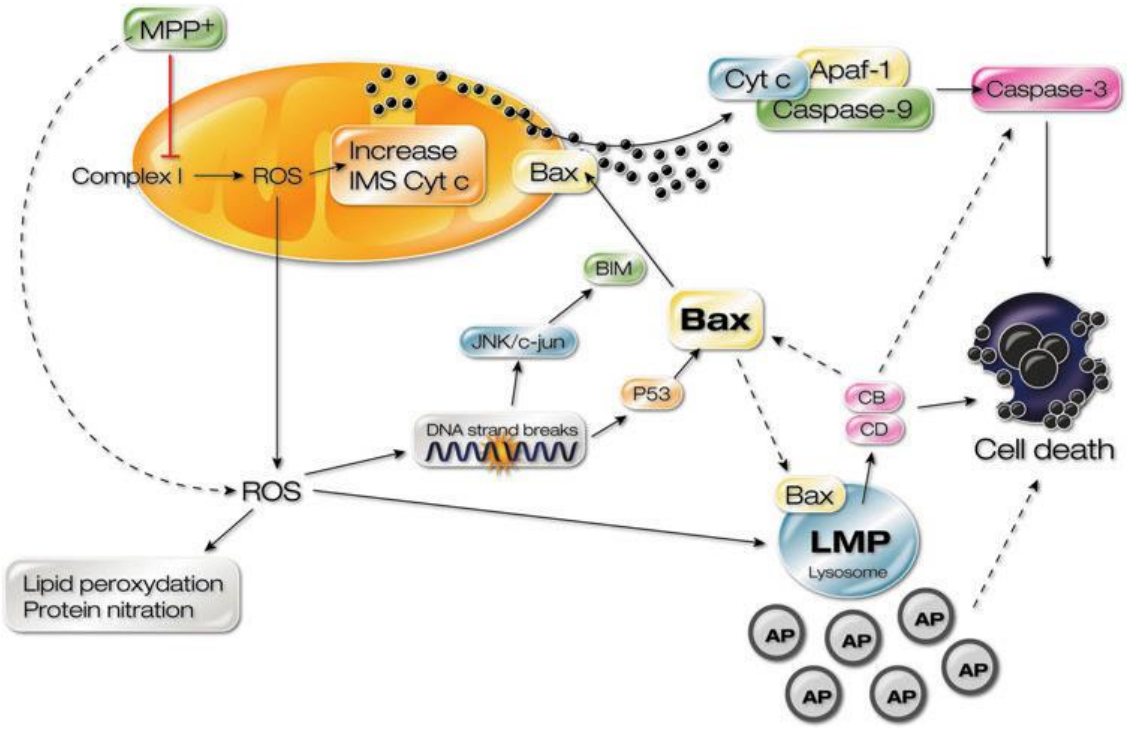

Figure 10. Pathogenic mechanisms of programmed cell death. Inhibition of complex I increases ROS production in both cytoplasm and mitochondria, leading to an activation of the JNK pathway and an increase of the releasable pool of cytochrome c in the IMS, respectively. Both activation of BAX by p53 and BAX translocation into the mitochondria outer membrane by BIM, induce MOMP and the release of cytochrome c into the cytosol, which, in turn, triggers the activation of caspase-9 and, consequently, the activation of the executioner caspase-3**.** The LMP and the ectopic release of lysosomal proteases induced by BAX translocation into the lysosomes cause, together with activated caspase-3, neuronal cell death. From Perier *et al.*, 2012 *Antioxid. Redox. Signal.*

It is believed that other proteins located in the OMM, such as voltage-dependent anion channel 1 (VDAC1), could also promote the cytochrome c release and therefore playing an important role in mediating mitochondria-mediated cell death (Shimizu *et al.*, 1999; Zaid *et al.*, 2005; Abu-Hamad *et al.*, 2008; Weisthal *et al.*, 2014). However, there is some controversy and the precise role of VDAC1 in mediating apoptosis is still debated (McCommis and Baines, 2012).

Supporting the role of apoptosis in PD, increased activated caspase-9 (Viswanath *et al.*, 2001; Kawamoto *et al.*, 2014) and caspase-3 (Tatton, 2000) have been observed in SNpc dopaminergic neurons. In this line, higher levels of BAX (Tatton, 2000) and cytochrome c (Kawamoto *et al.*, 2014) have also been documented. Moreover, levels

of p53 protein, which is known to be involved in apoptosis by activating BAX, are increased in PD brains (Sunico *et al.*, 2013). However, most of the insights regarding the mechanistic role of apoptosis in PD come from experimental models. In this line, dopaminergic neurodegeneration in the MPTP model occur by activation of apoptotic pathways (Vila and Przedborski, 2003; Perier *et al.*, 2012) through the cytochrome c release followed by activation of caspase-9 and caspase-3 (Perier *et al.*, 2005). BAX seems to play an important role in dopaminergic neurodegeneration, since when activated is translocated to both the mitochondrial membrane and lysosomal membrane, inducing MOMP and lysosomal membrane permeabilization (LMP) with an ectopic release of lysosomal proteases, respectively, and thereby contributing to cell death (Perier *et al.*, 2005, 2007; Bové *et al.*, 2014). In contrast, MPTP-induced dopaminergic cell death was abolished by either genetic ablation of BAX (Vila *et al.*, 2001) or pharmacologically targeting both MOMP and LMP with BAX channel inhibitor (Bci), which is a compound capable of blocking the pore-forming activity of BAX in lipid membranes (Bové *et al.*, 2014). Moreover, deletion of p53 (Trimmer *et al.*, 1996; Biswas *et al.*, 2005), genetic ablation (Perier *et al.*, 2007) or knocking down (Liou *et al.*, 2005) BIM, inactivating caspase-9 (Viswanath *et al.*, 2001) or overexpressing the anti-apoptotic protein BCL-2 (Yang *et al.*, 1998; Vila *et al.*, 2001) and BCL-XL (Dietz *et al.*, 2008) have also been reported to confer neuroprotection in dopaminergic neurons from neurotoxic insults, such as MPTP.

1.1.5.4. α-synuclein pathology

For many years α-synuclein has been the backbone of PD pathogenesis. Since mutations in *SNCA* gene cause an unequivocally inherited form of PD (Lesage and Brice, 2009) and α-synuclein is the major component of LBs (Spillantini *et al.*, 1998), which is a neuropathological hallmark required for the diagnosis of PD, mounting strategies to elucidate its role in PD have been gathered. The normal function of α-synuclein is still not well understood, even though it is believed to interact with membrane phospholipids and to have a presynaptic role (Bendor *et al.*, 2013). In PD

patients, increased levels of pathological post-translational-modified forms S129-phosphorylated (Mahul-Mellier *et al.*, 2014) and nitrated (Giasson *et al.*, 2000) α-synuclein have been documented. Since transgenic α-synuclein animal models only display subtle functional defects and no degeneration is observed (Fernagut and Chesselet, 2004), most of the insights of the mechanism of α-synuclein to contribute to neuronal death come from models that favor α-synuclein accumulation or oligomerization, as it happens in the disease.

Several studies in which they overexpress the WT or mutated α-synuclein have shown neurodegeneration (Kirik *et al.*, 2002; Decressac *et al.*, 2012a; Oliveras-Salvá *et al.*, 2013) probably due to α-synuclein is able to affect all these pathological events listed below that have been observed in numerous works: alteration of the ubiquitin-dependent degradation system and loss of DA release (Stefanis *et al.*, 2001), decreased proteasome activity (Tanaka *et al.*, 2001; Snyder *et al.*, 2003; Zondler *et al.*, 2017), mitochondrial dysfunction and increased endoplasmic reticulum (ER) stress (Smith *et al.*, 2005), increased sensitivity to mitochondria-mediated cell death (Tanaka *et al.*, 2001) and suppression of autophagy (Pupyshev *et al.*, 2018). Moreover, some studies have added another piece of the puzzle stating that α-synuclein could exert a cell-to-cell transmission (Emmanouilidou *et al.*, 2010; Recasens and Dehay, 2014; Rey *et al.*, 2016; Minakaki *et al.*, 2018) and a prion-like mechanism in which toxic forms of α-synuclein trigger the pathological conversion of endogenous α-synuclein (Recasens *et al.*, 2014). These features could, in fact, explain the progression of Braak stages as disease progresses (Braak *et al.*, 2003).

Since all these pathological events commented above have been demonstrated to contribute to PD pathogenesis, increased interest in lowering α-synuclein levels emerged as a potential therapeutic approach for PD. In this regard, a selective α-synuclein knock down in monoamine neurons by intranasal oligonucleotide delivery conjugated with indatraline was shown to increase DA neurotransmission in mice (Alarcón-Arís *et al.*, 2018). Besides, knocking down α-synuclein by means of a short

hairpin RNA (shRNA) prevented the PD-related neurodegeneration and improved behavioral deficits in rats (Tai *et al.*, 2014; Zharikov *et al.*, 2015).

1.1.5.5. Protein handling dysfunction

Maintaining the continuous turnover of proteins and organelles is crucial for the well-being of the cell. To deal with this, neurons, like other eukaryotic cells, evolved two major mechanisms: the ubiquitin-proteasome system (UPS) and the autophagy-lysosomal pathway (ALP) (Martinez-Vicente, 2015) (**Figure 11**).

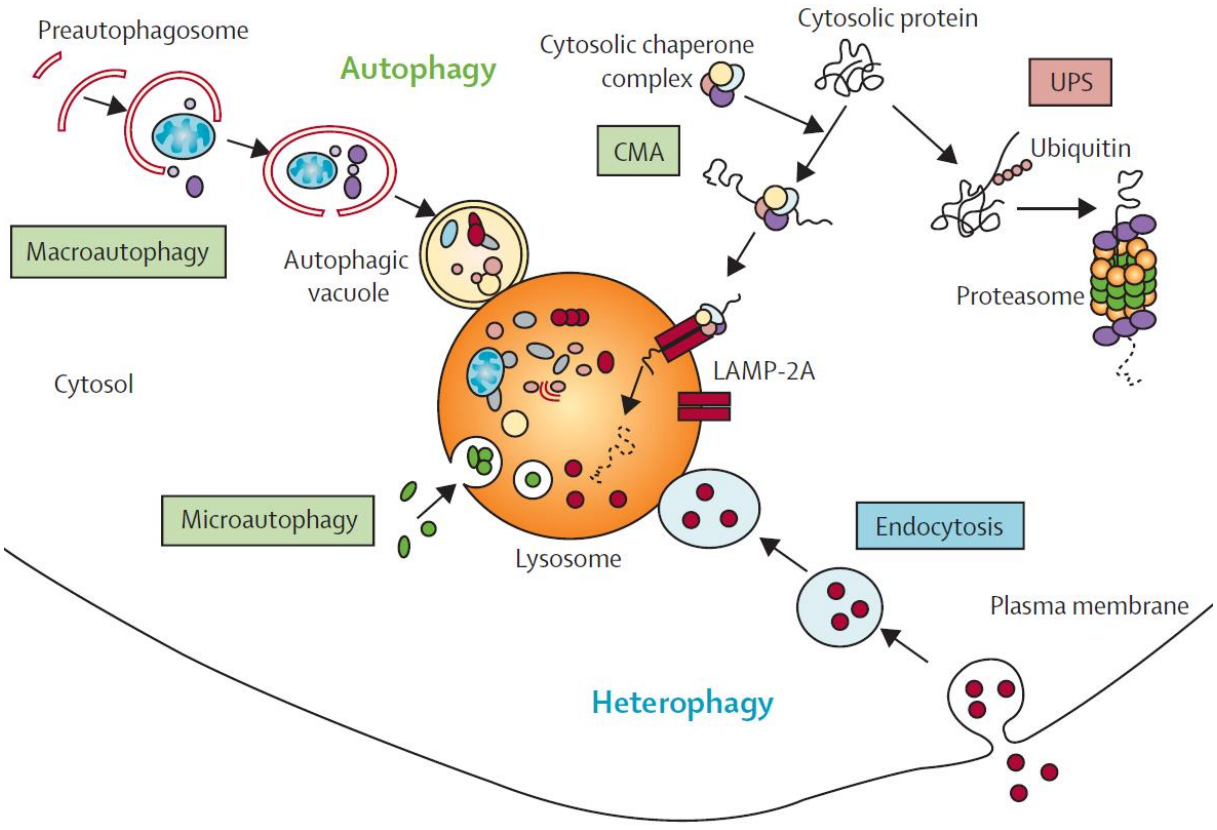

Figure 11. Mechanisms of protein and organelles degradation. The cell has two major mechanisms to keep the correct homeostasis of the cell: the UPS and the ALP. While UPS is a selective system based on the degradation of proteins tagged with a small protein (ubiquitin), the ALP involves the engulfment of cytosolic regions containing proteins and aggregates (in bulk) or organelles (selective), which are delivered to lysosomes for degradation. From Martinez-Vicente and Cuervo, 2007 *Lancet Neurol.*

1.1.5.5.1. Ubiquitin-proteasome system

The UPS is a highly regulated multi-catalytic enzymatic complex that covalently tags short-lived and misfolded proteins with a polymeric ubiquitin chain (Finley, 2009). This ligation requires the sequential actions of various enzymes including ubiquitin-activating enzymes (E1), ubiquitin-conjugating enzymes (E2) and ubiquitin-protein ligases (E3) (Lim and Tan, 2007). Since many proteins of the UPS are found in LBs (Wakabayashi *et al.*, 2007) and many different PD-associated genes, such as *PRKN* and *FBX07*, codify for proteins that are crucial for the proper UPS function, it boosted to the notion that UPS dysfunction may contribute to PD pathogenesis (Zhou and Tan, 2016). In this regard, UPS activity is decreased in the SNpc of PD patients (McNaught and Jenner, 2001) and some studies revealed that α-synuclein could bind to the proteasome and thereby contributing to UPS inhibition (Tanaka *et al.*, 2001; Snyder *et al.*, 2003; Zondler *et al.*, 2017) and triggering dopaminergic cell death (Stefanis *et al.*, 2001). In contrast, overexpression of several components of the UPS machinery, especially Parkin, have a general neuroprotective effect in various PD models (Petrucelli *et al.*, 2002; Yang *et al.*, 2003).

1.1.5.5.2. Autophagy-lysosomal pathway

Autophagy is a catabolic mechanism by which long-lived proteins, aggregates and even organelles are delivered to lysosomes for degradation. There are three types of autophagy to promote proteolytic degradation: macroautophagy, microautophagy and chaperone-mediated autophagy (CMA). Even though they differ in their regulation or the substrates targeted, they share the same endpoint, the lysosome, and that's why autophagy is also known as the autophagy-lysosomal pathway (ALP) (Martinez-Vicente and Cuervo, 2007). Macroautophagy is the most studied type of autophagy and thereby is frequently referred to simply as autophagy.

As commented previously, mTORC1 is the main negative regulator of autophagy by repressing ULK1, which is necessary for autophagy initiation (Ganley *et al.*, 2009;

Hosokawa *et al.*, 2009). Under starvation conditions and nutrients become limiting, mTORC1 is inactivated and thereby allows the recovery of ULK1 kinase activity triggering the translocation of the Vps34 complex, which is formed by Vps30/Atg6/Beclin 1, autophagy and Beclin 1 regulator 1 (AMBRA), Vps15, Vps34, and Atg14L, to the preautophagosomal structure (Ohashi *et al.*, 2019). Then, nucleation step starts after generating phosphatidylinositol 3-phosphate (PI3P) by Vps34 complex, which allows the autophagosome elongation via the conjugation of light chain 3 (LC3-I) protein with phosphatidylethanolamine (PE) to form LC3-II (He and Klionsky, 2009; Mizushima *et al.*, 2011). Then, the cargo (e.g. proteins and organelles) is engulfed with a double-membrane vesicle known as autophagosome (AP), which is then fused with lysosomes. Lysosomes contain structural proteins, such as lysosomal-associated membrane protein 1 (LAMP1) and 2A (LAMP2A), and numerous types of acid hydrolases like proteases (e.g. cathepsins (CTS)), nuclease and lipases, which allow the degradation of the cargo internalized therein (Martinez-Vicente, 2015) (**Figure 12**).

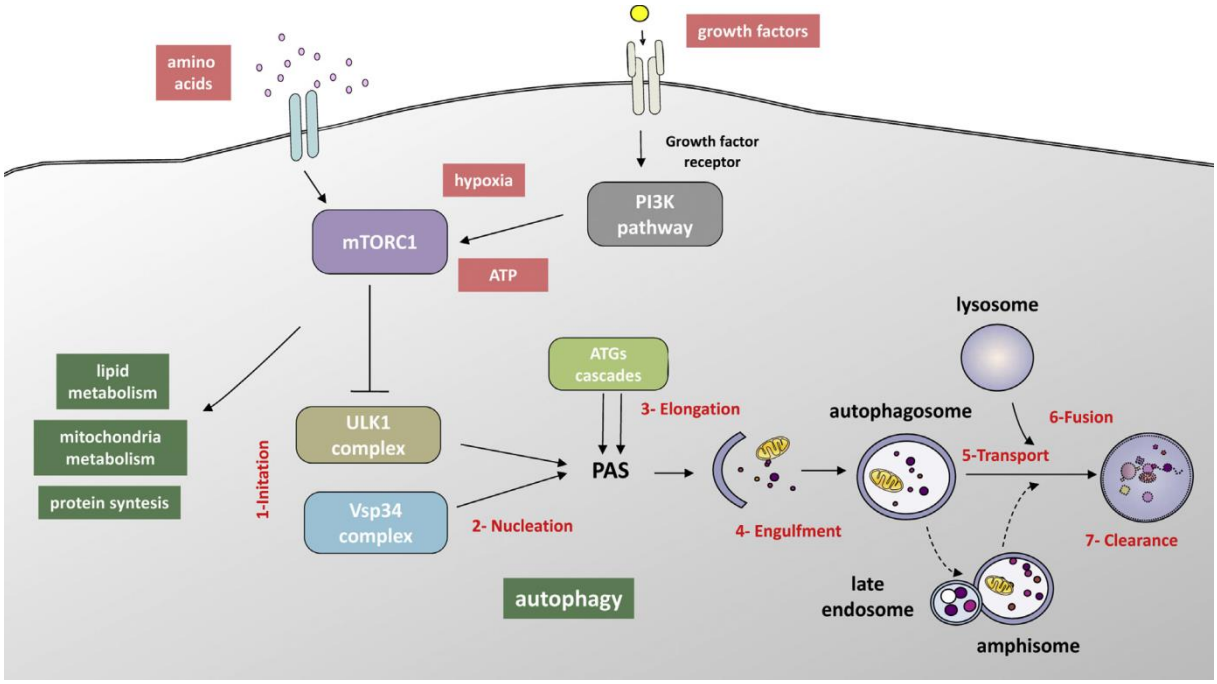

Figure 12. Autophagy regulation steps. In fed conditions, mTORC1 acts as a negative regulator of autophagy by inactivating ULK1 kinase activity. Upon starvation, the inactivation of mTORC1 leads to the activation of ULK1, which allows the formation of the preautophagosome structure in cooperation with Vps34 complex. Then, the lipidation of LC3-I to LC3-II lets the formation of the autophagosome that engulf the proteins or organelles to be delivered to the lysosome, where they are degraded. From Martinez-Vicente, 2015 *Semin. Cell. Dev. Biol.*

Autophagy plays a crucial role in neuronal homeostasis, since neurons need a constant autophagic flux to prevent the accumulation of debris, misfolded proteins and damaged organelles (Martinez-Vicente and Vila, 2013). The contribution of impaired autophagy to the PD pathology is evident considering that in PD there is an accumulation of misfolded proteins and the existence of LBs, which are especially rich for α-synuclein. As commented above, α-synuclein has been described to suppress UPS but it can also impair autophagy by multiple mechanisms including: inhibition of Rab1 (Winslow *et al.*, 2010), a small GTPase important for membrane tethering and autophagosome formation via Atg9; inhibition of high-mobility group box 1 (HMGB1) (Wang *et al.*, 2016a), which is important for Beclin 1 regulation; excessive binding to LAMP2A and thus collapsing CMA (Cuervo *et al.*, 2004); and alteration of mitophagy through PINK1-Parkin deficiency (Chen *et al.*, 2015). Moreover, in dopaminergic neurons of PD patients there is a pathogenic lysosomal depletion, as indicated by decreased levels of LAMP1 (Chu *et al.*, 2009; Dehay *et al.*, 2010), LAMP2A (Alvarez-Erviti *et al.*, 2010), GCase (Gegg *et al.*, 2012), CTSD (Chu *et al.*, 2009) and ATP13A2 (Dehay *et al.*, 2012) protein levels. This lysosomal depletion induces a subsequent accumulation of undegraded autophagosomes in PD brains due to defective clearance, contributing to autophagy impairment (Dehay *et al.*, 2010). Recently, we have also demonstrated that the continuous accumulation of NM within dopaminergic neurons exhausts the autophagic capacity of the cell, leading to neuronal dysfunction and degeneration (Carballo-Carbajal *et al.*, 2019). Furthermore, post-mortem studies in PD patients demonstrated decreased levels of LIM homeobox transcription factor 1 beta (LMX1B) (Laguna *et al.*, 2015) and transcription factor EB (TFEB) (Decressac *et al.*, 2013), which are both enhancers of the ALP (Sardiello *et al.*, 2009; Settembre *et al.*, 2011; Laguna *et al.*, 2015), in the SNpc dopaminergic neurons. In contrast, promoting the ALP by either genetic overexpression of autophagy proteins such as Atg5 (Hu *et al.*, 2017), or pharmacologically using rapamycin (Dehay *et al.*, 2010), which is a well-known inhibitor of some mTORC1 actions (Thoreen *et al.*, 2009), partially attenuated dopaminergic degeneration. In this line, overexpression of TFEB was also shown to counteract dopaminergic degeneration both *in vitro* (Dehay *et al.*, 2010) and *in vivo*

(Decressac *et al.*, 2013; Carballo-Carbajal *et al.*, 2019) PD models by increasing the ALP and lysosomal exocytosis.

1.1.5.5.3. Unfolded protein response and ER stress

Besides the UPS and the ALP, cells also have another different mechanism to tackle aberrant protein load, named unfolded protein response (UPR) (Bravo *et al.*, 2013). Misfolded and unfolded proteins are detected by transmembrane receptors located in the ER and thus result in ER stress, which is known to contribute to PD pathogenesis (Selvaraj *et al.*, 2012). ER stress activates the UPR, which, in turn, activates three mechanisms to restore normal protein homeostasis: (i) inhibition of protein translation through phosphorylation and activation of PRKR-like ER kinase (PERK) in order to decrease the amount of new proteins entering to the ER that would need to be folded; (ii) activation of activating transcription factor 6 (ATF6) that boosts the transcription of genes involved in protein folding, such as chaperones; and (iii) transport of misfolded proteins into the cytoplasm to be degraded for the UPS (Ron and Walter, 2007). In PD patients, activation of the UPR has been detected as determined by increased levels of phosphorylated/activated PERK (Hoozemans *et al.*, 2007). Moreover, some markers of ER stress and UPR activation have also been demonstrated in PD-derived neurons (Chung *et al.*, 2013) and in several PD models (Holtz and O'Malley, 2003; Silva *et al.*, 2005; Bellucci *et al.*, 2011), while restoring UPR activity to normal levels conferred neuroprotection (Smith *et al.*, 2005).

1.1.5.6. Non-cell-autonomous mechanisms dysregulation

Besides the intrinsic mechanisms of the neuron, mounting evidence point out that other non-cell-autonomous mechanisms could play a role in PD pathogenesis. It is well stablished that threatened neurons can induce an immune response mediated by other cells, being glia the most studied so far (Xing and Lo, 2017). In this scenario,

PD patients have an increased number of astroglial and microglial cells in the SNpc (Lastres-Becker *et al.*, 2012), as well as alterations in a wide number of inflammatory cytokines (Hunot and Hirsch, 2003). These changes are consistent with those seen in PD models (Yasuda *et al.*, 2008; Huang *et al.*, 2017). However, the exact role of astroglia and microglia when activated and their involvement in PD remains controversial. While activated microglia has been strongly suggested to participate in neuronal cell death in different neurotoxic-based PD models (Liberatore *et al.*, 1999; Pabon *et al.*, 2011), the role of activated astroglia is still debated since both protective (Saura *et al.*, 2003) and pathogenic (Pil Yun *et al.*, 2018b) roles have been proposed, probably due to its different reactive states (Liddelow and Barres, 2017).

Furthermore, although the brain has always been considered immune-privileged, some studies suggest that peripheral immune system may also be involved in PD pathogenesis (Hasegawa *et al.*, 2000; Mosley *et al.*, 2012). In this context, both $CD4^+$ and $CD8^+$ T cell lymphocytes have been observed to infiltrate into the SNpc of PD patients as well as in the MPTP mouse model (Brochard *et al.*, 2009), reinforcing the concept that immune system may play a significant role in PD pathogenesis.

1.2. Transcription factor EB

1.2.1. MiT/TFE family of transcription factors

The microphthalmia/transcription factor E (MiT/TFE) family is a physiologic regulator of proliferation, differentiation and survival in several non-nervous tissues, and is made up of four transcription factors: microphthalmia-associated transcription factor (MITF), transcription factor EB (TFEB), transcription factor EC (TFEC) and transcription factor E3 (TFE3) (Haq and Fisher, 2011). In invertebrates, however, only one ortholog form exists, named HLH-30 in *Caenorhabditis elegans* (Rehli *et al.*, 1999) and Mitf in *Drosophila melanogaster* (Hallsson *et al.*, 2004), and may explain the large degree of overlap between MiT/TFE transcription factors functions (Puertollano *et al.*, 2018). However, these transcription factors seem to have also specific roles, since MITF deficiency affects melanocyte viability (Haq and Fisher, 2011) and because only TFEB KO mice are embryonic lethal at E9.5-10.5 due to defective placental vascularization (Steingrímsson *et al.*, 1998).

MiT/TFE transcription factors share a common structure, which includes: (i) a basic region required for DNA contact and binding; (ii) a basic helix-loop-helix (bHLH) leucine zipper (ZIP) motif, which is important for their dimerization; (iii) and a transactivation domain (Steingrímsson *et al.*, 2004). These transcription factors bind the palindromic DNA sequence CANNTG, termed E-box, located in the proximal promoter of many genes to regulate their expression. While MITF, TFEB and TFE3 activate gene transcription, TFEC is believed to inhibit, rather than activate, gene transcription (Napolitano and Ballabio, 2016). Binding DNA can occur in the form of both homodimers and heterodimers with other members of the MiT/TFE family (Hemesath *et al.*, 1994), although their relevance to transcription remains unknown. E-box is also recognized by other transcription factors that also have the bHLH-ZIP motif, such as MYC, albeit they cannot heterodimerize with the MiT/TFE family of transcription factors probably due to the latter present a specific ZIP domain with a three-residue shift (Pogenberg *et al.*, 2012; Napolitano and Ballabio, 2016).

In 2009, however, a new role for the MiT/TFE transcription factors emerged after the discovery that TFEB was able to promote lysosomal biogenesis and autophagy by binding a palindromic E-box-like sequence (GTCACGTGAC), termed Coordinated Lysosomal Expression and Regulation (CLEAR) element (Sardiello *et al.*, 2009; Settembre *et al.*, 2011).

1.2.2. TFEB as a master regulator of lysosomal biogenesis and autophagy

The autophagy-lysosomal pathway needs to be finely tuned at transcriptional level in order to adapt the cell to different physiological conditions. In this regard, TFEB is considered the master transcriptional enhancer of both lysosomal biogenesis and autophagy by promoting the transcription of numerous lysosomal and autophagic genes that participate in multiple steps of autophagy from autophagosome initiation to degradation of the cargo into the lysosomes (Sardiello *et al.*, 2009; Settembre *et al.*, 2011). Additionally, TFEB has also been shown to induce lysosomal exocytosis, a process in which lysosomes are docked to the cellular membrane and directly empty their content to the extracellular space (Medina *et al.*, 2011). In contrast to TFEB, lysosomal biogenesis and autophagy are transcriptionally repressed by zing finger protein with KRAB and SCAN domains 3 (ZKSCAN3), which is considered the master repressor of the ALP (Chauhan *et al.*, 2013). Thus, TFEB and ZKSCAN3 are regulated in an opposite manner in order to orchestrate the ALP to different cellular responses.

1.2.2.1. Regulation of TFEB activity

Regulation of TFEB activity relies on its phosphorylation status and thereby subcellular localization. In this regard, under nutrient-rich conditions, TFEB remains phosphorylated and therefore inactive in the cytosol, whereas under several cellular stressors (e.g. starvation, infection, inflammation, ER stress or physical exercise),

TFEB is rapidly dephosphorylated and translocates to the nucleus to activate the ALP (Sardiello *et al.*, 2009; Settembre *et al.*, 2011; Martina *et al.*, 2014; Puertollano *et al.*, 2018). To date, TFEB has been shown to be phosphorylated at least at 20 different residues by several kinases including mTORC1, ERK2, AKT and glycogen synthase kinase 3 (GSK3), being most of them inhibitory phosphorylations that retain TFEB in the cytosol (Puertollano *et al.*, 2018) (**Figure 13**).

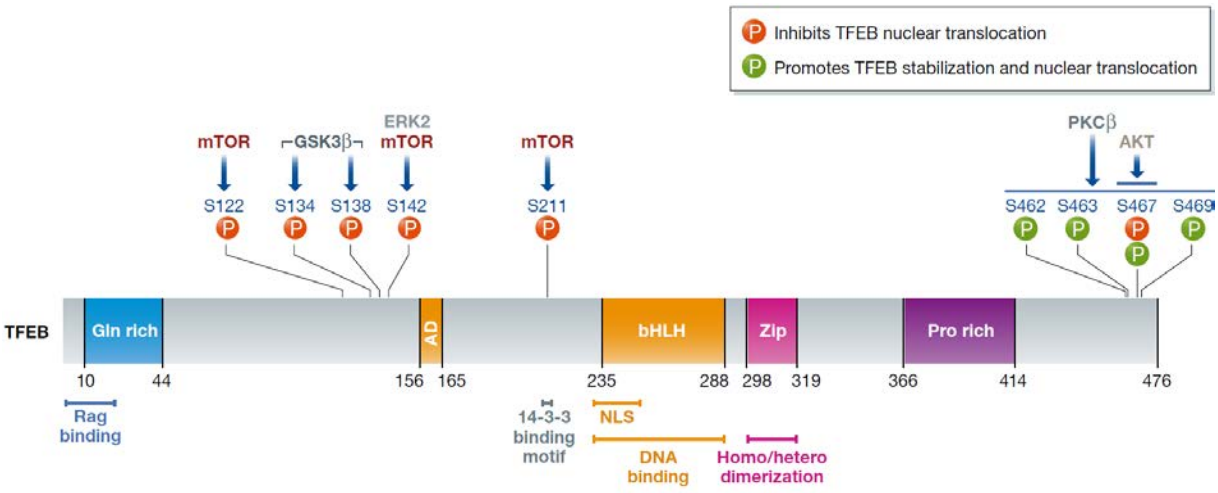

Figure 13. Most studied phosphorylation residues of TFEB. Numerous serine residues of TFEB protein have been described to be subject to phosphorylation. Although some of these phosphorylations could stabilize TFEB and promote its nuclear translocation, most of them are inhibitory phosphorylations that retain TFEB in the cytosol. From Puertollano *et al.*, 2018 *EMBO J.*

In fact, inhibition of either mTORC1 (Settembre *et al.*, 2012), ERK2 (Settembre *et al.*, 2011), AKT (Palmieri *et al.*, 2017) or GSK3 (Li *et al.*, 2016) are sufficient *per se* to induce TFEB activation by boosting its translocation into the nucleus. Among these kinases, mTORC1-mediated TFEB phosphorylation is the most studied by far (Martina *et al.*, 2012; Roczniak-Ferguson *et al.*, 2012; Settembre *et al.*, 2012). In this regard, phosphorylation of TFEB by mTORC1 is believed to take place in the lysosomal membrane (Settembre *et al.*, 2012), where both proteins are recruited by Ras-related GTP-binding (Rag) GTPases (Sancak *et al.*, 2010; Martina and Puertollano, 2013). Once TFEB is phosphorylated, it is sent back to the cytosol, triggering TFEB binding to 14-3-3 protein, which sequesters TFEB in the cytosol by

masking a nuclear localization signal (NLS) required for TFEB nuclear translocation (Martina *et al.*, 2012; Roczniak-Ferguson *et al.*, 2012) (**Figure 14**). Reinforcing the concept that interaction between mTORC1 and TFEB occurs at the lysosome membrane, a recent study has demonstrated that not only TFEB is phosphorylated by mTORC1 at the lysosomal surface but also that TFEB is actually a positive regulator of mTORC1 signaling under nutrient replenishment in the same place by promoting the transcriptional regulation of RagD GTPase, which is a direct target of TFEB (Di Malta *et al.*, 2017). Therefore, there is a feedback loop under fed conditions by which TFEB promotes mTORC1 signaling and this, in turn, decreases TFEB activity by phosphorylation (Di Malta and Ballabio, 2017). mTORC1-mediated phosphorylation of TFEB occur mainly at S122, S142 and S211, although only Ser-to-Ala mutations of the last two (S142A, S211A) result in a constitutive activation of TFEB, which is always nuclear translocated (Settembre *et al.*, 2012). Moreover, when TFEB is phosphorylated at S142 and S211, the chaperone-dependent E3 ubiquitin ligase STUB1 mediates TFEB degradation through the UPS (Sha *et al.*, 2017).

In contrast, when nutrients become limiting or under stress conditions, two events concomitantly occur in order to promote TFEB nuclear translocation. On the one hand, mTORC1 is inactivated by releasing from the lysosomal membrane (Sancak *et al.*, 2010). On the other hand, dephosphorylation and therefore activation of TFEB by calcineurin (CN) occurs after stress-induced lysosomal Ca^{2+} release through mucolipin 1 calcium channel (MCOLN1) (Medina *et al.*, 2015). Finally, upon nutrient refeeding, TFEB is exported to the cytosol by exportin 1/chromosomal maintenance 1 (CRM1) (Napolitano *et al.*, 2018), thereby creating a continuous TFEB shuttling between the cytosol and the nucleus that fine-tunes its activity upon nutrient availability.

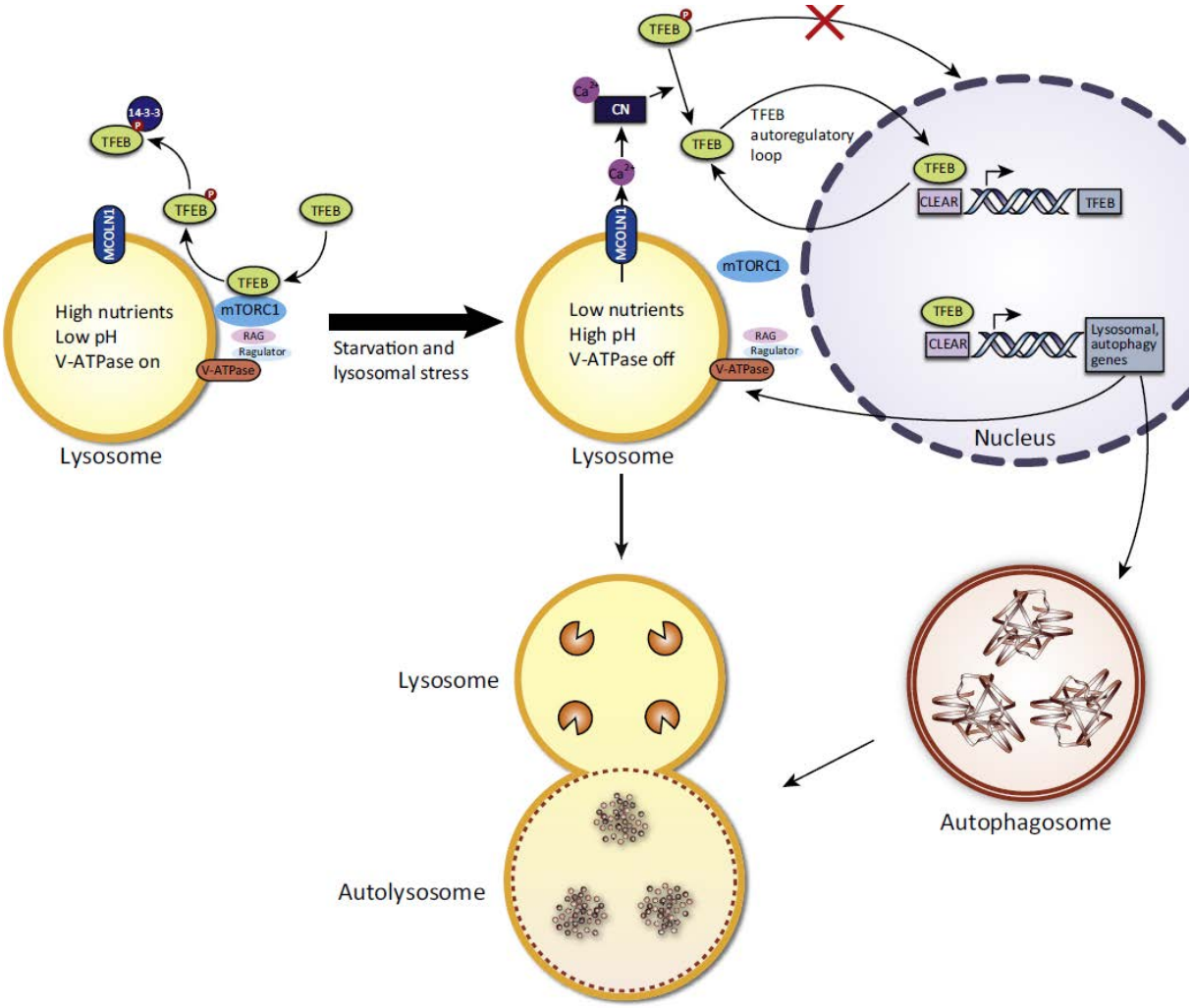

Figure 14. Regulation of TFEB activity. In normal conditions, mTORC1 is activated by a complex formed by V-ATPase, Rag GTPases and Ragulator. Once mTORC1 is activated, it phosphorylates TFEB and inhibits its nuclear translocation by promoting its binding to 14-3-3 protein. In contrast, under starvation or stressed conditions, the complex that activates mTORC1 is dissociated and thereby turned off, allowing calcineurin to dephosphorylate TFEB and permitting TFEB to be translocated into the nucleus, where it regulates numerous genes related to the ALP. From Martini-Stoica *et al.*, 2016 *Trends Neurosci.*

1.2.2.2. TFEB and ALP in neurodegenerative diseases

Increased levels of proteins related to the ALP and a subsequent enhancement of macroautophagy (Settembre *et al.*, 2011) and organelle-specific autophagy like mitophagy (Nezich *et al.*, 2015) and lipophagy (Settembre *et al.*, 2013), have been achieved after TFEB overexpression. Therefore, TFEB stands as a potential therapeutic target for those diseases in which lysosomal or autophagic dysfunction

have been documented, such as lysosomal storage disorders (LSDs) and neurodegenerative diseases. Regarding LSDs, such as Pompe disease or Batten disease, several studies have demonstrated the protective role of overexpressing TFEB by lowering substrate accumulation (Spampanato *et al.*, 2013; Rega *et al.*, 2016; Palmieri *et al.*, 2017).

In the neurodegenerative diseases research field, much interest and effort has been carried out to tackle neurodegeneration by enhancing TFEB activation as a therapeutic strategy. These studies have been summarized in **Table 2**. Importantly, histological examination of post-mortem tissue revealed a decreased TFEB activity in PD, as determined by decreased TFEB nuclear-positive SNpc dopaminergic neurons compared to healthy controls, indicating that TFEB dysfunction could play a central role in PD pathogenesis (Decressac *et al.*, 2013). Therefore, promoting TFEB activation may hold great promise for the development of disease-modifying strategies for PD.

Table 2. TFEB-based therapeutic approaches in neurodegenerative diseases experimental models

Neurodegenerative disease	Experimental model	References
Parkinson's disease	MPP^+ *in vitro*	Dehay *et al.*, 2010
	AAV-α-syn rat	Decressac *et al.*, 2013
	α-syn *in vitro*	Kilpatrick *et al.*, 2015
	AAV-hTyr rat	Carballo-Carbajal *et al.*, 2019
Alzheimer's disease	rTg4510 mouse	Polito *et al.*, 2014
	APP/PS1 mouse	Xiao *et al.*, 2014, 2015
	hTau (T231D/S235D) *in vitro*	Chauhan *et al.*, 2015
	5XFAD mouse	Chandra *et al.*, 2018, 2019
	TauP301L mouse TauP301S *in vitro* gmr-Gal4 > tau-2N4R *D. melanogaster*	Song *et al.*, 2019

	PS19 mouse	Martini-Stoica *et al.*, 2018
	TauP301S	Wang, *et al.*, 2016b
Huntington's disease	HD43 *in vitro*	Sardiello *et al.*, 2009
	N171-82Q mouse	Tsunemi *et al.*, 2012
	HDQ175/Q7 mouse	Vodicka *et al.*, 2016
Spinal and bulbar muscular atrophy	ARpolyQ	Rusmini *et al.*, 2019
Amyotrophic lateral sclerosis	TARDBP-25/TDP-25 *in vitro* $SOD1^{A4V}$ *in vitro* $SOD1^{G93A}$ *in vitro*	Rusmini *et al.*, 2019
	TDP-43 *in vitro*	Wang *et al.*, 2018
Cochlear degeneration	Kanamycin sulfate + furosemide, mouse	Ye *et al.*, 2019
Cerebral ischemia	pMCAO rat	Liu *et al.*, 2019
Juvenile neuronal ceroid lipofuscinosis	$Cln3^{\Delta ex7-8}$ mouse	Palmieri *et al.*, 2017

1.2.3. Targets and biological functions not related to the ALP regulated by TFEB

Although TFEB gained momentum since it was discovered that controls the ALP and that its activation might counteract lysosomal impairment and protein aggregation, the majority of putative direct targets of TFEB described to date is linked to a range of biological processes that are not related to the ALP (Palmieri *et al.*, 2011). In this line, only 64 out of 471 putative direct targets of TFEB are linked to this system, whereas hundreds of the other genes controlled by TFEB are linked to different biological processes, such as mitochondrial metabolism, cellular response to stress, regulation of gene expression, cell cycle and translation, among others (Palmieri *et al.*, 2011) (**Figure 15**).

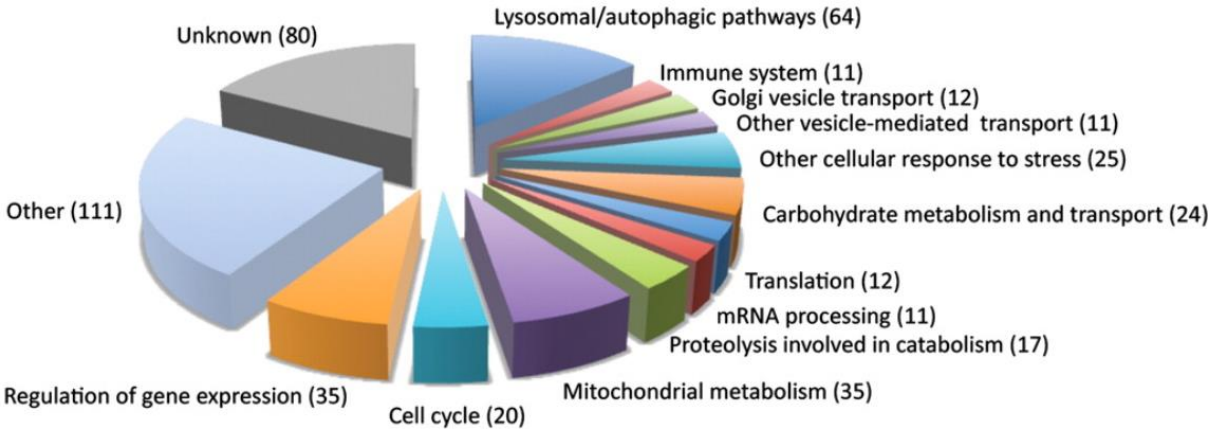

Figure 15. Biological processes of TFEB direct targets. Although some genes belong to the ALP, a considerable proportion of genes are associated with a variety of functions that are not connected to the ALP, such as mitochondrial or carbohydrate metabolism, mRNA processing, cell cycle or immune system. From Palmieri *et al.*, 2011 *Hum. Mol. Genet.*

Additional roles of TFEB were determined after the discovery that genetic ablation of TFEB caused a lethal defect in placental vascularization (Steingrímsson *et al.*, 1998). In fact, the MiT/TFE family has been long associated to tumorigenesis (Steingrímsson *et al.*, 2004; Haq and Fisher, 2011). In particular, chromosomal translocations or amplifications of *TFEB* gene have been linked to renal cell carcinoma and pancreatic ductal adenocarcinoma (Kauffman *et al.*, 2014; Durinck *et al.*, 2015; Perera *et al.*, 2015). In this context, TFEB-associated tumors display an induction of RagD GTPase and a subsequent mTORC1 hyperactivation (Di Malta *et al.*, 2017), suggesting that TFEB may have a key role in the proliferation and survival of dividing cells. Moreover, osteoclast differentiation and bone resorption seem to also depend on TFEB activity (Ferron *et al.*, 2013). Interestingly, TFEB was shown to control liver lipid metabolism via PGC-1α (Settembre *et al.*, 2013), as well as mitochondrial biogenesis in muscle (Mansueto *et al.*, 2017) and both maturation and antigen presentation by major histocompatibility complexes in dendritic cells (Samie and Cresswell, 2015).

All above commented unraveled that TFEB has several functions in different tissues. However, the contribution of these other pathways not related to the ALP to TFEB's

protective effect has been neglected in all the studies related to the neuroscience field and may account for its potential beneficial outcome. Therefore, to deepen our knowledge on TFEB function in neurons may be crucial to develop a potential therapeutic strategy for PD and other related neurological disorders.

HYPOTHESIS AND AIMS

2. Hypothesis and aims

The working hypothesis of this PhD thesis is that overexpressing TFEB in the dopaminergic neurons of the mouse substantia nigra will not only activate the autophagy-lysosomal pathway but also turn on other signaling pathways that can contribute in fighting neuronal cell death and dysfunction, which are characteristic of PD.

Hence, the main aim of this study is to deepen our knowledge of the different molecular mechanisms activated upon *in vivo* TFEB overexpression that may offer potential benefits in the context of PD. To this end, we established the following specific objectives:

1. To explore the effect of TFEB overexpression in mice SNpc dopaminergic neurons of several cellular pathways affected in PD including the autophagy-lysosomal pathway, dopamine metabolism, survival signaling pathways and mitochondria.
2. To determine the therapeutic potential of TFEB overexpression in an *in vivo* model of PD-related dopaminergic neurodegeneration.
3. To analyze the contribution of several molecular pathways in the neuroprotective and neurotrophic effects elicited by TFEB overexpression in an *in vivo* model of PD-related dopaminergic neurodegeneration.
4. To assess the actual neuroprotective extent of inducing lysosomal biogenesis and autophagy by knocking down ZKSCAN3 in an *in vivo* model of PD-related dopaminergic neurodegeneration.

MATERIALS AND METHODS

3. Materials and Methods

3.1. Animals

8-11 weeks old male C57BL/6Ncrl mice were used for all the experiments. Mice were housed under controlled conditions (22ºC ± 1°C; 12 hours light/dark cycle) with food and water available *ad libitum*. The acquisition, care, housing, use, and disposition of laboratory animals in this research procedure, have been in compliance with applicable Catalan (Decret 214/97) and Spanish (RD53/2013) laws and regulations, institutional policies, and with international conventions to which the European Union is a party. All the studies were approved by the Ethical Committee of Animal Experimentation of Vall d'Hebron Research Institute.

3.2. Stereotaxic delivery of adeno-associated viral vectors

For viral vector injections, mice were anesthetized using isoflurane (Baxter, Ref. PDG9623) and placed in a stereotactic apparatus. Mice were stereotaxically injected into the region immediately above right SNpc of 8-week-old C57BL/6Ncrl mice (coordinates in mm: -2.9 AP, 1.3 ML, and -4.5 DV from Bregma) with 1 µl of adeno-associated viral vector using the Neuros Hamilton system (Hamilton, 701 RN, Ref. 7635-01). Each injection was performed with a flow rate of 0,4 µl/min, with the needle being left in place for 4 minutes before withdrawal. Control mice received vehicle. An empty vector with noncoding stuffer DNA (AAV-EV) was also used.

AAV serotype 2/9 containing the murine *Tfeb* cDNA fused to 3 Flag epitopes under control of the cytomegalovirus (CMV) promoter was produced at TIGEM AAV Vector Core Facility (Italy), as previously described (Settembre *et al.*, 2011), and was used for the overexpression of TFEB in dopaminergic neurons of the SNpc. The titer of the AAV batch used in this study was 3×10^{12} gc/mL.

An AAV containing the sequence coding a short double-stranded hairpin RNA (shRNA) directed against rodent ZKSCAN3 has been used to knock down ZKSCAN3. To generate AAV vectors expressing shZKSCAN3, oligonucleotides containing 19 targeting nucleotides were synthesized. shZKSCAN3: 5'-AGCTTC CGGTCAGACTTGGAACTCTTTTCAAGAGAAAGAGTTCCAAGTCTGACCTTTTTGG AAG-3'. The shRNA was cloned downstream of the H1 RNA polymerase III promoter and the construct was cloned into a self-complementary pAAV2 backbone to generate pAAV2/9-shZKSCAN3. Recombinant AAV2/9 were produced by polyethylenimine (PEI) mediated triple transfection of low passage HEK-293T /17 cells (ATCC, Molsheim, France; cat number CRL-11268). The AAV expression plasmids (pAAV2-H1-shZKSCAN3-pA) was co-transfected with the adeno helper pAd Delta F6 plasmid (Penn Vector Core, Philadelphia, USA; Ref. PL-F-PVADF6) and AAV Rep Cap pAAV2/9 plasmid (Penn Vector Core, Philadelphia, USA; Ref. PL-T-PV008). AAV vectors were purified as previously described (Zolotukhin *et al.*, 1999). Cells were harvested 72h post-transfection, resuspended in lysis buffer (150 mM NaCl, 50 mM Tris-HCl pH 8.5) and lysed by 3 freeze-thaw cycles (37°C/-80°C). The cell lysate was treated with 150units/ml Benzonase (Sigma, St Louis, USA) for 1 hour at 37°C and the crude lysate was clarified by centrifugation. Vectors were purified by iodixanol step gradient centrifugation, and concentrated and buffer exchanged into Lactated Ringer's solution (Baxter, Deerfield, USA) using vivaspin20 100kDa cut off concentrator (Sartorius Stedim, Goettingen, Germany). Titrations were performed at the platform study of the transcriptome (Neurocentre Magendie, INSERM U862, Bordeaux, France). The genome-containing particle (gcp) titer was determined by quantitative real-time PCR using the Light Cycler 480 SYBR green master mix (Roche, Meylan, France; Ref. 04887352001) with primers specific for the AAV2 ITRs (fwd 5′-GGAACCCCTAGTGATGGAGTT-3′; rev 5′-CGGCCTCAGTGAGCGA-3′) (Aurnhammer *et al.*, 2012) on a Light Cycler 480 instrument. Purity assessment of vector stocks was estimated by loading 10 µl of vector stock on 10% SDS acrylamide gels, total proteins were visualized using the Krypton Infrared Protein Stain according to the manufacturer's instructions (Thermo Fisher Scientific, Waltham, USA). Finally,

the titer of the AAV batch used for the *in vivo* application in this study was 2.58 x 10^{13} gc/mL for AAV2/9-shZKSCAN3.

3.3. MPTP intoxication

An intraperitoneal injection of MPTP-HCl (30 mg/kg/day of free base; Sigma-Aldrich, Ref. M0896) was administrated for five consecutive days 4 weeks after the stereotaxic administration of AAV-TFEB, vehicle, AAV-EV or AAV-shZKSCAN3. Control mice received saline injections instead of MPTP. Mice were euthanized 1 or 21 days after the last MPTP or saline injection.

3.4. Immunofluorescence/Immunohistochemistry

Mice were deeply anesthetized with an intraperitoneal injection of 5% pentobarbital sodium (Dr Carreras, Ref. 39916) and perfused through the ascending aorta at 9 mL/min flow rate with physiological saline (0.9% NaCl, Fresenius Kabi, Ref. B314801) for 3 minutes followed by 4% ice-cold paraformaldehyde (PanReac ApplyChem, Ref. A3697.9010) diluted in 0.2 M phosphate buffer containing 0.15 M sodium phosphate dibasic (Sigma-Aldrich, Ref. S0876) and phosphate dibasic (Sigma-Aldrich, Ref. S9638) for 8 minutes. Brains were removed, post-fixed in 4% ice-cold paraformaldehyde for 24h at 4°C and crioprotected with 30% sucrose (Sigma-Aldrich, Ref. S9378) at 4°C for 48 hours. Brain were then frozen in 2-methylbutane (Sigma-Aldrich, Ref. M32631) and stored at -80°C until cut at a thickness of 30 µm in the coronal plane, recollecting the sections in 48-well plates with phosphate buffer 0.1 M + 0.01% sodium azide (Sigma-Aldrich, Ref. S8032).

Immunofluorescence. Immunofluorescence was performed on free-floating 30 um-thick midbrain sections. Sections were rinsed with PBS, blocked in 5% NGS and permeabilized with 0.3% Triton X-100 in PBS for 1 hour at RT, and incubated

overnight at 4°C with corresponding primary antibodies in 2% NGS and 0.3% Triton X-100 in PBS. After washing, sections were then incubated with secondary Alexa Fluor antibodies in 2% NGS and 0.3% Triton X-100 in PBS for 1 hour at RT. Sections were rinsed and the cell nuclei were stained with Hoechst 33342 (Thermo Fisher Scientific, Ref. H3570) at 1:2000 dilution in PBS for 10 minutes. Sections were washed and mounted onto Superfrost Ultra Plus slides using DakoCytomation Fluorescent medium (DAKO, Ref. S3023). Fluorescence was analyzed using an Olympus FV1000 confocal microscopy with FV 4.1 software (Olympus Corporation) or using an Olympus BX61 fluorescence microscope with CellSens software (Olympus Corporation).

Immunohistochemistry. Immunohistochemistry was performed on free-floating 30 µm-thick sections including the midbrain or the striatum. Sections were rinsed with TBS and quenched with 10% methanol (PanReac AppliChem, Ref. 131091.1212) and 3% H_2O_2 (Sigma-Aldrich, Ref. H1009) in TBS to inhibit endogenous peroxidases for 5 minutes at RT. Sections were then rinsed with TBS, blocked in 5% NGS (Vector Laboratories, Ref. S100) for 1 hour at RT, and incubated with the primary antibody in 2% NGS in TBS for 24-48 hours at 4°C. After washing, sections were incubated with the corresponding secondary antibody in 2% NGS in TBS for 1 hour at RT, followed by an incubation for 1 hour with the avidin-biotin-peroxidase complex Standard (Thermo Fisher Scientific, Ref. 32020) for midbrain sections or avidin-biotin-peroxidase complex Ultra-sensitive Plus (Thermo Fisher Scientific, Ref. 32050) for striatum sections. Finally, staining was visualized using 3,3-diaminobenzidine (DAB) as a chromogen, and sections were mounted onto Superfrost Ultra Plus slides (Thermo Fisher Scientific, Ref. J3800AMNZ) and air-dried overnight at RT. Slides were dehydrated by a consecutive incubation with 70% ethanol, 95% ethanol, 100% ethanol and xylene (Panreac, Ref. A2476), and mounted using DPX medium (Sigma-Aldrich, Ref. 06522).

For VMAT2 and DAT immunostainings, an additional previous step of antigen retrieval with 10 mM sodium citrate (Sigma-Aldrich, Ref. S1804) pH 6.0 was performed for 20 minutes in a 95°C pre-heated water bath.

3.5. Transduction efficiency

To assess rAAV-3xFlag-TFEB transduction efficiency, a double immunofluorescence of two coronal midbrain sections through the SN were immunostained with antibodies against TH and Flag to analyze TFEB expression of the nigral dopaminergic cells. Sections were visualized using an Olympus FSX100 with FSX-BSW software (Olympus Corporation), and photographs were taken with DP72 incorporated camera using a 4x objective. Photomontages were made from multiple 4x objective images using Adobe Photoshop CS6, and analyzed using a Cell Counter plugin on ImageJ 1.50i software. Different color channels were split, which allowed first to mark SNpc TH-positive cells, and then those that also expressed Flag. Data are expressed as percentage of DAergic neurons that coexpress exogenous TFEB (TH^+ $Flag^+$).

3.6. Quantitative morphology

Midbrain sections were immunostained against TH to assess different parameters of the SNpc and their dopaminergic neurons using a computerized stereology system (StereoInvestigator, MBF Bioscience, Williston, VT) and ImageJ 1.50i software (National Institutes of Health, USA). The researcher was blind to the experimental condition of the animal being studied.

SNpc volume. The volume of the SNpc, expressed in μm^3, was estimated on the basis of SNpc area obtained from contour measurements of every fourth section of the SNpc, yielding 12 sections per animal.

Neuronal cell body area. The mean area of dopaminergic neurons, expressed in μm^2, was measured with a stereological nucleator probe. Neurons randomly selected from four sections including the SNpc were measured for each animal. The size of counting frame was 50x50 µm spaced 175x100 µm.

Dendritic arborization. Neuronal branches were assessed by optical densitometry of transmitted-light microscopy images of TH–immunostained midbrain sections. Three sections per animal were analyzed using ImageJ 1.50i.

Intraneuronal TH optical density. The intracellular optical density of transmitted-light microscopy images of TH–positive neurons from four sections per animal was analyzed using ImageJ 1.50i. Neurons transversely cut were selected for the analysis. At least 40 neurons were analyzed in each animal.

Nigral dopaminergic neuron counts. A Nissl counterstaining with Cresyl Violet (Sigma-Aldrich, Ref. C5042) for 10 minutes prior to the dehydration step was performed on TH-immunostained midbrain sections. Assessment of the total number of TH/Nissl-positive neurons in the SNpc was made in both sides of every fourth section throughout the SN, yielding 12 sections per animal (**Figure 16**), using stereological quantification methods by employing the optical fractionator principle. SNpc was delineated by using a 4x objective, whereas the actual counting was performed using a 100x oil objective on a Zeiss ImagerD1 microscope. The size of counting frame was 50x50 µm spaced 125x100 µm. In MPTP experiments, the total number of neurons was estimated at 21 days after the last MPTP or saline injection.

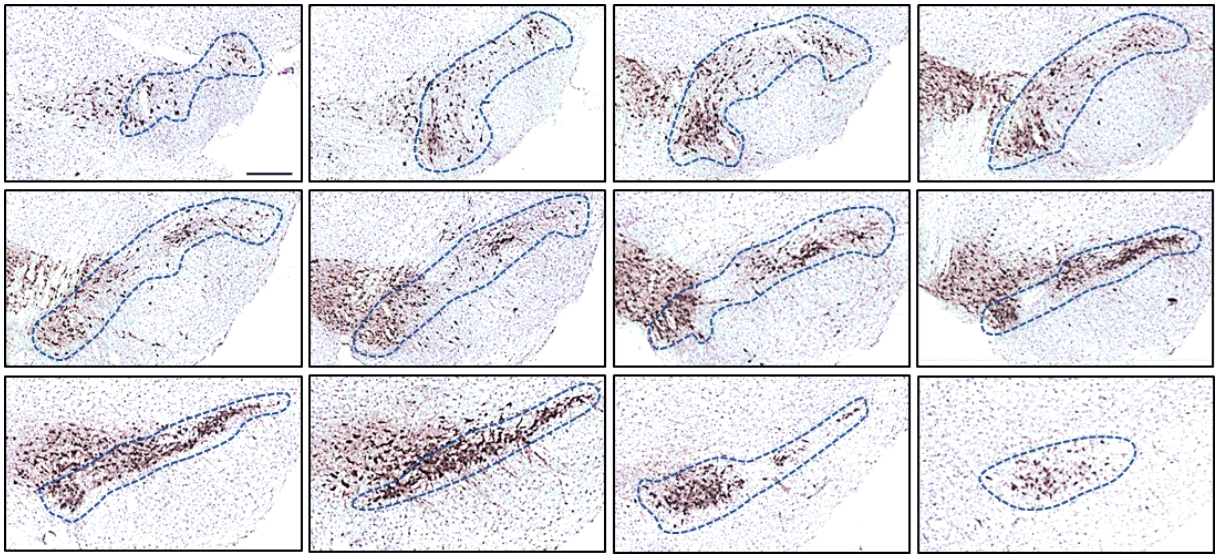

Figure 16. Coronal midbrain sections across the SNpc from caudal to rostral. For SNpc dopaminergic counts, a total of 12 sections throughout the SN with a fourth section interval were immunostained against TH. SNpc was delineated (dashed blue line) and counted by employing the optical fractionator principle. Scale bar = 300 µm

3.7. Optical densitometry analyses

The intraneuronal intensity of fluorescence or transmitted-light microscopy images of SNpc sections after TOM20, TIM23, ZKSCAN3, LAMP1, phospho-ERK1/2$^{Thr202/Tyr204}$ or phospho-AKT^{S473} immunostaining was analyzed using ImageJ 1.50i. Neurons transversely cut were selected for the analysis. For each staining condition quantified, a total of three sections were analyzed per animal, computing at least 60 neurons analyzed in each animal.

Striatal TH, VMAT2 and DAT-positive fiber density was assessed by optical densitometry (OD) at three-four coronal levels from each animal, covering the entire striatum (**Figure 17**). Slides were scanned with an Epson Perfection V750 PRO scanner and intensity was analyzed with SigmaScan Pro 5.0 software (Systate Software, Inc, USA). The measured striatal values (IStr) were corrected for non-specific background staining by subtracting values obtained from the corpus callosum (ICc). OD was assessed with the following formula:

$$OD = -log\left(\frac{IStr}{ICc}\right)$$

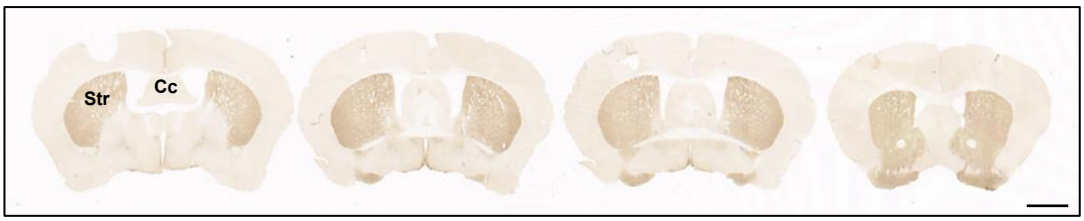

Figure 17. Coronal striatum sections from caudal to rostral. For striatal OD quantification, 4-regularly spaced 30 µm-thick sections were analyzed after TH immunohistochemistry. Cc, corpus callosum; Str, striatum. Scale bar = 500 µm

All quantifications were performed by an investigator blinded to the experimental groups.

3.8. *In vivo* microdialysis and HPLC measurements

Striatal homogenate levels of dopamine and metabolites, DOPAC and HVA, were measured by HPLC with electrochemical detection (Waters model 2465; +0.7V), as previously described (Bortolozzi and Artigas, 2003). Mice were euthanized and their brains were quickly removed and placed over a cold plate. Caudate putamen were carefully dissected out, weight, frozen on dry ice and kept at -80°C until assayed. The tissue were homogenized in 200 µl of buffer containing 0.4 M perchloric acid containing 0.1% sodium metabisulphite, 0.01% EDTA, 0.1% cysteine and centrifuged at 12000 g for 30 min. Aliquots of supernatants were then filtered through 0.45 µm filters (Millex, Barcelona, Spain) and analyzed by HPLC as described. The mobile phase consisted of 0.1 M KH2PO4, 1 mM octyl sodium sulphate, 0.1 mM EDTA (pH 2.65) and 18% methanol. DA and their metabolites were separated on a Mediterranea Sea (18, 3 µm, 10 cm x 6.4 mm) (Teknokroma, Ref. TR010042, Barcelona, Spain).

To assess local effects of D-amphetamine sulfate or veratridine on striatal DA release in microdialysis experiments, they were dissolved in artificial cerebrospinal fluid (aCSF: 125 mM NaCl, 2.5 mM KCl, 1.26 mM $CaCl_2$ and 1.18 mM $MgCl_2$) and administered by reverse dialysis at the stated concentration (uncorrected for membrane recovery).

Extracellular DA concentration was measured by *in vivo* microdialysis, as previously described (Díaz-Mataix *et al.*, 2005), at 5 weeks after AAV-TFEB or vehicle injections. In the MPTP experiments, microdialysis was performed at 21 days after the last MPTP or saline injection. Briefly, one concentric dialysis probe (Cuprophan membrane; 6000 Da molecular weight cut-off; 1.5 mm-long) was implanted in the right striatum (coordinates in mm: AP, 0.5; ML, -1.7; DV, -4.5) of pentobarbital-anaesthetized mice (40 mg/kg ip). Microdialysis experiments were performed 24-48h after surgery in freely moving mice. The aCSF was pumped (WPI model, SP220i) at 1.5 µl/min and 20-min samples were collected. Following an initial 100-min stabilization period, five or six baseline samples were collected (20 min each) before

local drug application by reverse dialysis and then successive dialysate samples were collected. The concentration of DA in dialysate samples was determined by HPLC with electrochemical detection (Hewlett Packard 1049, Palo Alto, CA, USA). Striatal dialysates were collected on microvials containing 5 µL of 10 mM perchloric acid and were rapidly injected into the HPLC. DA was detected at 5–7.5 min with a limit of detection of 3 fmol/sample using an oxidation potential of +0.75 V.

3.9. Western blot analyses

Mice ventral midbrains were dissected and stored at -80°C. Tissues were homogenized on ice in 1M Tris HCl (pH 7.5), 5 M NaCl, 0.5 M EDTA, 1% SDS, Nonidet P-40, protease inhibitors (Complete Mini; Roche Diagnostics, Ref. 11836153001) and protease/phosphatase inhibitors (Cell Signaling Technology®, Ref. 5872), performing 10-15 up-and-down strokes with a 18G syringe and then 10-15 up-and-down strokes with a 23G syringe. The suspension was centrifuged at 13000 rpm at 4°C for 30 min and the supernatant (protein) was quantified by the bicinchoninic assay method (Thermo Fisher Scientific, Reagent A Ref. 23228 and Reagent B Ref. 23224) with BSA (Thermo Fisher Scientific, Ref. 23209) as standard protein.

Proteins were then separated by sodium dodecyl sulfate polyacrylamide gel electrophoresis (SDS-PAGE) on different percentage of polyacrylamide gels, ranging from 6% to 15%, and run for 90-120 min at 105V in running buffer containing 25 mM Trizma Base (Sigma-Aldrich, Ref. T6066), 192 mM glycine (Sigma-Aldrich, Ref. G7126) and 1% SDS (Sigma-Aldrich, Ref. L3771). Protein All Blue Standards (BioRad, Ref. 161-0373) was used as a ladder. Resolved proteins were transferred to nitrocellulose membranes (GE Healtchare, Ref. 10600002) for 90 minutes at 200 mA per gel in transfer buffer containing 25 mM Trizma Base, 192 mM glycine and 20% methanol. Membranes were immediately blocked with 5% BSA (Sigma-Aldrich, Ref. A4503) for phospho-proteins or 5% non-fat milk powder (Sigma-Aldrich, Ref.

70166) for 1 hour and incubated with the corresponding primary antibody diluted in 4% BSA in TBS-T overnight at 4°C. Membranes were then rinsed three times with TBS-T for 5 minutes each and incubated with the corresponding secondary antibody coupled with horseradish peroxidase in 5% non-fat milk in TBS-T for 1 hour at RT. Finally, membranes were rinsed again three times with TBS-T for 10 minutes each and developed using West Pico SuperSignal (Thermo Fisher Scientific, Ref. 34080) or West Femto SuperSignal (Thermo Fisher Scientific, Ref. 34095) on an ImageQuant RT ECL Capture imaging system (GE Healthcare). Bands were quantified by densitometry using the 1D plugin on ImageQuant RT ECL Capture software. GAPDH and Tubulin were used as loading controls.

3.10. Isolation of midbrain mitochondria

10 midbrains from mice were pooled for each experimental group and homogenized in isolation buffer containing 225 mM mannitol (Sigma-Aldrich, Ref. M4125), 75 mM sucrose, 1 mM EGTA (Sigma-Aldrich, Ref. E4378), 5 mM HEPES (Sigma-Aldrich, Ref. H3375), and 2 mg/ml fat-free BSA (Sigma-Aldrich, Ref. A6003) using a Dounce homogenizer with eight up-and-down strokes on ice. The homogenate was centrifuged at 1000 g for 10 minutes at 4°C, and the resulting supernatant was layered onto 4 ml of 7.5% Ficoll on top of 4 ml of 10% Ficoll in Ficoll medium (0.3 M sucrose, 50 µM EGTA, and 10 mM HEPES) and centrifuged at 79000 g for 30 minutes at 4°C using a Sorvall WX Ultra 90 ultracentrifuge (Thermo Fisher Scientific). The pellet (nonsynaptosomal mitochondria) was gently washed with isolation buffer (–BSA), resuspended in 100 µl with the same buffer and quantified by the bicinchoninic assay method with BSA as a standard protein. Purity of mitochondria was checked by western blot.

For western blot experiments with isolated mitochondria, 50 µg were loaded and separated by SDS-PAGE as previously commented. HSP60 was used as a loading control.

3.11. RNA extraction and gene expression analysis by RT-qPCR

Total RNA from mouse tissue was extracted from injected ventral midbrains using RNeasy Lipid Tissue Mini Kit (Qiagen, Ref. 74804) according to the supplier's recommendations. RNA concentration was determined using the NanoDrop 1000 assay (Thermo Fisher Scientific) and RNA integrity was assessed by running the samples on an Agilent RNA 6000 Nano chip on an Agilent 2100 BioAnalyzer (Agilent Technologies). One microgram of RNA was used for reverse transcription with oligo(dT)12–18 primers (Invitrogen, Ref. 18418012) and SuperScript™ II reverse transcriptase (Invitrogen, Ref. 18064014). Quantitative real-time PCR was performed with 20 ng of cDNA, Taqman Gene Expression Master Mix with UNG (Applied Biosystems, Ref. 4440038) and Taqman gene expression assays (Applied Biosystems. **Table 3**) on an ABI PRISM 7900HT (Applied Biosystems). Fold change was calculated with the ΔΔCt-method using the software SDS version v2.4 (Applied Biosystems), RQ Manager v1.2.1 (Applied Biosystems) and DataAssist v3.01 (Applied Biosystems), and normalized to *Gapdh* and *Rpl19* gene expression.

Table 3. List of Taqman gene expression assays used

Gene	Reactivity	Taqman Ref.
Tfeb	Mouse	#Mm00448968_m1
Ppargc1a	Mouse	#Mm01208835_m1
Tfam	Mouse	#Mm00447485_m1
Lamp1	Mouse	#Mm00495262_m1
Ctsd	Mouse	#Mm00515586_m1
Rps6kb1	Mouse	#Mm01310033_m1
Eif4e	Mouse	#Mm00725633_s1
Bcl2l11	Mouse	#Mm00437796_m1
Gapdh	Mouse	#Mm99999915_g1
Rpl19	Mouse	#Mm02601633_g1

3.12. Mitochondrial DNA copy number measurements

Total DNA (genomic and mitochondrial) was isolated from right ventral midbrains using the QIAmp DNA Mini Kit (Qiagen, Ref. 51306) according to the supplier's recommendations. DNA was eluted in 200 µl of distilled water and quantified using the NanoDrop 1000 assay (Thermo Scientific). All samples were diluted at 8 ng/µl in 10 mM Tris HCl pH 8. To quantifiy mtDNA content, we analyzed relative mtDNA (*16S* rRNA gene and *ND4* gene) versus nuclear DNA (*ANG1* gene) copy number. The sequences for 16S primers used are: 5'-AATGGTTCGTTTGTTCAACGATT-3' (forward) and 5'-AGAAACCGACCTGGATTGCTC-3' (reverse), with a FAM-labeled probe sequence 5'-FAM-AAGTCCTACGTGATCTGAGTT-MGB-3'. The sequences for ND4 primers used are: 5'-TGCATCAATCATAATCCAAACTCCATGA-3' (forward) and 5'-GGCAGAATAGGAGTGATGATGTGA-3' (reverse), with a VIC-labeled probe sequence 5'-VIC-CCGACATCATTACCGGGTTTTCCTCTTG-TAMRA-3'. For ANG1 we used a commercial assay (Applied Biosystems, Ref. Mm00833184_s1).

Calibration curves were used for absolute quantification of mtDNA and nDNA copy number, which were based on the linear relationship between the crossing point cycle values and the logarithm of the starting copy number, as previously described (Andreu *et al.*, 2009). Quantitative real-time PCR was performed with 10 ng of DNA with Taqman Gene Expression Master Mix with UNG (Applied Biosystems, Ref. 4440038) on an ABI PRISM 7900HT. Data were analyzed using the software SDS v2.4 (Applied Biosystems), RQ Manager v1.2.1 (Applied Biosystems) and DataAssist v3.01 (Applied Biosystems).

3.13. Transmission electron microscopy analyses

Mice were perfused transcardially with 4% ice-cold paraformaldehyde and 0.1% glutaraldehyde (Merck Millipore, Ref. G5882). Brains were removed and post-fixed for 4 hours at 4°C in the same fixative, washed in ice-cold PBS and sectioned into 100 µm-thickness slices using a HM 650V vibratome (Thermo Fisher Scientific).

Free-floating sections were blocked in 10% NGS and 0.1% Triton X-100 in PBS for 1 hour at RT, and incubated with primary antibody against TH in 10% NGS in PBS overnight at 4°C. Sections were rinsed with 10% NGS in PBS for 1 hour at 4°C, incubated with a secondary goat anti-rabbit antibody conjugated to biotin for 1 hour at RT, and incubated with the avidin-biotin-peroxidase complex Standard. Finally, staining was visualized using DAB as a chromogen. The sections were post-fixed in 3% glutaraldehyde and in 1% osmium tetroxide in 0.1M cacodylate buffer (pH 7.4), dehydrated in ethanol, and embedded in Spurr's epoxy resin. Survey sections (2 µm) and ultrathin sections (70 nm) were cut with a diamond knife (Diatome) using an ultramicrotome Ultracut E (Reichert-Jung). Ultrathin sections were collected onto copper grids, counterstained with 2% uranyl acetate and led citrate, and visualized in a JEOL 1010 100kV (tungsten filament) transmission electron microscope. Images were acquired with an Orius CCD camera by using GATAN Digital Micrograph software.

TEM images were analyzed with ImageJ 1.50i to assess different mitochondrial parameters in both control (n = 2) and AAV-TFEB-injected (n = 2) mice:

Mitochondrial density. Mitochondrial density of a given neuron was computed as follows: (number of mitochondria)/(neuronal area). In control mice, a total of 12 TH-positive neurons were analyzed. In AAV-TFEB-injected mice, a total of 21 TH-positive neurons were analyzed.

Neuronal area occupied by mitochondria. The neuronal area that was occupied by mitochondria was computed as follows: (the sum of mitochondria areas)/(neuronal area). In control mice, a total of 12 TH-positive neurons were analyzed. In AAV-TFEB-injected mice, a total of 21 TH-positive neurons were analyzed.

Mitochondrial area. The mean area of mitochondria, expressed in μm^2, was measured by drawing a ROI to each mitochondrion. In control mice, a total of 569 mitochondria were analyzed. In AAV-TFEB-injected mice, a total of 1308 mitochondria were analyzed.

Mitochondria type. Mitochondria were binned into three different categories depending on their shape: rounded (class I), intermediate (class II) and elongated (class III). Data is represented as the mean of the percentage of each type of mitochondria in TH-positive neurons. In control mice, a total of 12 TH-positive neurons were analyzed. In AAV-TFEB-injected mice, a total of 19 TH-positive neurons were analyzed.

Mitochondrial Feret's diameter. Feret's diameter represents the longest distance, expressed in µm, between any two points within a given mitochondrion. In control mice, a total of 419 mitochondria were analyzed. In AAV-TFEB-injected mice, a total of 970 mitochondria were analyzed.

Mitochondrial aspect ratio (AR). AR, which reflects the length-to-width ratio of a given mitochondrion, was computed as follows: (major axis)/(minor axis). In control mice, a total of 419 mitochondria were analyzed. In AAV-TFEB-injected mice, a total of 970 mitochondria were analyzed.

3.14. Amphetamine-induced rotation test

Mice were placed in a cylinder in a closed room to avoid any environmental disturbance, and allowed to habituate for 1 hour. Then, mice were injected intraperitoneally with D-amphetamine (5 mg/kg; Tocris, Ref. 2813) and recorded for 60 min. Each subject was scored for full body rotations in 10 min intervals. The net contralateral rotations were obtained as follows: total left − total right 360° turns.

3.15. Cytochrome c release study

For cytochrome c release experiments, 200 µg of isolated brain mitochondria were incubated with 100 µM MPP^+ (Sigma-Aldrich, Ref. D048) and/or different amounts (100-150 nM) of recombinant Bax (Thermo Fisher Scientific, Ref. RP-800) for 1 hour

at 4°C. Incubation with Alamethicin (Alm, 40 µg/ml) from *Trichoderma viride* (Sigma-Aldrich, Ref. A5361) was used as a positive control of the maximal cytochrome c release. Mitochondria were then pelleted at 17000 g for 15 minutes and both the pellet and the supernatant were analyzed by western blot. The percentage of cytochrome c release was estimated by assessing the intensities of the immunoblot bands for the soluble fractions versus total fractions (soluble plus particulate). Mitochondrial protein HSP60 was used as a control of the experiment.

3.16. Antibodies

A complete list of the primary (**Table 4**) and secondary (**Table 5**) antibodies used in all experimental procedures is listed below.

Table 4. List of primary antibodies used

Protein	Host	Source	Reference	Dilution
TH	Rabbit polyclonal	Merck Millipore	657012	IHC: 1:2000-1:5000 IF: 1:1000 EM: 1:1000
TH	Mouse monoclonal	Merck Millipore	MAB5280	IF: 1:1000
Flag	Mouse monoclonal	Sigma-Aldrich	F3165	IF: 1:1000
LAMP1	Rabbit polyclonal	GeneTex	GTX19294	WB: 1:750 IF: 1:1000 IHC: 1:250
Cathepsin D	Goat polyclonal	Santa Cruz Biotechnology	sc-6494	WB: 1:1000
LC3	Rabbit polyclonal	Novus Biologicals	NB100-2220	WB: 1:750 IF: 1:1000

eIF4E	Rabbit monoclonal	Cell Signaling Technology	9742	WB: 1:1000
p4E-BP1^{S65}	Rabbit polyclonal	Cell Signaling Technology	9451	WB: 1:1000
p4E-BP1$^{T37/46}$	Rabbit monoclonal	Cell Signaling Technology	2855	WB: 1:1000
4E-BP1	Rabbit monoclonal	Cell Signaling Technology	9452	WB: 1:1000
non-p4E-BP1	Rabbit monoclonal	Cell Signaling Technology	4923	WB: 1:1000
S6K1^{T389}	Rabbit polyclonal	Cell Signaling Technology	9202	WB: 1:1000
pS6K1	Rabbit polyclonal	Cell Signaling Technology	9205	WB: 1:1000
pRPS6$^{S235/236}$	Rabbit monoclonal	Cell Signaling Technology	4857	IHC: 1:300
ERK1/2	Rabbit monoclonal	Cell Signaling Technology	4695	WB: 1:1000
pERK1/2$^{Thr202/Tyr204}$	Rabbit monoclonal	Cell Signaling Technology	4370	WB: 1:1000 IHC: 1:200
p-p90RSK$^{T359/S363}$	Rabbit polyclonal	Cell Signaling Technology	9344	WB: 1:1000
p90RSK	Rabbit polyclonal	Cell Signaling Technology	9347	WB: 1:500
pAKT^{S473}	Rabbit polyclonal	Cell Signaling Technology	9271	WB: 1:1000
pAKT^{S473}	Rabbit monoclonal	Cell Signaling Technology	4060	IHC: 1:200
AKT	Rabbit polyclonal	Cell Signaling Technology	9272	WB: 1:1000
NDRG1	Rabbit polyclonal	Cell Signaling Technology	5196	WB: 1:500
pNDRG1^{T346}	Rabbit polyclonal	Cell Signaling Technology	3217	WB: 1:1000
pTBK1^{S172}	Rabbit polyclonal	Merck Millipore	106835	WB: 1:1000

TBK1	Rabbit monoclonal	Cell Signaling Technology	3504	WB: 1:500
pCASP9^{T125}	Rabbit polyclonal	Novus Biologicals	NB100-92677	WB: 1:1000
p-eIF4E^{S209}	Rabbit monoclonal	Cell Signaling Technology	9741	WB: 1:1000
PGC-1α	Rabbit polyclonal	Abcam	ab54481	WB: 1:500
OXPHOS cocktail	Mouse monoclonal	Abcam	ab110411	WB: 1:1000
Complex IV	Mouse monoclonal	ThermoFisher Scientific	A21348	WB: 1:1000
TOM20	Mouse monoclonal	Abcam	ab56783	IF: 1:1000
TIM23	Mouse monoclonal	BD Biosciences	611222	IF: 1:1000 WB: 1:1000
OPA1	Mouse monoclonal	BD Biosciences	612606	WB: 1:1000
MFN1	Chicken polyclonal	Abcam	ab60939	WB: 1:500
MFN2	Rabbit polyclonal	Abcam	ab50838	WB: 1:500
BCL-XL	Rabbit monoclonal	Abcam	ab32370	WB: 1:1000
VDAC1	Rabbit polyclonal	Abcam	ab15895	WB: 1:2000
Cytochrome c	Mouse monoclonal	Zymed	33-8500	WB: 1:500
HSP60	Rabbit polyclonal	Abcam	ab46798	WB: 1:1000
ZKSCAN3	Rabbit polyclonal	Proteintech	20800-1-AP	IF: 1:50
DAT	Mouse monoclonal	Novus Biologicals	NBP2-22164	IHC: 1:500
VMAT2	Rabbit polyclonal	Novus Biologicals	NBP1-69750	WB: 1:2000

VMAT2	Guinea pig polyclonal	Progen	16085	IHC: 1:2000-1:3000
GAPDH	Mouse monoclonal	Merck Millipore	MAB374	WB: 1:3000
Tubulin	Mouse monoclonal	Sigma-Aldrich	T5168	WB: 1:5000
Tubulin	Rabbit monoclonal	Abcam	ab52866	WB: 1:5000

IHC: immunohistochemistry; IF: immunofluorescence; EM: electron microscopy; WB: western blot

Table 5. List of secondary antibodies used

Antibody	Host	Source	Reference	Dilution
Anti-mouse HRP	Sheep	GE Healthcare	NXA93IV	WB: 1:2000
Anti-rabbit HRP	Donkey	GE Healthcare	NA934V	WB: 1:2000
Anti-goat HRP	Donkey	Santa Cruz Biotechnology	sc-2020	WB: 1:2000
Anti-chicken HRP	Goat	Santa Cruz Biotechnology	sc-2428	WB: 1:2000
Anti-mouse biotinylated	Goat	Vector Laboratories	BA-9200	IHC: 1:1000
Anti-rabbit biotinylated	Goat	Vector Laboratories	BA-1000	IHC: 1:1000 EM: 1:500
Anti-guinea pig biotinylated	Goat	Santa Cruz Biotechnology	sc-2440	IHC: 1:1000
Alexa Fluor 488 anti-mouse	Goat	ThermoFisher Scientific	A11001	IF: 1:1000
Alexa Fluor 488 anti-rabbit	Goat	ThermoFisher Scientific	A11008	IF: 1:1000
Alexa Fluor 594 anti-mouse	Goat	ThermoFisher Scientific	A11005	IF: 1:1000
Alexa Fluor 594 anti-rabbit	Goat	ThermoFisher Scientific	A11012	IF: 1:1000

IHC: immunohistochemistry; IF: immunofluorescence; EM: electron microscopy; WB: western blot

3.17. Statistical analysis

All values are expressed as the mean ± standard error of the mean (SEM). Statistical comparisons were performed with GraphPad Prism software (v6, GraphPad Software Inc, USA) using the appropriate statistical tests, as indicated in each figure legend. Differences among means were analyzed by using Mann-Whitney test and 1- or 2-way analysis of variance (ANOVA), as appropriate. When ANOVA showed significant differences, pairwise comparisons between means were subjected to Tukey *post hoc* test. In all analyses, the null hypothesis was rejected at the 0.05 level.

RESULTS

4. Results

4.1. Overexpressed TFEB translocates to the nucleus of substantia nigra dopaminergic neurons and activates the autophagy-lysosomal pathway

Here we studied the effect of overexpressing TFEB by means of an adeno-associated viral vector (AAV-TFEB) in mice SNpc dopaminergic neurons. For such, 8-week-old C57BL/6Ncrl mice received a single unilateral stereotaxic inoculation of AAV-TFEB into the region immediately above right SNpc. After 5 weeks, animals were euthanized and their brains were processed for different analyses (**Figure 18A**).

We aimed to analyze TFEB overexpression levels by RT-qPCR, and we found that AAV-TFEB injection in mice ventral midbrain yielded a 17-fold increase of TFEB expression (**Figure 18B**). Accordingly, confocal immunofluorescence revealed that TFEB overexpression in dopaminergic neurons induced its translocation to the nucleus shown by a strong nuclear staining (**Figure 18C**). TFEB translocates to the nucleus to trigger the transcription of its target genes only when is activated, therefore its nuclear localization confirms that TFEB is activated (Napolitano and Ballabio, 2016). Next, to study the AAV-TFEB transduction efficiency, we determined the percentage of dopaminergic nigral cells that coexpressed exogenous TFEB (TH^+ $Flag^+$). Detailed confocal microscopy analyses displayed a good co-localization of TH and Flag resulting on high transduction efficiency whose values were uniformly distributed between ~60-70%, indicating that most of SNpc neurons overexpressed TFEB. Moreover, no changes on transduction efficiencies were observed between anterior (A) and posterior (P) SNpc sections, demonstrating that transgene expression remained homogenous along the anteroposterior axis (**Figure 18D**).

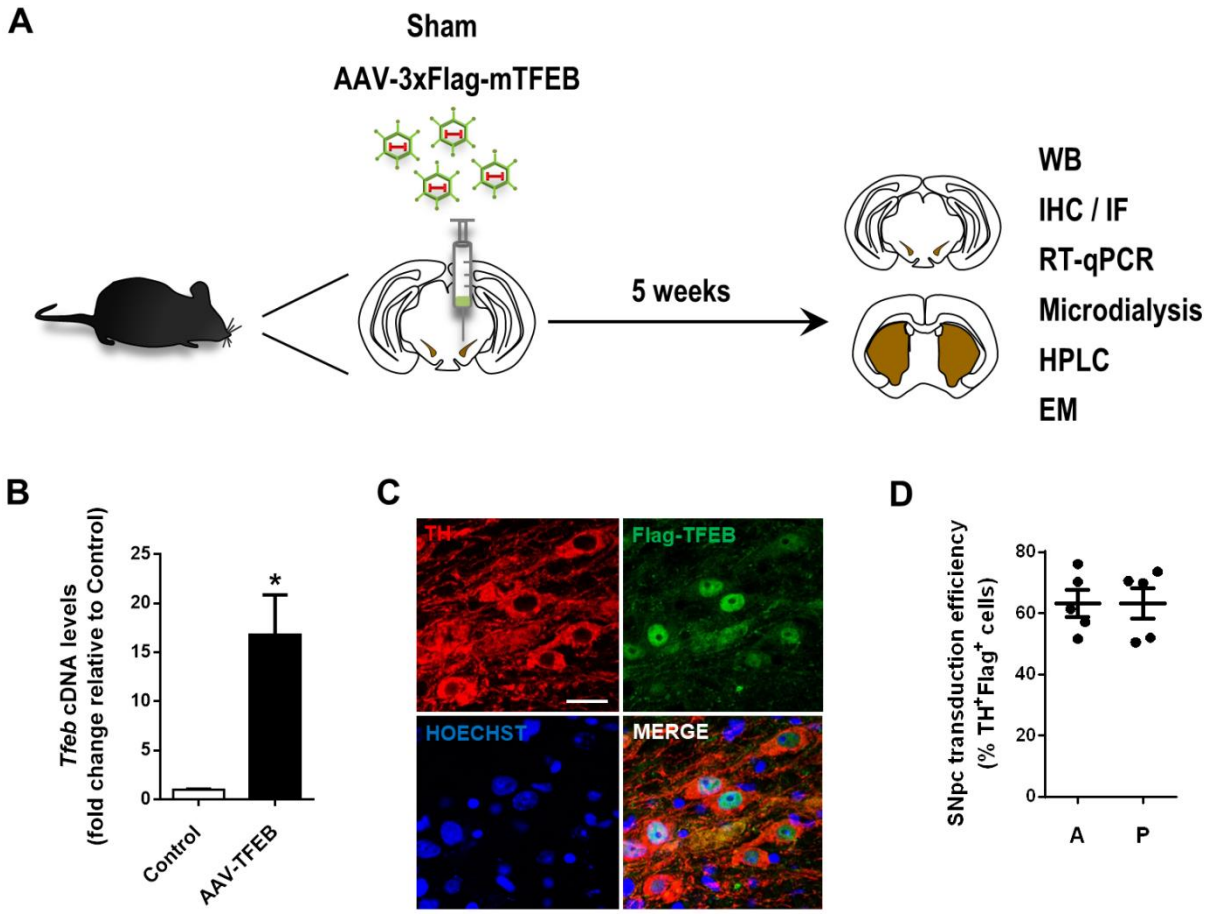

Figure 18. Injection of AAV-TFEB results in high TFEB overexpression in mice SNpc dopaminergic neurons. (**A**) Diagram representing the workflow and experiments carried out with AAV-TFEB-injected mice. (**B**) *Tfeb* cDNA levels measured by RT-qPCR in ventral midbrain homogenates of mice after vehicle (*n* = 6) or AAV-TFEB nigral injection (*n* = 5); Mann-Whitney test. **P* < 0.05 compared to control. (**C**) Immunofluorescence for tyrosine hydroxylase (red), Flag (green) and nucleus (blue) in substantia nigra sections showing TFEB translocation into the nucleus after AAV-TFEB nigral injection. Scale bar = 25 μm. (**D**) AAV-TFEB transduction efficiency analysis, as determined by dopaminergic neurons (TH^+) that co-express exogenous TFEB (TH^+Flag^+), in both anterior (A) and posterior (P) midbrain sections. In all panels, samples were collected 5 weeks after AAV-TFEB or vehicle injections. All data are represented as mean ± SEM.

It is well established that TFEB binds to the promoter regions of numerous autophagy-lysosomal genes to induce autophagosome and lysosome biogenesis and autophagosome-lysosome fusion (Settembre *et al.*, 2011). To confirm that TFEB overexpression was able to boost the autophagy-lysosomal degradation pathway machinery in mice dopaminergic neurons, we measured by western blot the levels of

two lysosomal markers, LAMP1 and cathepsin D (CTSD), and the levels of the autophagic vacuole marker LC3-II, expressed as the ratio LC3-II/LC3-I. As expected, protein levels of both lysosomal markers were clearly raised, particularly in the case of CTSD, which was increased fivefold (**Figures 19A, B**). The increase of lysosomal markers confirms previously published results where TFEB was overexpressed *in vivo* in neurons and lysosomal proteins or mRNA levels were raised (Decressac *et al.*, 2013; Polito *et al.*, 2014). LC3-II/LC3-I ratio was also raised 226% compared to control mice (**Figure 19C**), corroborating that TFEB overexpression was also inducing autophagosome formation in dopaminergic neurons *in vivo*.

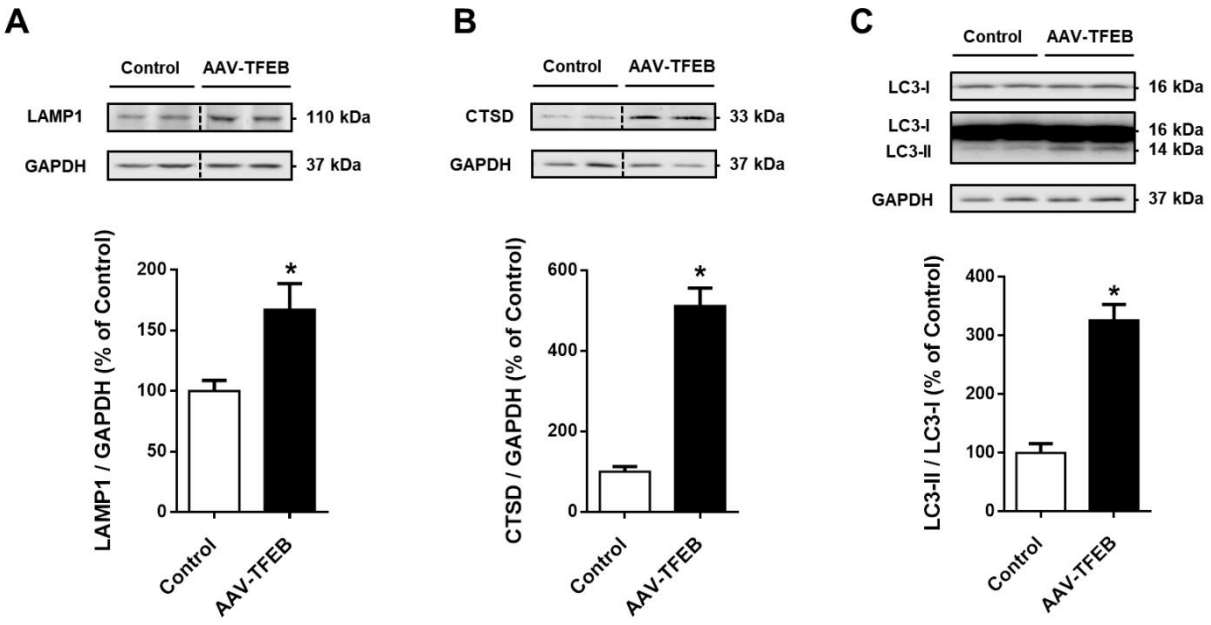

Figure 19. TFEB overexpression activates the autophagy-lysosomal pathway. (**A-C**) Representative western blots and protein levels in ventral midbrain homogenates from mice overexpressing TFEB (n = 6) compared to vehicle-injected mice (n = 5-6) of (**A**) LAMP1; (**B**) cathepsin D (CTSD) and (**C**) LC3-I and II. Mann-Whitney test. *P < 0.05 compared to control. In all panels, samples were collected 5 weeks after AAV-TFEB or vehicle injections. All data are represented as mean ± SEM.

4.2. TFEB overexpression drives a neurotrophic effect that increases dopaminergic function

After performing tyrosine hydroxylase immunohistochemistry we observed a patent enlargement of the AAV-TFEB injected SNpc (**Figure 20A**). We determined that this enlargement represented a 30% increase in the total volume of the SNpc when compared to the contralateral or the vehicle-injected SNpc (**Figure 20B**). At a cellular level, this increased SNpc volume was attributable to a 40% increase in the average cell body area of the dopaminergic neurons (**Figure 20C**), which was notably apparent on visual inspection of cells under the light microscope (**Figure 20A**). Moreover, not only cell body was actually increased but also dendritic arborization by 130% compared to vehicle-injected mice (**Figure 20D**), suggesting that TFEB overexpression was indeed inducing a trophic effect in SNpc dopaminergic neurons. Besides, stereological cell counts of the total number of dopaminergic neurons in the TFEB-overexpressing SNpc was no different than the number estimated in the contralateral or the vehicle-injected SNpc (**Figure 20E**), ruling out not only a deleterious effect of overexpressing TFEB but also an effect on neurogenesis. Taken together, these results strongly demonstrate that TFEB overexpression, in addition to the activation of the autophagy-lysosomal pathway, triggers a trophic effect that resembles the one elicited by neurotrophic factors.

Because neurotrophic factors like GDNF or neurturin were shown to increase, in addition to neuronal size, dopaminergic phenotypic markers such as tyrosine hydroxylase (Hyman *et al.*, 1994; Herzog *et al.*, 2007) and enhancing neuronal function (Grondin *et al.*, 2002), we carried out various histological, biochemical and functional experiments in order to ascertain whether TFEB was also mimicking neurotrophic factors at these levels. Once dopamine (DA) is synthesized, it is stored into synaptic vesicles through the vesicular monoamine transporter 2 (VMAT2) preventing DA oxidation due to low vesicular pH levels (Segura-Aguilar and Paris, 2014). Thus, VMAT2 is a good readout of vesicular DA packaging and handling (Lohr *et al.*, 2015). This vesicular DA is transported to the neuronal terminal, where it is released into the synaptic space and picked up by the dopamine transporter (DAT)

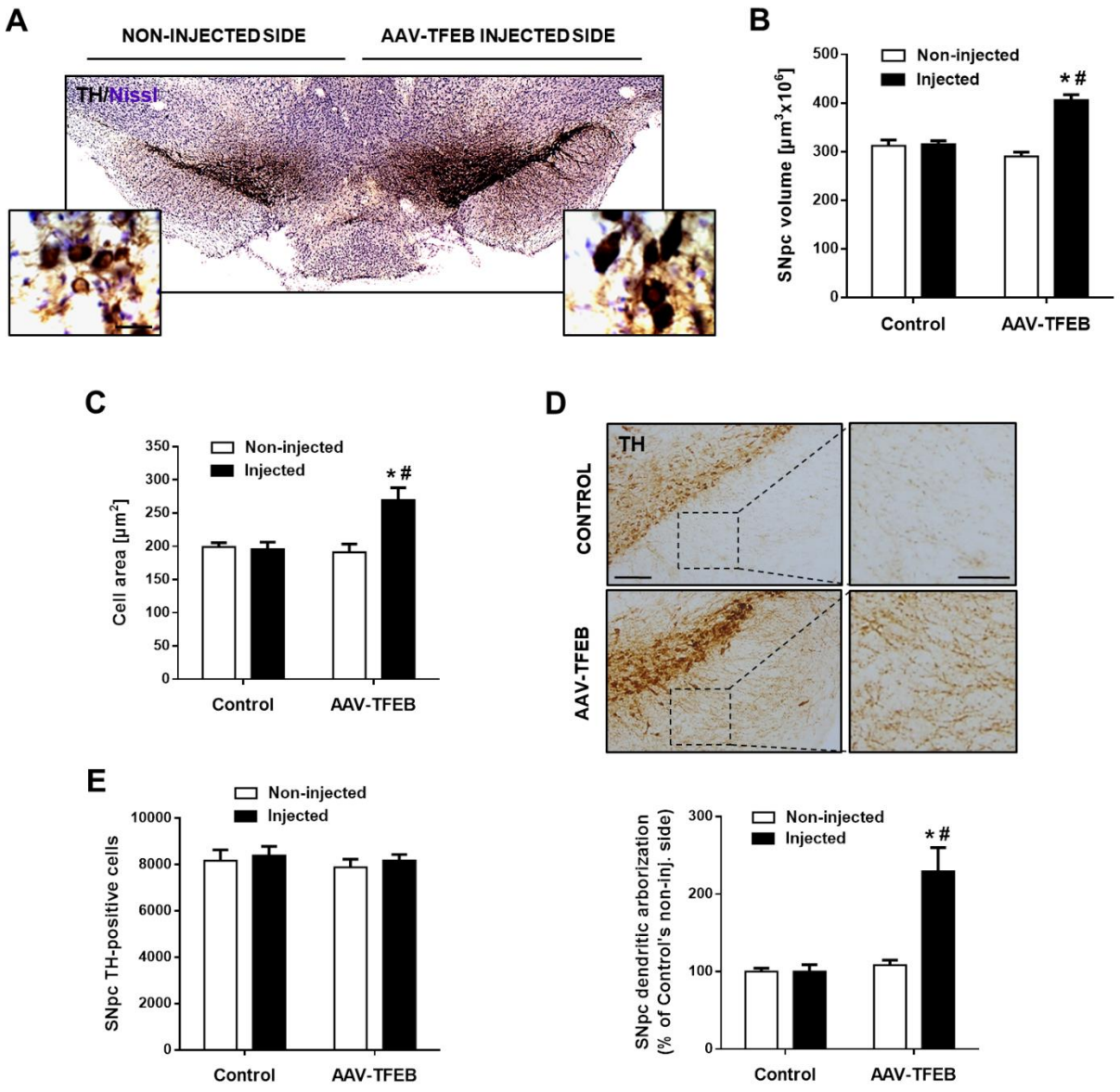

Figure 20. TFEB overexpression induces a neurotrophic effect in SNpc dopaminergic neurons. (**A**) Representative photomicrograph of tyrosine hydroxylase-immunostained substantia nigra section of a mouse injected with AAV-TFEB into the right SN. Scale bar = 25 µm. (**B**) Stereological volumes of both SNpc of unilateral vehicle-injected (*n* = 7) and AAV-TFEB-injected mice (*n* = 8). (**C**) Average cell area of SNpc dopaminergic neurons of vehicle-injected (*n* = 7) and AAV-TFEB-injected mice (*n* = 8). (**D**) Top, representative images of SNpc dendritic arborization of vehicle-injected (*n* = 6) and AAV-TFEB-injected mice (*n* = 5). Scale bar = 150 µm and 200 µm (zoom). Bottom, quantification of SNpc dendritic arborization in both groups of animals. (**E**) Stereological cell counts of dopaminergic neurons in substantia nigra pars compacta of mice injected with vehicle (*n* = 7) or AAV-TFEB (*n* = 9). In all panels, two-way ANOVA, *post hoc* Tukey's. **P* < 0.05 compared to control injected side. $^{\#}P$ < 0.05 compared to AAV-TFEB non-injected side. Samples were collected 5 weeks after AAV-TFEB or vehicle injections. All data are represented as mean ± SEM.

and either recycled into synaptic vesicles or metabolized to 3,4-dihydroxyphenylacetic acid (DOPAC) and homovanillic acid (HVA), the final metabolite of DA.

First, we determined the optical density (OD) of tyrosine hydroxylase, the rate-limiting enzyme on DA biosynthesis, in SNpc dopaminergic neurons. We found that this enzyme was 20% higher in TFEB-overexpressing neurons compared to vehicle-injected mice (**Figure 21A**), indicating that DA biosynthesis may be boosted. To check whether this event was accompanied by an increase of DA packaging, we examined by western blot the levels of VMAT2 in ventral midbrain homogenates and found that VMAT2 levels were increased more than sevenfold in TFEB-overexpressing mice (**Figure 21B**). This result was further confirmed by a detected intensification of VMAT2 immunolabeling in the AAV-TFEB injected SNpc dopaminergic neurons (**Figure 21C**). To determine whether these findings correlated with an enhancement of dopaminergic function at the synaptic level, we again checked VMAT2 levels in the striatum by performing an immunohistochemistry against VMAT2 in coronal sections of this region and measured the optical density of VMAT2. As expected, VMAT2 levels were also raised (70%) in the striatum of AAV-TFEB-injected mice (**Figure 21D**), indicating that vesicular DA is properly trafficked to the synaptic space to be released. No statistical changes were observed in striatal DAT levels (**Figure 21E**), suggesting that although DA handling may be enhanced by increased VMAT2 levels upon TFEB overexpression conditions, DA reuptake seems not to be affected.

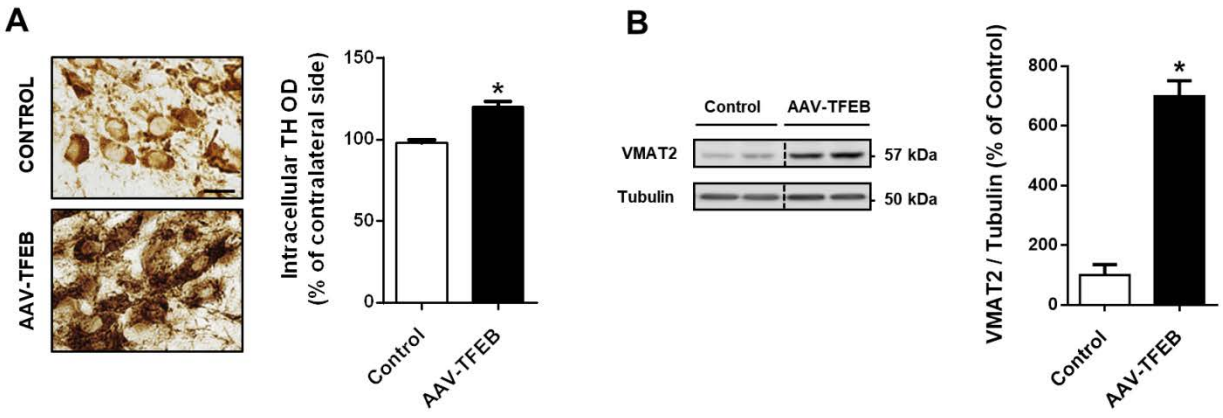

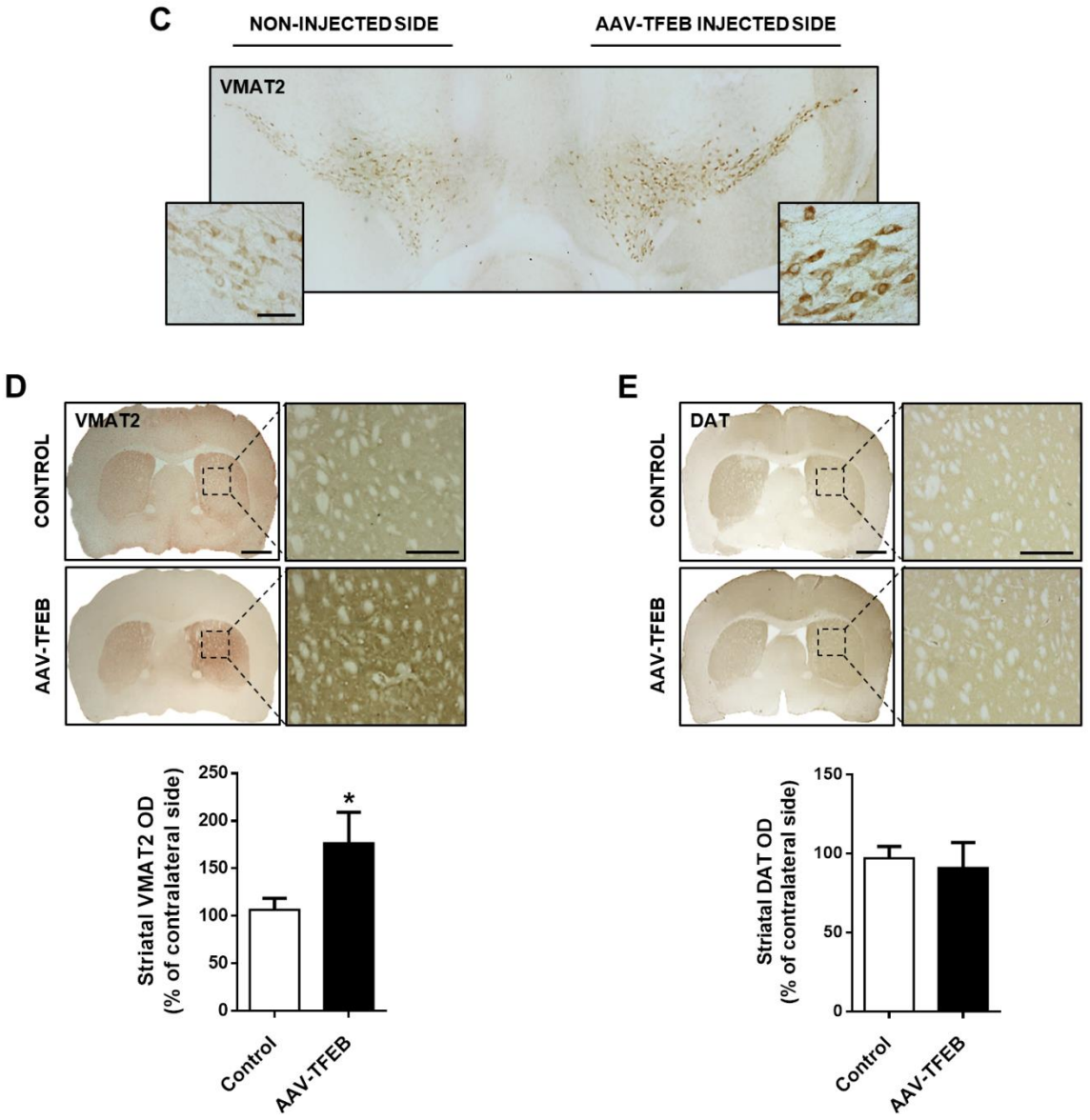

Figure 21. TFEB overexpression increases TH expression and enhances dopamine handling. (**A**) Left, representative images of tyrosine hydroxylase levels of dopaminergic neurons from vehicle-injected (*n* = 6) and AAV-TFEB-injected mice (*n* = 5). Scale bar = 25 µm. Right, intraneuronal optical densitometry of tyrosine hydroxylase immunoreactivity of both groups of animals. (**B**) Representative western blot and protein levels of VMAT2 in ventral midbrain homogenates from mice overexpressing TFEB (*n* = 6) compared to vehicle-injected mice (*n* = 6). (**C**) Representative photomicrograph of VMAT2-immunostained SN section of a mouse injected with AAV-TFEB into the right SN. Scale bar = 50 µm. (**D-E**) Representative photomicrographs and quantification levels of (**D**) VMAT2 and (**E**) DAT-immunostained striata from mice overexpressing TFEB (*n* = 6) compared to vehicle-injected mice (*n* = 6). Scale bar = 500 µm and 150 µm (zoom). In all panels, Mann-Whitney test. *$P < 0.05$ compared to control. Samples were collected 5 weeks after AAV-TFEB or vehicle injections. All data are represented as mean ± SEM.

Next, to assess whether these molecular changes were associated with correlated neurochemical changes, we checked by HPLC the content of the neurotransmitter DA and its metabolites DOPAC and HVA in the striatum. TFEB-overexpressing mice exhibited a decrease in both dopamine (20%) and DOPAC (18%) content but an increase in the postsynaptic metabolite HVA content (36%) (**Figure 22A**). The DOPAC/DA ratio, which represents dopamine metabolism, did not change, while the HVA/DA ratio, which represents dopamine release, was almost doubled in the striatum of TFEB-overexpressing mice **(Figure 22A**). Interestingly, the same pattern is achieved when GDNF (Grondin *et al.*, 2002) or BDNF (Altar *et al.*, 1992) are chronically delivered, with only increases in HVA levels and the HVA/DA ratio having been reported. Serotonin (5-HT) levels remained unchanged, indicating that the effect was specific for the catecholaminergic neurotransmitter system **(Figure 22A**).

Finally, to further confirm that dopaminergic neurons' function was enhanced and that dopamine release was increased in AAV-TFEB mice, we carried out *in vivo* microdialysis studies. First, we measured intrastriatal veratridine-evoked dopamine release in both vehicle and AAV-TFEB-injected mice. When stimulated with the depolarizing agent veratridine, striatal DA release was much more prominent in AAV-TFEB-injected mice compared to the increased evoked in vehicle-injected animals (**Figure 22B**). Then, we also assessed intrastriatal d-amphetamine-evoked dopamine overflow. D-amphetamine elevates dopamine extracellular levels by three major mechanisms: (i) it is a substrate for DAT that competitively inhibits dopamine uptake; (ii) it facilitates the movement of dopamine out of vesicles; and (iii) it mediates DAT-mediated reverse-transport of dopamine into the synaptic cleft (Fleckenstein *et al.*, 2007). D-amphetamine-evoked increase of extracellular dopamine levels in the striatum of TFEB-overexpressing mice doubled the increase evoked in control mice (**Figure 22C**), demonstrating that TFEB overexpression not only increases the dopamine release but also the available pool of dopamine, as previous VMAT2 results indicated.

All together, these results demonstrate that TFEB overexpression in dopaminergic neurons triggers a neurotrophic effect that is accompanied by an increase of dopaminergic neuronal function.

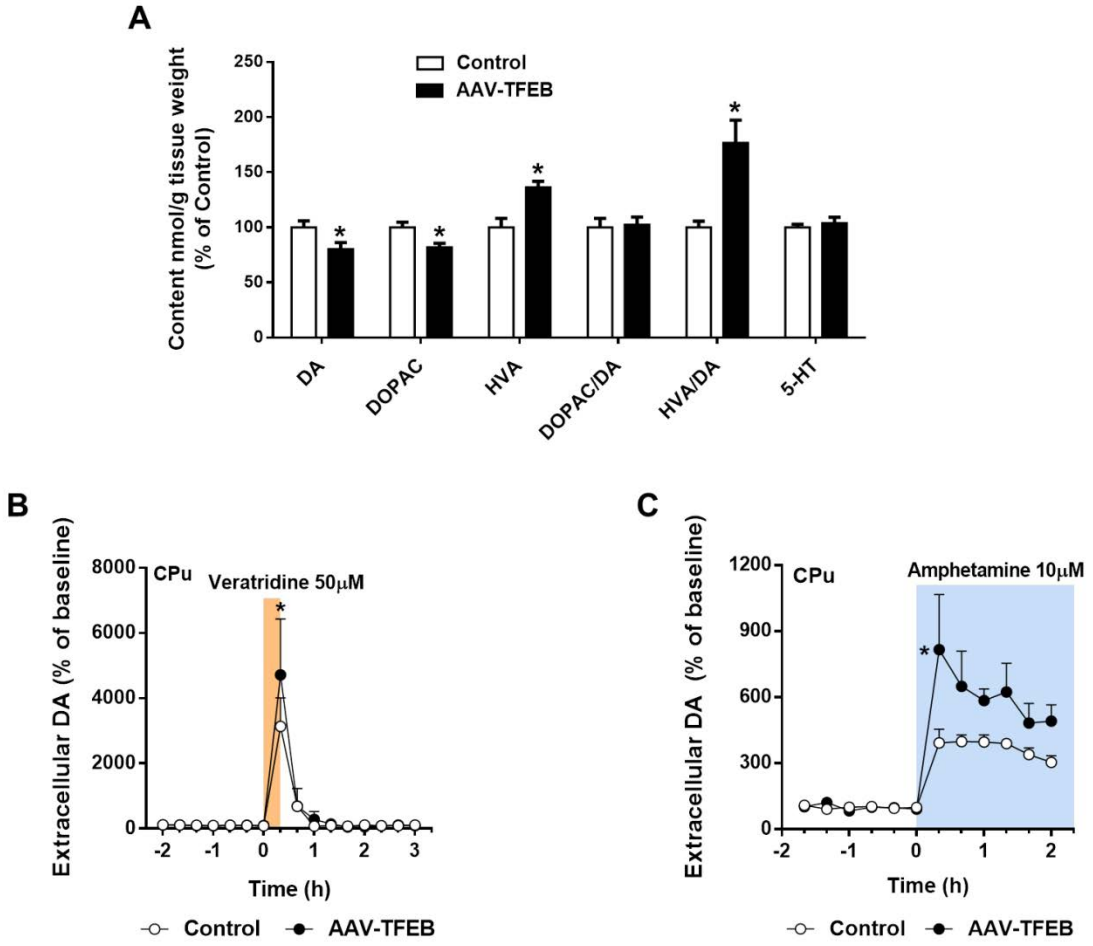

Figure 22. TFEB overexpression increases both the available pool of DA and DA release in the striatum. (**A**) Content of dopamine (DA) and its metabolites 3,4-Dihydroxyphenylacetic acid (DOPAC) and homovanillic acid (HVA), and DOPAC/DA and HVA/DA ratios in striatal homogenates measured by HPLC of vehicle-injected (*n* = 6) and AAV-TFEB-injected mice (*n* = 6). Serotonin (5-HT) levels were measured as a control of the experiment; Mann-Whitney test. **P* < 0.05 compared to control. (**B-C**) Striatal DA relative amounts in AAV-TFEB (*n* = 4-5) and vehicle-injected mice (*n* = 6-7) measured by microdialysis in the ipsilateral striatum following local (**B**) veratridine (50 µM) or (**C**) d-amphetamine (10 µM) administration by reverse-dialysis; ANOVA for repeated measures, *post hoc* Tukey's. **P* < 0.05 compared to control. In all panels, samples were collected 5 weeks after AAV-TFEB or vehicle injections. All data are represented as mean ± SEM.

4.3. mTORC1 signaling is boosted in TFEB-overexpressing mice

Cell growth involves increasing cellular biomass, which is achieved by enhanced protein synthesis that is controlled by mTORC1. mTORC1 activates protein synthesis and cell growth by phosphorylating p70 ribosomal S6 kinase 1 (S6K1) and eukaryotic translation initiation factor 4E (eIF4E)-binding protein 1 (4E-BP1). eIF4E is a component of the complex eIF4F and binds the 5' cap in translation initiation. Binding of eIF4F to the cap is hindered by 4E-BP1, which, when hypophosphorylated, sequesters eIF4E and impedes translation initiation. When 4E-BP1 is phosphorylated on Thr37/46 by mTORC1, it serves as a priming event followed by Ser65 phosphorylation, which finally allows the release of eIF4E and permits the formation of eIF4F complex and the subsequent translation initiation (Gingras *et al.*, 1999; Wang *et al.*, 2003). Since eIF4E has been identified as a TFEB direct target, we expected the involvement of this initiation factor in TFEB-induced cell growth (Palmieri *et al.*, 2011). To test this hypothesis, we carried out the necessary western blot analysis with ventral midbrain protein homogenates. As anticipated, we found an increase of eIF4E levels (43%) in AAV-TFEB injected mice (**Figure 23A**). We next determined the phosphorylation status of 4E-BP1 on Thr37/46 and found that it was increased (**Figure 23B**), as well as the ratio of Ser65-phosphorylated to total 4E-BP that serves as an indicator of free and active eIF4E (**Figure 23C**). These results indicate a translation initiation enhancement in TFEB-overexpressing SNpc.

Regarding S6K1, once it is phosphorylated on Thr389 by mTORC1, mRNA translation is promoted by the phosphorylation of or binding to multiple proteins, including ribosomal protein S6 (RPS6) (Ruvinsky and Meyuhas, 2006; Magnuson *et al.*, 2012). A prominent increase of activated/phosphorylated S6K1 (176%) and the phosphorylated/total ratio (100%) was detected in ventral midbrain homogenates of TFEB-overexpressing mice (**Figure 23D**). This was accompanied by an increase in the intensity of phosphorylated/activated RPS6 immunohistochemistry in the SNpc (**Figure 23E**).

Taken together, these results demonstrate that mTORC1 signaling is boosted and both the 4E-BP1/eIF4E and S6K1 pathways collaborate to increase the protein synthesis necessary for the TFEB-induced neurotrophic effect. We confirm that TFEB overexpression increases mTORC1 signaling and protein synthesis in neurons as it has also recently demonstrated in other cell types (Di Malta *et al.*, 2017).

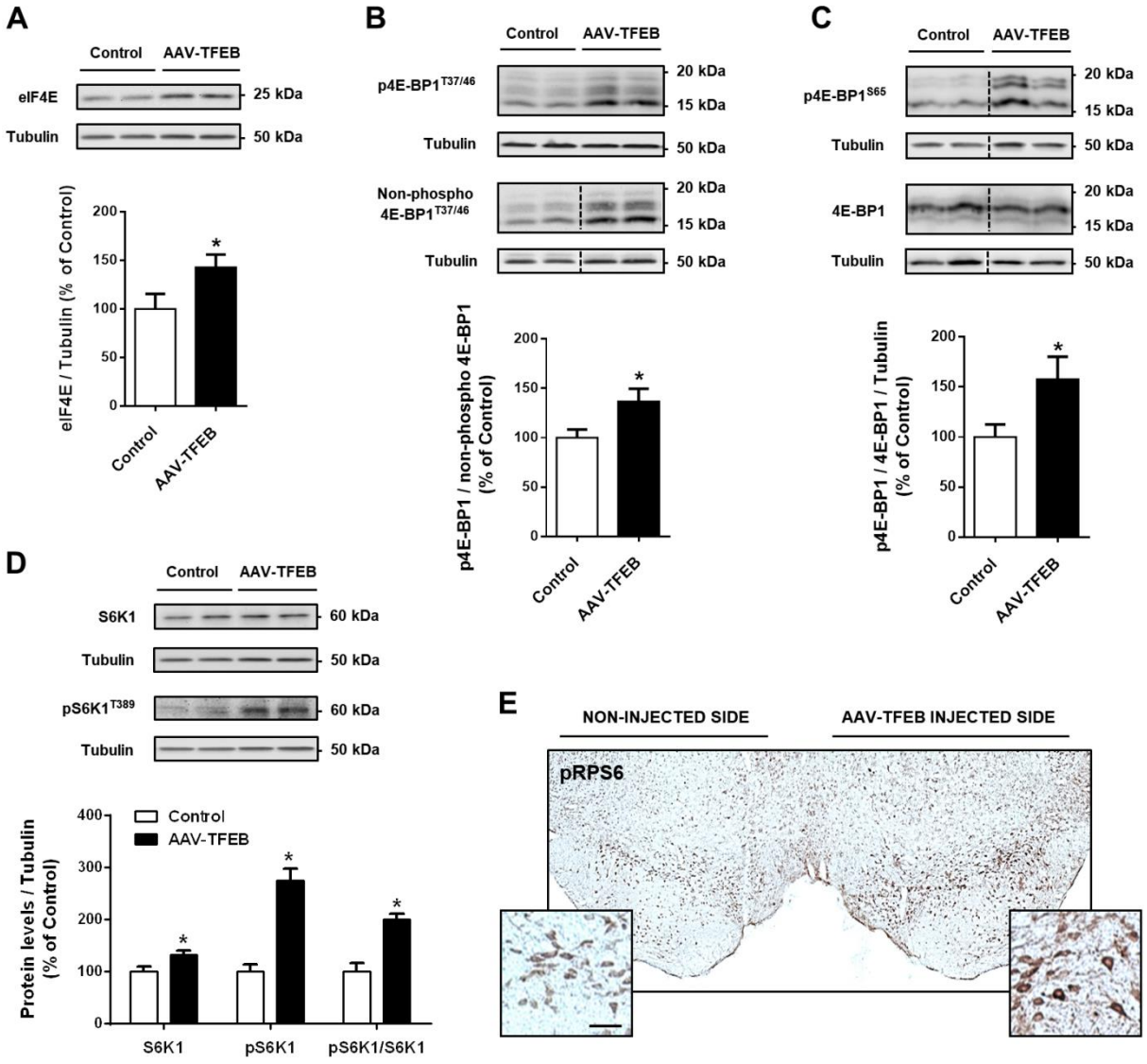

Figure 23. Activation of the mTORC1 protein synthesis inducers eIF4E and S6K1. (**A-D**) Representative western blots and protein levels in ventral midbrain homogenates from mice overexpressing TFEB (*n* = 6) compared to control mice (*n* = 5-6) of (**A**) eIF4E, (**B**) phosphorylated and non-phosphorylated 4E-BP1 at Thr37/46, expressed as a ratio, (**C**) phosphorylated 4E-BP1 at Ser65 versus total 4E-BP1 levels, and (**D**) S6K1, its activated form (pS6K1^{T389}) and the ratio. Mann-Whitney test. **P* < 0.05 compared to control. (**E**) Representative photomicrograph of a SN section immunostained for the phosphorylated/activated RPS6, pRPS6$^{S235/236}$, of a mouse injected with AAV-TFEB into the right SN. Scale bar = 50 µm. In all panels, samples were collected 5 weeks after AAV-TFEB or vehicle injections. All data are represented as mean ± SEM.

4.4. Pro-survival AKT/mTOR and ERK1/2 signaling pathways are activated upon TFEB overexpression

We next determined whether the AKT/mTOR pathway, which is the main pathway that activates mTORC1 signaling and therefore mediates neurotrophic activity (Besset *et al.*, 2000; Hsuan *et al.*, 2006; Robinet and Pellerin, 2010), could be involved in the TFEB-mediated neurotrophic effect. For such, we measured the relative amount of AKT as well as phosphorylated/activated AKT levels and found that, although total amounts of AKT were downregulated by half, phosphorylated AKT at S473 was dramatically increased (233%) in TFEB-overexpressing neurons, as well as the phosphorylated/total protein ratio (603%) (**Figure 24A**). To determine whether mTORC2, known to phosphorylate AKT at S473 (Sarbassov *et al.*, 2005), was responsible of the strong activation of AKT, we measured the total and phosphorylated/activated form of N-Myc downstream regulated 1 protein (NDRG1), which is a proxy indicator of mTORC2 activity (Weiler *et al.*, 2014). Total NDRG1 was downregulated (47%) and activated NDRG1 was decreased even further (72%) (**Figure 24B**), suggesting that the mTORC2 pathway was not involved. We subsequently looked for a putative TFEB direct target that could be responsible for this AKT activation/phosphorylation (Palmieri *et al.*, 2011). Among the possible options, TANK-binding kinase 1 (TBK1) is known to phosphorylate/activate AKT independently of PDPK1 and mTORC2 (Ou *et al.*, 2011). We therefore assessed both TBK1 total and phosphorylated/activated levels and found a threefold increase of both (**Figure 24C**), demonstrating that TBK1 is not only overexpressed under TFEB-overexpressing conditions but activated probably by autophosphorylation (Shu *et al.*, 2013). TBK1 only binds to AKT when activated and non-phosphorylated TBK1 is not interfering the activation of AKT (Ou *et al.*, 2011), therefore TBK1 is a strong candidate for AKT phosphorylation. Moreover, we are also demonstrating that despite mTORC1 activation, mTORC2 pathway is not activated upon TFEB overexpression.

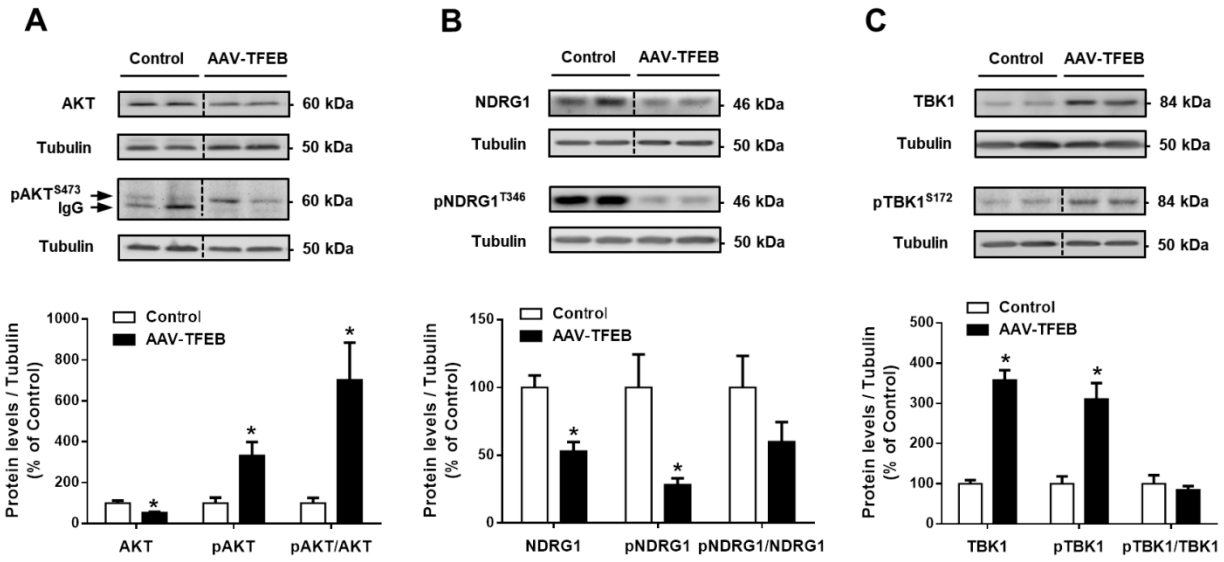

Figure 24. Activation of AKT/mTOR signaling pathway after TFEB overexpression. (**A-C**) Representative western blots and protein levels in ventral midbrain homogenates from mice overexpressing TFEB (*n* = 6) compared to vehicle-injected mice (*n* = 5-6) of (**A**) total AKT, phosphorylated/activated AKT (pAKT^{S473}) and the ratio; (**B**) total NDRG1, its phosphorylated/activated form (pNDRG1^{T346}) and the ratio; and (**C**) TBK1, its phosphorylated/activated form (pTBK1^{S172}) and the ratio. In all panels, Mann-Whitney test. **P* < 0.05 compared to control. Samples were collected 5 weeks after AAV-TFEB or vehicle injections. All data are represented as mean ± SEM.

Our initial hypothesis pointed out that the ERK1/2 pathway, which is the other relevant signaling pathway that mediates neurotrophic activity (Melillo *et al.*, 2001; Nicole *et al.*, 2001; Hetman and Gosdz, 2004; Gomes *et al.*, 2007; Herzog *et al.*, 2007), might be activated after TFEB overexpression because both ERK 1 and 2 have been identified as TFEB direct targets (Palmieri *et al.*, 2011). ERK1/2 are known to activate, among others: (i) mTORC1 upstream proteins like Rheb by inhibiting TSC2 (Parmar and Tamanoi, 2010; Winter *et al.*, 2011); and (ii) mTORC1 downstream proteins like S6K1 and RPS6 (Roux *et al.*, 2007). Therefore, ERK1/2 activation could also explain the neurotrophic effect we had found in AAV-TFEB-injected mice. To test this hypothesis, we determined the total levels and the Thr202/Tyr204-phosphorylated/ activated form of ERK1/2. Not only were the total ERK1/2 levels were upregulated (43%), but we also found a threefold increase in the activated form (**Figure 25A**). To further confirm ERK1/2 pathway activation, we measured the levels of phosphorylated/activated p90 ribosomal S6 kinase (p-

p90RSK), which is known to be a ubiquitous and versatile mediator of ERK1/2 signal transduction (Carriere *et al.*, 2008), and again found a threefold increase of activated p90RSK in TFEB-overexpressing SNpc (**Figure 25B**).

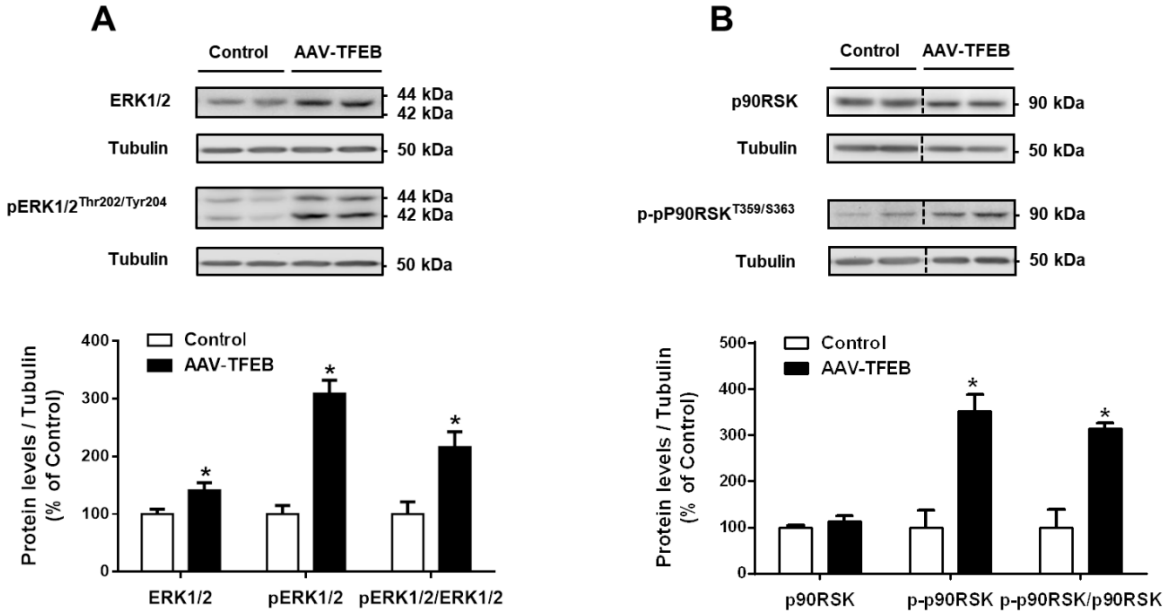

Figure 25. Activation of ERK1/2 signaling pathway after TFEB overexpression. (**A-B**) Representative western blots and protein levels in ventral midbrain homogenates from mice overexpressing TFEB (*n* = 6) compared to vehicle-injected mice (*n* = 5) of (**A**) ERK1/2, their activated forms (pERK1/2$^{Thr202/Tyr204}$) and the ratio; and (**B**) p90RSK, its phosphorylated/activated form (p-p90RSK$^{T359/S363}$) and the ratio. In both panels, Mann-Whitney test. **P* < 0.05 compared to control. Samples were collected 5 weeks after AAV-TFEB or vehicle injections. All data are represented as mean ± SEM.

Our results demonstrate that both ERK1/2 and AKT/mTOR pro-survival signaling pathways are activated after TFEB overexpression, which are likely to synergistically contribute to the TFEB-induced neurotrophic effect.

4.5. TFEB overexpression increases mitochondrial size and promotes mitochondrial fusion in substantia nigra dopaminergic neurons

Another group of TFEB putative direct target genes particularly relevant to PD are those involved in mitochondria. Since more than thirty TFEB putative direct targets are linked to mitochondria metabolism (Palmieri *et al.*, 2011), we expected that TFEB overexpression could somehow be modifying mitochondrial function in neurons, as it has also recently reported in other non-brain tissues (Mansueto *et al.*, 2017). Boosting mitochondrial function may potentially contribute to halt the progression of PD since growing evidence suggests that impaired mitochondrial function is instrumental in this disease (Perier *et al.*, 2007, 2012; Franco-Iborra *et al.*, 2018b).

To assess mitochondrial status in SNpc dopaminergic neurons we first checked the mitochondrial marker TOM20, which is a component of the outer mitochondrial membrane widely used to check mitochondrial status (Wurm *et al.*, 2011; Bové *et al.*, 2014; Mot *et al.*, 2016), and found a threefold increase of TOM20 intensity in TFEB-overexpressing compared to control neurons (**Figure 26A**). We next determined whether respiratory chain components were also modified by TFEB overexpression. We measured the protein levels of one subunit of various mitochondrial respiratory chain complexes including NADH:ubiquinone oxido-reductase subunit B8 (NDUFB8, complex I), cytochrome c oxidase subunit 4 isoform 1 (COX4I1, complex IV) and succinate dehydrogenase complex iron sulfur subunit B (SDHB, complex II). All three subunits were raised in ventral midbrain homogenates of TFEB-injected mice (**Figure 26B**), suggesting that TFEB is involved in mitochondrial respiration. This result is in agreement with a previous work in which increased levels of many OXPHOS subunits were reported after TFEB overexpression (Mansueto *et al.*, 2017). To confirm that this event was indeed occurring in the SNpc dopaminergic neurons, a double immunofluorescence experiment for TH and COX IV was performed in both control and AAV-TFEB-injected mice. TFEB-overexpressing neurons clearly displayed higher levels of COX IV, as determined by immunofluorescence confocal microscopy visualization (**Figure 26C**).

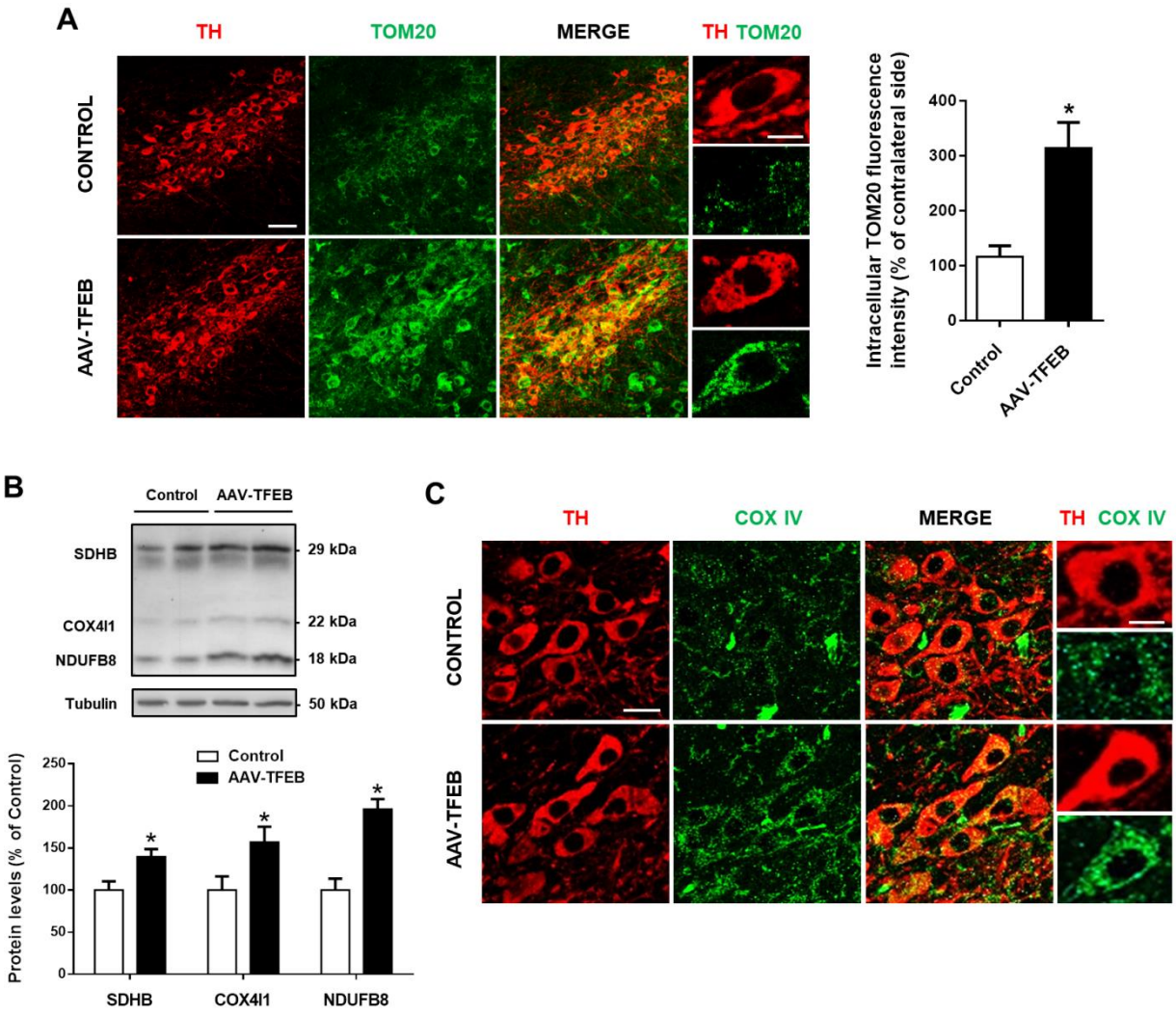

Figure 26. Mitochondrial markers are heightened in TFEB-overexpressing dopaminergic neurons. (**A**) Left, representative confocal images of a double immunofluorescence for TH (red) and TOM20 (green) in SN sections of mice injected with vehicle (*n* = 6) or AAV-TFEB (*n* = 5). Scale bar = 50 µm and 10 µm (zoom). Right, quantification of TOM20 fluorescence intensity in SN dopaminergic neurons of both groups of mice, represented as a percentage of the non-injected side. (**B**) Representative western blot and protein levels in ventral midbrain homogenates from mice overexpressing TFEB (*n* = 6) compared to vehicle-injected mice (*n* = 6) of SDHB (complex II), COX4I1 (complex IV) and NDUFB8 (complex I). (**C**) Representative confocal images of a double immunofluorescence for TH (red) and COX IV (green) in SN sections of mice injected with vehicle (*n* = 5) or AAV-TFEB (*n* = 6). Scale bar = 25 µm and 10 µm (zoom). In all panels, Mann-Whitney test. *P < 0.05 compared to control. Samples were collected 5 weeks after AAV-TFEB or vehicle injections. All data are represented as mean ± SEM.

Because the data obtained, we hypothesized that TFEB overexpression would increase the number of mitochondria by triggering mitochondrial biogenesis since the master regulator of mitochondrial biogenesis peroxisome-proliferator-activated receptor gamma co-activator-1alpha (PGC-1α) is considered a TFEB direct target (Palmieri *et al.*, 2011). To validate this hypothesis, we first measured the levels of PGC-1α in ventral midbrain homogenates of vehicle and AAV-TFEB-injected mice, but found that the levels were equivalent in both groups (**Figure 27A**). We then assessed *Ppargc1a* mRNA levels, but again no changes were detected (**Figure 27B**). We also determined the mRNA levels of *Tfam*, a key activator of mitochondrial transcription that participates in mitochondrial genome replication, and yet again found that TFEB overexpression did not induce any increase (**Figure 27B**). To evaluate whether the steady-state number of mitochondria was higher in TFEB-overexpressing conditions, we assessed mitochondrial DNA (mtDNA) copy number by measuring the number of *16S* and *ND4* mitochondrial-encoded gene copies, relative to nuclear genomic DNA by using the angiogenin 1 (*Ang1*) gene. No statistical differences were observed between vehicle and AAV-TFEB-injected mice (**Figure 27C**). Taken together, these results suggested that sustained TFEB activation was not inducing mitochondrial biogenesis, or at least not in a sustained manner. To further confirm these results, TH-labeled SNpc sections were ultrastructural examined by transmission electron microscopy (TEM) to specifically visualize the mitochondrial morphology in dopaminergic neurons of both groups of animals (**Figure 27D**). Quantification of TEM images revealed no differences in mitochondrial density (**Figure 27E**), although the dopaminergic neuronal area occupied by mitochondria was increased in AAV-TFEB-injected animals (**Figure 27F**). This seeming paradox was explained by the fact that mitochondrial area was vastly increased (83%) rather than increased number of mitochondria upon TFEB overexpression (**Figure 27G**). Importantly, these enlarged mitochondria exhibited normal internal ultrastructure, with fairly dark uniform matrix filled with densely distributed cristae, indicating that mitochondria conserved an appropriate internal morphology (**Figure 27D**).

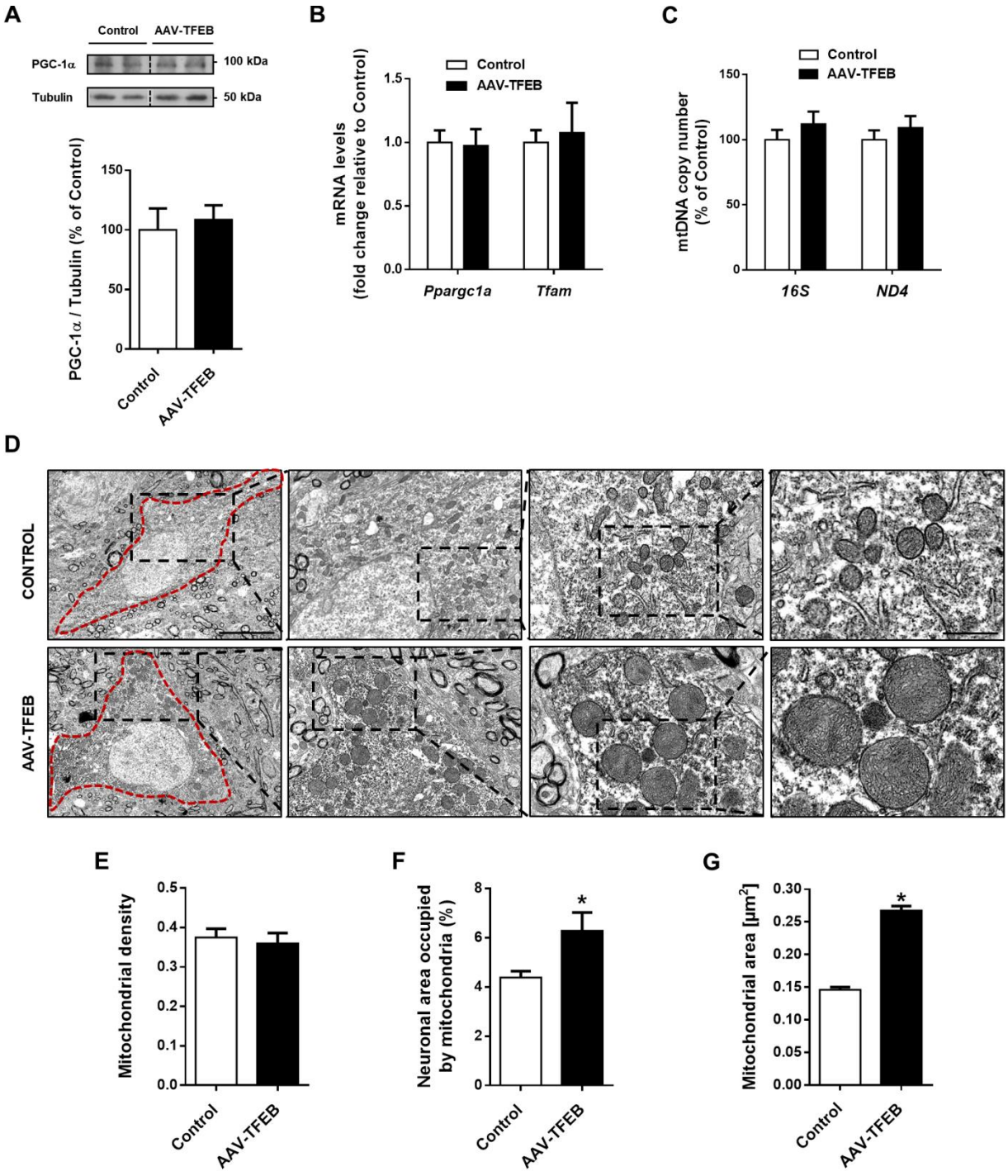

Figure 27. TFEB overexpression does not induce mitochondrial biogenesis but does increase mitochondrial size in dopaminergic neurons. (**A**) Representative western blot and protein levels of the master regulator of mitochondrial biogenesis, PGC-1α, from mice overexpressing TFEB (*n* = 5) compared to vehicle-injected mice (*n* = 6). (**B**) mRNA levels of *Ppargc1a* and *Tfam* determined by RT-qPCR in ventral midbrain homogenates from mice overexpressing TFEB (*n* = 5) compared to vehicle-injected mice (*n* = 6). (**C**) Determination of mitochondrial DNA (mtDNA) copy number in ventral midbrain extracts of unilaterally injected mice with AAV-TFEB (*n* = 10) or vehicle (*n* = 8). (**D**) Electron microscopy images of TH-labeled SNpc dopaminergic neurons (dashed red line) from mice overexpressing TFEB (*n* = 2) compared to vehicle-injected mice (*n* = 2). Scale bar = 10 μm and 1 μm

(zoom). (**E-F**) Quantification of (**E**) mitochondrial density and (**F**) percentage of neuronal area occupied by mitochondria of AAV-TFEB-injected mice (*n* = 21 neurons) and vehicle-injected mice (*n* = 12 neurons), as determined by electron microscopy studies. (**G**) Mitochondrial area quantification of AAV-TFEB-injected mice (*n* = 1308 mitochondria) and vehicle-injected mice (*n* = 569 mitochondria), as assessed by electron microscopy. In all panels, Mann-Whitney test. *P < 0.05 compared to control. Samples were collected 5 weeks after AAV-TFEB or vehicle injections. All data are represented as mean ± SEM.

We next determined whether this increase in mitochondrial size was accompanied by changes in mitochondrial fusion/fission balance. Since TOM20 overexpression *in vitro* not only stimulates protein transport but also triggers changes in mitochondrial dynamics that could fit with fusion events (Yano *et al.*, 1997), we postulated whether mitochondrial fusion status was increased in the SNpc of AAV-TFEB-injected mice.

We relied on TEM studies that allowed us to bin dopaminergic neurons' mitochondria into three categories: rounded mitochondria (class I), intermediate mitochondria that could fit with fusion/fission events (class II), and elongated mitochondria (class III). While in control mice the number of class II mitochondria was below 10% of total mitochondria and class III mitochondria were nearly undetectable, in TFEB-overexpressing neurons we observed that class II mitochondria were almost doubled and class III mitochondria were more than three times abundant compared to control mice (**Figure 28A**). These results suggested that mitochondria were more dynamic and tipping the balance towards mitochondrial fusion events that make mitochondria to adopt an elongated form. Additional morphometry analyses were carried out to further confirm these results. On the one hand, mitochondrial length was assessed by measuring the Feret's diameter, which represents the longest distance between any two points within a given mitochondrion. Feret's diameter was far larger in mitochondria from TFEB-overexpressing mice than those in control mice (**Figure 28B**). On the other hand, to demonstrate that this increase in Feret's diameter was indeed due to an increase of mitochondrial length instead of a reflection of the increased mitochondrial size that we also previously observed (**Figure 27G**), we measured the aspect ratio (AR) of mitochondria, which is computed as (major

axis)/(minor axis) and reflects the length-to-width ratio of mitochondria. Mitochondrial AR ratio was much higher in AAV-TFEB-injected mice (**Figure 28C**), corroborating that mitochondria were both larger and more elongated compared to control mice. To verify that these observed events were accompanied by increased levels of mitochondrial fusion proteins, we measured by western blot the relative levels of three essential proteins that are necessary to ensure an appropriate mitochondrial fusion: (i) optic atrophy 1 (OPA1); (ii) mitofusin 1 (MFN1); and (iii) mitofusin 2 (MFN2) (Chen *et al.*, 2005). All three mitochondrial fusion proteins were raised in TFEB-overexpressing ventral midbrain homogenates when compared to control animals, particularly in the case of both mitofusins, which were increased more than threefold (**Figure 28D**).

While mitochondrial fission is often associated to high levels of stress, such as those induced by neurotoxins damage (Van der Bliek *et al.*, 2013) and to participate in apoptosis (Frank *et al.*, 2001; Meuer *et al.*, 2007), mitochondrial fusion attenuates the potential deleterious effects of mutated mtDNA or misfolded proteins (Chen *et al.*, 2010; Van der Bliek *et al.*, 2013) and extends the mitochondrial network, maximizing ATP synthesis (Westermann, 2012). Therefore, our results strongly demonstrate that increased mitochondrial fusion entails a potential beneficial effect in dopaminergic neurons of TFEB-overexpressing mice.

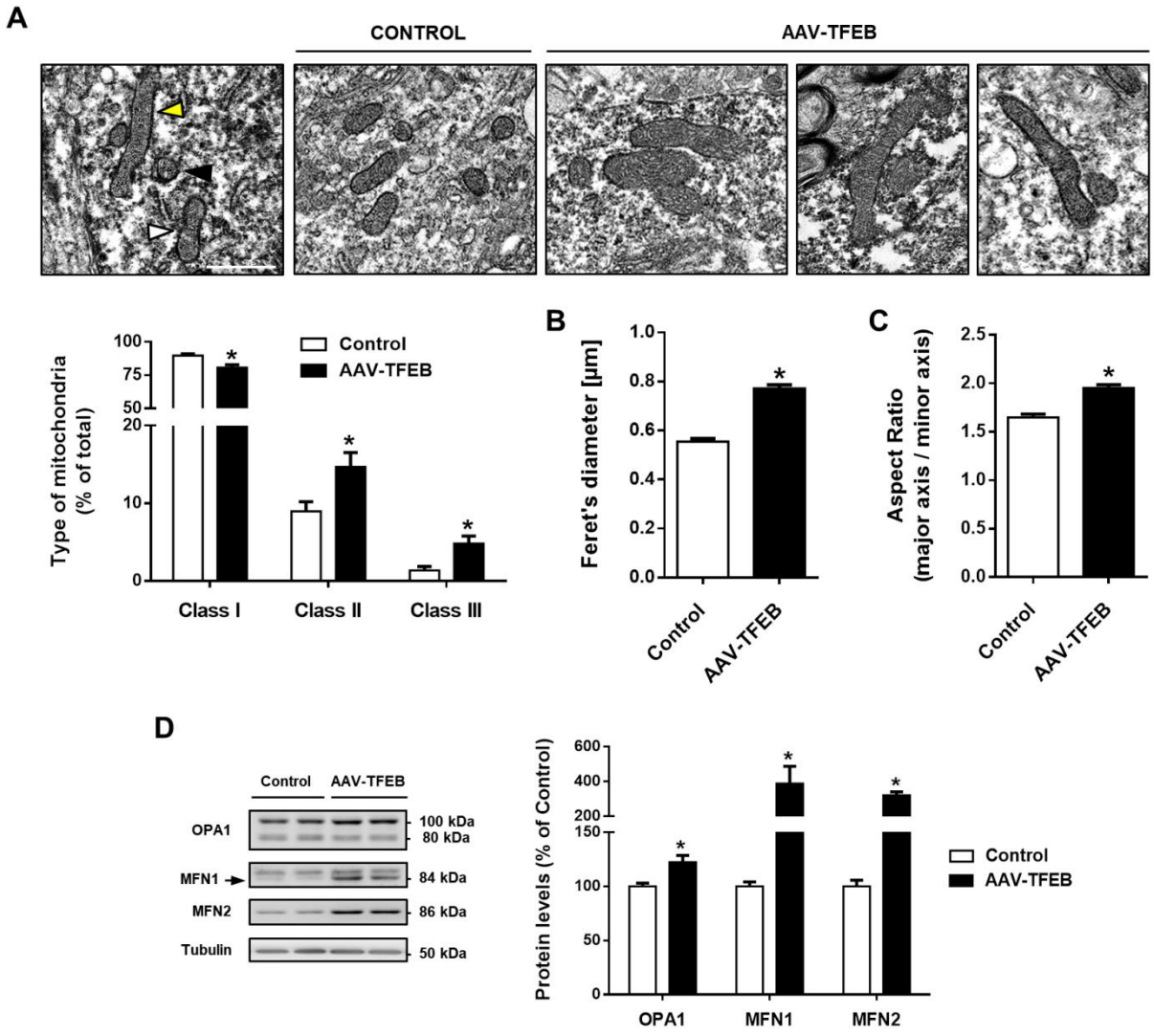

Figure 28. TFEB overexpression induces mitochondrial fusion in dopaminergic neurons. (**A**) Top, electron microscopy images of TH-labeled SNpc dopaminergic neurons from mice overexpressing TFEB (*n* = 2) compared to vehicle-injected mice (*n* = 2). Mitochondria were binned into three different categories: rounded (class I, black arrowhead), intermediate (class II, white arrowhead) and elongated (class III, yellow arrowhead). Scale bar = 1 µm. Bottom, quantification of all three types of mitochondria from AAV-TFEB-injected mice (*n* = 19 neurons) and vehicle-injected mice (*n* = 12 neurons). (**B-C**) Quantification of (**B**) mitochondria Feret's diameter and (**C**) the aspect ratio (AR) from AAV-TFEB-injected mice (*n* = 970 mitochondria) and vehicle-injected mice (*n* = 419 mitochondria), as determined by electron microscopy studies. (**D**) Representative western blot and protein levels in ventral midbrain homogenates from mice overexpressing TFEB (*n* = 6) compared to vehicle-injected mice (*n* = 6) of the mitochondrial fusion proteins OPA1, MFN1 and MFN2. In all panels, Mann-Whitney test. *P < 0.05 compared to control. Samples were collected 5 weeks after AAV-TFEB or vehicle injections. All data are represented as mean ± SEM.

Mitochondrial proteins synthesized in the cytoplasm are imported into the mitochondrial matrix through the TOM complex of the outer membrane and the TIM23 complex of the inner membrane (Pfanner *et al.*, 2019). These translocases, when overexpressed, are described to stimulate mitochondrial protein import and are often associated to neuroprotective effects (Yano *et al.*, 1997; Bender *et al.*, 2013; Di Maio *et al.*, 2016; Franco-Iborra *et al.*, 2018a). Thus, TOM20 and TIM23 protein levels are a good readout of the mitochondrial protein import status. As we previously observed an increase of TOM20 levels (**Figure 26A**), we believed that mitochondrial protein import machinery could be boosted in TFEB-overexpressing dopaminergic neurons. To delve further into this concept, we next determined the immunofluorescence intensity of TIM23 in SNpc dopaminergic neurons and found that it was 50% increased (**Figure 29A**), suggesting that those mitochondria were actively incorporating newly synthesized proteins. The relative expression of TIM23 was also increased in isolated midbrain mitochondria from TFEB-overexpressing compared to control mice (**Figure 29B**), indicating that TIM23 is properly trafficked and incorporated into the mitochondria, and at the same time corroborating that mitochondrial protein import machinery is increased upon TFEB overexpression.

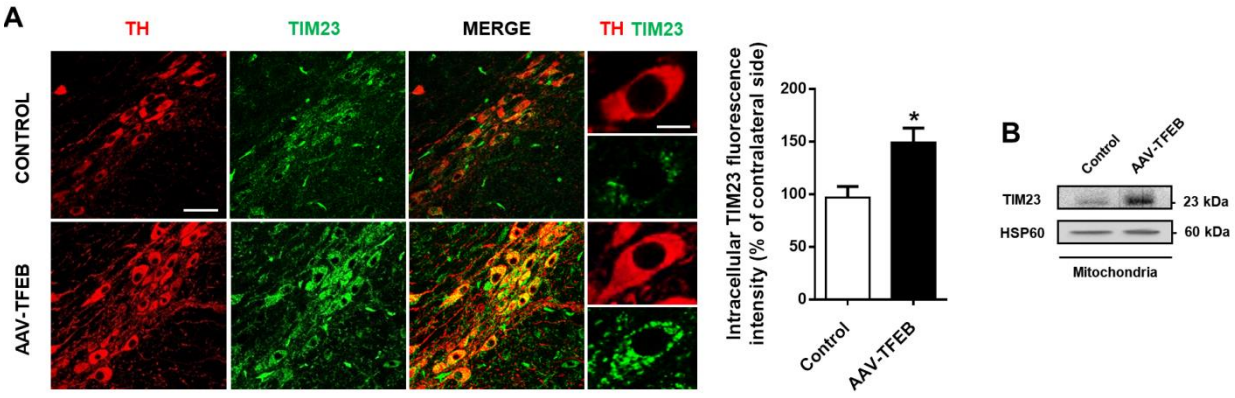

Figure 29. Mitochondrial protein import machinery is increased in TFEB-overexpressing neurons. (**A**) Left, representative confocal images of a double immunofluorescence for TH (red) and TIM23 (green) in SN sections of mice injected with vehicle (*n* = 6) or AAV-TFEB (*n* = 5). Scale bar = 50 µm and 10 µm (zoom). Right, quantification of TOM20 fluorescence intensity in SN dopaminergic neurons of both groups of mice, represented as a percentage of the non-injected side; Mann-Whitney test. *P < 0.05 compared to control. (**B**) Western blot analyses of TIM23 in isolated midbrain mitochondria of AAV-TFEB-injected mice (pool of *n* = 10 midbrains) and vehicle-injected mice (pool of *n* = 10 midbrains). In all panels, samples were collected 5 weeks after AAV-TFEB or vehicle injections. All data are represented as mean ± SEM.

4.6. TFEB confers a complete neuroprotection and counteracts atrophy in the MPTP mouse model of Parkinson's disease

Targeting TFEB has been used to boost the autophagy-lysosomal pathway as a strategy to eliminate protein accumulation in numerous *in vivo* experimental models of neurodegenerative diseases including PD (Decressac *et al.*, 2013), Alzheimer's disease (Polito *et al.*, 2014; Xiao *et al.*, 2014, 2015; Chandra *et al.*, 2018, 2019; Song *et al.*, 2019) and Huntington's disease (Tsunemi *et al.*, 2012; Rusmini *et al.*, 2019), among others, resulting in a neuroprotective effect. Here, we wanted to assess the neuroprotective effect of overexpressing TFEB in a PD model in which neurodegeneration is not induced by the accumulation of a protein. For that purpose we used the MPTP mouse model in which neuronal cell death is triggered by the inhibition of mitochondrial complex I (Bové and Perier, 2012). Thus, mice received a single unilateral stereotaxic inoculation of AAV-TFEB into the region immediately above right SNpc and after 4 weeks they were treated with a sub-acute MPTP regimen (30 mg/kg per day for five consecutive days). Mice were euthanized at different time points after the last MPTP administration depending on the experiment to be performed (**Figure 30A**).

First, we aimed to analyze TFEB overexpression levels by RT-qPCR and found that AAV-TFEB injection in MPTP mice ventral midbrain yielded a 23-fold increase of TFEB expression, ruling out an interaction between MPTP and the capacity of the AAV to properly overexpress TFEB (**Figure 30B**). Then, we assessed the integrity of the nigrostriatal dopaminergic system 21 days after the last MPTP injection, once the dopaminergic lesion is stabilized (Vila *et al.*, 2001; Perier *et al.*, 2007). Stereological dopaminergic cell counts showed that MPTP intoxication induced a 30% loss of SNpc dopaminergic neurons that was completely prevented on the side in which TFEB was overexpressed (**Figure 30C**). Vehicle stereotaxic injection had no effect on the MPTP-induced neuronal death (**Figure 30C**). To determine whether this total preservation of dopaminergic cell bodies was accompanied by a preservation of the dopaminergic terminals in the striatum, we measured the OD of TH staining in this region. MPTP intoxication induced a 75% reduction of striatal TH OD, and again we

found a complete preservation of the fibers in the TFEB-injected side (**Figure 30D**). The non-injected side of MPTP+AAV-TFEB mice appeared partially preserved, probably due to the existence of contralateral nigrostriatal projections, as anatomic and functional studies have demonstrated (Jaeger *et al.*, 1983; Fox *et al.*, 2016).

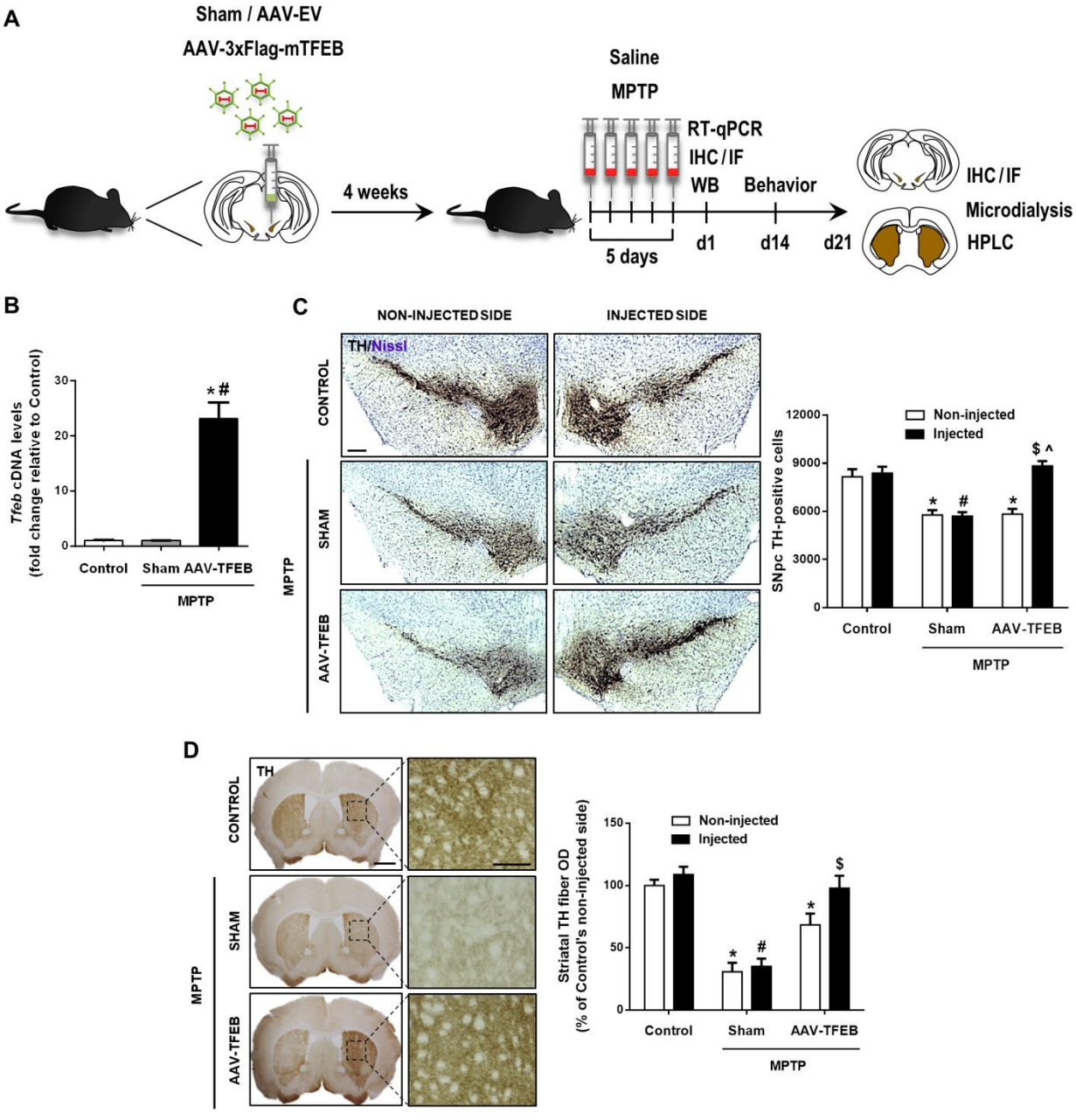

Figure 30. Neuroprotective effect of TFEB overexpression in the MPTP mouse model of Parkinson's disease. (**A**) Diagram representing the workflow and experiments carried out with MPTP+AAV-TFEB-injected mice. (**B**) *Tfeb* cDNA levels measured by RT-qPCR in ventral midbrain homogenates of MPTP-intoxicated mice previously injected with AAV-TFEB (n = 6) or vehicle (n = 6), and control mice treated with saline and previously injected with vehicle (n = 6); one-way ANOVA, *post*

hoc Tukey's. **P* < 0.05 compared to control. $^{\#}$*P* < 0.05 compared to MPTP+Sham group. (**C**) Left, representative photomicrographs of TH-immunostained SN counterstained with Nissl of MPTP-intoxicated mice previously injected with AAV-TFEB (*n* = 14) or vehicle (*n* = 10), and control mice treated with saline and previously injected with vehicle (*n* = 7). Scale bar = 200 μm. Right, stereological cell counts of dopaminergic neurons in SNpc of all groups of animals. (**D**) Left, representative photomicrographs of TH-immunostained striata of MPTP-intoxicated mice previously injected with AAV-TFEB (*n* = 14) or vehicle (*n* = 10), and control mice treated with saline and previously injected with vehicle (*n* = 7). Scale bar = 500 μm and 150 μm (zoom). Right, optical densitometry of striatal TH-positive dopaminergic fibers of all groups of animals. In panels C-E, two-way ANOVA *post hoc* Tukey's. *P < 0.05 compared to control non-injected side. $^{\#}$P < 0.05 compared to control injected side. $^{\$}$P < 0.05 compared to MPTP+Sham injected side. ^P < 0.05 compared to MPTP+AAV-TFEB non-injected side. All samples were collected 1 day (in panel B) or 21 days (in panels C-E) after the last administration of MPTP. All data are represented as mean ± SEM.

Morphological assessment of SNpc dopaminergic neurons in human postmortem samples has demonstrated that cell body shrinkage that is accompanied by a loss of phenotype that involves TH downregulation (Kastner *et al.*, 1993; Rudow *et al.*, 2008; Kordower *et al.*, 2013) is linked to programmed cell death in PD patients (Anglade *et al.*, 1997).

To determine whether cellular atrophy was also occurring in the MPTP mouse model, and could be prevented as we had hypothesized by TFEB overexpression, we measured the cell body size of SNpc dopaminergic neurons in MPTP-intoxicated mice before cell death occurred (one day post-MPTP) (**Figure 31A**, top). The average cell area of the MPTP-intoxicated mice decreased 20% compared to control mice, with this neuronal atrophy prevented by TFEB-overexpression (**Figure 31A**, bottom, left graph). To assess the evolution of these atrophic neurons, we next determined the cell body size of neurons 21 days after the last MPTP administration, when cell counts were performed and cell death was stabilized. We found that the surviving dopaminergic neurons were still atrophic. However, TFEB-overexpressing neurons reached the size that we had previously determined for the TFEB trophic effect, going from 25% to 37% of control neurons (**Figure 31A**, bottom, right graph), suggesting that TFEB overexpression can also reverse neuronal atrophy. Furthermore, we also assessed TH optical density of SNpc dopaminergic neurons

and found that MPTP-intoxicated neurons displayed a mild downregulation of TH as early as one day after the last MPTP injection. In contrast, MPTP mice treated with AAV-TFEB not only TH levels were preserved but also reached the levels (20%) we had previously determined for the TFEB trophic effect (**Figure 31B**), which was also apparent on visual inspection of cells under the light microscope (**Figure 31A**, top). To further confirm that TFEB was not only preventing neuronal atrophy but also inducing a *bona fide* neurotrophic effect even in MPTP conditions, we measured the dendritic arborization of SNpc dopaminergic neurons (**Figure 31C**, top). We found a decrease of dendritic arborization in MPTP-intoxicated neurons, partly probably attributed to TH downregulation. However, MPTP mice injected with AAV-TFEB displayed a 140% increase in dendrite branching (**Figure 31C**, bottom).

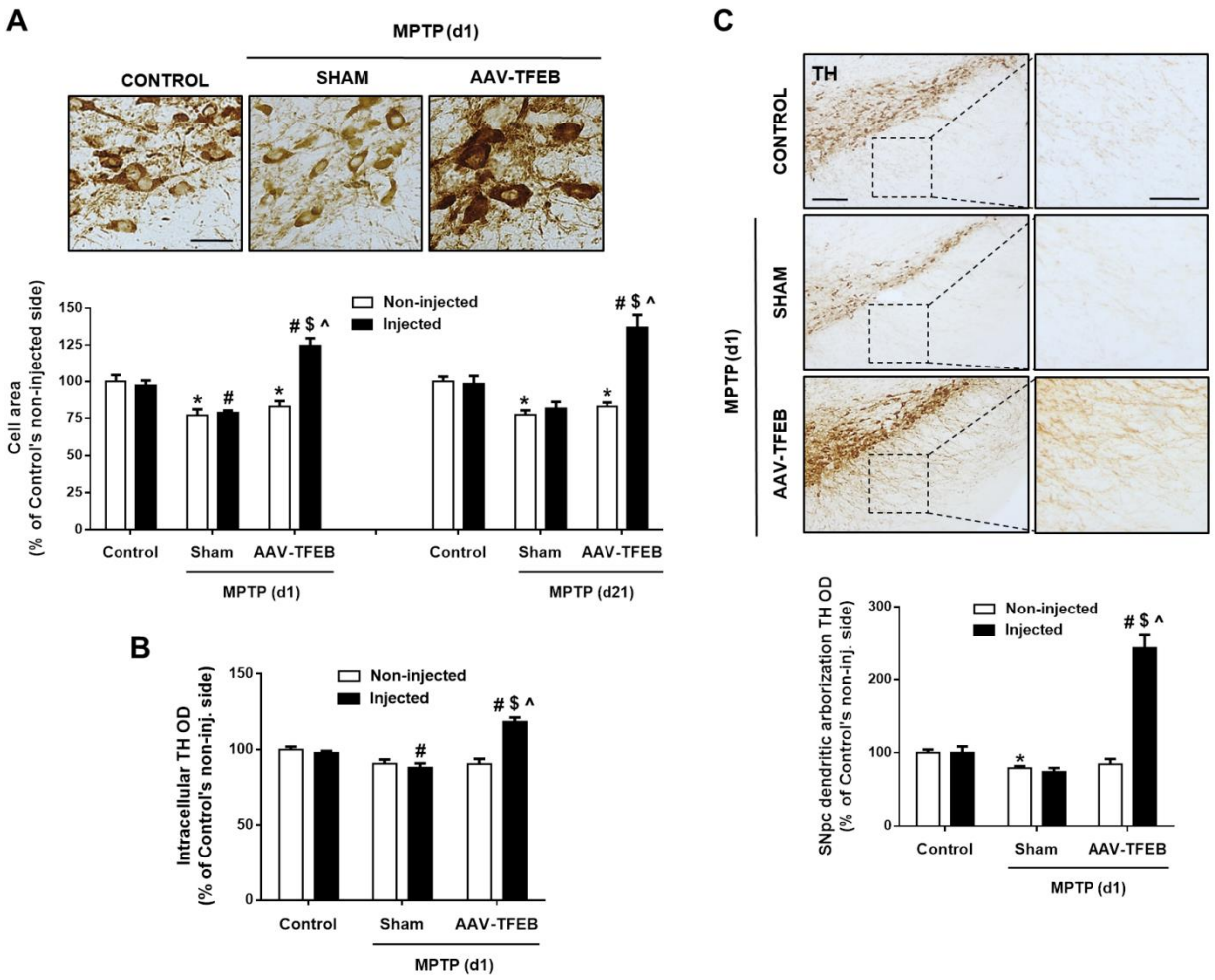

Figure 31. TFEB induces a neurotrophic effect that counteracts atrophy in the MPTP mouse model of Parkinson's disease. (**A**) Top, representative images of dopaminergic neuronal area of MPTP-intoxicated mice previously injected with AAV-TFEB (*n* = 6) or vehicle (*n* = 6), and control mice

treated with saline and previously injected with vehicle (*n* = 6). Scale bar = 30 μm. Bottom, average cell area of all groups of animals (*n* = 6-10 mice per group) at one day (MPTP d1) and at 21 days (MPTP d21) after the last MPTP injection. (**B**) Intraneuronal optical densitometry of tyrosine hydroxylase immunoreactivity of all groups of animals. (**C**) Top, representative images of SN sections showing SNpc dendritic arborization of MPTP-intoxicated mice previously injected with AAV-TFEB (*n* = 6) or vehicle (*n* = 6), and control mice treated with saline and previously injected with vehicle (*n* = 6). Scale bar = 150 μm and 200 μm (zoom). Bottom, quantification of SNpc dendritic arborization in all groups of animals. In all panels, two-way ANOVA, *post hoc* Tukey's. *P < 0.05 compared to control non-injected side. $^{\#}$P < 0.05 compared to control injected side. $^{\$}$P < 0.05 compared to MPTP+Sham injected side. ^P < 0.05 compared to MPTP+AAV-TFEB non-injected side. All samples were collected 1 day (in panel A left graph, B-C) or 21 days (in panel A right graph) after the last administration of MPTP. All data are represented as mean ± SEM.

To rule out any possible effect of the vector itself in the both observed TFEB neuroprotective and neurotrophic effects we carried out an additional experiment with an AAV empty vector (AAV-EV). Mice were stereotaxically injected with the AAV-EV and intoxicated with MPTP following exactly the same protocol that we followed for the AAV-TFEB mice. AAV-EV injection did not prevent MPTP-induced SNpc cell body loss (**Figure 32A**) or dopaminergic striatal terminals (**Figure 32B**). Accordingly, AAV-EV nor did affect dopaminergic cell size, neither in saline nor MPTP treatments (**Figure 32C**).

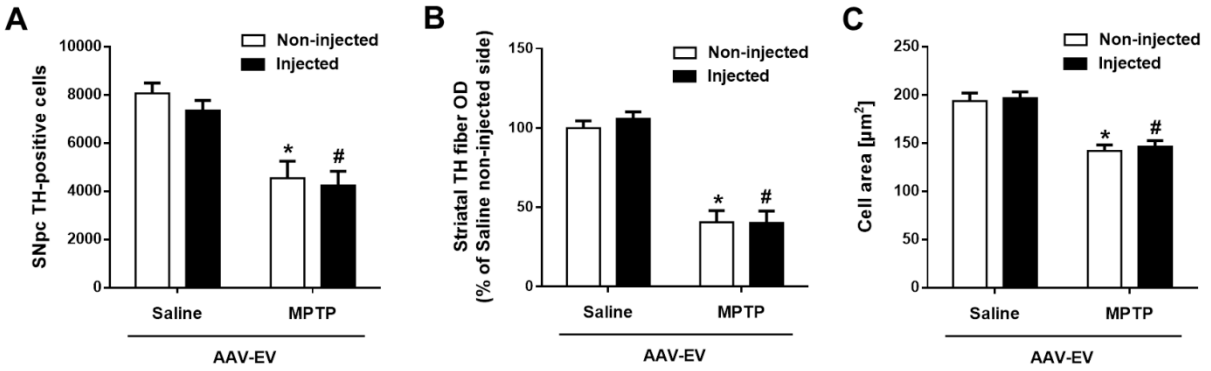

Figure 32. AAV-EV injection does not modify neuronal size and does not prevent neuronal cell loss or atrophy in the MPTP model. (**A**) Stereological cell counts of dopaminergic neurons in SNpc in MPTP-intoxicated mice previously injected with AAV-EV (*n* = 7), and mice treated with saline and previously injected with AAV-EV (*n* = 8). (**B**) Optical densitometry of striatal TH-positive dopaminergic fibers in MPTP-intoxicated mice previously injected with AAV-EV (*n* = 7), and mice treated with saline and previously injected with AAV-EV (*n* = 8). (**C**) Average cell area of dopaminergic neurons in MPTP-intoxicated mice previously injected with AAV-EV (*n* = 7), and mice treated with saline and previously

injected with AAV-EV (*n* = 7). In all panels, two-way ANOVA, post hoc Tukey's. *P < 0.05 compared to Saline+AAV-EV non-injected side. #P < 0.05 compared to Saline+AAV-EV injected side. Quantifications were performed 21 days after the last MPTP or saline administration. All data are represented as mean ± SEM.

Taken together, these results strongly confirm that TFEB overexpression confers a complete neuroprotection both at the level of cell body and axon terminals, as well as its neurotrophic effect counteracts neuronal atrophy in the MPTP mouse model of PD.

4.7. TFEB preserves neuronal function in the MPTP model

To determine whether TFEB expression was not only preserving the integrity of nigral dopaminergic neurons but also their function after MPTP intoxication, we carried out both histological and functional experiments. In this regard, we performed an immunohistochemistry against DAT in the striatum to corroborate that the occurrence of a synaptic failure in MPTP-intoxicated mice was completely prevented in TFEB-injected animals. Striatal DAT optical density was dramatically reduced in MPTP mice, reaching up to 70% depletion, concomitant with TH-positive fiber loss. In contrast, MPTP+AAV-TFEB mice displayed a significant conservation of DAT-positive fibers (**Figure 33A**), suggesting that synaptic function was preserved. To confirm this result, mice were subjected to a rotational behavioral test. Since TFEB is only overexpressed in the right substantia nigra there should be an imbalance between both sides in the MPTP-intoxicated mice if neuronal function is preserved in the AAV-TFEB injected side. This imbalance between the two dopaminergic systems triggers a measurable rotational behavior when a dopaminomimetic drug is systemically injected. When a drug that stimulates the release of dopamine, such as amphetamine, is administered, the rodent exhibits a contralateral rotation due to the fact that the non-lesioned side is able to release more dopamine than the lesioned side (Bové and Perier, 2012) (**Figure 33B**, left). AAV-TFEB MPTP-intoxicated mice

exhibited a sustained contralateral rotation unlike Sham MPTP-intoxicated mice after d-amphetamine systemic administration (**Figure 33B**, right). This result demonstrates that TFEB overexpression is indeed preserving neuronal function in the PD MPTP mouse model.

To further confirm that this rotational behavior was accompanied by a preservation of striatal monoamine levels, we measured the content of dopamine and its metabolites DOPAC and HVA in the striatum by HPLC. Although less striking than the preservation of dopaminergic nerve terminals, MPTP-intoxicated mice injected with AAV-TFEB displayed a markedly attenuation of monoamine levels compared to Sham+MPTP mice as early as 1 day after the last MPTP injection prior to neuronal cell death taking place. Similar results were obtained 21 days after the last MPTP injection when cell death was stabilized, being as well HVA levels completely preserved (**Figure 33C**). Again, we carried out *in vivo* microdialysis studies to further confirm that TFEB-overexpressing neurons were functional even in a parkinsonian scenario. When stimulated with the depolarizing agent veratridine, striatal dopamine release was significantly more prominent in AAV-TFEB MPTP-intoxicated mice compared to Sham MPTP-intoxicated animals (**Figure 33D**). Strikingly, d-amphetamine-evoked increase of extracellular dopamine levels in the striatum of MPTP TFEB-overexpressing mice were even much prominent than control mice (**Figure 33E**), demonstrating that TFEB expression increased the pool of dopamine in the model.

With these results we demonstrate that TFEB-induced neuroprotective and neurotrophic effects preserves neuronal integrity and function in the MPTP-based PD model.

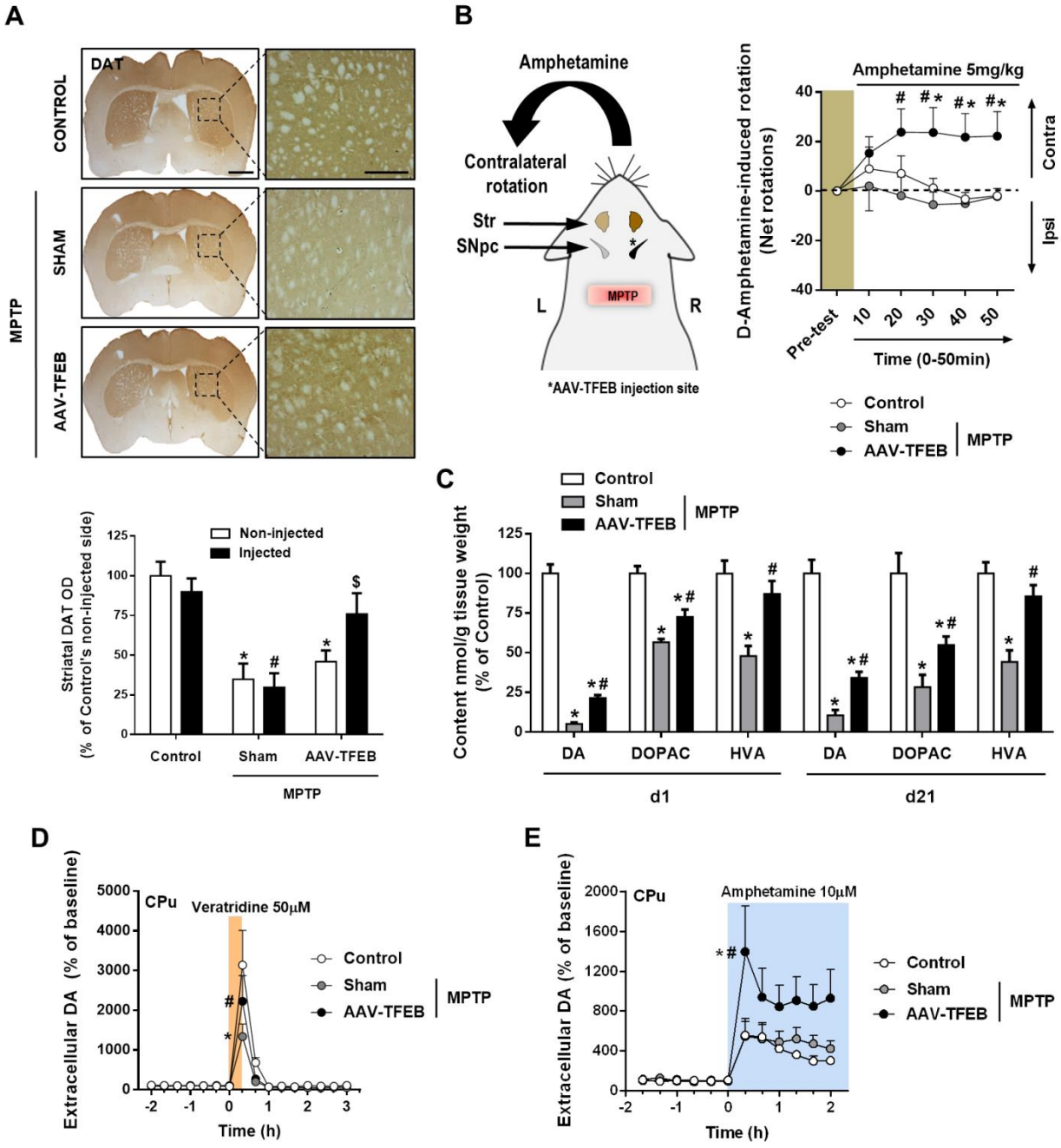

Figure 33. TFEB preserves neuronal function in the MPTP model of Parkinson's disease. (**A**) Top, representative photomicrographs of DAT-immunostained striata of MPTP-intoxicated mice previously injected with AAV-TFEB (*n* = 6) or vehicle (*n* = 6), and control mice treated with saline and previously injected with vehicle (*n* = 6). Scale bar = 500 μm and 150 μm (zoom). Bottom, optical densitometry of striatal DAT-positive dopaminergic fibers of all groups of animals; two-way ANOVA, *post hoc* Tukey's. *P < 0.05 compared to control non-injected side. $^{\#}$P < 0.05 compared to control injected side. $^{\$}$P < 0.05 compared to MPTP+Sham injected side. (**B**) Left, representative scheme of the effect following amphetamine injection (5 mg/kg) in MPTP AAV-TFEB-injected mice. L, left side. R, right side. Right, cumulative rotations induced by systemic administration of amphetamine during 10 min intervals 14 days after the last administration of MPTP. The net contralateral rotations were obtained as follows: total left − total right 360º turns. The test was performed with MPTP-intoxicated mice previously injected with AAV-TFEB (*n* = 9) or vehicle (*n* = 13), and control mice treated with

saline and previously stereotaxically injected with vehicle (*n* = 10). Ipsi, ipsilateral rotation. Contra, contralateral rotation. (**C**) Content of dopamine (DA) and its metabolites 3,4-Dihydroxyphenylacetic acid (DOPAC) and homovanillic acid (HVA) in striatal homogenates measured by HPLC of MPTP-intoxicated mice previously injected with AAV-TFEB (*n* = 9 at d1, *n* = 7 at d21) or vehicle (*n* = 7 at d1, n = 8 at d21), and control mice treated with saline and previously injected with vehicle (*n* = 6 at d1, *n* = 7 at d21); one-way ANOVA, *post hoc* Tukey's. **P* < 0.05 compared to control. $^{\#}$*P* < 0.05 compared to MPTP+Sham group. (**D-E**) Striatal DA relative amounts in MPTP-intoxicated mice previously injected with AAV-TFEB (*n* = 5) or vehicle (*n* = 5-10), and control mice treated with saline and previously stereotaxically injected with vehicle (*n* = 7), measured by microdialysis in the ipsilateral striatum following local (**D**) veratridine (50 µM) or (**E**) amphetamine (10 µM) administration. In panels B, D and E, two-way ANOVA for repeated measures, *post hoc* Tukey's. **P* < 0.05 compared to control. $^{\#}$P < 0.05 compared to MPTP+Sham. All samples were collected 1 day (in panel C left graph), 14 days (in panel B) or 21 days (in panel A, C right graph, D-E) after the last administration of MPTP. All data are represented as mean ± SEM.

4.8. MPTP-induced protein synthesis decline is prevented by TFEB overexpression

As previously discussed, cell size is mainly controlled by the 4E-BP/eIF4E and S6K1 pathways. We hypothesized that MPTP-induced neuronal dysfunctional atrophy was mediated by the inhibition of at least one of these two pathways that control protein biosynthesis, and that TFEB might be preventing this inhibition. To test this hypothesis, we first assessed the effect of MPTP in protein synthesis at the transcriptional level at 1 day after MPTP treatment. We measured the mRNA levels of *Rps6kb1* and *Eif4e* and both transcripts were notably decreased in MPTP-intoxicated mice, suggesting that MPTP shuts down protein synthesis machinery. In contrast, TFEB overexpression was able to completely prevent the diminution of both transcripts (**Figure 34A**). We next determined the total and Ser65-phosphorylated 4E-BP1 levels and found that MPTP triggered a dramatic reduction of this phosphorylated form showing no band in the western blot. This reduction was not prevented by TFEB overexpression at this time point (**Figure 34B**). When 4E-BP1 is phosphorylated on the sites located carboxy-terminal to the eIF4E-binding site, including Ser65 and Thr70, it releases from eIF4E. These phosphorylations cannot occur if 4E-BP1 is not previously phosphorylated on Thr37 and Thr46 (Gingras *et al.*,

1999). To determine whether these phosphorylations were also altered by MPTP intoxication and modulated by TFEB overexpression we measured the Thr37/46 phosphorylated-4E-BP1/non-Thr37/46 phosphorylated-4E-BP1 ratio. In this case, we found that MPTP intoxication substantially reduced this ratio and that this reduction was prevented by TFEB overexpression (**Figure 34C**).

Then, to assess whether eIF4E activity was also inhibited at a post-translational level we measured S209-phosphorylation that, although not required for translation initiation, has been shown to enhance the translation of specific proteins in neurons (Cao *et al.*, 2015), while its dephosphorylation has been linked to apoptosis (Bushell *et al.*, 2000). MPTP intoxication reduced S209-phosphorylated eIF4E levels by half compared to control mice, while TFEB overexpression prevented this diminution (**Figure 7D**). The fact that eIF4E phosphorylation is known to be mediated by MAP kinase interacting kinase 1 (MNK1) (Waskiewicz *et al.*, 1999), the downstream kinase of the ERK1/2 signaling pathway, may explain this prevention. In line with this, it has been demonstrated that the BDNF-induced upregulation of protein synthesis is triggered by the MNK1-mediated phosphorylation of eIF4E (Genheden *et al.*, 2015).

To determine whether S6K1 pathway was also affected in the MPTP mouse model of PD, we measured both S6K1 total and phosphorylated/activated protein levels. We found that MPTP intoxication did not induce any statistically significant variation of these forms, but TFEB overexpression in MPTP-intoxicated mice increased both of them, in particular it doubled the activated form and increased the activated/total protein ratio (**Figure 34E**).

These results demonstrate that neuronal atrophy is mediated by inhibition of the 4E-BP/eIF4E pathway in the MPTP mouse model, and that TFEB counteracts atrophy by the activation of both the eIF4E and S6K1 pathways.

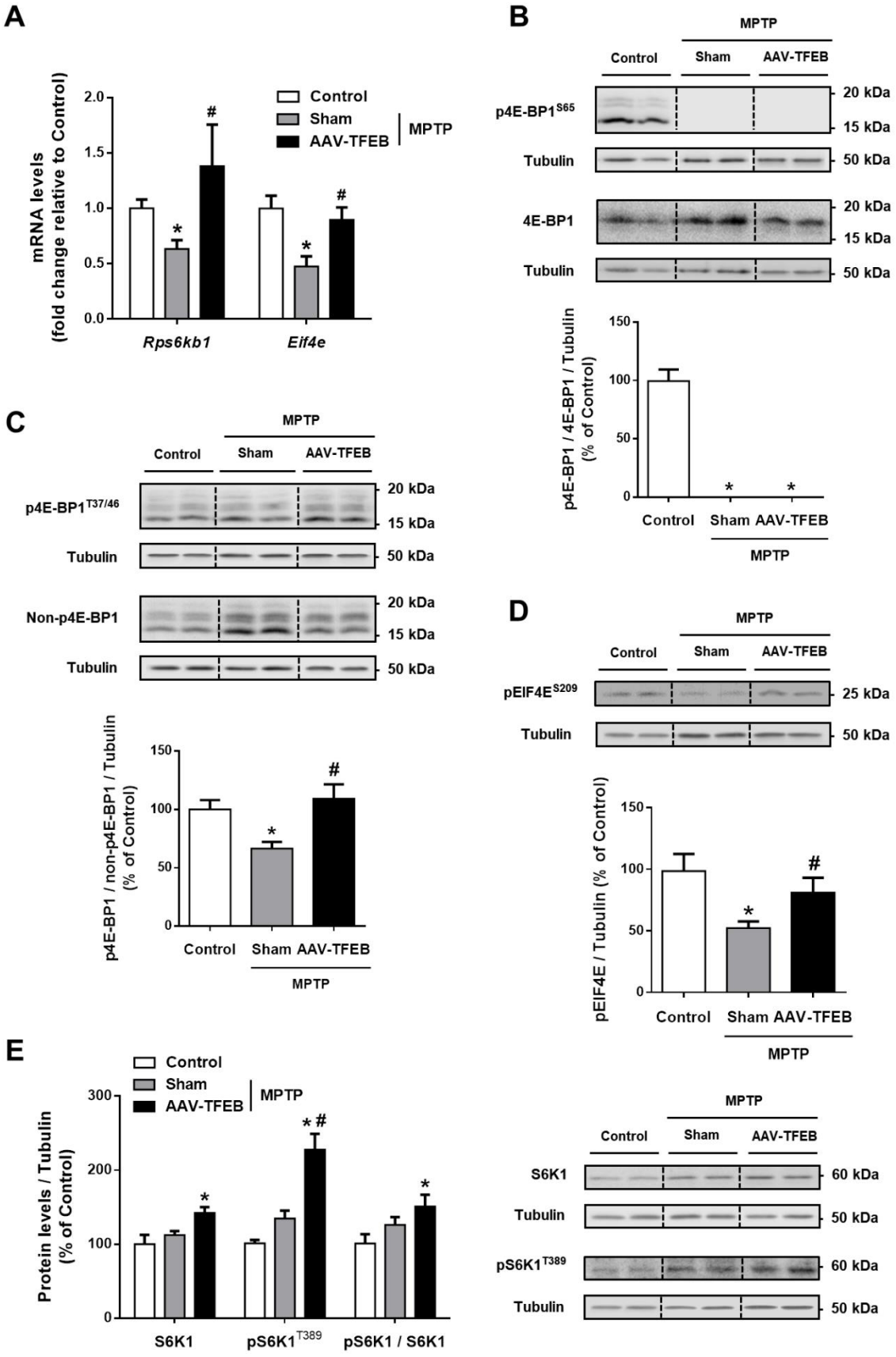

Figure 34. TFEB overexpression prevents the decline of protein synthesis that occurs in the MPTP model of Parkinson's disease. (**A**) *Rps6kb1* and *Eif4e* mRNA levels of ventral midbrain

homogenates in MPTP-intoxicated mice previously injected with AAV-TFEB (n = 7) or vehicle (n = 6), and control mice treated with saline and previously injected with vehicle (n = 6). (**B-E**) Representative western blot and protein levels of ventral midbrain homogenates in MPTP-intoxicated mice previously injected with AAV-TFEB (n = 7-8) or vehicle (n = 7), and control mice treated with saline and previously injected with vehicle (n = 5-6), of (**B**) Ser65-phosphorylated and total 4E-BP1, expressed as a ratio, (**C**) Thr-37/46 phosphorylated-4E-BP1/non-Thr-37/46 phosphorylated-4E-BP1 ratio, (**D**) S209-phosphorylated eIF4E, p-eIF4E^{S209}, and (**E**) S6K1, its activated form (pS6K1^{T389}) and the ratio. In all panels, one-way ANOVA, *post hoc* Tukey's. $^{*}P < 0.05$ compared to control. $^{\#}P < 0.05$ compared to MPTP+Sham group. All samples were collected 1 day after the last administration of MPTP prior to neuronal cell death taking place. All data are represented as mean ± SEM.

4.9. TFEB counteracts the autophagy-lysosomal defect in the MPTP model

We have previously reported that lysosomal depletion and a subsequent lysosomal-autophagy defect that involves accumulation of autophagic vacuoles precedes cell death in the MPTP model (Dehay *et al.*, 2010; Bové *et al.*, 2014). To determine whether TFEB overexpression could also prevent these events, we assessed by western blot the protein levels of several lysosomal and autophagic markers. As expected, MPTP intoxication induced lysosomal depletion, as determined by decreased levels of LAMP1, while TFEB overexpression was able to prevent this diminution (**Figure 35A**). TFEB-induced lysosomal enhancement was further confirmed with increased levels of lysosomal enzymes, such as cathepsin D, which was doubled compared to control mice (**Figure 35B**). As expected, lysosomal depletion was accompanied by a defective autophagic degradation in Sham MPTP mice, as determined by an increase of LC3-II/LC3-I ratio, whereas TFEB overexpression was able to counteract this autophagic accumulation (**Figure 35C**). To confirm that these events were occurring in the SNpc dopaminergic neurons, we performed double immunofluorescence experiments for TH and LAMP1. MPTP-intoxicated mice indeed showed a clear decrease in LAMP1 immunofluorescence inside the SNpc dopaminergic neurons that was completely prevented in TFEB-overexpressing mice (**Figure 35D**). We hypothesized that MPTP intoxication would also impair lysosomal damage at a transcriptional level, and that TFEB overexpression would be able to counteract this defect. To test this hypothesis, we measured mRNA levels of the lysosomal proteins *Lamp1* and *Ctsd*. Levels of both

mRNAs were diminished in MPTP-intoxicated mice, and significantly increased in TFEB-overexpressing compared to Sham mice after MPTP intoxication (**Figure 35E**).

These results demonstrate that TFEB counteracts the autophagy-lysosomal defect in the MPTP model, as we have previously shown in an *in vitro* system (Dehay *et al.*, 2010).

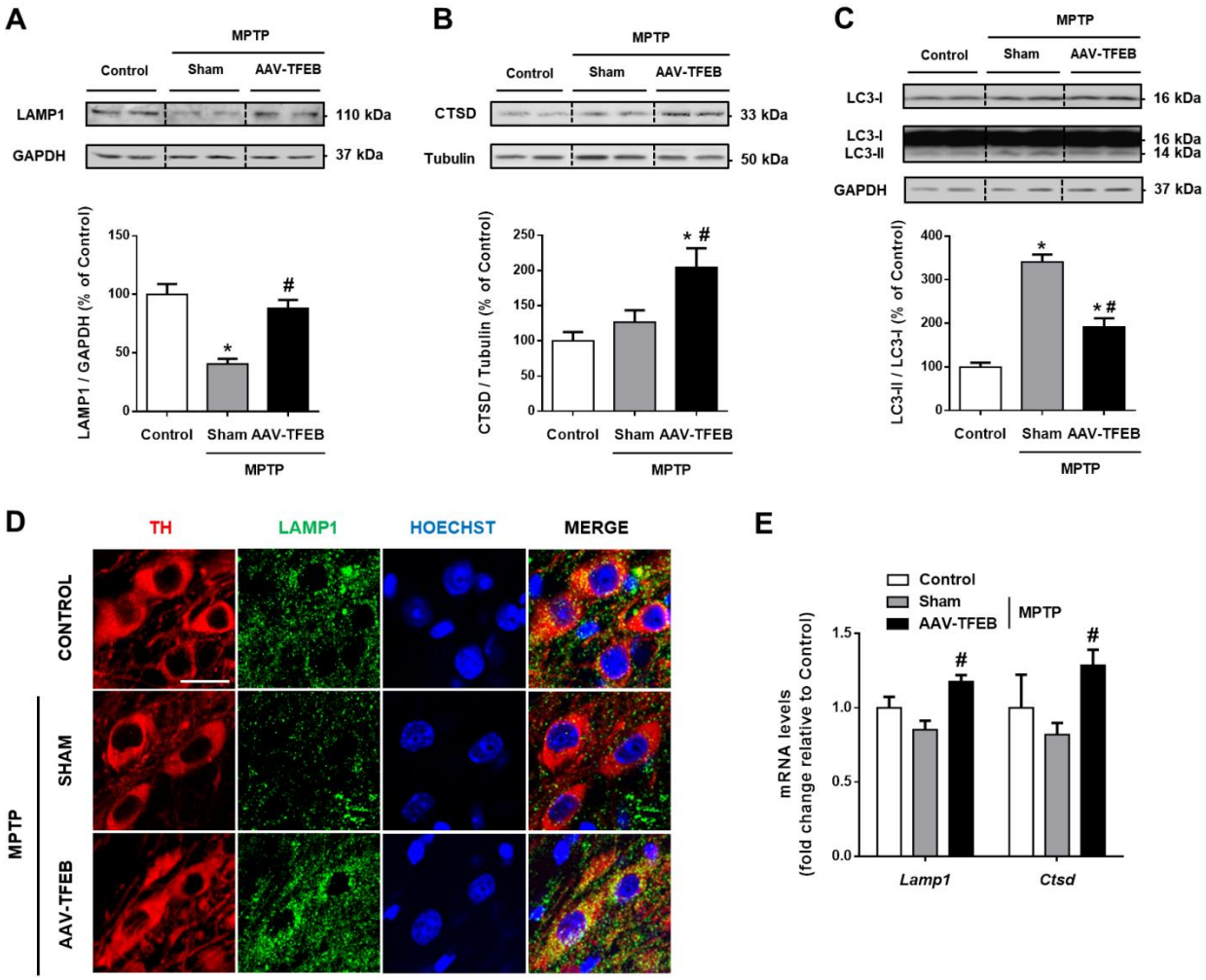

Figure 35. Overexpression of TFEB counteracts the autophagy-lysosomal impairment of the MPTP mouse model of Parkinson's disease. (**A-C**) Representative western blots and protein levels of ventral midbrain homogenates in MPTP-intoxicated mice previously injected with AAV-TFEB (*n* = 7-8) or vehicle (*n* = 7), and control mice treated with saline and previously injected with vehicle (*n* = 6), of (**A**) LAMP1, (**B**) cathepsin D (CTSD) and (**C**) LC3-I and II. (**D**) Confocal images showing immunofluorescence for TH (red), LAMP1 (green) and nuclei (blue). Scale bar = 25 µm. (**E**) *Lamp1* and *Ctsd* mRNA levels in ventral midbrain extracts in MPTP-intoxicated mice previously injected with AAV-TFEB (*n* = 6) or vehicle (*n* = 6), and control mice treated with saline and previously injected with vehicle (*n* = 4-6). In all panels, one-way ANOVA *post hoc* Tukey's. **P* < 0.05 compared to control. $^{\#}P$ < 0.05 compared to MPTP+Sham. Samples were collected 1 day after the last administration of MPTP prior to neuronal cell death taking place. All data are represented as mean ± SEM.

4.10. Knocking down the master transcriptional repressor of autophagy ZKSCAN3 does not prevent MPTP-induced neurodegeneration or atrophy

TFEB sustained overexpression triggers a pleiotropic neurotrophic effect that involves a myriad of direct and indirect targets of this transcription factor. To elucidate which are the most relevant events or pathways and how they work synergistically to build up this neurotrophic/neuroprotective effect is not an easy task. So far, as we discussed above, it is believed that TFEB neuroprotective effect is mainly due to its effect on the autophagy-lysosomal pathway. Our results demonstrate that TFEB is indeed boosting this degradation system but also activating pro-survival pathways that could explain by themselves the neuroprotective effect. Therefore, we believe that it is very relevant for the neurodegenerative diseases field to determine the actual neuroprotective extent of inducing lysosomal biogenesis and autophagy. ZKSCAN3 is a master transcriptional repressor of autophagy and lysosome biogenesis and function, and is regulated in an opposite manner than TFEB by starvation (Chauhan *et al.*, 2013). As previously demonstrated, knocking down ZKSCAN3 activates autophagy and increases lysosomal biogenesis (Chauhan *et al.*, 2013). Therefore, we decided to knock down ZKSCAN3 in mice dopaminergic neurons with an adeno-associated vector containing the sequence coding a short double-stranded hairpin RNA (shRNA) directed against rodent ZKSCAN3 (AAV-shZKSCAN3), and test its neuroprotective effect in the same MPTP PD model that we tested TFEB neuroprotective effect (**Figure 36A**).

To demonstrate that we were certainly knocking down ZKSCAN3 we performed an immunofluorescence assay that showed a strong nuclear staining in the control group that was dramatically reduced in the shZKSACN3 group. The reduction of the intensity elicited was more than 60% (**Figure 36B**). Then, we assessed the levels of the lysosomal marker LAMP1 by means of measuring substantia nigra intensity in midbrain sections after performing immunohistochemistry, and we found a 30% increase in LAMP1 intensity in shZKSCAN3 ventral midbrains (**Figure 36C**). We also performed an immunofluorescence for the autophagic vacuole marker LC3 and

analyzed LC3 puncta inside dopaminergic neurons, which displayed higher amounts of autophagosomes in ZKSCAN3-knocked down mice (**Figure 36D**).

These results are compatible with an increase of lysosomal biogenesis and activation of autophagy that have been described *in vitro* with several cell lines, including a neuronal cell line, after knocking down ZKSCAN3 (Chauhan *et al.*, 2013).

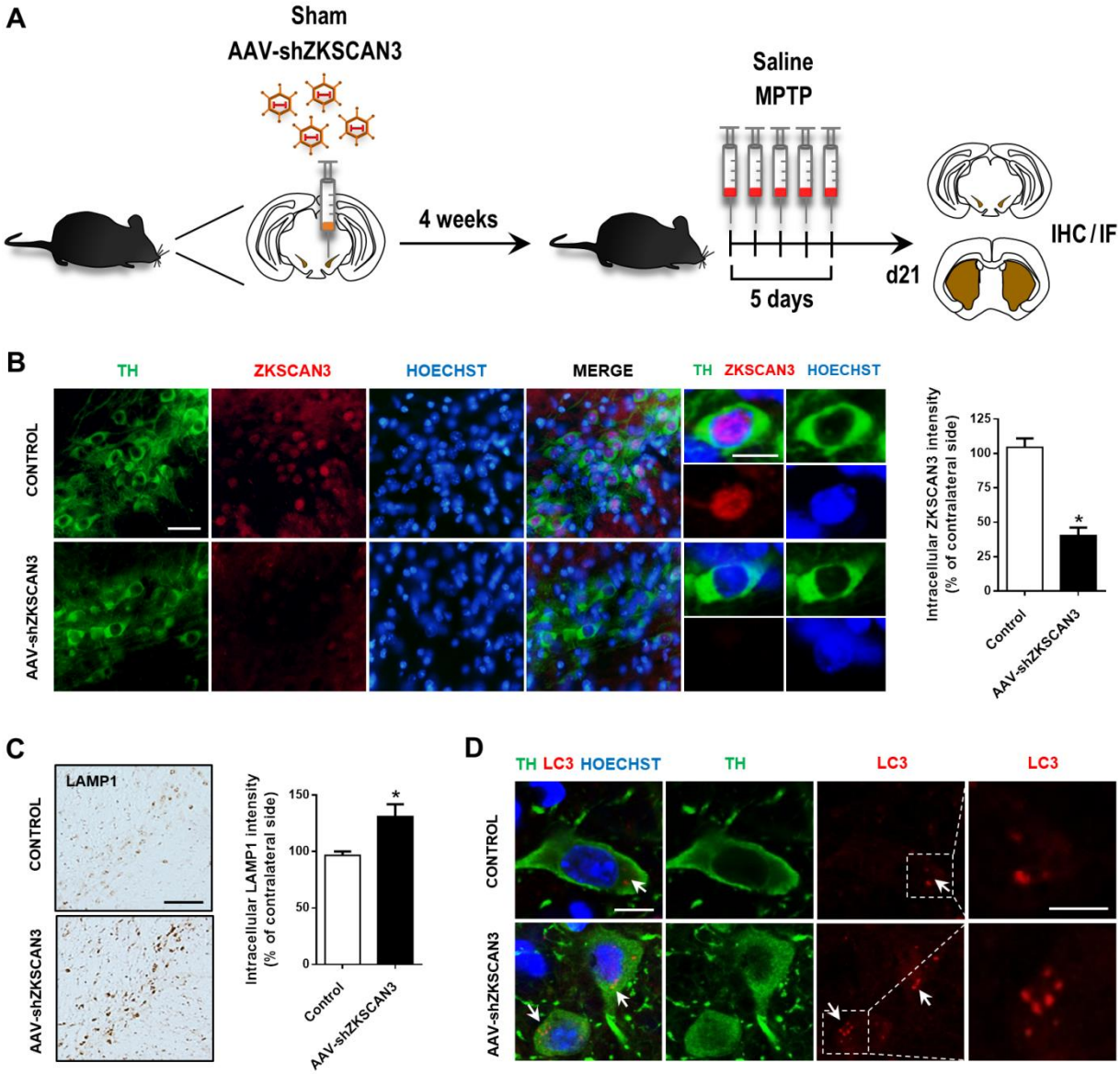

Figure 36. Autophagy-lysosomal pathway is activated after knocking down the master transcriptional repressor of autophagy ZKSCAN3. (**A**) Diagram representing the workflow and experiments carried out with MPTP+AAV-shZKSCAN3-injected mice. (**B**) *Left*, Representative images showing immunofluorescence for TH (green), ZKSCAN3 (red) and nuclear staining (blue) in SN sections in mice after vehicle (n = 5) or AAV-shZKSCAN3 (n = 6) nigral injection. Scale bar = 50 µm and 20 µm (zoom). *Right*, Quantification of intracellular ZKSCAN3 immunolabeling intensity of both

groups of animals. (**C**) Left, Representative photomicrographs of LAMP1-immunostained SN in mice after vehicle (*n* = 4) or AAV-shZKSCAN3 (*n* = 4) nigral injection. Scale bar = 200 μm. Right, Quantification of intracellular LAMP1 immunolabeling intensity of both groups of animals. (**D**) Representative images showing immunofluorescence for TH (green), LC3 (red) and nuclear staining (blue) in SN sections of mice after vehicle (*n* = 4) or AAV-shZKSCAN3 (*n* = 4) nigral injection. White arrows indicate autophagosomes, as determined by LC3 puncta staining. Scale bar = 10 μm and 5 μm (zoom). In panels B-C, Mann-Whitney test. **P* < 0.05 compared to control. Samples were collected 21 days after the last MPTP or saline administration. All data are represented as mean ± SEM.

Then, we assessed the integrity of the nigrostriatal dopaminergic system in the MPTP model in control and AAV-shZKSCAN3 mice at day 21 after the last MPTP injection. Stereological dopaminergic cell counts were performed in all groups and we observed that, although MPTP intoxication induced a significant cell body loss, it was not prevented in MPTP AAV-shZKSCAN3 mice group (**Figure 37A**). We next assessed the integrity of the dopaminergic terminals in the striatum by measuring the optical density of TH-positive fibers in this region. MPTP intoxication induced a 65% reduction of striatal OD and, again, the same levels of TH-positive striatal terminals were detected in MPTP-intoxicated mice group that were injected with AAV-shZKSCAN3 (**Figure 37B**), indicating that neither cell bodies nor axon terminals were protected in MPTP ZKSCAN3-knocked down mice. No neurodegeneration was detected in saline AAV-shZKSCAN3-injected animals, ruling out a deleterious effect of knocking down this transcription factor in SNpc dopaminergic neurons (**Figure 37A**, **B**).

These results suggest that boosting the autophagy-lysosomal pathway does not suffice *per se* to counteract neurodegeneration in this PD model.

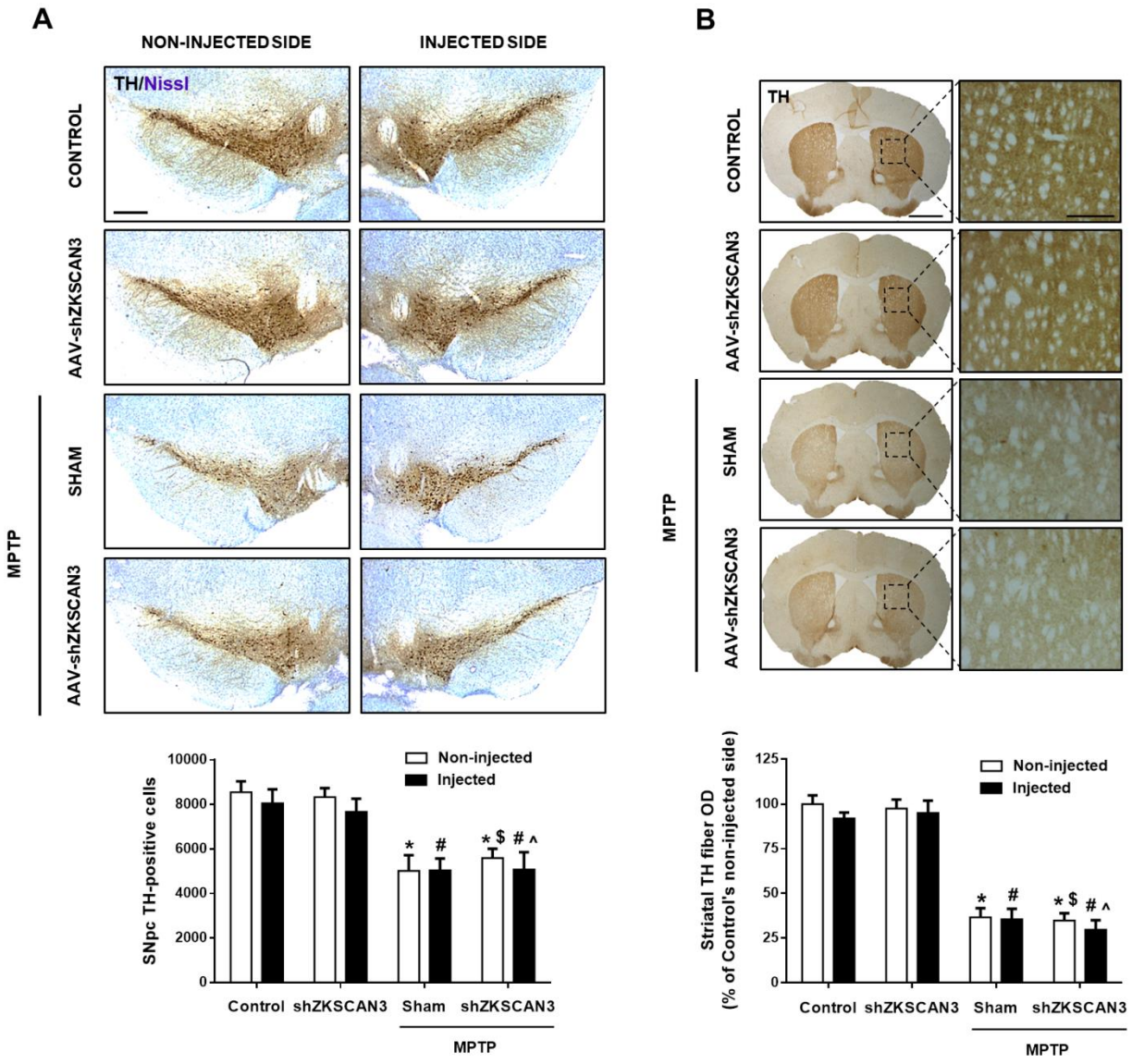

Figure 37. Boosting the autophagy-lysosomal pathway is not sufficient to induce neuroprotection in the MPTP mouse model of Parkinson's disease. (**A**) Top, representative photomicrographs of TH-immunostained SN counterstained with Nissl of MPTP-intoxicated mice previously injected with AAV-shZKSCAN3 (*n* = 5) or vehicle (*n* = 5), and mice treated with saline and previously injected with vehicle (*n* = 6) or AAV-shZKSCAN3 (*n* = 5). Scale bar = 250 µm. Bottom, stereological cell counts of dopaminergic neurons in SNpc of all groups of animals. (**B**) Top, representative photomicrographs of TH-immunostained striata of MPTP-intoxicated mice previously injected with AAV-shZKSCAN3 (*n* = 8) or vehicle (*n* = 7), and mice treated with saline and previously injected with vehicle (*n* = 7) or AAV-shZKSCAN3 (*n* = 7). Bottom, optical densitometry of striatal TH-positive dopaminergic fibers of all groups of animals. In both panels, two-way ANOVA *post hoc* Tukey's. *P < 0.05 compared to control non-injected side. $^{\#}$P < 0.05 compared to control injected side. $^{\$}$P < 0.05 compared to saline AAV-shZKSCAN3 non-injected side. ^P < 0.05 compared to saline AAV-shZKSCAN3 injected side. Samples were collected 21 days after the last MPTP or saline administration. All data are represented as mean ± SEM.

Furthermore, to confirm that activation of the autophagy-lysosomal system was not accompanied with the activation of ERK1/2 and AKT signaling pathways we measured the intensities after Thr202/Tyr204-phosphorylated/activated form of ERK1/2 and Ser473-phosphorylated form of AKT. No differences were observed neither in phospho-ERK1/2 (**Figure 38A**) nor phospho-AKT (**Figure 38B**) between control and AAV-shZKSCAN3 mice, indicating that these pro-survival signaling pathways are not activated in ZKSCAN3-knocked down animals. We next measured the cell body size of SNpc dopaminergic neurons in the MPTP model in control and AAV-shZKSCAN3 mice. As we expected, we found that under MPTP conditions dopaminergic neurons were still atrophic after silencing ZKSCAN3 (**Figure 38C**), indicating that activation of ERK1/2 and AKT pathways may be crucial for TFEB-induced neurotrophic effect.

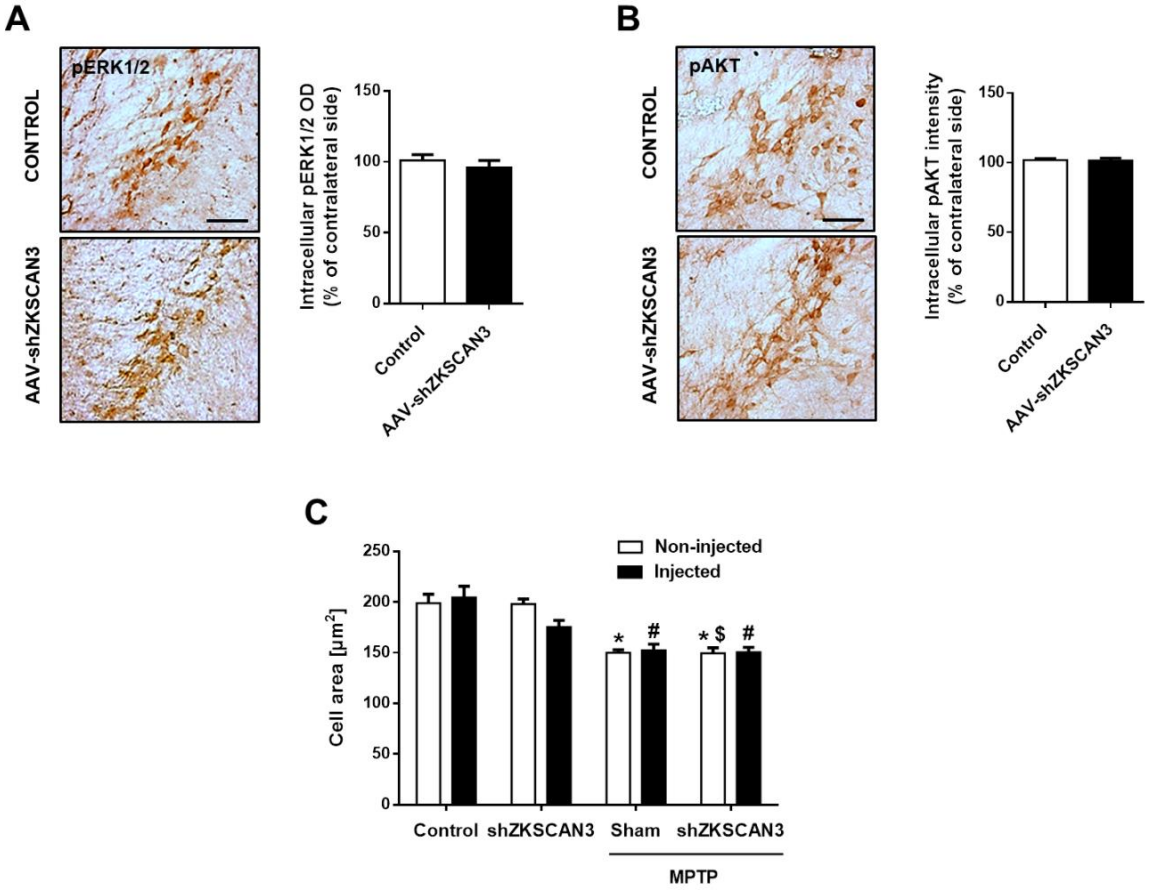

Figure 38. Knocking down ZKSCAN3 does not reverse MPTP-induced neuronal atrophy. (**A-B**) Left, representative photomicrographs of (A) Thr202/Tyr204-phosphorylated ERK1/2 and (B) S473-phosphorylated AKT-immunostained SN in mice after vehicle (*n* = 4) or AAV-shZKSCAN3 (*n* = 4)

nigral injection. Scale bar = 125 μm. Right, quantification of intracellular (A) Thr202/Tyr204-phosphorylated ERK1/2 and (B) S473-phosphorylated AKT-immunolabeling intensity of both groups of animals; Mann-Whitney test. (**C**) Average cell area of dopaminergic neurons in MPTP-intoxicated mice previously injected with AAV-shZKSCAN3 (*n* = 5) or vehicle (*n* = 5), and mice treated with saline and previously injected with vehicle (*n* = 6) or AAV-shZKSCAN3 (*n* = 6); two-way ANOVA, *post hoc* Tukey's. *P < 0.05 compared to control non-injected side. $^{\#}$P < 0.05 compared to control injected side. $^{\$}$P < 0.05 compared to saline AAV-shZKSCAN3 non-injected side. In all panels, samples were collected 21 days after the last MPTP or saline administration. All data are represented as mean ± SEM.

4.11. Mitochondria-mediated cell death is counteracted at multiple levels by TFEB overexpression

In PD, the mitochondrial/intrinsic pathway is believed to play a greater role in triggering programmed cell death than the extrinsic pathway (Venderova and Park, 2012). We have previously demonstrated that dopaminergic neurodegeneration in the MPTP model occur by activation of the intrinsic apoptotic pathway (Bové and Perier, 2012; Perier *et al.*, 2012) through the cytochrome c release followed by activation of caspase-9 (Perier *et al.*, 2005). Taking into account the above shown results demonstrating that TFEB overexpression was activating ERK1/2 (**Figure 24**) and AKT pathways (**Figure 25**) and also inducing structural and morphological mitochondrial changes (**Figures 26-29**), we hypothesized that the neuroprotective effect elicited by TFEB overexpression in the MPTP model may also involve the regulation of pro- and anti-apoptotic mechanisms by targeting the mitochondria-mediated cell death pathway. In fact, both AKT and ERK pathways are known to block this apoptotic pathway at multiple levels by: (i) inducing a transcriptional repression or decreasing the activity of pro-apoptotic molecules, such as BIM and various caspases, being the former one of the most powerful killers among the BH3-only proteins because its ability to bind to all Bcl-2 family of pro-survival proteins and thereby facilitating BAX activation and cytochrome c release (Letai *et al.*, 2002; Kuwana *et al.*, 2005; Perier *et al.*, 2007); and (ii) upregulating anti-apoptotic proteins, such as BCL-XL, via enhancement both its transcription and activity (Lu and Xu, 2006; Levy *et al.*, 2009; Winter *et al.*, 2011). Moreover, while inducing fusion

prevents cell death induced by several stimuli including parkinsonian toxins (Chen *et al.*, 2005; Zorzano and Claret, 2015), cells unable to react with mitochondrial hyperfusion are more vulnerable to stress and programmed cell death (Chen *et al.*, 2005; Tondera *et al.*, 2009; Rolland *et al.*, 2013; Zorzano and Claret, 2015).

To delve further into this concept, we started by measuring by western blot the levels of BCL-XL, an anti-apoptotic protein that when overexpressed was shown to block mitochondria-mediated cell death by inhibiting cytochrome c release (Reshi *et al.*, 2017). We found that BCL-XL levels were 30% raised in ventral midbrain homogenates of AAV-TFEB-injected mice when compared to control mice (**Figure 39A**). To determine whether this increase was indeed due to an increase of BCL-XL into mitochondria, we also measured BCL-XL levels in isolated midbrain mitochondria of TFEB-overexpressing mice, and found that it was markedly increased compared to mitochondria of control mice (**Figure 39B**). We next measured the levels of VDAC1, which is known to play a role in programmed cell death by inducing mitochondrial outer membrane permeabilization and the subsequent cytochrome c release and programmed cell death (Rostovtseva and Bezrukov, 2008; McCommis and Baines, 2012; Weisthal *et al.*, 2014). We found that VDAC1 levels were reduced by half in ventral midbrain homogenates of AAV-TFEB injected mice (**Figure 39C**), as well as in isolated midbrain mitochondria (**Figure 39D**), demonstrating that VDAC1 downregulation may contribute to the generation of mitochondria that were less prone to programmed cell death. We have previously demonstrated that *Bcl2l11* transcript levels, corresponding to the pro-apoptotic protein BIM, peaked at 1 day after the last MPTP injection and covered the entire period of MPTP-induced apoptotic neuronal death (Perier *et al.*, 2007). Therefore, we decided to measure *Bcl2l11* transcript levels by RT-qPCR and we observed an induction of *Bcl2l11* mRNA levels 1 day after the last MPTP injection that it was completely prevented in MPTP AAV-TFEB-injected mice (**Figure 39E**), suggesting that TFEB overexpression was blocking the transcription of BIM. Because cytochrome c release activates caspase-9, we also decided to assess whether TFEB overexpression was able to inactivate caspase-9 in MPTP conditions. Phosphorylation of caspase-9 at Thr125 is

known to prevent its cleavage and the subsequent activation of the intrinsic apoptotic pathway (Allan and Clarke, 2009). There are three known possible protein kinases that can phosphorylate caspase-9 at Thr125: (i) ERK1/2 when activated by extracellular growth/survival signals; (ii) CDK1-cyclin B1 in mitosis; and (iii) DYRK1A, which regulates apoptosis during development (Allan and Clarke, 2009). Taking into account that ERK1/2 is activated in TFEB-overexpressing mice, we assessed Thr125-phosphorylated caspase-9 (pCASP9) levels in ventral midbrain homogenates of mice, before cell death occurred. MPTP intoxication reduced Thr125-pCASP9 levels by half compared to control mice, while TFEB overexpression in MPTP mice not only prevented the MPTP-induced diminution but also showed much higher levels than control mice (**Figure 39F**). This finding suggests that TFEB overexpression is also acting at the downstream level by blocking caspase-9, the main instigator of mitochondria-mediated cell death, thereby turning neurons less prone to cell death.

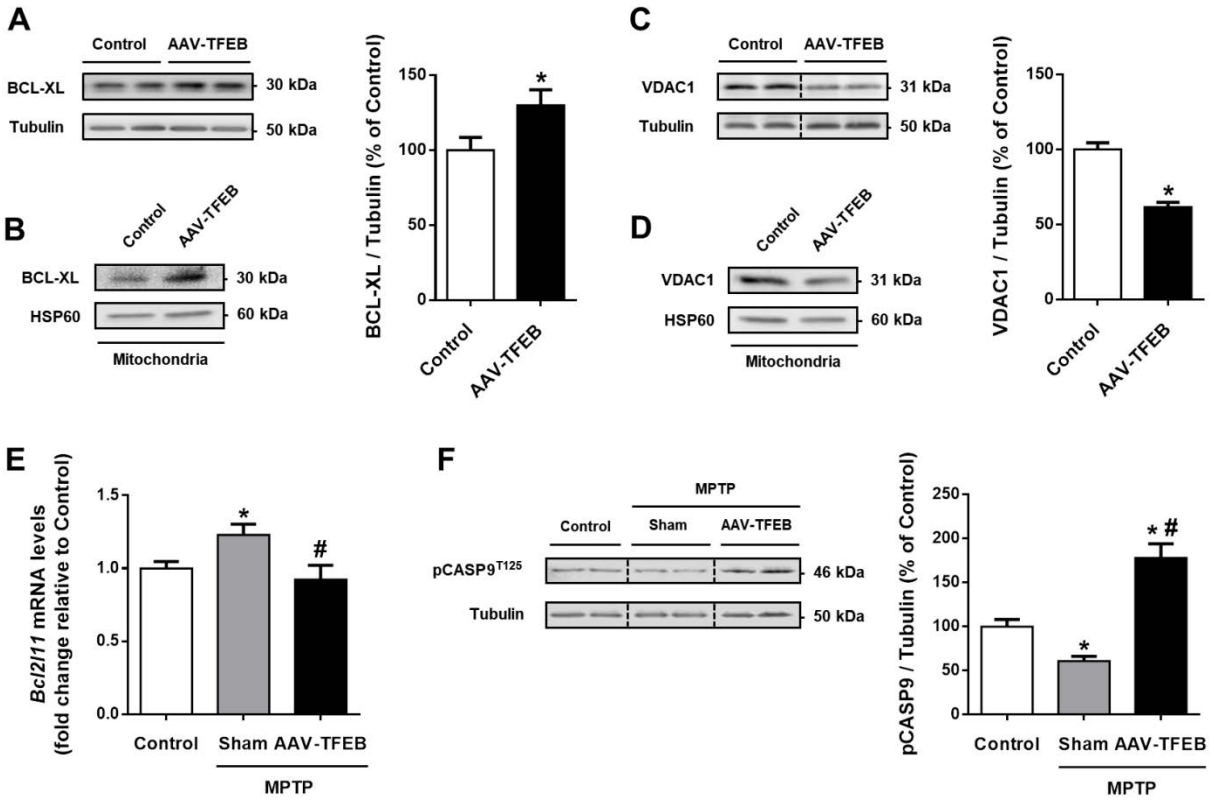

Figure 39. TFEB overexpression modulates mitochondria-mediated cell death effectors and turns neurons less prone to programmed cell death. (**A**, **C**) Representative western blot and protein levels of (**A**) the anti-apoptotic protein BCL-XL and (**C**) the pro-apoptotic protein VDAC1 from mice overexpressing TFEB (*n* = 6) compared to vehicle-injected mice (*n* = 6); Mann-Whitney test. *P <

0.05 compared to control. (**B**, **D**) Western blot analyses of (**B**) BCL-XL and (**D**) VDAC1 in isolated midbrain mitochondria of AAV-TFEB-injected mice (pool of *n* = 10 midbrains) and vehicle-injected mice (pool of *n* = 10 midbrains). (**E**) *Bcl2l11* mRNA levels of ventral midbrain homogenates in MPTP-intoxicated mice previously injected with AAV-TFEB (*n* = 7) or vehicle (*n* = 6), and control mice treated with saline and previously injected with vehicle (*n* = 5); one-way ANOVA *post hoc* Tukey's. **P* < 0.05 compared to control. $^{\#}P$ < 0.05 compared to MPTP+Sham. (**F**) Representative western blots and protein levels of Thr125-phosphorylated/inactivated caspase-9 (pCASP9) in ventral midbrain homogenates of MPTP-intoxicated mice previously injected with AAV-TFEB (*n* = 7) or vehicle (*n* = 7), and control mice treated with saline and previously injected with vehicle (*n* = 6); one-way ANOVA *post hoc* Tukey's. **P* < 0.05 compared to control. $^{\#}P$ < 0.05 compared to MPTP+Sham. In panels A-D, samples were collected 5 weeks after AAV-TFEB or vehicle injections. In panels E-F, samples were collected 1 day after the last administration of MPTP prior to neuronal cell death taking place. All data are represented as mean ± SEM.

We next ascertained whether these TFEB-induced changes of mitochondria-mediated cell death modulators were indeed contributing to block cytochrome c release of mitochondria in TFEB-overexpressing mice. First, we carried out a validation study in which isolated midbrain mitochondria were incubated with MPTP's active metabolite, MPP^+, and/or different amounts of recombinant BAX. After centrifugation, both pellets and supernatants were subjected to western blot anaylses in order to assess cytochrome c release (**Figure 40A**). Accordingly to our previous work (Perier *et al.*, 2005), this experiment confirmed that in purified midbrain mitochondria only when inhibition of complex I is accompanied by an increase of a cell death agonist, such as BAX, cytochrome c located in the mitochondrial membrane space is significantly released to the cytosol (**Figure 40B**), triggering mitochondria-mediated cell death. Importantly, none of the tested conditions (complex I inhibition by MPP^+, recombinant BAX, or combination of both) caused a release of the matrix mitochondrial heat shock protein 60 (HSP60), ruling out the possibility that the cytochrome c release observed by combining both MPP^+ and recombinant BAX resulted from a mitochondrial structural damage (**Figure 40B**).

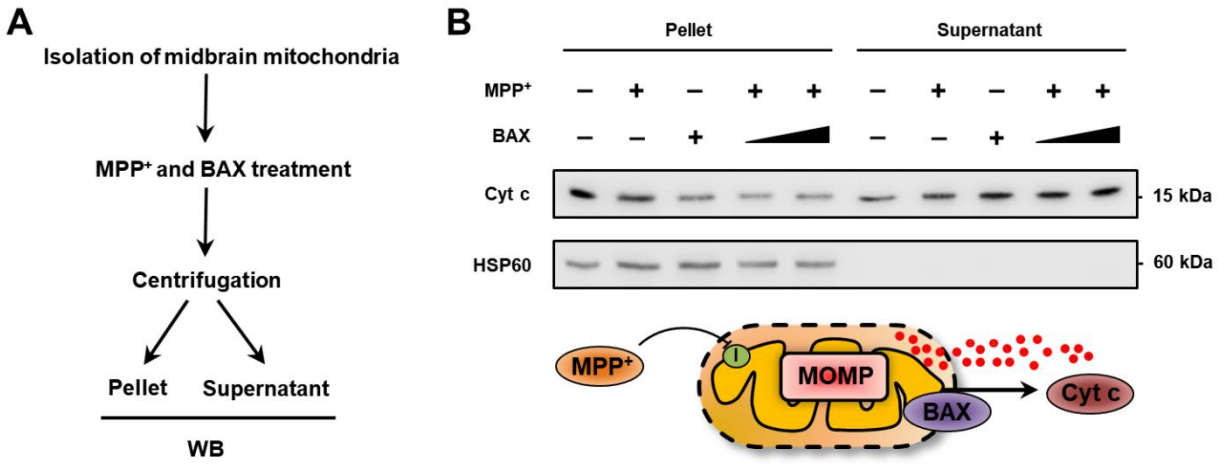

Figure 40. Complex I inhibition promotes BAX-dependent cytochrome c release. (**A**) Diagram representing the workflow of cytochrome c release experiments in isolated midbrain mitochondria. (**B**) Combined complex I inhibition (100 µM MPP^+) and incubation with recombinant BAX (100-150 nM) trigger significant cytochrome c release from isolated midbrain mitochondria (pool of *n* = 10 midbrains), as assessed by western blot analyses. MOMP, mitochondrial outer membrane permeabilization.

Then, we performed the experiment with isolated midbrain mitochondria of vehicle and AAV-TFEB-injected mice. As expected and in agreement with our previous results (**Figure 40B**), we detected a marked release (32%) of mitochondrial cytochrome c when mitochondria of vehicle-injected mice were incubated with both MPP^+ and recombinant BAX (**Figure 41A**). In contrast, almost no cytochrome c was detected in the supernatant unlike the pellet of MPP^++BAX-treated isolated midbrain mitochondria from AAV-TFEB-injected mice (**Figure 41B**), indicating that TFEB overexpression was completely abolishing mitochondrial cytochrome c release. Incubation with alamethicin (Alm), which is a potent channel-forming antibiotic that allows the passive diffusion of cytochrome c (Ritov *et al.*, 1992), induced a complete cytochrome c release and was used in both groups of animals as a positive control of the experiment (**Figure 41A**, **B**).

Hence, these results demonstrate that the neuroprotective effect elicited by TFEB overexpression also involves anti-apoptotic mechanisms that target both upstream and downstream instigators of mitochondria-mediated cell death.

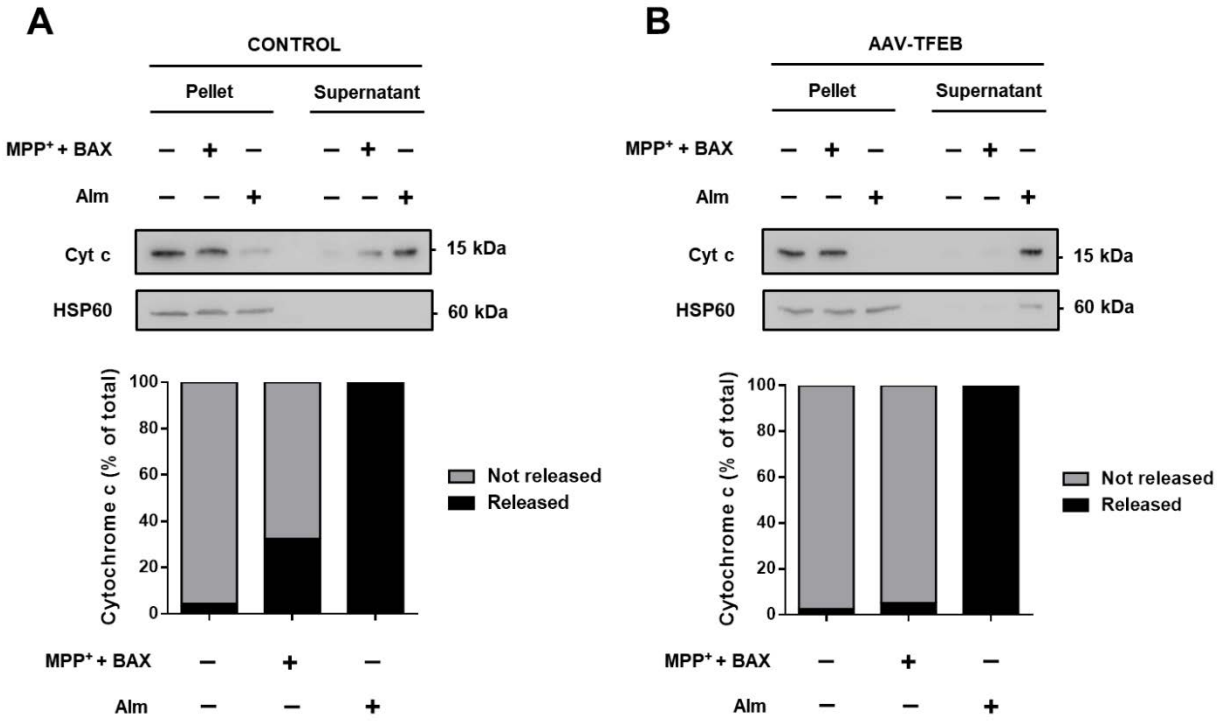

Figure 41. MPP$^+$/BAX-induced cytochrome c release is blocked by TFEB overexpression. (**A**-**B**) Assessment of cytochrome c release by western blot analyses in isolated midbrain mitochondria of (**A**) vehicle-injected mice (pool of *n* = 10 midbrains) and (**B**) AAV-TFEB-injected mice (pool of *n* = 10 midbrains) after combined incubation of MPP$^+$ (100 µM) and recombinant BAX (100 nM). Incubation with alamethicin (Alm, 40 µg/ml) was used as a positive control of the maximal cytochrome c release. In all panels, samples were collected 5 weeks after AAV-TFEB or vehicle injections.

DISCUSSION

5. Discussion

Our work has focused on the study of different molecular processes activated upon TFEB overexpression that may offer potential benefits in the context of PD. In this regard, we have demonstrated that TFEB overexpression in mice substantia nigra dopaminergic neurons by means of an adeno-associated viral vector drove a previously unknown *bona fide* neurotrophic effect giving rise to cell growth, neurite outgrowth, increased TH expression, enhanced dopamine handling and higher amounts of releasable dopamine in the striatum. We also demonstrated that TFEB overexpression boosted mTORC1 signaling, activated both pro-survival AKT and ERK1/2 signaling pathways, increased mitochondrial size, promoted mitochondrial fusion and enhanced mitochondrial protein import in substantia nigra dopaminergic neurons. In a parkinsonian scenario, we have unraveled that TFEB overexpression protected SNpc dopaminergic neurons both at the cell body level as well as striatal dopaminergic terminals and restored their activity/function and phenotype in the MPTP mouse model of PD. TFEB overexpression also counteracted the deleterious events like lysosomal depletion and mitochondria-mediated cell death that are linked to MPTP neurotoxicity and PD. Moreover, we also showed that knocking down the master repressor of autophagy ZKSCAN3 did not prevent MPTP-induced neurodegeneration or atrophy. Altogether, our results highlight TFEB as an alternative candidate to neurotrophic factor-based therapies for PD.

None of the clinical trials carried out to date to halt the progression of PD have been fully satisfactory (Ferreira *et al.*, 2018). One possible explanation for this systematic failure is that the majority of the strategies tested, with the exception of the neurotrophic factors, target only one of the pathogenic mechanisms involved in the development of the disease. This insight becomes even clearer after the failure of anti-apoptotic drugs such as TCH346 and CEP-1347 in clinical trials (Parkinson Study Group PRECEPT Investigators, 2007; Athauda and Foltynie, 2015). Another paradigmatic example is the use of antioxidants to reduce mitochondrial dysfunction

as a treatment for PD. Antioxidant drugs such as creatine or ubiquinone (coenzyme Q_{10}) successfully worked in preclinical studies (Beal, 2011; Tóth *et al.*, 2014) but again failed to show any clinical benefit in high-profile clinical trials (Athauda and Foltynie, 2015). It is precisely because of the holistic effect of the neurotrophic factors that neurotrophic factor-based therapy stands as the most promising disease-modifying therapeutic approach for PD. Since various neurotrophic factors have been reported to be decreased in PD patients (Toulorge *et al.*, 2016) and the subsequent neurotrophic signaling lost is believed to contribute to neuronal death (Decressac *et al.*, 2012b; Kang *et al.*, 2017), a large amount of interest in rising neurotrophic factors levels to protect and repair the degenerating nigrostriatal pathway has been for years a rationale for developing therapeutic strategies for PD. In this line, delivery of many neurotrophic factors conferred beneficial effects in diverse PD animal models (summarized in **Table 6**).

Table 6. List of neurotrophic factor-based strategies in PD animal models

Neurotrophic factor	PD model	Beneficial effect	References
GDNF	Mouse MPTP	Nigrostriatal protection, functional improvement	Tomac *et al.*, 1995 Date *et al.*, 1998
	Monkey MPTP	Nigrostriatal protection, functional improvement	Kordower *et al.*, 2000 Grondin *et al.*, 2002 Garbayo *et al.*, 2016
	Monkey MPTP	Functional improvement	Gerhardt *et al.*, 1999
	Marmoset MPTP	Nigral protection, functional improvement	Iravani *et al.*, 2001
	Rat 6-OHDA	Functional improvement	Hoffer *et al.*, 1994
	Rat 6-OHDA	Nigrostriatal protection	Rosenblad *et al.*, 1999
	Rat 6-OHDA	Nigrostriatal protection, functional improvement	Shults *et al.*, 1996 Choi-Lundberg *et al.*, 1998 Aoi *et al.*, 2000

	Rat 6-OHDA	Nigral protection	Sauer *et al.*, 1995 Winkler *et al.*, 1996
	AAV/LV-α-syn rat	None	Lo Bianco *et al.*, 2004 Decressac *et al.*, 2011
BDNF	Rat 6-OHDA	Functional improvement	Klein *et al.*, 1999
	Rat MPP^+	Nigral protection	Frim *et al.*, 1994
	Monkey MPTP	Nigral protection, functional improvement	Tsukahara *et al.*, 1995
Neurturin	Rat 6-OHDA	Nigrostriatal protection	Rosenblad *et al.*, 1999
	Rat 6-OHDA	Nigrostriatal protection, functional improvement	Horger *et al.*, 1998 Oiwa *et al.*, 2002 Fjord-Larsen *et al.*, 2005 Bartus *et al.*, 2011 Reyes-Corona *et al.*, 2017
	Monkey MPTP	Nigrostriatal protection, functional improvement	Kordower *et al.*, 2006
CDNF	Mouse MPTP	Nigrostriatal protection, functional improvement	Airavaara *et al.*, 2012
	Rat 6-OHDA	Nigrostriatal protection, functional improvement	Lindholm *et al.*, 2007 Voutilainen *et al.*, 2011 Bäck *et al.*, 2013 Ren *et al.*, 2013
	Marmoset 6-OHDA	Functional improvement	Garea-Rodríguez *et al.*, 2016

Neurotrophic factors are known to activate the RAS/ERK and PI3K/AKT signaling pathways (Besset *et al.*, 2000; Melillo *et al.*, 2001), both of which lead to the activation of several transcription factors and increase the expression of genes involved in neuronal survival, neurite outgrowth, synaptic plasticity and the

expression of enzymes involved in dopamine biosynthesis (Lei *et al.*, 2011; Olanow *et al.*, 2015). In fact, extensive evidence from experimental animal models of neurological diseases suggests that neurotrophic factors are both neuroprotective and neurorestorative (Domanskyi *et al.*, 2015; Olanow *et al.*, 2015). In particular, GDNF and neurturin have demonstrated a clear beneficial effect including nigrostriatal protection and functional improvement in multiple PD experimental models from rodents to nonhuman primates. In this line, several early phase clinical trials with neurotrophic factors like GDNF or CERE-120 (AAV-neurturin), or drugs that promote GDNF release, such as PYM50028, have shown the potential of neurotrophic factors; however, no neurotrophic factor-based protein or gene therapy has yet demonstrated sufficient efficacy in later phases (Domanskyi *et al.*, 2015; Ferreira *et al.*, 2018). This bewildering poor success could be explained by two facts: impaired axonal transport (Olanow *et al.*, 2015) and downregulation of GDNF/neurturin receptor RET (Decressac *et al.*, 2012b). Once GDNF or neurturin binds to the presynaptic striatal RET receptors, delivering signaling molecules to the soma relies on retrograde axonal transport (Ito and Enomoto, 2016). Consequently, the axonal impairment that occurs in PD may interfere with the activation of pro-survival pathways. RET downregulation in nigral dopaminergic neurons observed in PD patients also compromises the therapeutic effect of the GDNF family of ligands, and has encouraged scientists in the field to seek RET-independent neurotrophic factors. An alternative to delivering neurotrophic factors to overcome these hurdles is to directly activate the intracellular signaling pathways responsible for their effect (Ries *et al.*, 2006).

Ballabio and colleagues identified TFEB as the master transcriptional enhancer of both lysosomal biogenesis and autophagy by promoting the transcription of numerous lysosomal and autophagic genes that participate in multiple steps of autophagy from autophagosome initiation to the delivery of the cargo into the lysosomes for degradation (Sardiello *et al.*, 2009; Settembre *et al.*, 2011). This significant finding resulted in focusing on TFEB as a new therapeutic approach for those diseases in which lysosomal or autophagic dysfunction have been

documented, such as lysosomal storage disorders and neurodegenerative diseases. Some years ago, Decressac *et al.* found that TFEB expression in the nuclear compartment of SNpc dopaminergic neurons was much reduced when compared to healthy controls. In the same study, this phenomenon was not observed in the mesolimbic dopaminergic neurons of the ventral tegmental area (VTA), providing evidence that TFEB dysfunction is likely to contribute to PD pathogenesis since relative sparing of VTA neurons has been described in the disease (Dauer and Przedborski, 2003; Decressac *et al.*, 2013). Our group was the first in demonstrating that increasing TFEB activity may hold great promise for PD patients by combating neurodegeneration. In this line, we previously demonstrated that *in vitro* TFEB overexpression counteracted lysosomal depletion, increased autophagosomes clearance and attenuated MPP^+-induced cell death (Dehay *et al.*, 2010). Subsequently, a few other studies used TFEB to tackle neurodegeneration by enhancing the autophagy-lysosomal pathway and lowering aggregate load (Decressac *et al.*, 2013; Kilpatrick *et al.*, 2015). Nevertheless, all these works neglected the possibility that TFEB could exert a neuroprotective effect by activating also other molecular pathways not related to the autophagy-lysosomal system. This hypothesis was supported by the fact that the majority of putative direct targets of TFEB described to date is linked to a variety of biological processes that are not related to this degradative pathway (Palmieri *et al.*, 2011). In fact, only 64 out of 471 putative direct targets of TFEB are linked to the autophagy-lysosomal pathway, whereas hundreds of other genes controlled by TFEB are related to different cellular processes, such as mitochondrial metabolism, cell cycle and translation, mRNA processing, among others (Palmieri *et al.*, 2011).

Here, we have not only characterized the effect of TFEB overexpressing in activating the autophagy-lysosomal pathway in substantia nigra dopaminergic neurons but also other pathways implicated in different processes of the cell that could provide neuroprotective mechanisms, such as dopamine metabolism, mTORC1 signaling, pro-survival signaling pathways and mitochondria. All these pathways when deregulated not only have been described to contribute to PD pathogenesis but also

to cross-interact with each other (Levy *et al.*, 2009; Fahn *et al.*, 2011; Zeng *et al.*, 2018), generating an even more complex network and thereby limiting the effectiveness of single-targeting neuroprotective strategies. Hence, a neuroprotective approach that acts at multiple levels may increase the likelihood of developing a better disease-modifying treatment for PD.

We show here for first time that TFEB overexpression induces a trophic effect on SNpc dopaminergic neurons, characterized by a striking increase of cell area that increases SNpc volume, neurite outgrowth and increased phenotypic dopaminergic markers, mimicking RET-mediated effects (Hyman *et al.*, 1994; Grondin *et al.*, 2002; Herzog *et al.*, 2007; Lei *et al.*, 2011; Kramer and Liss, 2015; Olanow *et al.*, 2015). These findings are unexpected and surprising since the up-to-date documented effects of TFEB are mainly related to the induction of the autophagy-lysosomal pathway. A very similar trophic effect was observed by Burke and collaborators in various studies in which several components of the AKT/mTOR pathway were overexpressed. In this regard, overexpression of a myristoylated, constitutively active form of AKT (Myr-AKT) by means of an AAV induced a pronounced trophic effect and conferred neuroprotection *in vivo* (Ries *et al.*, 2006). Similarly, viral vector overexpression of a constitutive form of the principal upstream activator of mTOR, Rheb(S16H), induced many neurotrophic effects in mice, including the ability to both preserve and restore the nigrostriatal dopaminergic pathway in the intrastriatal 6-OHDA mouse model (Kim *et al.*, 2011a, 2012). Therefore, to our knowledge, our study is one of the few that demonstrated a trophic effect similar to the one elicited by neurotrophic factors and probably the first in achieving it without requiring a direct overexpression of a protein belonging to the AKT/mTOR or ERK1/2 pathways. Moreover, we also demonstrated at the histological, biochemical and functional levels that TFEB was also mimicking neurotrophic factors by increasing dopaminergic function. Although the main effect of neurotrophic factors described to date related to dopaminergic function is the increased tyrosine-hydroxylase amount and dopamine release (Altar *et al.*, 1992; Grondin *et al.*, 2002), we also found an increase of dopamine packaging and handling that heightened the available pool of dopamine at

the level of the striatum. These results are of great interest considering that mishandling of dopamine in mice with reduced VMAT2 expression has been reported to cause DA-mediated toxicity and progressive loss of dopaminergic neurons (Caudle *et al.*, 2007). In contrast, other studies reported that VMAT2 overexpression was sufficient to oppose MPTP-induced neurodegeneration *in vivo* (Lohr *et al.*, 2014, 2016). Thus, the increased VMAT2 levels that we observed, probably in addition to other molecular changes related to dopamine metabolism that were not depicted in our work, would most likely contribute to TFEB's neuroprotective effect.

We also have investigated which molecular pathways could be responsible of the neurotrophic effect of TFEB. To that end, we focused in analyzing mTOR signaling since is the main pathway that promotes cell growth and protein synthesis by activating S6K1 and eIF4E, being the later activated through 4E-BP1 phosphorylation/inhibition. Our results pointed out to increased mTORC1 signaling, a result that seems plausible considering that growing cells require stimulated anabolic processes to suit the increased cellular biomass. The observation that TFEB activates mTORC1 is consistent with existing literature that was running simultaneously to our work. In this line, Di Malta *et al.* showed that TFEB overexpression in the liver of mice boosted mTORC1 signaling whereas *Tfeb* liver-specific conditional knockout mice displayed a significant reduction of both mTORC1 signaling and protein synthesis (Di Malta *et al.*, 2017). Furthermore, mTOR signaling has been described to be especially relevant to PD because RTP801/REDD1, a pro-apoptotic protein that acts like Torin1 by suppressing all mTOR activities and induces neuronal cell death (Brugarolas *et al.*, 2004; Malagelada *et al.*, 2006), was found increased in dopaminergic neurons of PD patients (Malagelada *et al.*, 2006).

We also observed an activation of both AKT and ERK1/2 pro-survival signaling pathways, which are both well-known to boost mTORC1 signaling and mediate neurotrophic activity when activated (Besset *et al.*, 2000; Hsuan *et al.*, 2006; Roux *et al.*, 2007; Parmar and Tamanoi, 2010; Robinet and Pellerin, 2010; Winter *et al.*, 2011). Given the importance of AKT in neuronal survival since deactivation of AKT was found in SNpc dopaminergic neurons of PD patients (Malagelada *et al.*, 2008)

and to contribute to neurodegeneration in different experimental models of PD (Malagelada *et al.*, 2008; Tasaki *et al.*, 2010), TFEB-induced activation of AKT may therefore play a key role in the neuroprotective and neurotrophic effects elicited by TFEB. This hypothesis is strengthened by the fact that overexpression of AKT has been shown to confer neuroprotection *in vivo* against MPTP (Aleyasin *et al.*, 2010) and 6-OHDA toxicity (Ries *et al.*, 2006), as well as in other *in vitro* PD models (Salinas *et al.*, 2001; Malagelada *et al.*, 2008; Aleyasin *et al.*, 2010; Tasaki *et al.*, 2010). Conversely, AAV delivery of a dominant-negative form of AKT induced neurodegeneration and shrinkage of SNpc neurons (Ries *et al.*, 2009). Instead, the role of ERK1/2 signaling in promoting neuronal survival, plasticity and growth, as some studies have demonstrated (Xia *et al.*, 1995; Xue *et al.*, 2000; Sweatt, 2001; Thiels and Klann, 2001), has been questioned several times by other works that suggest that ERK1/2 activation induces deleterious effects in neurons permitting neuron degeneration and cell death (Kulich and Chu, 2001; Gómez-Santos *et al.*, 2002; Cheung and Slack, 2004). These differences could be explained in some cases as a neuroprotective compensatory mechanism to counteract death signals (Hetman *et al.*, 1999) or due to the intrinsic characteristics of each cellular type. However, our results support the hypothesis of ERK1/2 in favoring neuronal survival since no degeneration was observed after TFEB-induced ERK1/2 activation, which conversely seems to play, at least in part, a role in the neurotrophic and neuroprotective effects of TFEB.

TFEB activity is controlled by its subcellular localization that is regulated by phosphorylation (Puertollano *et al.*, 2018). We observed an activation of mTORC1, AKT and ERK2 kinases, which are the main protein kinases known to phosphorylate/inactivate TFEB (Napolitano and Ballabio, 2016). However, as we show, TFEB translocates to the nucleus after being overexpressed confirming its activation. This seeming paradox can be explained by the fact that, although both AKT and ERK signaling pathways activate mTORC1, TFEB by itself is also a positive regulator of mTORC1 signaling in the lysosomal surface by promoting the transcriptional regulation of RagD GTPase, which is a direct target of TFEB (Di Malta

et al., 2017). Besides, ERK2 and TBK1, a known AKT activator, are also direct targets of TFEB (Palmieri *et al.*, 2011), so it is reasonable and sound to find both pathways activated upon TFEB overexpression. Although we currently know that there is a feedback loop under fed conditions by which TFEB promotes mTORC1 signaling and this, in turn, decreases TFEB activity by phosphorylation (Di Malta and Ballabio, 2017), the advantage of our system relies on the detail that when TFEB is overexpressed it saturates the ability of mTORC1, AKT and ERK2 to phosphorylate it. Thus, the reason why TFEB is mainly found in the nucleus in normally fed neurons is because, while some of TFEB is found in the cytoplasm boosting mTORC1 signaling together with AKT and ERK1/2, most of the overexpressed TFEB escapes the phosphorylation by these kinases and translocates to the nucleus (Medina *et al.*, 2011; Puertollano *et al.*, 2018), where it regulates both anabolic and catabolic genes (**Figure 42**). A similar effect was found in another study in which they expressed a constitutive activated form of TFEB that was Ser-to-Ala mutated (S142A, S211A), which evaded mTORC1 and ERK2-induced phosphorylation and thereby most TFEB was nuclear translocated (Settembre *et al.*, 2012). It is important to point out that both activation of anabolic pathways such as mTORC1 and catabolic pathways such as autophagy seems to happen simultaneously in our model. This fact could be explained because of under conditions conducive to cell growth, a relative lower rate of autophagic flux is maintained for the proper cellular homeostasis and well-being of the cell.

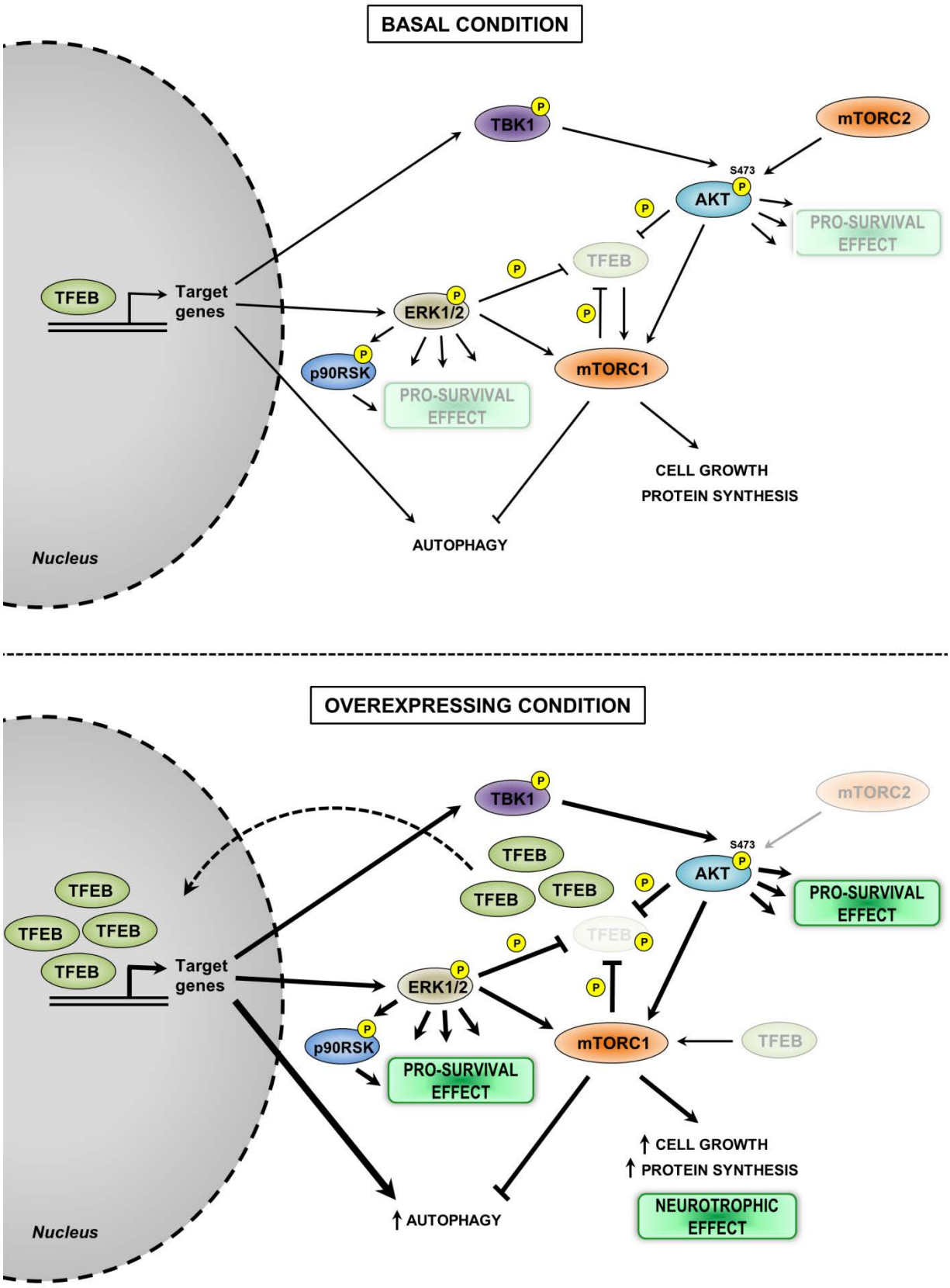

Figure 42. Schematic representation of TFEB activity. Under basal conditions (top panel), TFEB promotes transcription of several genes, including TBK1, ERK1/2 and genes implicated to the induction of the autophagy-lysosomal pathway. However, there is a feedback loop under fed

conditions by which TFEB promotes mTORC1 signaling and this, in turn, decreases TFEB activity by phosphorylation. In addition to AKT- and ERK2-induced phosphorylation, TFEB remains inactive in the cytosol. mTORC1 signaling is not favored. Under overexpressing conditions (bottom panel), some of TFEB is found in the cytoplasm boosting mTORC1 signaling, whereas most of the overexpressed TFEB escapes the phosphorylation/inactivation by AKT, ERK2 and mTORC1, thereby translocating to the nucleus, where it is mainly found. TFEB target genes are highly induced, including TBK1, ERK1/2 and those related to the induction of the autophagy-lysosomal system. In this situation, S473-phosphorylated form of AKT seems to be mediated through TBK1 rather than mTORC2. Activated AKT and ERK1/2 pathways boost mTORC1 signaling, which induces cell growth and protein synthesis.

Because lysosomal and mitochondrial impairment are two deleterious events that are linked to PD, we assessed the effect of overexpressing TFEB in these two organelles. As expected, and as previously reported (Dehay *et al.*, 2010; Decressac *et al.*, 2013), TFEB overexpression induced lysosomal biogenesis paralleling the induction of autophagy. However, the effect of TFEB on mitochondria of neurons has never been assessed previously. In this line, our study is the first to demonstrate that TFEB overexpression induces mitochondrial fusion and mitochondrial protein expression changes that render neurons less prone to cell death. However, our findings do not support the presence of mitochondrial biogenesis, or at least not in a sustained manner. This observation seems also to mimic the GDNF/RET signaling effect on mitochondria since they have proven to be necessary for normal mitochondrial function and morphology and to prevent mitochondrial fragmentation and associated cell death. This effect on mitochondrial integrity is accompanied by a lack of GDNF to trigger mitochondrial biogenesis (Klein *et al.*, 2014; Meka *et al.*, 2015), which contrasts with other trophic or neurotrophic factors like BDNF (Mattson *et al.*, 2018). Indeed, BDNF and GDNF were shown to increase the efficiency of respiratory coupling and rescued bioenergetics deficits in *Drosophila melanogaster* Pink1 mutants and Parkin-deficient cells, respectively (Markham *et al.*, 2004; Klein *et al.*, 2014; Meka *et al.*, 2015). Although in our study we did not check specific OXPHOS complex activities or ATP production, we did check the levels of some OXPHOS subunits that pointed out that TFEB was involved in mitochondrial

respiration, possibly increasing or enhancing its function. This hypothesis is strengthened by a recent study from Mansueto and collaborators, which was running parallel to ours, that unraveled that TFEB overexpression improved respiratory chain complex activities and increased ATP production in skeletal muscle (Mansueto *et al.*, 2017). In the same study, authors demonstrated that TFEB induced mitochondrial biogenesis, contrasting with our results, through a PGC-1α- and PGC-1β-independent mechanism. This result is surprising considering that PGC-1α, which is the master regulator of mitochondrial biogenesis, is rated as a TFEB direct target (Palmieri *et al.*, 2011). Nevertheless, special caution must be taken by extrapolating these results to neurons since the networks of genes regulated by TFEB have been described to be context specific, supporting diverse tissue-specific metabolic functions (Settembre *et al.*, 2013; Mansueto *et al.*, 2017). Moreover, we also reported that TFEB overexpression induced an increase of mitochondrial size that partly may be explained by the boosted mitochondrial fusion that we observed, as determined by both western blot and electron microscopy studies. This effect of TFEB on mitochondrial size was already reported by Mansueto and collaborators in muscle tissue, although, intriguingly, authors did not discuss this important observation (Mansueto *et al.*, 2017). This striking fact can be explained from a physiological point of view since extended mitochondrial networks achieved by increased mitochondrial size and/or mitochondrial fusion are of great advantage, especially under conditions of high energy demand (Westermann, 2012). In addition to the other beneficial outcomes of a hyperfused mitochondrial network like to attenuate the potential deleterious effects of mutated mtDNA or misfolded proteins (Chen *et al.*, 2010; Van der Bliek *et al.*, 2013), mitochondrial fusion also seems to play an important role in maximizing ATP biosynthesis by allowing the OXPHOS complexes to cooperate more efficiently (Westermann, 2012) and thereby favoring cell growth. In this line, cells with disrupted mitochondrial fusion by targeted mutations in *Mfn1/2* genes display a loss of respiratory capacity and poor cell growth (Chen *et al.*, 2005). Therefore, is very tempting to speculate that in our TFEB-overexpressing model in which neurons undergo a trophic effect more energy is needed to suit the metabolic needs of the cell. Further confirming this insight, a study by Liang *et al.* demonstrated

that mitochondrial size in neurons is correlated to soma's size since the largest mitochondria are found in bigger neurons like those of the red nucleus, while the smallest mitochondria are found in smaller neurons like SNpc dopaminergic neurons (Liang *et al.*, 2007). Consequently, the relative low mitochondrial mass of dopaminergic nigral neurons may contribute to the selective vulnerability of these neurons to degenerate in PD, while increased mitochondrial size in TFEB-overexpressing neurons may potentially account for its neuroprotective effect.

Even though the effect of neurotrophic factors on the mitochondrial protein import machinery is not known, we also found a striking increase in the levels of TOM20 and TIM23 after TFEB overexpression. In the light of new evidences that demonstrated that knocking down this family of translocases in primary cortical and striatal neurons triggered neuronal death (Yano *et al.*, 2014) and that mitochondrial protein import was impaired in PD due to the blockage of TOM20 by certain post-translationally modified species of α-synuclein and that this impairment can be reverted by TOM20 overexpression *in vitro* (Di Maio *et al.*, 2016), TFEB-mediated TOM20 and TIM23 overexpression is a relevant contributor to the neuroprotective effect of TFEB.

In addition to the above commented results, our study has also focused on demonstrating that these TFEB-overexpressing neurons were indeed able to block neurodegeneration in a parkinsonian context, that induced by the neurotoxin MPTP. We chose this experimental model for various reasons. First, MPTP is the only toxin that has been proven to cause PD in humans. Second, all the pathways that have been described in MPTP models are still valid since most PD models only replicate what has been described in the MPTP model. And third, neuronal cell death in this model is triggered by the inhibition of mitochondrial complex I rather than the accumulation of a protein. Thus, stereotaxic delivery of TFEB was followed after four weeks by a sub-acute MPTP treatment to test the neuroprotective effect of TFEB. We found that TFEB overexpression completely prevented MPTP-induced neurodegeneration of SNpc dopaminergic neurons. In addition to TFEB's ability to protect dopaminergic cell bodies, it also fully preserved the dopaminergic terminals in the striatum. This is an important observation that distinguishes our work from many

others considering the difficulty to preserve the dopaminergic axonal projections rather than the cell bodies due to the former constitute a different cellular compartment that degenerates earlier in the disease through distinct molecular mechanisms (Burke and O'Malley, 2013).

Hypertrophy of pigmented SNpc neurons has been reported to be a compensatory mechanism within individual neurons to preserve motor function despite the loss of SNpc neurons in normal ageing. However, such mechanism is overwhelmed in PD and subsequently neurons undergo atrophy (Rudow *et al.*, 2008). In our MPTP mouse model we observed that cell soma shrinkage, decreased dendritic arborization and tyrosine hydroxylase downregulation preceded neuronal loss. These results agree with those observed in PD, with neuronal dysfunction and atrophy accompanied by a markedly decrease in dendritic arborization and a loss of phenotype that involves tyrosine hydroxylase downregulation, which precede actual neuronal death, having been reported (Patt and Gerhard, 1993; Kordower *et al.*, 2013). However, some neurons that underwent atrophy were able to overcome MPTP's deleterious effects and survive. This observation suggests that remaining atrophic neurons are still viable and are possible targets for neurorestorative therapies. In fact, some experimental data suggest that neuronal atrophy and programmed cell death can be dissociated in experimental PD (Kim *et al.*, 2011b), and the same seems to occur in PD (Cheng *et al.*, 2010). Consequently, targeting programmed cell death alone as a strategy to halt the progression of the disease would therefore not prevent neuronal dysfunction and associated symptoms. Therefore, elucidating the mechanisms of neuronal dysfunction and atrophy is essential to develop a therapeutic approach that blocks neurodegeneration in all senses of the word. Our results suggested that TFEB overexpression not only was capable of preserving the cell body and axon terminals in the MPTP model but also the activity and phenotype of these dopaminergic neurons. In this regard, we demonstrated that even in MPTP conditions, TFEB mediated an increase of tyrosine hydroxylase expression, cellular size and dendrite branching, and probably also triggered the expression of other proteins relevant to the dopaminergic phenotype

that were not assessed here. Moreover, TFEB also preserved synaptic function in the MPTP model, as indicated by a conservation of DAT-positive fibers and striatal monoamine levels, as well as boosting the available pool of dopamine in the striatum. These molecular changes had behavioral correlates in the d-amphetamine-induced rotation test, in which MPTP TFEB-treated mice exhibited a contralateral rotation due to the fact that the non-lesioned side was able to release more dopamine than the lesioned side. It is significant that TFEB was able to block all the neuropathology induced by MPTP, making these findings especially relevant for PD.

Furthermore, we demonstrated that TFEB overexpression counteracted the diminution of lysosomal biogenesis and protein synthesis associated with neuronal atrophy that occurs in neurodegeneration. While the first observation is in accordance with a previous work from our laboratory in which TFEB was able to prevent the pathogenic lysosomal depletion and the subsequent lysosomal-autophagy defect that precedes cell death *in vitro* (Dehay *et al.*, 2010), the molecular mechanisms of protein synthesis and their role in the disease have remained poorly understood. Our results indicated that neuronal atrophy in the MPTP mouse model was mediated by inhibition of the 4E-BP/eIF4E pathway, and that TFEB counteracted atrophy mainly by the activation of S6K1 pathway and, in part, by the preservation of eIF4E phosphorylation. Further confirming this insight, evidence for disrupted eIF4 and S6K1 signaling have been found in individually isolated SNpc dopaminergic neurons of PD patients (Elstner *et al.*, 2011). Conversely, other studies pointed out that S6K1 pathway seems to contribute to neuronal cell death in both neurotoxin PD models and PD by increasing the translation of RTP801 (Malagelada *et al.*, 2010). Another study reported some years ago that inhibition of 5' cap-dependent translation by increasing 4E-BP activation conferred neuroprotection by promoting the upregulation of stress response factors such as GstS1 (Tain *et al.*, 2009). Such divergent outcomes seem to point that only when enhanced protein synthesis is accompanied by other favorable cellular processes, as our results indicate, neurons seem to have no harmful effect at all. Instead, shutting down protein synthesis

machinery and thereby undergoing neuronal atrophy may be a neuroprotective mechanism for the neuron to cope with unfavorable situations.

Our results highlighted that TFEB neuroprotective effect could be due to several mechanisms that went beyond autophagy, which is greatly significant for the neurodegenerative diseases field. Autophagy has become a field of rapidly growing interest and has been suggested to fight neurodegeneration, since autophagy dysfunction and the presence of aggregated proteins have long been described in neurodegenerative diseases, including PD (Scrivo *et al.*, 2018). In this line, the majority of studies that demonstrated a protective effect of autophagy have used rapamycin, an inhibitor of some mTORC1 activities including the main known factor restricting autophagy induction. However, mTORC1 functions as a negative regulator of TFEB by impeding its nuclear translocation. Hence, pharmacological inhibition of mTORC1 with rapamycin alleviates the repression of TFEB and promotes its shuttling to the nucleus (Martina *et al.*, 2012; Decressac *et al.*, 2013), which could explain most, if not all, the neuroprotective effect that has been attributed to rapamycin at boosting autophagy in many *in vivo* experimental models of PD (Pan *et al.*, 2008; Bjedov *et al.*, 2010; Crews *et al.*, 2010; Dehay *et al.*, 2010; Liu *et al.*, 2013). Moreover, as discussed above, rapamycin has also been shown to confer neuroprotection both *in vitro* and *in vivo* in PD models by other mechanisms beyond autophagy, such as blocking of mTOR-mediated RTP801 translation (Malagelada *et al.*, 2010). Another strategy described to activate autophagy is trehalose, a disaccharide of glucose that has been reported to counteract pathologic autophagosome accumulation and attenuating cell death in MPP^+-treated cells (Dehay *et al.*, 2010). However, trehalose effect is mediated by activation of TFEB (Dehay *et al.*, 2010), entailing the stimulation of the other molecular pathways described in this thesis.

Despite we agree that neurons need a constitutive basal autophagic activity for the proper cellular homeostasis, some studies unraveled that activation of autophagy in a PD model of α-synuclein overexpression appears to be detrimental and contributes to neuronal cell death (Xilouri *et al.*, 2009). For this reason, we strongly believe that

activating exclusively autophagy may be not sufficient to develop an effective disease-modifying treatment for PD. To delve further into this concept, we decided to knock down the master transcriptional repressor of autophagy ZKSCAN3 in nigral dopaminergic neurons, thereby boosting the autophagy-lysosomal pathway in the same MPTP-based PD model that we tested TFEB neuroprotective effect. Only a previous work has used this interesting approach to activate the autophagy-lysosomal pathway by knocking down ZKSCAN3, although in an *in vitro* context (Chauhan *et al.*, 2013). In our *in vivo* model, even though we successfully knocked down ZKSCAN3, we observed that neurons underwent neurodegeneration and atrophy after MPTP intoxication, suggesting that boosting autophagy-lysosomal system did not suffice *per se* to confer neuroprotection, at least in our model. This result was accompanied by a lack of activation of ERK1/2 and AKT signaling pathways, indicating that these pathways could be of most importance for both TFEB-induced neuroprotective and neurotrophic effects. However, further studies should be conducted to dissect all the relevant neuroprotective mechanisms triggered by TFEB overexpression, including autophagy. In fact, TFEB overexpression has proven to exert a neuroprotective effect in other experimental models (Decressac *et al.*, 2013; Polito *et al.*, 2014), suggesting that the neuroprotective effect of TFEB is independent of the pathogenic mechanisms underlying neurodegeneration, as in the case of neurotrophic factors.

Finally, in addition to the results regarding increased mitochondrial size, mitochondrial fusion and mitochondrial protein import, we also demonstrated that TFEB overexpression also involved anti-apoptotic mechanisms that targeted both upstream and downstream instigators of mitochondria-mediated cell death, which together rendered neurons less prone to apoptosis (**Figure 43**). These results could be simply attributed to the observed activation upon TFEB overexpression of both AKT and ERK1/2 signaling pathways, which are known to inhibit apoptosis at multiple levels by inducing a transcriptional repression or decreasing the activity of pro-apoptotic molecules, and by upregulating anti-apoptotic proteins via enhancement both its transcription and activity (Lu and Xu, 2006; Levy *et al.*, 2009; Winter *et al.*,

2011). Our results are consistent with those observed with neurotrophic factors like BDNF, which has been previously reported to inhibit neuronal apoptosis by inducing the expression of anti-apoptotic BCL-2 family of proteins, such as BCL-XL, and by inhibiting pro-apoptotic proteins such as BAD and BAX (Marosi and Mattson, 2014). While it has been demonstrated that there is a tight correlation between the increase in VDAC1 expression levels and VDAC1 oligomerization and programmed cell death (Keinan *et al.*, 2010; Weisthal *et al.*, 2014), we found that VDAC1 levels were reduced in AAV-TFEB injected mice, demonstrating that VDAC1 downregulation was contributing to the generation of mitochondria that were less prone to programmed cell death. In further support of this insight, Shimizu *et al.* demonstrated that increasing BCL-XL levels prevented the release of cytochrome c by VDAC1 (Shimizu *et al.*, 1999). Accordingly, delivery of BCL-XL linked to a peptide that allowed its delivery across the blood-brain barrier prevented MPTP-induced neurodegeneration (Dietz *et al.*, 2008). Furthermore, genetic ablation of BIM attenuated BAX activation, cytochrome c release and dopaminergic neuronal death in MPTP-intoxicated mice (Perier *et al.*, 2007). In line with this, inactivating caspase-9 was reported to confer neuroprotection in dopaminergic neurons from neurotoxic insults, such as MPTP (Viswanath *et al.*, 2001). All these results regarding the blockade of mitochondria-mediated cell death are in keeping with the increased mitochondrial fusion and mitochondrial protein import that we also observed, since both have been shown to counteract cell death induced by several stimuli including parkinsonian toxins (Chen *et al.*, 2005; Zorzano and Claret, 2015; Franco-Iborra *et al.*, 2018a). In that connection, we previously demonstrated that inhibiting the cytochrome c release by remodeling the cristae structure through overexpression of the mitochondrial fusion protein OPA1 induced a neuroprotective effect in the MPTP model (Ramonet *et al.*, 2013). Therefore, all these TFEB-induced mitochondrial changes are likely to play a key role in the neuroprotective effect elicited by TFEB.

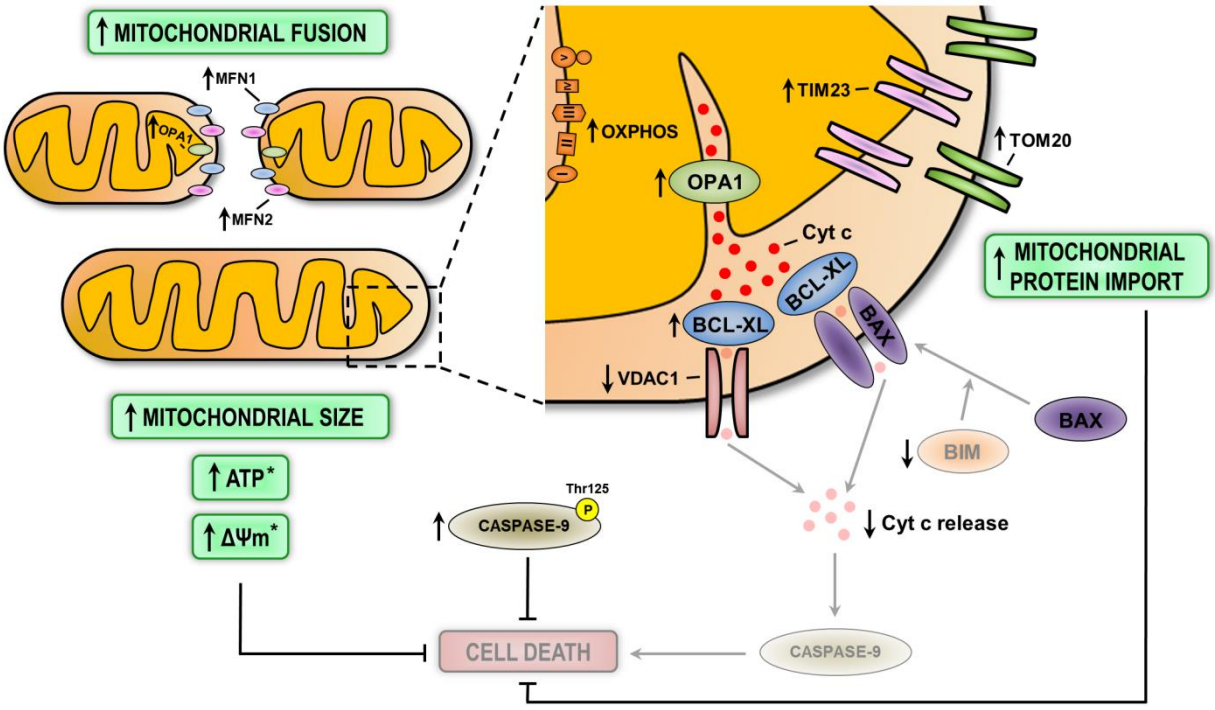

Figure 43. Schematic representation of TFEB-induced effects on mitochondria. TFEB overexpression promotes mitochondrial fusion and increases mitochondrial size, thereby extending mitochondrial network and probably, although not checked (indicated by an asterisk), maximizing ATP biosynthesis and increasing mitochondrial membrane potential (Δψm). Moreover, TFEB also enhances mitochondrial protein import in substantia nigra dopaminergic neurons, and blocks at multiple levels the mitochondria-mediated cell death by increasing anti-apoptotic proteins, such as BCL-XL, and decreasing both upstream (like BIM or VDAC1) and downstream (like caspase-9) instigators of mitochondria-mediated cell death. Consequently, cytochrome c release is inhibited, which, together with increased phosphorylated/inactivated caspase-9, contribute to block cell death.

Our findings here, in spite of being promising, represent an early proof-of-principle step since our experimental setting bolster a prevention of the pathological events associated with the disease rather than an actual rescue. We are aware that translating our results directly into clinical practice might raise some concerns regarding the risk of neoplastic transformation due to the constant high overexpression levels of TFEB that results in a sustained activation of both AKT and ERK1/2 pathways, which hyper-activate mTORC1 signaling. Although a constant mTORC1 signaling has been described to be necessary not only for the surveillance of the neuron but also for synaptic plasticity processes, mutations in TSC1/TSC2 that

implicate an augmented mTORC1 activity result in tuberous sclerosis, an autosomal dominant disorder characterized by the formation of multiple tumors mainly in the central nervous system. We did not observe any sign of neoplasia or aberrant behavior in TFEB-injected mice as long as 56 days after stereotaxic injection, although some caution should be taken in long-term studies, especially considering that TFEB was originally characterized as a lineage survival oncogene.

We propose some strategies to challenge these above commented limitations. One way would be the use of adeno-associated viral vectors with a tetracycline-controlled transcriptional activation for inducible and reversible control of transgene expression, which can be controlled by doxycycline at any time point desired (Dogbevia *et al.*, 2016). Although less striking than a constitutive AAV, both AAV equipped with rtTA (TetON) and tTA (TetOFF) have been successfully used in the neuroscience field (Haberman *et al.*, 2002; Bockstael *et al.*, 2008; Dogbevia *et al.*, 2016), providing evidence that temporal control of gene expression is achievable. TFEB has so far been used exclusively as a transgene, thereby being solely limited to gene therapy. An alternative of gene therapy would be the direct administration of TFEB to the local area. Pending the identification of an appropriate endocytosis of the full-length TFEB protein into neurons, an interesting method to go one step further and as an alternative of gene therapy would be by means of a purified cell-penetrating polypeptide from TFEB. This strategy unveils promising perspectives since a recent work unraveled that a purified tetrapeptide from mesencephalic astrocyte-derived neurotrophic factor (MANF) was able to penetrate cells and potently promoted survival of cultured primary dopaminergic neurons (Božok *et al.*, 2018). In this line, recent preclinical results obtained from Kang and collaborators demonstrated that a cell-penetrating peptide-conjugated with metallothionein 1A alleviated mitochondrial damage and neurodegeneration in *in vivo* and *in vitro* PD experimental models (Kang *et al.*, 2018). Finally, another alternative method to gene therapy would be the pharmacological approach. Some drugs have been described to activate TFEB, especially focused on inhibiting mTORC1, the main repressor of TFEB. However, given that mTORC1 controls a wide range of biological functions, by suppressing all

mTORC1 activities with some inhibitors such as Torin1 actually results in neuronal cell death (Malagelada *et al.*, 2010). Therefore, the discovery of TFEB activators without inhibiting the mTORC1 pathway would be preferred and undoubtedly less deleterious to neurons. Although rapamycin is known to allosterically inhibit only some actions of mTORC1 without impeding neuronal survival (Rüegg *et al.*, 2007) and to activate TFEB (Martina *et al.*, 2012; Decressac *et al.*, 2013), there might be important issues with long-term use of rapamycin given its side effects as an immunosuppressant. An mTORC1-independent drug that has been used to activate TFEB is trehalose (Palmieri *et al.*, 2017). Nevertheless, the mechanism by which trehalose activates TFEB is through inhibition of AKT (Palmieri *et al.*, 2017), thereby losing relevance for the PD field because AKT it is known to be an important kinase for the surveillance of SNpc dopaminergic neurons (Burke, 2007; Malagelada *et al.*, 2008). Other mTORC1-independent pharmacological strategies have recently been shown to activate TFEB, such as the curcumin analogue C1 that binds directly to TFEB interfering its binding to inhibitory 14-3-3 proteins (Song *et al.*, 2016), or ambroxol (Magalhaes *et al.*, 2018), although in the latter the mechanism by which TFEB is activated remains mysterious. Overall, the current available drugs capable of activating TFEB are rather limited and some of them might raise serious concerns in the context of PD because of their mechanism of action. Hence, further work on drug discovery through high-throughput screening or by means of drug repositioning may be innovative ways for the breakthrough of new activators of TFEB that could be of great relevance to PD and related disorders.

To sum up, our results (briefly summarized in **Figure 44**) suggest that TFEB gene therapy or TFEB pharmacological activation are alternative candidates to neurotrophic factor-based therapies for PD and other neurodegenerative diseases. In any event, the potential beneficial effect of TFEB has become evident so further research should be conducted to elucidate the safest and most efficient ways to translate the results presented in this thesis into clinical practice.

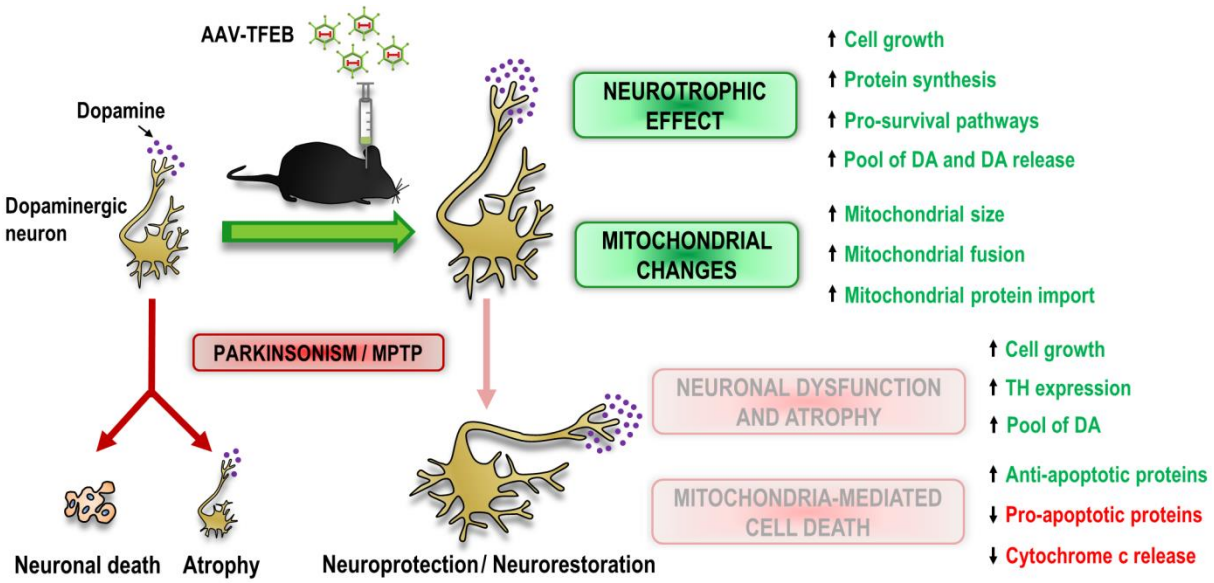

Figure 44. Schematic representation of the pleiotropic effect induced by TFEB overexpression in mouse SNpc dopaminergic neurons. In Parkinson's disease-related neurodegeneration, SNpc dopaminergic neurons undergo neuronal atrophy and programmed cell death, which can be dissociated. AAV-TFEB unilateral overexpression induces a neurotrophic affect in SNpc dopaminergic neurons that is accompanied by several mitochondrial changes. All these TFEB-induced molecular changes contribute in preventing MPTP-induced neurodegeneration by blocking mitochondria-mediated cell death at multiple levels. Besides, TFEB overexpression is able to preserve neuronal function in MPTP conditions.

CONCLUSIONS

6. Conclusions

1. TFEB overexpression induces a neurotrophic effect in mouse substantia nigra dopaminergic neurons.
2. TFEB overexpression enhances dopaminergic function by increasing TH expression levels and boosting both the available pool of DA and DA release in the striatum.
3. mTORC1 signaling and protein synthesis are boosted in TFEB-overexpressing mice.
4. Pro-survival AKT/mTOR and ERK1/2 signaling pathways are activated upon TFEB overexpression.
5. TFEB overexpression increases mitochondrial size, mitochondrial fusion and mitochondrial protein import in substantia nigra dopaminergic neurons.
6. TFEB overexpression confers a complete neuroprotection both at the level of cell body and striatal dopaminergic terminals in the MPTP mouse model of Parkinson's disease.
7. The neurotrophic effect elicited by TFEB counteracts neuronal atrophy and preserves neuronal function in MPTP mice.
8. MPTP-induced protein synthesis decline is prevented by TFEB overexpression.
9. TFEB counteracts the autophagy-lysosomal impairment of the MPTP mice.
10. Knocking down the master transcriptional repressor of autophagy ZKSCAN3 does not prevent MPTP-induced neurodegeneration or atrophy.
11. Mitochondria-mediated cell death is blocked at multiple levels by TFEB overexpression.

BIBLIOGRAPHY

7. Bibliography

Abu-Hamad, S., Zaid, H., Israelson, A., Nahon, E., and Shoshan-Barmatz, V. (2008) Hexokinase-I protection against apoptotic cell death is mediated via interaction with the voltage-dependent anion channel-1: Mapping the site of binding. *J. Biol. Chem.*, 283, 13482–13490.

Airavaara, M., Harvey, B.K., Voutilainen, M.H., Shen, H., Chou, J., Lindholm, P., Lindahl, M., Tuominen, R.K., Saarma, M., Hoffer, B., and Wang, Y. (2012) CDNF Protects the Nigrostriatal Dopamine System and Promotes Recovery After MPTP Treatment in Mice. *Cell Transplant.*, 21, 1213–1223.

Alarcón-Arís, D., Recasens, A., Galofré, M., Carballo-Carbajal, I., Zacchi, N., Ruiz-Bronchal, E., Pavia-Collado, R., Chica, R., Ferrés-Coy, A., Santos, M., Revilla, R., Montefeltro, A., Fariñas, I., Artigas, F., Vila, M., and Bortolozzi, A. (2018) Selective α-Synuclein Knockdown in Monoamine Neurons by Intranasal Oligonucleotide Delivery: Potential Therapy for Parkinson's Disease. *Mol. Ther.*, 26, 550–567.

Alcalay, R.N., Levy, O.A., Waters, C.C., Fahn, S., Ford, B., Kuo, S.H., Mazzoni, P., Pauciulo, M.W., Nichols, W.C., Gan-Or, Z., Rouleau, G.A., Chung, W.K., Wolf, P., Oliva, P., Keutzer, J., Marder, K., and Zhang, X. (2015) Glucocerebrosidase activity in Parkinson's disease with and without GBA mutations. *Brain*, 138, 2648–2658.

Aleyasin, H., Rousseaux, M.W.C., Marcogliese, P.C., Hewitt, S.J., Irrcher, I., Joselin, A.P., Parsanejad, M., Kim, R.H., Rizzu, P., Callaghan, S.M., Slack, R.S., Mak, T.W., and Park, D.S. (2010) DJ-1 protects the nigrostriatal axis from the neurotoxin MPTP by modulation of the AKT pathway. *Proc. Natl. Acad. Sci.*, 107, 3186–3191.

Allan, L.A. and Clarke, P.R. (2009) Apoptosis and autophagy: Regulation of caspase-9 by phosphorylation. *FEBS J.*, 276, 6063–6073.

Altar, C.A., Boylan, C.B., Jackson, C., Hershenson, S., Miller, J., Wiegand, S.J., Lindsay, R.M., and Hyman, C. (1992) Brain-derived neurotrophic factor augments rotational behavior and nigrostriatal dopamine turnover in vivo. *Proc. Natl. Acad. Sci.*, 89, 11347–11351.

Altomare, D.A. and Khaled, A.R. (2012) Homeostasis and the Importance for a Balance Between AKT/mTOR Activity and Intracellular Signaling. *Curr. Med. Chem.*, 19, 3748–3762.

Alvarez-Erviti, L., Rodriguez-Oroz, M.C., Cooper, J.M., Caballero, C., Ferrer, I., Obeso, J.A., and Schapira, A.H.V. (2010) Chaperone-mediated autophagy markers in Parkinson disease brains. *Arch. Neurol.*, 67, 1464–1472.

Anderson, C., Checkoway, H., Franklin, G., Beresford, S., Smith-Weller, T., and Swanson, P. (1999) Dietary factors in Parkinson's disease: The role of food groups and specific foods. *Mov. Disord.*, 14, 21–27.

Andreu, A.L., Martinez, R., Marti, R., and García-Arumí, E. (2009) Quantification of mitochondrial DNA copy number: Pre-analytical factors. *Mitochondrion*, 9, 242–246.

Anglade, P., Vyas, S., Javoy-Agid, F., Herrero, M., Michel, P., Marquez, J., Mouatt-Prigent, A., Ruberg, M., Hirsch, E., and Agid, Y. (1997) Apoptosis and autophagy in nigral neurons of patients with Parkinson's disease. *Histol. Histopathol.*, 12, 25–31.

Aoi, M., Date, I., Tomita, S., and Ohmoto, T. (2000) The effect of intrastriatal single injection of GDNF on the nigrostriatal dopaminergic system in hemiparkinsonian rats: behavioral and histological studies using two different dosages. *Neurosci. Res.*, 36, 319–325.

Asanuma, M., Hirata, H., and Cadet, J.L. (1998) Attenuation of 6-hydroxydopamine-induced dopaminergic nigrostriatal lesions in superoxide dismutase transgenic mice. *Neuroscience*, 85, 907–917.

Athauda, D. and Foltynie, T. (2015) The ongoing pursuit of neuroprotective therapies in Parkinson disease. *Nat. Rev. Neurol.*, 11, 25–40.

Aurnhammer, C., Haase, M., Muether, N., Hausl, M., Rauschhuber, C., Huber, I., Nitschko, H., Busch, U., Sing, A., Ehrhardt, A., and Baiker, A. (2012) Universal Real-Time PCR for the Detection and Quantification of Adeno-Associated Virus Serotype 2-Derived Inverted Terminal Repeat Sequences. *Hum. Gene Ther. Methods*, 28, 18–28.

Back, S., Peränen, J., Galli, E., Pulkkila, P., Lonka-Nevalaita, L., Tamminen, T., Voutilainen, M.H., Raasmaja, A., Saarma, M., Männistö, P.T., and Tuominen, R.K. (2013) Gene therapy with AAV2-CDNF provides functional benefits in a rat model of Parkinson's disease. *Brain Behav.*, 3, 75–88.

Barron, A.B., Søvik, E., and Cornish, J.L. (2010) The Roles of Dopamine and Related Compounds in Reward-Seeking Behavior Across Animal Phyla. *Front. Behav. Neurosci.*, 4, 1–9.

Bartus, R.T., Brown, L., Wilson, A., Kruegel, B., Siffert, J., Johnson, E.M., Kordower, J.H., and Herzog, C.D. (2011) Properly scaled and targeted AAV2-NRTN (neurturin) to the substantia nigra is safe, effective and causes no weight loss: Support for nigral targeting in Parkinson's disease. *Neurobiol. Dis.*, 44, 38–52.

Beal, M.F. (2011) Neuroprotective effects of creatine. *Amino Acids*, 40, 1305–1313.

Bellucci, A., Navarria, L., Zaltieri, M., Falarti, E., Bodei, S., Sigala, S., Battistin, L., Spillantini, M., Missale, C., and Spano, P. (2011) Induction of the unfolded protein response by α-synuclein in experimental models of Parkinson's disease. *J. Neurochem.*, 116, 588–605.

Ben-Sahra, I., Hoxhaj, G., Ricoult, S., Asara, J., and Manning, B. (2016) mTORC1 induces purine synthesis through control of the mitochondrial tetrahydrofolate cycle. *Science (80-.).*, 351.

Benabid, A-L., Koudsié, A., Benazzouz, A., Fraix, V., Ashraf, A., Le Bas, J. F., Chabardes, S., and Pollak, P. (2000) Subthalamic Stimulation for Parkinson. *Arch. Med. Res.*, 31, 282–289.

Bender, A., Desplats, P., Spencer, B., Rockenstein, E., Adame, A., Elstner, M., Laub, C., Mueller, S., Koob, A.O., Mante, M., Pham, E., Klopstock, T., and Masliah, E. (2013) TOM40 Mediates Mitochondrial Dysfunction Induced by α-Synuclein Accumulation in Parkinson's Disease. *PLoS One*, 8.

Bendor, J.T., Logan, T.P., and Edwards, R.H. (2013) The function of α-synuclein. *Neuron*, 79, 1044–1066.

Besset, V., Scott, R.P., and Ibáñez, C.F. (2000) Signaling complexes and protein-protein interactions involved in the activation of the Ras and phosphatidylinositol 3-kinase pathways by the c-Ret receptor tyrosine kinase. *J. Biol. Chem.*, 275, 39159–39166.

Betarbet, R., Sherer, T.B., Mackenzie, G., Garcia-osuna, M., Panov, A. V, and Greenamyre, J.T. (2000) Chronic systemic pesticide exposure reproduces features of Parkinson's disease. *Nat. Neurosci.*, 3, 1301–1306.

Bhardwaj, R. and Deshmukh, R. (2018) Neurotrophic factors and Parkinson's disease. *Clin. Investig. (Lond).*, 8, 53–62.

Biswas, S.C., Ryu, E., Park, C., Malagelada, C., and Greene, L.A. (2005) Puma and p53 play required roles in death evoked in a cellular model of Parkinson disease. *Neurochem. Res.*, 30, 839–845.

Bjedov, I., Toivonen, J.M., Kerr, F., Slack, C., Jacobson, J., Foley, A., and Partridge, L. (2010) Mechanisms of Life Span Extension by Rapamycin in the Fruit Fly Drosophila melanogaster. *Cell Metab.*, 11, 35–46.

Blesa, J. and Przedborski, S. (2014) Parkinson's disease: animal models and dopaminergic cell vulnerability. *Front. Neuroanat.*, 8, 1–12.

Bockstael, O., Chtarto, A., Wakkinen, J., Yang, X., Melas, C., Levivier, M., Brotchi, J., and Tenenbaum, L. (2008) Differential Transgene Expression Profiles in Rat Brain, Using rAAV2/1 Vectors with Tetracycline-Inducible and Cytomegalovirus Promoters. *Hum. Gene Ther.*, 19, 1293–1306.

Bortolozzi, A. and Artigas, F. (2003) Control of 5-hydroxytryptamine release in the dorsal raphe nucleus by the noradrenergic system in rat brain. Role of α-adrenoceptors. *Neuropsychopharmacology*, 28, 421–434.

Bosco, D.A., Fowler, D.M., Zhang, Q., Nieva, J., Powers, E.T., Wentworth, P., Lerner, R.A., and Kelly, J.W. (2006) Elevated levels of oxidized cholesterol metabolites in Lewy body disease brains accelerate α-synuclein fibrilization. *Nat. Chem. Biol.*, 2, 249–253.

Bové, J., Prou, D., Perier, C., and Przedborski, S. (2005) Toxin-Induced Models of Parkinson's Disease. *NeuroRx*, 2, 484–494.

Bové, J. and Perier, C. (2012) Neurotoxin-based models of Parkinson's disease. *Neuroscience*, 211, 51–76.

Bové, J., Martínez-Vicente, M., Dehay, B., Perier, C., Recasens, A., Bombrun, A., Antonsson, B., and Vila, M. (2014) BAX channel activity mediates lysosomal disruption linked to Parkinson disease. *Autophagy*, 10, 889–900.

Božok, V., Yu, L., Palgi, J., and Arumäe, U. (2018) Antioxidative CXXC Peptide Motif From Mesencephalic Astrocyte-Derived Neurotrophic Factor Antagonizes Programmed Cell Death. *Front. Cell Dev. Biol.*, 6, 1–15.

Braak, H., Del, K., Rüb, U., Vos, R.A.I. De, Jansen, E.N.H., and Braak, E. (2003) Staging of brain pathology related to sporadic Parkinson's disease. *Neurobiol. Aging*, 24, 197–211.

Bravo, R., Parra, V., Gatica, D., Rodriguez, A., Torrealba, N., Paredes, F., Wang, Z., Zorzano, A., Hill, J., Jaimovich, E., Quest, A., and Lavandero, S. (2013) Endoplasmic Reticulum and the Unfolded Protein Response: Dynamics and Metabolic Integration. *Int. Rev. Cell Mol. Biol.*, 301, 215–290.

Brochard, V., Combadière, B., Prigent, A., Laouar, Y., Perrin, A., Beray-berthat, V., Bonduelle, O., Alvarez-fischer, D., Callebert, J., Launay, J., Duyckaerts, C., Flavell, R.A., Hirsch, E.C., and Hunot, S. (2009) Infiltration of CD4+ lymphocytes into the brain contributes to neurodegeneration in a mouse model of Parkinson disease. *J. Clin. Invest.*, 119, 182–192.

Brugarolas, J., Lei, K., Hurley, R.L., Manning, B.D., Reiling, J.H., Hafen, E., Witters, L.A., Ellisen, L.W., and Kaelin, W.G. (2004) Regulation of mTOR function in response to hypoxia by REDD1 and the TSC1/TSC2 tumor suppressor complex. *Genes Dev.*, 18, 2893–2904.

Burbulla, A.L.F., Song, P., Mazzulli, J.R., Zampese, E., Strojny, C., Savas, J.N., Kiskinis, E., and Zhuang, X. (2017) Dopamine oxidation mediates a human-specific cascade of mitochondrial and lysosomal dysfunction in Parkinson ' s disease. *Science (80-.)*., 357, 1255–1261.

Burke, R.E. (2007) Inhibition of mitogen-activated protein kinase and stimulation of Akt kinase signaling pathways: Two approaches with therapeutic potential in the treatment of neurodegenerative disease. *Pharmacol. Ther.*, 114, 261–277.

Burke, R. E. and O'Malley, K. (2013) Axon Degeneration in Parkinson's Disease. *Exp. Neurol.*, 246, 72–83.

Bushell, M., Poncet, D., Marissen, W.E., Flotow, H., Lloyd, R.E., Clemens, M.J., and Morley, S.J. (2000) Cleavage of polypeptide chain initiation factor eIF4GI during apoptosis in lymphoma cells: Characterisation of an internal fragment generated by caspase-3-mediated cleavage. *Cell Death Differ.*, 7, 628–636.

Buyan-Dent, B.L., Mangin, T., and Shannon, K.M. (2018) Pharmaceutical Treatment of Parkinson's Disease. *Pract. Neurol.*, 32–37.

Cao, R., Gkogkas, C.G., De Zavalia, N., Blum, I.D., Yanagiya, A., Tsukumo, Y., Xu, H., Lee, C., Storch, K.F., Liu, A.C., Amir, S., and Sonenberg, N. (2015) Light-regulated translational control of circadian behavior by eIF4E phosphorylation. *Nat. Neurosci.*, 18, 855–862.

Cappelletti, G., Surrey, T., and Maci, R. (2005) The parkinsonism producing neurotoxin MPP+ affects microtubule dynamics by acting as a destabilising factor. *FEBS Lett.*, 579, 4781–4786.

Carballo-Carbajal, I., Laguna, A., Romero-Giménez, J., Cuadros, T., Bové, J., Martinez-Vicente, M., Parent, A., Gonzalez-Sepulveda, M., Peñuelas, N., Torra, A., Rodríguez-Galván, B., Ballabio, A., Hasegawa, T., Bortolozzi, A., Gelpi, E., and Vila, M. (2019) Brain tyrosinase overexpression implicates age-dependent neuromelanin production in Parkinson's disease pathogenesis. *Nat. Commun.*, 10.

Carriere, A., Ray, H., Blenis, J., and Roux, P.P. (2008) The RSK factors of activating the Ras/MAPK signaling cascade. *Front. Biosci.*, 1, 4258–4275.

Caudle, W.M., Richardson, J.R., Wang, M.Z., Taylor, T.N., Guillot, T.S., McCormack, A.L., Colebrooke, R.E., Di Monte, D.A., Emson, P.C., and Miller, G.W. (2007) Reduced Vesicular Storage of Dopamine Causes Progressive Nigrostriatal Neurodegeneration. *J. Neurosci.*, 27, 8138–8148.

Caudle, W.M., Colebrooke, R.E., Emson, P.C., and Miller, G.W. (2008) Altered vesicular dopamine storage in Parkinson's disease: a premature demise. *Trends Neurosci.*, 31, 303–308.

Chambers, J.W., Pachori, A., Howard, S., Ganno, M., Hansen, D., Kamenecka, T., Song, X., Duckett, D., Chen, W., Ling, Y.Y., Cherry, L., Cameron, M.D., Lin, L., Ruiz, C.H., and Lograsso, P. (2011) Small molecule c-jun-N-terminal kinase inhibitors protect dopaminergic neurons in a model of Parkinson's Disease. *ACS Chem. Neurosci.*, 2, 198–206.

Chambers, J.W., Howard, S., and LoGrasso, P. V. (2013) Blocking c-Jun N-terminal kinase (JNK) translocation to the mitochondria prevents 6-hydroxydopamine-induced toxicity in vitro and in vivo. *J. Biol. Chem.*, 288, 1079–1087.

Chan, C.S., Guzman, J.N., Ilijic, E., Mercer, J.N., Rick, C., Tkatch, T., Meredith, G.E., and Surmeier, D.J. (2007) "Rejuvenation" protects neurons in mouse models of Parkinson's disease. *Nature*, 447, 1081–1086.

Chandra, S., Jana, M., and Pahan, K. (2018) Aspirin Induces Lysosomal Biogenesis and Attenuates Amyloid Plaque Pathology in a Mouse Model of Alzheimer's Disease via PPARα. *J. Neurosci.*, 38, 6682–6699.

Chandra, S., Roy, A., Jana, M., and Pahan, K. (2019) Cinnamic acid activates PPARα to stimulate Lysosomal biogenesis and lower Amyloid plaque pathology in an Alzheimer's disease mouse model. *Neurobiol. Dis.*, 124, 379–395.

Chauhan, N.B., Siegel, G.J., and Lee, J.M. (2001) Depletion of glial cell line-derived neurotrophic factor in substantia nigra neurons of Parkinson's disease brain. *J. Chem. Neuroanat.*, 21, 277–288.

Chauhan, S., Goodwin, J.G., Chauhan, S., Manyam, G., Wang, J., Kamat, A.M., and Boyd, D.D. (2013) ZKSCAN3 Is a Master Transcriptional Repressor of Autophagy. *Mol. Cell*, 50, 16–28.

Chauhan, S., Ahmed, Z., Bradfute, S.B., Arko-Mensah, J., Mandell, M.A., Won Choi, S., Kimura, T., Blanchet, F., Waller, A., Mudd, M.H., Jiang, S., Sklar, L., Timmins, G.S., Maphis, N., Bhaskar, K., Piguet, V., and Deretic, V. (2015) Pharmaceutical screen identifies novel target processes for activation of autophagy with a broad translational potential. *Nat. Commun.*, 6, 1–15.

Chen, H., Zhang, S.M., Schwarzschild, M.A., Hernán, M.A., and Ascherio, A. (2005a) Physical activity and the risk of Parkinson disease. *Neurology*, 64, 664–669.

Chen, H., Chomyn, A., and Chan, D.C. (2005b) Disruption of fusion results in mitochondrial heterogeneity and dysfunction. *J. Biol. Chem.*, 280, 26185–26192.

Chen, H., McCaffery, J.M., and Chan, D.C. (2007) Mitochondrial Fusion Protects against Neurodegeneration in the Cerebellum. *Cell*, 130, 548–562.

Chen, H., Vermulst, M., Wang, Y.E., Chomyn, A., Prolla, T.A., McCaffery, J.M., and Chan, D.C. (2010) Mitochondrial fusion is required for mtdna stability in skeletal muscle and tolerance of mtDNA mutations. *Cell*, 141, 280–289.

Chen, L., Xie, Z., Turkson, S., and Zhuang, X. (2015) A53T Human -Synuclein Overexpression in Transgenic Mice Induces Pervasive Mitochondria Macroautophagy Defects Preceding Dopamine Neuron Degeneration. *J. Neurosci.*, 35, 890–905.

Cheng, H., Ulane, C., Burke, R. (2010) Clinical Progression in Parkinson's Disease and the Neurobiology of Axons. *Ann. Neurol.*, 67, 715–725.

Cheng, B., Yang, X., An, L., Gao, B., Liu, X., and Liu, S. (2009) Ketogenic diet protects dopaminergic neurons against 6-OHDA neurotoxicity via up-regulating glutathione in a rat model of Parkinson's disease. *Brain Res.*, 1286, 25–31.

Cheung, E.C.C. and Slack, R.S. (2004) Emerging Role for ERK as a Key Regulator of Neuronal Apoptosis. *Sci. Signal.*, 2004, pe45–pe45.

Choi-Lundberg, D.L., Lin, Q., Schallert, T., Crippens, D., Davidson, B.L., Chang, Y.N., Chiang, Y.L., Qian, J., Bardwaj, L., and Bohn, M.C. (1998) Behavioral and cellular protection of rat dopaminergic neurons by an adenoviral vector encoding glial cell line-derived neurotrophic factor. *Exp. Neurol.*, 154, 261–275.

Choi, B.S., Kim, H., Lee, H.J., Sapkota, K., Park, S.E., Kim, S., and Kim, S.J. (2014) Celastrol from "Thunder God Vine" Protects SH-SY5Y cells through the preservation of mitochondrial function and inhibition of p38 mapk in a rotenone model of parkinson's disease. *Neurochem. Res.*, 39, 84–96.

Choi, W.S., Yoon, S.Y., Oh, T.H., Choi, E.J., O'Malley, K.L., and Oh, Y.J. (1999) Two distinct mechanisms are involved in 6-hydroxydopamine- and MPP+- induced dopaminergic neuronal cell death: Role of caspases, ROS, and JNK. *J. Neurosci. Res.*, 57, 86–94.

Chu, Y., Dodiya, H., Aebischer, P., Olanow, C.W., and Kordower, J.H. (2009) Alterations in lysosomal and proteasomal markers in Parkinson's disease: Relationship to alpha-synuclein inclusions. *Neurobiol. Dis.*, 35, 385–398.

Chuang, J.I., Pan, I.L., Hsieh, C.Y., Huang, C.Y., Chen, P.C., and Shin, J.W. (2016) Melatonin prevents the dynamin-related protein 1-dependent mitochondrial fission and oxidative insult in the cortical neurons after 1-methyl-4-phenylpyridinium treatment. *J. Pineal Res.*, 1, 230–240.

Chung, C.Y., Khurana, V., Auluck, P.K., Tardiff, D.F., Mazzulli, J.R., Soldner, F., Baru, V., Lou, Y., Freyzon, Y., Cho, S., Mungenast, A.E., Muffat, J., Mitalipova, M., Pluth, M.D., Jui, N.T., Schuïe, B., Lippard, S.J., Tsai, L.H., Krainc, D., Buchwald, S.L., Jaenisch, R., and Lindquist, S. (2013) Identification and rescue of α-synuclein toxicity in Parkinson patient-derived neurons. *Science (80-.).*, 342, 983–987.

Cochemé, H.M. and Murphy, M.P. (2008) Complex I is the major site of mitochondrial superoxide production by paraquat. *J. Biol. Chem.*, 283, 1786–1798.

Coquillard, C., Vilchez, V., Marti, F., and Gedaly, R. (2015) mTOR Signaling in Regulatory T Cell Differentiation and Expansion. *SOJ Immunol.*, 3.

Costa, J., Lunet, N., Santos, C., Santos, J., and Vaz-Carneiro, A. (2010) Caffeine exposure and the risk of Parkinson's disease: A systematic review and meta-analysis of observational studiess. *J. Alzheimer's Dis.*, 20.

Crews, L., Spencer, B., Desplats, P., Patrick, C., Paulino, A., Rockenstein, E., Hansen, L., Adame, A., Galasko, D., and Masliah, E. (2010) Selective molecular alterations in the autophagy pathway in patients with lewy body disease and in models of α-synucleinopathy. *PLoS One*, 5.

Crocker, C.E., Khan, S., Cameron, M.D., Robertson, H.A., Robertson, G.S., and Lograsso, P. (2011) JNK inhibition protects dopamine neurons and provides behavioral improvement in a rat 6-hydroxydopamine model of Parkinson's disease. *ACS Chem. Neurosci.*, 2, 207–212.

Cuervo, A.M., Stafanis, L., Fredenburg, R., Lansbury, P.T., and Sulzer, D. (2004) Impaired degradation of mutant α-synuclein by chaperone-mediated autophagy. *Science (80-.).*, 305, 1292–1295.

Date, I., Aoi, M., Tomita, S., Collins, F., and Ohmoto, T. (1998) GDNF administration induces recovery of the nigrostriatal dopaminergic system both in young and aged Parkinsonian mice. *Neuroreport*, 9, 2365–2369.

Dauer, W. and Przedborski, S. (2003) Parkinson's Disease: Mechanisms and Models. *Neuron*, 39, 889–909.

Dawson, T.M., Ko, H.S., and Dawson, V.L. (2010) Genetic Animal Models of Parkinson's Disease. *Neuron*, 66, 646–661.

de Lau, L. and Breteler, M. (2006) Epidemiology of Parkinson's disease. *Lancet Neurol.*, 5, 54–58.

Decressac, M., Ulusoy, A., Mattsson, B., Georgievska, B., Romero-Ramos, M., Kirik, D., and Björklund, A. (2011) GDNF fails to exert neuroprotection in a rat α-synuclein model of Parkinson's disease. *Brain*, 134, 2302–2311.

Decressac, M., Mattsson, B., Lundblad, M., Weikop, P., and Björklund, A. (2012a) Progressive neurodegenerative and behavioural changes induced by AAV-mediated overexpression of α-synuclein in midbrain dopamine neurons. *Neurobiol. Dis.*, 45, 939–953.

Decressac, M., Kadkhodaei, B., Mattsson, B., Laguna, A., Perlmann, T., and Björklund, A. (2012b) α-synuclein-induced down-regulation of Nurr1 disrupts GDNF signaling in nigral dopamine neurons. *Sci. Transl. Med.*, 4.

Decressac, M., Mattsson, B., Weikop, P., Lundblad, M., Jakobsson, J., and Bjorklund, A. (2013) TFEB-mediated autophagy rescues midbrain dopamine neurons from -synuclein toxicity. *Proc. Natl. Acad. Sci.*, 110, E1817–E1826.

Dehay, B., Bové, J., Rodriguez-Muela, N., Perier, C., Recasens, A., Boya, P., and Vila, M. (2010) Pathogenic Lysosomal Depletion in Parkinson's Disease. *J. Neurosci.*, 30, 12535–12544.

Dehay, B., Ramirez, A., Martinez-Vicente, M., Perier, C., Canron, M.-H., Doudnikoff, E., Vital, A., Vila, M., Klein, C., and Bezard, E. (2012) Loss of P-type ATPase ATP13A2/PARK9 function induces general lysosomal deficiency and leads to Parkinson disease neurodegeneration. *Proc. Natl. Acad. Sci.*, 109, 9611–9616.

Delettre, C., Lenaers, G., Griffoin, J.M., Gigarel, N., Lorenzo, C., Belenguer, P., Pelloquin, L., Grosgeorge, J., Turc-Carel, C., Perret, E., Astarie-Dequeker, C., Lasquellec, L., Arnaud, B., Ducommun, B., Kaplan, J., and Hamel, C.P. (2000) Nuclear gene OPA1, encoding a mitochondrial dynamin-related protein, is mutated in dominant optic atrophy. *Nat. Genet.*, 26, 207–210.

Di Maio, R., Barrett, P.J., Hoffman, E.K., Barrett, C.W., Zharikov, A., Borah, A., Hu, X., Mccoy, J., Chu, C.T., Burton, E.A., Hastings, T.G., and Greenamyre, J.T. (2016) α-Synuclein binds TOM20 and inhibits mitochondrial protein import in Parkinson's disease HHS Public Access. *Sci. Transl. Med.*, 8, 342–378.

Di Malta, C., Siciliano, D., Calcagni, A., Monfregola, J., Punzi, S., Pastore, N., Eastes, A.N., Davis, O., De Cegli, R., Zampelli, A., Di Giovannantonio, L.G., Nusco, E., Platt, N., Guida, A., Ogmundsdottir, M.H., Lanfrancone, L., Perera, R.M., Zoncu, R., Pelicci, P.G., Settembre, C., and Ballabio, A. (2017) Transcriptional activation of RagD GTPase controls mTORC1 and promotes cancer growth. *Science,* 356, 1188–1193.

Di Malta, C. and Ballabio, A. (2017) TFEB-mTORC1 feedback loop in metabolism and cancer. *Cell Stress*, 1(1), 7.

Díaz-Mataix, L., Scorza, M., Bortolozzi, A., Toth, M., Celada, P., and Artigas, F. (2005) Involvement of 5-HT1A Receptors in Prefrontal Cortex in the Modulation of Dopaminergic Activity: Role in Atypical Antipsychotic Action. *J. Neurosci.*, 25, 10831–10843.

Dietz, G.P.H., Stockhausen, K. V., Dietz, B., Falkenburger, B.H., Valbuena, P., Opazo, F., Lingor, P., Meuer, K., Weishaupt, J.H., Schulz, J.B., and Bähr, M. (2008) Membrane-permeable Bcl-xL prevents MPTP-induced dopaminergic neuronal loss in the substantia nigra. *J. Neurochem.*, 104, 757–765.

Dogbevia, G.K., Roßmanith, M., Sprengel, R., and Hasan, M.T. (2016) Flexible, AAV-equipped Genetic Modules for Inducible Control of Gene Expression in Mammalian Brain. *Mol. Ther. - Nucleic Acids*, 5, e309.

Domanskyi, A., Saarma, M., and Airavaara, M. (2015) Prospects of Neurotrophic Factors for Parkinson's Disease: Comparison of Protein and Gene Therapy. *Hum. Gene Ther.*, 26, 550–559.

Donovan, N., Becker, E.B.E., Konishi, Y., and Bonni, A. (2002) JNK phosphorylation and activation of bad couples the stress-activated signaling pathway to the cell death machinery. *J. Biol. Chem.*, 277, 40944–40949.

Durinck, S., Stawiski, E.W., Pavía-Jiménez, A., Modrusan, Z., Kapur, P., Jaiswal, B.S., Zhang, N., Toffessi-Tcheuyap, V., Nguyen, T.T., Pahuja, K.B., Chen, Y.J., Saleem, S., Chaudhuri, S., Heldens, S., Jackson, M., Peña-Llopis, S., Guillory, J., Toy, K., Ha, C., Harris, C.J., Holloman, E., Hill, H.M., Stinson, J., Rivers, C.S., Janakiraman, V., Wang, W., Kinch, L.N., Grishin, N. V., Haverty, P.M., Chow, B., Gehring, J.S., Reeder, J., Pau, G., Wu, T.D., Margulis, V., Lotan, Y., Sagalowsky, A., Pedrosa, I., De Sauvage, F.J., Brugarolas, J., and Seshagiri, S. (2015) Spectrum of diverse genomic alterations define non-clear cell renal carcinoma subtypes. *Nat. Genet.*, 47, 13–21.

Dzamko, N., Zhou, J., Huang, Y., and Halliday, G.M. (2014) Parkinson's disease-implicated kinases in the brain; insights into disease pathogenesis. *Front. Mol. Neurosci.*, 7, 1–15.

Edvardson, S., Cinnamon, Y., Ta-Shma, A., Shaag, A., Yim, Y.I., Zenvirt, S., Jalas, C., Lesage, S., Brice, A., Taraboulos, A., Kaestner, K.H., Greene, L.E., and Elpeleg, O. (2012) A deleterious mutation in DNAJC6 encoding the neuronal-specific clathrin-uncoating Co-chaperone auxilin, is associated with juvenile parkinsonism. *PLoS One*, 7, 4–8.

Ekstrand, M.I., Terzioglu, M., Galter, D., Zhu, S., Hofstetter, C., Lindqvist, E., Ekstrand, M.I., Thams, S., Bergstrand, A., Hansson, F.S., Trifunovic, A., Hoffer, B., Cullheim, S., Mohammed, A.H., and Olson, L. (2007) Progressive parkinsonism in mice with respiratory-chain-deficient dopamine neurons. *Proc. Natl. Acad. Sci.*, 104, 1325–1330.

Elstner, M., Morris, C.M., Heim, K., Bender, A., Mehta, D., Jaros, E., Klopstock, T., Meitinger, T., Turnbull, D.M., and Prokisch, H. (2011) Expression analysis of dopaminergic neurons in Parkinson's disease and aging links transcriptional dysregulation of energy metabolism to cell death. *Acta Neuropathol.*, 122, 75–86.

Emmanouilidou, E., Melachroinou, K., Roumeliotis, T., Garbis, S.D., Ntzouni, M., Margaritis, L.H., Stefanis, L., and Vekrellis, K. (2010) Cell-Produced -Synuclein Is Secreted in a Calcium-Dependent Manner by Exosomes and Impacts Neuronal Survival. *J. Neurosci.*, 30, 6838–6851.

Fahn, S., Jankovic, J., and Hallett, M. (2011) Current concepts on the etiology and pathogenesis of Parkinson disease. *Princ. Pract. Mov. Disord.*, 93–118.

Fearnley, J.M. and Lees, A.J. (1991) Ageing and Parkinson's disease: substantia nigra regional selectivity. *Brain*, Oct;114 (Pt 5):2283-301.

Fernagut, P.O. and Chesselet, M.F. (2004) Alpha-synuclein and transgenic mouse models. *Neurobiol. Dis.*, 17, 123–130.

Ferreira, R.N., de Miranda, A.S., Rocha, N.P., Simoes, E-S. A.C., Teixeira, A.L., and da Silva Camargos, E.R. (2018) Neurotrophic Factors in Parkinson's Disease: What Have we Learned from Pre-Clinical and Clinical Studies? *Curr. Med. Chem.* 25(31):3682-3702.

Ferron, M., Settembre, C., Shimazu, J., Lacombe, J., Kato, S., Rawlings, D.J., Ballabio, A., and Karsenty, G. (2013) A RANKL-PKCβ-TFEB signaling cascade is necessary for lysosomal biogenesis in osteoclasts. *Genes Dev.*, 27, 955–969.

Figueroa, C., Tarras, S., Taylor, J., and Vojtek, A.B. (2003) Akt2 Negatively Regulates Assembly of the POSH-MLK-JNK Signaling Complex. *J. Biol. Chem.*, 278, 47922–47927.

Filichia, E., Hoffer, B., Qi, X., and Luo, Y. (2016) Inhibition of Drp1 mitochondrial translocation provides neural protection in dopaminergic system in a Parkinson's disease model induced by MPTP. *Sci. Rep.*, 6, 1–13.

Finley, D. (2009) Recognition and Processing of Ubiquitin-Protein Conjugates by the Proteasome. *Annu. Rev. Biochem.*, 78, 477–513.

Fjord-Larsen, L., Johansen, J.L., Kusk, P., Tornøe, J., Grønborg, M., Rosenblad, C., and Wahlberg, L.U. (2005) Efficient in vivo protection of nigral dopaminergic neurons by lentiviral gene transfer of a modified Neurturin construct. *Exp. Neurol.*, 195, 49–60.

Fleckenstein, A.E., Volz, T.J., Riddle, E.L., Gibb, J.W., and Hanson, G.R. (2007) New Insights into the Mechanism of Action of Amphetamines. *Annu. Rev. Pharmacol. Toxicol.*, 47, 681–698.

Fornai, F., Schluter, O.M., Lenzi, P., Gesi, M., Ruffoli, R., Ferrucci, M., Lazzeri, G., Busceti, C.L., Pontarelli, F., Battaglia, G., Pellegrini, A., Nicoletti, F., Ruggieri, S., Paparelli, A., and Sudhof, T.C. (2005) Parkinson-like syndrome induced by continuous MPTP infusion: Convergent roles of the ubiquitin-proteasome system and -synuclein. *Proc. Natl. Acad. Sci.*, 102, 3413–3418.

Fox, M.E., Mikhailova, M.A., Bass, C.E., Takmakov, P., Gainetdinov, R.R., Budygin, E.A., and Wightman, R.M. (2016) Cross-hemispheric dopamine projections have functional significance. *Proc. Natl. Acad. Sci.*, 113, 6985–6990.

Franco-Iborra, S., Vila, M., and Perier, C. (2016) The Parkinson Disease Mitochondrial Hypothesis: Where Are We at? *Neuroscientist*, 22, 266–277.

Franco-Iborra, S., Cuadros, T., Parent, A., Romero-Gimenez, J., Vila, M., and Perier, C. (2018a) Defective mitochondrial protein import contributes to complex I-induced mitochondrial dysfunction and neurodegeneration in Parkinson's disease. *Cell Death Dis.*, 9.

Franco-Iborra, S., Vila, M., and Perier, C. (2018b) Mitochondrial quality control in neurodegenerative diseases: Focus on Parkinson's disease and Huntington's disease. *Front. Neurosci.*, 12, 1–25.

Frank, S., Gaume, B., Bergmann-Leitner, E.S., Leitner, W.W., Robert, E.G., Catez, F., Smith, C.L., and Youle, R.J. (2001) The Role of Dynamin-Related Protein 1, a Mediator of Mitochondrial Fission, in Apoptosis. *Dev. Cell*, 1, 515–525.

Frim, D.M., Uhler, T.A., Galpern, W.R., Beal, M.F., Breakefield, X.O., and Isacson, O. (1994) Implanted fibroblasts genetically engineered to produce brain-derived neurotrophic factor prevent 1-methyl-4-phenylpyridinium toxicity to dopaminergic neurons in the rat. *Proc. Natl. Acad. Sci. U. S. A.*, 91, 5104–5108.

Ganley, I.G., Lam, D.H., Wang, J., Ding, X., Chen, S., and Jiang, X. (2009) ULK1·ATG13·FIP200 complex mediates mTOR signaling and is essential for autophagy. *J. Biol. Chem.*, 284, 12297–12305.

Garbayo, E., Ansorena, E., Lana, H., Carmona-Abellan, M. del M., Marcilla, I., Lanciego, J.L., Luquin, M.R., and Blanco-Prieto, M.J. (2016) Brain delivery of microencapsulated GDNF induces functional and structural recovery in parkinsonian monkeys. *Biomaterials*, 110, 11–23.

Garcia-Esparcia, P., Hernández-Ortega, K., Koneti, A., Gil, L., Delgado-Morales, R., Castaño, E., Carmona, M., and Ferrer, I. (2015) Altered machinery of protein synthesis is region- and stage-dependent and is associated with α-synuclein oligomers in Parkinson's disease. *Acta Neuropathol. Commun.*, 3, 1–25.

Garea-Rodríguez, E., Eesmaa, A., Lindholm, P., Schlumbohm, C., König, J., Meller, B., Krieglstein, K., Helms, G., Saarma, M., and Fuchs, E. (2016) Comparative Analysis of the Effects of Neurotrophic Factors CDNF and GDNF in a Nonhuman Primate Model of Parkinson's Disease. *PLoS One*, 11.

Gegg, M.E., Burke, D., Heales, S.J.R., Cooper, J.M., Hardy, J., Wood, N.W., and Schapira, A.H.V. (2012) Glucocerebrosidase deficiency in substantia nigra of parkinson disease brains. *Ann. Neurol.*, 72, 455–463.

Genheden, M., Kenney, J.W., Johnston, H.E., Manousopoulou, A., Garbis, S.D., and Proud, C.G. (2015) BDNF Stimulation of Protein Synthesis in Cortical Neurons Requires the MAP Kinase-Interacting Kinase MNK1. *J. Neurosci.*, 35, 972–984.

Gerhardt, G.A., Cass, W.A., Huettl, P., Brock, S., Zhang, Z., and Gash, D.M. (1999) GDNF improves dopamine function in the substantia nigra but not the putamen of unilateral MPTP-lesioned rhesus monkeys. *Brain Res.*, 817, 163–171.

Giasson, B., Duda, J., Murray, I., Chen, Q., Souza, J., Hurtig, H., Ischiropoulos, H., Trojanowski, J., and Lee, V.-Y. (2000) Oxidative Damage Linked to Neurodegeneration by Selective a-Synuclein Nitration in Synucleinopathy Lesions. *Science*, 290, 985–989.

Gingras, A., Raught, B., and Sonenberg, N. (1999) eIF4 Initiation Factors: Effectors of mRNA Recruitment to Ribosomes and Regulators of Translation. *Annu. Rev. Biochem.*, 68, 913–963.

Giovanni, A., Sieber, B.-A., Heikkiila, R.E., and Sossalla, P.K. (1994) Studies on species sensitivity to the dopaminergic neurotoxin. Part 1: Systemic. *J. Pharmacol. Exp. Ther.*, 270, 1000–1007.

Goldstein, D., Sullivan, P., Holmes, C., Kopin, I., Basile, M., and Mash, D. (2011) Catechols in post-mortem brain of patients with Parkinson disease. *Eur. J. Neurosci.*, 18, 703–710.

Gomes, E., Papa, L., Hao, T., and Rockwell, P. (2007) The VEGFR2 and PKA pathways converge at MEK/ERK1/2 to promote survival in serum deprived neuronal cells. *Mol. Cell. Biochem.*, 305, 179–190.

Gomez-Lazaro, M., Bonekamp, N.A., Galindo, M.F., Jordán, J., and Schrader, M. (2008) 6-Hydroxydopamine (6-OHDA) induces Drp1-dependent mitochondrial fragmentation in SH-SY5Y cells. *Free Radic. Biol. Med.*, 44, 1960–1969.

Gómez-Santos, C., Ferrer, I., Reiriz, J., Vials, F., Barrachina, M., and Ambrosio, S. (2002) MPP + increases α-synuclein expression and ERK/MAP-kinase phosphorylation in human neuroblastoma SH-SY5Y cells. *Brain Res.*, 935, 32–39.

Greene, J.C., Whitworth, A.J., Kuo, I., Andrews, L.A., Feany, M.B., and Pallanck, L.J. (2003) Mitochondrial pathology and apoptotic muscle degeneration in Drosophila parkin mutants. *Proc. Natl. Acad. Sci.*, 100, 4078–4083.

Grondin, R., Zhang, Z., Yi, A., Cass, W., Maswood, N., Adersen, A., Elsberry, D., Klein, M., Gerhardt, G., and Gash, D. (2002) Chronic, controlled GDNF infusion promotes structural and functional recovery in advanced parkinsonian monkeys. *Brain*, 125, 2191–2201.

Grünewald, A., Rygiel, K.A., Hepplewhite, P.D., Morris, C.M., Picard, M., and Turnbull, D.M. (2016) Mitochondrial DNA Depletion in Respiratory Chain-Deficient Parkinson Disease Neurons. *Ann. Neurol.*, 79, 366–378.

Haaxma, C.A., Bloem, B.R., Borm, G.F., Oyen, W.J.G., Leenders, K.L., Eshuis, S., Booij, J., Dluzen, D.E., and Horstink, M.W.I.M. (2007) Gender differences in Parkinson's disease. *J. Neurol. Neurosurg. Psychiatry*, 78, 819–824.

Haberman, R.P., Criswell, H.E., Snowdy, S., Ming, Z., Breese, G.R., Samulski, R.J., and McCown, T.J. (2002) Therapeutic liabilities of in vivo viral vector tropism: Adeno-associated virus vectors, NMDAR1 antisense, and focal seizure sensitivity. *Mol. Ther.*, 6, 495–500.

Halliday, G.M., Ophof, A., Broe, M., Jensen, P.H., Kettle, E., Fedorow, H., Cartwright, M.I., Griffiths, F.M., Shepherd, C.E., and Double, K.L. (2005) α-Synuclein redistributes to neuromelanin lipid in the substantia nigra early in Parkinson's disease. *Brain*, 128, 2654–2664.

Hallsson, J.H., Haflidadóttir, B.S., Stivers, C., Odenwald, W., Arnheiter, H., Pignoni, F., and Steingrímsson, E. (2004) The basic helix-loop-helix leucine zipper transcription factor Mitf is conserved in Drosophila and functions in eye development. *Genetics*, 167, 233–241.

Haq, R. and Fisher, D.E. (2011) Biology and clinical relevance of the micropthalmia family of transcription factors in human cancer. *J. Clin. Oncol.*, 29, 3474–3482.

Hasegawa, Y., Inagaki, T., Sawada, M., and Suzumura, A. (2000) Impaired cytokine production by peripheral blood mononuclear cells and monocytes/macrophages in Parkinson's disease. *Acta Neurol. Scand.*, 101, 159–164.

Hastings, T., Lewis, A., and Zigmond, M. (1996) Role of oxidation in the neurotoxic effects of intrastriatal dopamine injections. *Proc. Natl. Acad. Sci. U. S. A.*, 93, 1956–1961.

Hattingen, E., Magerkurth, J., Pilatus, U., Mozer, A., Seifried, C., Steinmetz, H., Zanella, F., and Hilker, R. (2009) Phosphorus and proton magnetic resonance spectroscopy demonstrates mitochondrial dysfunction in early and advanced Parkinson's disease. *Brain*, 132, 3285–3297.

Hauser, R.A. (2009) Levodopa: Past, present, and future. *Eur. Neurol.*, 62, 1–8.

He, C. and Klionsky, D.J. (2009) Regulation mechanisms and signaling pathways of autophagy. *Annu. Rev. Genet.*, 43, 67–93.

Hemesath, T., Steingrímsson, E., Mcgill, G., Mj, H., Vaught, J., Ca, H., Arnheiter, H., Copeland, N., Jenkins, N., and Fisher, D. (1994) Search : microphthalmia , a critical factor in melanocyte development , defines a discrete transcription factor family . *Genes Dev.*, 8, 2770–2780.

Hernán, M.A., Takkouche, B., Caamaño-Isorna, F., and Gestal-Otero, J.J. (2002) A meta-analysis of coffee drinking, cigarette smoking, and the risk of Parkinson's disease. *Ann. Neurol.*, 52, 276–284.

Herzog, C.D., Dass, B., Holden, J.E., Stansell, J., Gasmi, M., Tuszynski, M.H., Bartus, R.T., and Kordower, J.H. (2007) Striatal delivery of CERE-120, an AAV2 vector encoding human neurturin, enhances activity of the dopaminergic nigrostriatal system in aged monkeys. *Mov. Disord.*, 22, 1124–1132.

Hetman, M., Kanning, K., Cavanaugh, J.E., and Xia, Z. (1999) Neuroprotection by brain-derived neurotrophic factor is mediated by extracellular signal-regulated kinase and phosphatidylinositol 3-kinase. *J. Biol. Chem.*, 274, 22569–22580.

Hetman, M. and Gosdz, A. (2004) Role of extracellular signal regulated kinases 1 and 2 in neuronal survival. *Eur. J. Biochem.*, 271, 2050–2055.

Hirsch, E., Hunot, S., Faucheux, B., Agid, Y., Mizuno, Y., Mochizuki, H., Tatton, W., Tatton, N., and Olanow, W. (1999) Dopaminergic Neurons Degenerate by Apoptosis in Parkinson's Disease. *Mov. Disord.*, 14, 383–386.

Hoffer, B.J., Hoffman, A., Bowenkamp, K., Huettl, P., Hudson, J., Martin, D., Lin, L.F.H., and Gerhardt, G.A. (1994) Glial cell line-derived neurotrophic factor reverses toxin-induced injury to midbrain dopaminergic neurons in vivo. *Neurosci. Lett.*, 182, 107–111.

Holtz, W.A. and O'Malley, K.L. (2003) Parkinsonian mimetics induce aspects of unfolded protein response in death of dopaminergic neurons. *J. Biol. Chem.*, 278, 19367–19377.

Hoozemans, J.J.M., van Haastert, E.S., Eikelenboom, P., de Vos, R.A.I., Rozemuller, J.M., and Scheper, W. (2007) Activation of the unfolded protein response in Parkinson's disease. *Biochem. Biophys. Res. Commun.*, 354, 707–711.

Horger, B.A., Nishimura, M.C., Armanini, M.P., Wang, L.-C., Poulsen, K.T., Rosenblad, C., Kirik, D., Moffat, B., Simmons, L., Johnson, E., Milbrandt, J., Rosenthal, A., Bjorklund, A., Vandlen, R.A., Hynes, M.A., and Phillips, H.S. (1998) Neurturin Exerts Potent Actions on Survival and Function of Midbrain Dopaminergic Neurons. *J. Neurosci.*, 18, 4929–4937.

Hosokawa, N., Hara, T., Kaizuka, T., Kishi, C., Takamura, A., Miura, Y., Iemura, S., Natsume, T., Takehana, K., Yamada, N., Guan, J., Oshiro, N., and Mizushima, N. (2009) Nutrient-dependent mTORC1 Association with the ULK1–Atg13–FIP200 Complex Required for Autophagy. *Mol. Biol. Cell*, 20, 1981–1991.

Hsuan, S.-L., Klintworth, H.M., and Xia, Z. (2006) Basic Fibroblast Growth Factor Protects against Rotenone-Induced Dopaminergic Cell Death through Activation of Extracellular Signal-Regulated Kinases 1/2 and Phosphatidylinositol-3 Kinase Pathways. *J. Neurosci.*, 26, 4481–4491.

Hu, X., Weng, Z., Chu, C.T., Zhang, L., Cao, G., Gao, Y., Signore, A., Zhu, J., Hastings, T., Greenamyre, J.T., and Chen, J. (2011) Peroxiredoxin-2 Protects against 6-Hydroxydopamine-Induced Dopaminergic Neurodegeneration via Attenuation of the Apoptosis Signal-Regulating Kinase (ASK1) Signaling Cascade. *J. Neurosci.*, 31, 247–261.

Hu, Z.Y., Chen, B., Zhang, J.P., and Ma, Y.Y. (2017) Up-regulation of autophagy-related gene 5 (ATG5) protects dopaminergic neurons in a zebrafish model of Parkinson's disease. *J. Biol. Chem.*, 292, 18062–18074.

Huang, D., Xu, J., Wang, J., Tong, J., Bai, X., Li, H., Wang, Z., Huang, Y., Wu, Y., Yu, M., and Huang, F. (2017) Dynamic changes in the nigrostriatal pathway in the MPTP mouse model of Parkinson's disease. *Parkinsons. Dis.*, 2017.

Hunot, S. and Hirsch, E.C. (2003) Neuroinflammatory processes in Parkinson's disease. *Ann. Neurol.*, 53, S49–S60.

Hunot, S., Vila, M., Teismann, P., Davis, R.J., Hirsch, E.C., Przedborski, S., Rakic, P., and Flavell, R.A. (2004) JNK-mediated induction of cyclooxygenase 2 is required for neurodegeneration in a mouse model of Parkinson's disease. *Proc. Natl. Acad. Sci.*, 101, 665–670.

Hwang, O. (2013) Role of Oxidative Stress in Parkinson's Disease. *Exp. Neurobiol.*, 22, 11–17.

Hyman, C., Juhasz, M., Jackson, C., Wright, P., Ip, N., and Lindsay, R. (1994) Overlapping and Distinct Actions of the Neurotrophins BDNF, NT-3, and NT-4/5 on Cultured Dopaminergic and GABAergic Neurons of the Ventral Mesencephalon. *J. Neurosci.*, 14, 335–347.

Iravani, M.M., Costa, S., Jackson, M.J., Tel, B.C., Cannizzaro, C., Pearce, R.K.B., and Jenner, P. (2001) GDNF reverses priming for dyskinesia in MPTP-treated, L-DOPA-primed common marmosets. *Eur. J. Neurosci.*, 13, 597–608.

Itoh, K., Nakamura, K., Iijima, M., and Sesaki, H. (2013) Mitochondrial dynamics and neurodegeneration. *Trends Cell Biol.*, 23, 64–71.

Ito, K. and Enomoto, H. (2016) Retrograde transport of neurotrophic factor signaling: implications in neuronal development and pathogenesis. *J. Biochem.*, 160, 77–85.

Jackson-Lewis, V., Jakowec, M., Burke, R.E., and Przedborski, S. (1995) Time course and morphology of dopaminergic neuronal death caused by the neurotoxin 1-methyl-4-phenyl-1,2,3,6-tetrahydropyridine. *Neurodegeneration*, 4, 257–269.

Jaeger, C.B., Joh, T.H., and Reis, D.J. (1983) The effect of forebrain lesions in the neonatal rat: Survival of midbrain dopaminergic neurons and the crossed nigrostriatal projection. *J. Comp. Neurol.*, 218, 74–90.

Jiang, X. and Wang, X. (2000) Cytochrome c promotes caspase-9 activation by inducing nucleotide binding to Apaf-1. *J. Biol. Chem.*, 275, 31199–31203.

Kale, J., Osterlund, E.J., and Andrews, D.W. (2018) BCL-2 family proteins: Changing partners in the dance towards death. *Cell Death Differ.*, 25, 65–80.

Kang, S.S., Zhang, Z., Liu, X., Manfredsson, F.P., Benskey, M.J., Cao, X., Xu, J., Sun, Y.E., and Ye, K. (2017) TrkB neurotrophic activities are blocked by α-synuclein, triggering dopaminergic cell death in Parkinson's disease. *Proc. Natl. Acad. Sci. U. S. A.*, 114, 10773–10778.

Kang, Y.C., Son, M., Kang, S., Im, S., Piao, Y., Lim, K.S., Song, M.Y., Park, K.S., Kim, Y.H., and Pak, Y.K. (2018) Cell-penetrating artificial mitochondria-targeting peptide-conjugated metallothionein 1A alleviates mitochondrial damage in Parkinson's disease models. *Exp. Mol. Med.*, 50, 105.

Kann, O. and Kovács, R. (2006) Mitochondria and neuronal activity. *Am. J. Physiol. Physiol.*, 292, C641–C657.

Kastner, A., Hirsch, E.C., Agid, Y., and Javoy-Agid, F. (1993) Tyrosine hydroxylase protein and messenger RNA in the dopaminergic nigral neurons of patients with Parkinson's disease. *Brain Res.*, 606, 341–345.

Kauffman, E.C., Ricketts, C.J., Rais-Bahrami, S., Yang, Y., Merino, M.J., Bottaro, D.P., Srinivasan, R., and Linehan, W.M. (2014) Molecular genetics and cellular features of TFE3 and TFEB fusion kidney cancers. *Nat. Rev. Urol.*, 11, 465–475.

Kawamoto, Y., Ito, H., Ayaki, T., and Takahashi, R. (2014) Immunohistochemical localization of apoptosome-related proteins in Lewy bodies in Parkinsons disease and dementia with Lewy bodies. *Brain Res.*, 1571, 39–48.

Keeney, P.M., Xie, J., Capaldi, R.A., and Bennett Jr, J.P. (2006) Parkinson's Disease Brain Mitochondrial Complex I Has Oxidatively Damaged Subunits and Is Functionally Impaired and Misassembled. *J. Neurosci.*, 26, 5256–5264.

Keinan, N., Tyomkin, D., and Shoshan-Barmatz, V. (2010) Oligomerization of the Mitochondrial Protein Voltage-Dependent Anion Channel Is Coupled to the Induction of Apoptosis. *Mol. Cell. Biol.*, 30, 5698–5709.

Kett, L.R., Stiller, B., Bernath, M.M., Tasset, I., Blesa, J., Jackson-Lewis, V., Chan, R.B., Zhou, B., Di Paolo, G., Przedborski, S., Cuervo, A.M., and Dauer, W.T. (2015) a-Synuclein-Independent Histopathological and Motor Deficits in Mice Lacking the Endolysosomal Parkinsonism Protein Atp13a2. *J. Neurosci.*, 35, 5724–5742.

Kilpatrick, K., Zeng, Y., Hancock, T., and Segatori, L. (2015) Genetic and chemical activation of TFEB mediates clearance of aggregated α-synuclein. *PLoS One*, 10, 1–21.

Kim, A.H., Yano, H., Cho, H., Meyer, D., Monks, B., Margolis, B., Birnbaum, M.J., and Chao, M. V. (2002) Akt1 regulates a JNK scaffold during excitotoxic apoptosis. *Neuron*, 35, 697–709.

Kim, S.R., Chen, X., Oo, T.F., Kareva, T., Yarygina, O., Wang, C., During, M., Kholodilov, N., and Burke, R.E. (2011a) Dopaminergic pathway reconstruction by Akt/Rheb-induced axon regeneration. *Ann. Neurol.*, 70, 110–120.

Kim, T.W., Moon, Y., Kim, K., Lee, J.E., Koh, H.C., Rhyu, I.J., Kim, H., and Sun, W. (2011b) Dissociation of progressive dopaminergic neuronal death and behavioral impairments by bax deletion in a mouse model of parkinson's diseases. *PLoS One*, 6.

Kim, S.R., Kareva, T., Yarygina, O., Kholodilov, N., and Burke, R.E. (2012) AAV transduction of dopamine neurons with constitutively active rheb protects from neurodegeneration and mediates axon regrowth. *Mol. Ther.*, 20, 275–286.

Kirik, D., Rosenblad, C., Burger, C., Lundberg, C., Johansen, T.E., Muzyczka, N., Mandel, R.J., and Björklund, A. (2002) Parkinson-Like Neurodegeneration Induced by Targeted Overexpression of α-Synuclein in the Nigrostriatal System. *J. Neurosci.*, 22, 2780–2791.

Kish, S.J., Morito, C., and Hornykiewicz, O. (1985) Glutathione peroxidase activity in Parkinson's disease brain. *Neurosci. Lett.*, 58, 343–346.

Kitada, T., Tong, Y., Gautier, C.A., and Shen, J. (2009) Absence of nigral degeneration in aged parkin/DJ-1/PINK1 triple knockout mice. *J. Neurochem.*, 111, 696–702.

Kitamura, Y., Kakimura, J., and Taniguchi, T. (1998) Protective effect of talipexole on MPTP-treated planarian, a unique parkinsonian worm model. *Jpn. J. Pharmacol.*, 78, 23–29.

Klein, C. and Westenberger, A. (2012) Genetics of Parkinson's disease. *Cold Spring Harb. Perspect. Med.*, 2, a008888.

Klein, P., Kathrin, A., Uller-Rischart, M., Motori, E., Onbauer, C., Schnorrer, F., Winklhofer, K.F., and R€ Udiger Klein, and (2014) Ret rescues mitochondrial morphology and muscle degeneration of Drosophila Pink1 mutants. *EMBO J.*, 33, 341–355.

Klein, R.L., Lewis, M.H., Muzyczka, N., and Meyer, E.M. (1999) Prevention of 6-hydroxydopamine-induced rotational behavior by BDNF somatic gene transfer. *Brain Res.*, 847, 314–320.

Kordower, J.H., Emborg, M.E., Bloch, J., Ma, S., Chu, Y., Leventhal, L., Mcbride, J., Chen, E.-Y., Palfi, S., Roitberg, B.Z., Douglas, W., Holden, J., Pyzalski, R., Taylor, M.D., Carvey, P., Ling, Z., Trono, D., Hantraye, P., Deglon, N., and Aebischer, P. (2000) Neurodegeneration Prevented by Lentiviral Vector Delivery of GDNF in Primate Models of Parkinson's Disease. *Science*, 290, 767–773.

Kordower, J.H., Herzog, C.D., Dass, B., Bakay, R.A.E., Stansell, J., Gasmi, M., and Bartus, R.T. (2006) Delivery of neurturin by AAV2 (CERE-120)-mediated gene transfer provides structural and functional neuroprotection and neurorestoration in MPTP-treated monkeys. *Ann. Neurol.*, 60, 706–715.

Kordower, J.H., Olanow, C.W., Dodiya, H.B., Chu, Y., Beach, T.G., Adler, C.H., Halliday, G.M., and Bartus, R.T. (2013) Disease duration and the integrity of the nigrostriatal system in Parkinson's disease. *Brain*, 136, 2419–2431.

Kramer, E.R. and Liss, B. (2015) GDNF-Ret signaling in midbrain dopaminergic neurons and its implication for Parkinson disease. *FEBS Lett.*, 589, 3760–3772.

Krebs, C.E., Karkheiran, S., Powell, J.C., Cao, M., Makarov, V., Darvish, H., Di Paolo, G., Walker, R.H., Shahidi, G.A., Buxbaum, J.D., De Camilli, P., Yue, Z., and Paisán-Ruiz, C. (2013) The sac1 domain of SYNJ1 identified mutated in a family with early-onset progressive parkinsonism with generalized seizures. *Hum. Mutat.*, 34, 1200–1207.

Kulich, S.M. and Chu, C.T. (2001) Sustained extracellular signal-regulated kinase activation by 6-hydroxydopamine: Implications for Parkinson's disease. *J. Neurochem.*, 77, 1058–1066.

Kumar Jha, S., Jha, N.K., Kar, R., Ambasta, R.K., and Kumar, P. (2015) p38 MAPK and PI3K/AKT Signalling Cascades inParkinson's Disease. *Int. J. Mol. Cell. Med.*, 4, 67–86.

Kuwana, T., Bouchier-Hayes, L., Chipuk, J.E., Bonzon, C., Sullivan, B.A., Green, D.R., and Newmeyer, D.D. (2005) BH3 domains of BH3-only proteins differentially regulate Bax-mediated mitochondrial membrane permeabilization both directly and indirectly. *Mol. Cell*, 17, 525–535.

Kyriakis, J.M. and Avruch, J. (2012) Mammalian MAPK Signal Transduction Pathways Activated by Stress and Inflammation: A 10-Year Update. *Physiol. Rev.*, 92, 689–737.

Laguna, A., Schintu, N., Nobre, A., Alvarsson, A., Volakakis, N., Jacobsen, J.K., Gómez-Galán, M., Sopova, E., Joodmardi, E., Yoshitake, T., Deng, Q., Kehr, J., Ericson, J., Svenningsson, P., Shupliakov, O., and Perlmann, T. (2015) Dopaminergic control of autophagic-lysosomal function implicates Lmx1b in Parkinson's disease. *Nat. Neurosci.*, 18, 826–835.

Lai, B., Marion, S., Teschke, K., and Tsui, J. (2002) Occupational and environmental risk factors for Parkinson's disease. *Park. Relat. Disord.*, 8, 297–309.

Lang, A. and Lozano, A. (1998) Parkinson. *N. Engl. J. Med.*,.

Langston, J.W., Ballard, P., Tetrud, J.W., and Irwin, I. (1983) Chronic Parkinsonism in humans due to a product of meperidine-analog synthesis. *Science*, 219, 979–980.

Langston, J.W., Forno, L.S., Tetrud, J., Reeves, A.G., Kaplan, J.A., and Karluk, D. (1999) Evidence of active nerve cell degeneration in the substantia nigra of humans years after 1-methyl-4-phenyl-1,2,3,6-tetrahydropyridine exposure. *Ann. Neurol.*, 46, 598–605.

Laplante, M. and Sabatini, D.M. (2009) mTOR signaling at a glance. *J. Cell Sci.*, 122, 3589–3594.

Lastres-Becker, I., Ulusoy, A., Innamorato, N.G., Sahin, G., Rábano, A., Kirik, D., and Cuadrado, A. (2012) α-synuclein expression and Nrf2 deficiency cooperate to aggravate protein aggregation, neuronal death and inflammation in early-stage Parkinson's disease. *Hum. Mol. Genet.*, 21, 3173–3192.

Lee, Y., Dawson, V.L., and Dawson, T.M. (2012) Animal models of Parkinson's disease: Vertebrate genetics. *Cold Spring Harb. Perspect. Med.*, 2.

Lei, K. and Davis, R.J. (2003) JNK phosphorylation of Bim-related members of the Bcl2 family induces Bax-dependent apoptosis. *Proc. Natl. Acad. Sci.*, 100, 2432–2437.

Lei, Z., Jiang, Y., Li, T., Zhu, J., and Zeng, S. (2011) Signaling of glial cell line-derived neurotrophic factor and its receptor GFRα1 induce Nurr1 and Pitx3 to promote survival of grafted midbrain-derived neural stem cells in a rat model of Parkinson disease. *J. Neuropathol. Exp. Neurol.*, 70, 736–747.

Leret, M.L., San Millán, J.A., Fabre, E., Gredilla, R., and Barja, G. (2002) Deprenyl protects from MPTP-induced Parkinson-like syndrome and glutathione oxidation in rat striatum. *Toxicology*, 170, 165–171.

Lesage, S. and Brice, A. (2009) Parkinson's disease: From monogenic forms to genetic susceptibility factors. *Hum. Mol. Genet.*, 18, 48–59.

Lesage, S., Drouet, V., Majounie, E., Deramecourt, V., Jacoupy, M., Nicolas, A., Cormier-Dequaire, F., Hassoun, S.M., Pujol, C., Ciura, S., Erpapazoglou, Z., Usenko, T., Maurage, C.A., Sahbatou, M., Liebau, S., Ding, J., Bilgic, B., Emre, M., Erginel-Unaltuna, N., Guven, G., Tison, F., Tranchant, C., Vidailhet, M., Corvol, J.C., Krack, P., Leutenegger, A.L., Nalls, M.A., Hernandez, D.G., Heutink, P., Gibbs, J.R., Hardy, J., Wood, N.W., Gasser, T., Durr, A., Deleuze, J.F., Tazir, M., Destée, A., Lohmann, E., Kabashi, E., Singleton, A., Corti, O., Brice, A., Tison, F., Vidailhet, M., Corvol, J.C., Agid, Y., Anheim, M., Bonnet, A.M., Borg, M., Broussolle, E., Damier, P., Destée, A., Dürr, A., Durif, F., Krack, P., Klebe, S., Lohmann, E., Martinez, M., Pollak, P., Rascol, O., Tranchant, C., Vérin, M., Viallet, F., Lesage, S., Majounie, E., Tison, F., Vidailhet, M., Corvol, J.C., Nalls, M.A., Hernandez, D.G., Gibbs, J.R., Dürr, A., Arepalli, S., Barker, R.A., Ben-Shlomo, Y., Berg, D., Bettella, F., Bhatia, K., de Bie, R.M.A., Biffi, A., Bloem, B.R., Bochdanovits, Z., Bonin, M., Bras, J.M., Brockmann, K., Brooks, J., Burn, D.J., Charlesworth, G., Chen, H., Chinnery, P.F., Chong, S., Clarke, C.E., Cookson, M.R., Counsell, C., Damier, P., Dartigues, J.F., Deloukas, P., Deuschl, G., Dexter, D.T., van Dijk, K.D., Dillman, A., Dong, J., Durif, F., Edkins, S., Escott-Price, V., Evans, J.R., Foltynie, T., Gao, J., Gardner, M., Goate, A., Gray, E., Guerreiro, R., Harris, C., van Hilten, J.J., Hofman, A., Hollenbeck, A., Holmans, P., Holton, J., Hu, M., Huang, X., Huber, H., Hudson, G., Hunt, S.E., Huttenlocher, J., Illig, T., Jónsson, P. V., Kilarski, L.L., Jansen, I.E., Lambert, J.C., Langford, C., Lees, A., Lichtner, P., Limousin, P., Lopez, G., Lorenz, D., Lubbe, S., Lungu, C., Martinez, M., Mätzler, W., McNeill, A., Moorby, C., Moore, M., Morrison, K.E., Mudanohwo, E., O'sullivan, S.S., Owen, M.J., Pearson, J., Perlmutter, J.S., Pétursson, H., Plagnol, V., Pollak, P., Post, B., Potter, S., Ravina, B., Revesz, T., Riess, O., Rivadeneira, F., Rizzu, P., Ryten, M., Saad, M., Simón-Sánchez, J., Sawcer, S., Schapira, A., Scheffer, H., Schulte, C., Sharma, M., Shaw, K., Sheerin, U.M., Shoulson, I., Shulman, J., Sidransky, E., Spencer, C.C.A., Stefánsson, H., Stefánsson, K., Stockton, J.D., Strange, A., Talbot, K., Tanner, C.M., Tashakkori-Ghanbaria, A., Trabzuni, D., Traynor, B.J., Uitterlinden, A.G., Velseboer, D., Walker, R., Warrenburg, B. van de, Wickremaratchi, M., Williams-Gray, C.H., Winder-Rhodes, S., Wurster, I., Williams, N., Morris, H.R., Heutink, P., Hardy, J., Wood, N.W., Gasser, T., Singleton, A.B., and Brice, A. (2016) Loss of VPS13C Function in Autosomal-Recessive Parkinsonism Causes Mitochondrial Dysfunction and Increases PINK1/Parkin-Dependent Mitophagy. *Am. J. Hum. Genet.*, 98, 500–513.

Letai, A., Bassik, M.C., Walensky, L.D., Sorcinelli, M.D., Weiler, S., and Korsmeyer, S.J. (2002) Distinct BH3 domains either sensitize or activate mitochondrial apoptosis, serving as prototype cancer therapeutics. *Cancer Cell*, 2, 183–192.

Levy, O.A., Malagelada, C., and Greene, L.A. (2009) Cell death pathways in Parkinson's disease: Proximal triggers, distal effectors, and final steps. *Apoptosis*, 14, 478–500.

Lewis, C.A., Griffiths, B., Santos, C.R., Pende, M., and Schulze, A. (2011) Regulation of the SREBP transcription factors by mTORC1: Figure 1. *Biochem. Soc. Trans.*, 39, 495–499.

Li, Y., Xu, M., Ding, X., Yan, C., Song, Z., Chen, L., Huang, X., Wang, X., Jian, Y., Tang, G., Tang, C., Di, Y., Mu, S., Liu, X., Liu, K., Li, T., Wang, Y., Miao, L., Guo, W., Hao, X., and Yang, C. (2016) Protein kinase C controls lysosome biogenesis independently of mTORC1. *Nat. Cell Biol.*, 18, 1065–1077.

Liang, C.L., Wang, T.T., Luby-Phelps, K., and German, D.C. (2007) Mitochondria mass is low in mouse substantia nigra dopamine neurons: Implications for Parkinson's disease. *Exp. Neurol.*, 203, 370–380.

Liberatore, G.T., Jackson-Lewis, V., Vukosavic, S., Mandir, A.S., Vila, M., Mcauliffe, W.G., Dawson, V.L., Dawson, T.M., and Przedborski, S. (1999) Inducible nitric oxide synthase stimulates dopaminergic neurodegeneration in the MPTP model of Parkinson disease. *Nat. Med.*, 5, 1403–1409.

Liddelow, S.A. and Barres, B.A. (2017) Reactive Astrocytes: Production, Function, and Therapeutic Potential. *Immunity*, 46, 957–967.

Lim, K.-L. and Tan, J.-M. (2007) Role of the ubiquitin proteasome system in Parkinson's disease. *BMC Biochem.*, 8, S13.

Lindholm, P., Voutilainen, M.H., Laurén, J., Peränen, J., Leppänen, V.M., Andressoo, J.O., Lindahl, M., Janhunen, S., Kalkkinen, N., Timmusk, T., Tuominen, R.K., and Saarma, M. (2007) Novel neurotrophic factor CDNF protects and rescues midbrain dopamine neurons in vivo. *Nature*, 448, 73–77.

Liou, A.K.F., Zhou, Z., Pei, W., Lim, T.-M., Yin, X.-M., and Chen, J. (2005) BimEL up-regulation potentiates AIF translocation and cell death in response to MPTP. *FASEB J.*, 19, 1350–1352.

Liu, K., Shi, N., Sun, Y., Zhang, T., and Sun, X. (2013) Therapeutic effects of rapamycin on MPTP-induced Parkinsonism in mice. *Neurochem. Res.*, 38, 201–207.

Liu, Y., Xue, X., Zhang, H., Che, X., Luo, J., Wang, P., Xu, J., Xing, Z., Yuan, L., Liu, Y., Fu, X., Su, D., Sun, S., Zhang, H., Wu, C., and Yang, J. (2019) Neuronal-targeted TFEB rescues dysfunction of the autophagy-lysosomal pathway and alleviates ischemic injury in permanent cerebral ischemia. *Autophagy*, 15, 493–509.

Lo Bianco, C., Déglon, N., Pralong, W., and Aebischer, P. (2004) Lentiviral nigral delivery of GDNF does not prevent neurodegeneration in a genetic rat model of Parkinson's disease. *Neurobiol. Dis.*, 17, 283–289.

Lohr, K.M., Bernstein, A.I., Stout, K.A., Dunn, A.R., Lazo, C.R., Alter, S.P., Wang, M., Li, Y., Fan, X., Hess, E.J., Yi, H., Vecchio, L.M., Goldstein, D.S., Guillot, T.S., Salahpour, A., and Miller, G.W. (2014) Increased vesicular monoamine transporter enhances dopamine release and opposes Parkinson disease-related neurodegeneration in vivo. *Proc. Natl. Acad. Sci.*, 111, 9977–9982.

Lohr, K.M., Stout, K., Dunn, A., Wang, M., Salahpour, A., Guillot, T., and Miller, G.W. (2015) Increased Vesicular Monoamine Transporter 2 (VMAT2; Slc18a2) Protects against Methamphetamine Toxicity. *ACS Chem. Neurosci.*, 6, 790–799.

Lohr, K.M., Chen, M., Hoffman, C.A., McDaniel, M.J., Stout, K.A., Dunn, A.R., Wang, M., Bernstein, A.I., and Miller, G.W. (2016) Vesicular monoamine transporter 2 (VMAT2) level regulates MPTP vulnerability and clearance of excess dopamine in mouse striatal terminals. *Toxicol. Sci.*, 153, 79–88.

Lotharius, J. and O'Malley, K.L. (2000) The Parkinsonism-inducing Drug 1-Methyl-4-phenylpyridinium Triggers Intracellular Dopamine Oxidation. *J. Biol. Chem.*, 275, 38581–38588.

Lu, Z. and Xu, S. (2006) ERK1/2 MAP kinases in cell survival and apoptosis. *IUBMB Life*, 58, 621–631.

Magalhaes, J., Gegg, M.E., Migdalska-Richards, A., and Schapira, A.H. (2018) Effects of ambroxol on the autophagy-lysosome pathway and mitochondria in primary cortical neurons. *Sci. Rep.*, 8, 1–12.

Magnuson, B., Ekim, B., and Fingar, D.C. (2012) Regulation and function of ribosomal protein S6 kinase (S6K) within mTOR signalling networks. *Biochem. J.*, 441, 1–21.

Mahul-Mellier, A.L., Fauvet, B., Gysbers, A., Dikiy, I., Oueslati, A., Georgeon, S., Lamontanara, A.J., Bisquertt, A., Eliezer, D., Masliah, E., Halliday, G., Hantschel, O., and Lashuel, H.A. (2014) C-Abl phosphorylates α-synuclein and regulates its degradation: Implication for α-synuclein clearance and contribution to the pathogenesis of parkinson's disease. *Hum. Mol. Genet.*, 23, 2858–2879.

Malagelada, C., Ryu, E.J., Biswas, S.C., Jackson-Lewis, V., and Greene, L.A. (2006) RTP801 Is Elevated in Parkinson Brain Substantia Nigral Neurons and Mediates Death in Cellular Models of Parkinson's Disease by a Mechanism Involving Mammalian Target of Rapamycin Inactivation. *J. Neurosci.*, 26, 9996–10005.

Malagelada, C., Jin, Z.H., and Greene, L.A. (2008) RTP801 Is Induced in Parkinson's Disease and Mediates Neuron Death by Inhibiting Akt Phosphorylation/Activation. *J. Neurosci.*, 28, 14363–14371.

Malagelada, C., Jin, Z.H., Jackson-Lewis, V., Przedborski, S., and Greene, L.A. (2010) Rapamycin Protects against Neuron Death in In Vitro andIn Vivo Models of Parkinson's Disease. *J. Neurosci.*, 30, 1166–1175.

Mansueto, G., Armani, A., Viscomi, C., D'Orsi, L., De Cegli, R., Polishchuk, E. V., Lamperti, C., Di Meo, I., Romanello, V., Marchet, S., Saha, P.K., Zong, H., Blaauw, B., Solagna, F., Tezze, C., Grumati, P., Bonaldo, P., Pessin, J.E., Zeviani, M., Sandri, M., and Ballabio, A. (2017) Transcription Factor EB Controls Metabolic Flexibility during Exercise. *Cell Metab.*, 25, 182–196.

Markham, A., Cameron, I., Franklin, P., and Spedding, M. (2004) BDNF increases rat brain mitochondrial respiratory coupling at complex I, but not complex II. *Eur. J. Neurosci.*, 20, 1189–1196.

Marosi, K; Mattson, M. (2014) BDNF Mediates Adaptive Brain and Body Responses to Energetic Challenges. *Trends Endocrinol. Metab.*, 25, 89–98.

Martina, J., Chen, Y., Gucek, M., and Puertollano, R. (2012) MTORC1 functions as a transcriptional regulator of autophagy by preventing nuclear transport of TFEB. *Autophagy*, 8, 877–876.

Martina, J.A. and Puertollano, R. (2013) Rag GTPases mediate amino acid-dependent recruitment of TFEB and MITF to lysosomes. *J. Cell Biol.*, 200, 475–491.

Martina, J.A., Diab, H.I., Li, H., Puertollano, R., and Martina, JA; Diab, HI; Li, H; Puertollano, R. (2014) Novel roles for the MiTF/TFE family of transcription factors in organelle biogenesis, nutrient sensing, and energy homeostasis. *Cell. Mol. Life Sci.*, 71, 2483–2497.

Martinez-Vicente, M. and Cuervo, A.M. (2007) Autophagy and neurodegeneration: when the cleaning crew goes on strike. *Lancet Neurol.*, 6, 352–361.

Martinez-Vicente, M. and Vila, M. (2013) Alpha-synuclein and protein degradation pathways in Parkinson's disease: A pathological feed-back loop. *Exp. Neurol.*, 247, 308–313.

Martinez-Vicente, M. (2015) Autophagy in neurodegenerative diseases: From pathogenic dysfunction to therapeutic modulation. *Semin. Cell Dev. Biol.*, 40, 115–126.

Martinez, B.A., Caldwell, K.A., and Caldwell, G.A. (2017) C. elegans as a model system to accelerate discovery for Parkinson disease. *Curr. Opin. Genet. Dev.*, 44, 102–109.

Martini-Stoica, H., Cole, A.L., Swartzlander, D.B., Chen, F., Wan, Y.-W., Bajaj, L., Bader, D.A., Lee, V.M.Y., Trojanowski, J.Q., Liu, Z., Sardiello, M., and Zheng, H. (2018) TFEB enhances astroglial uptake of extracellular tau species and reduces tau spreading. *J. Exp. Med.*, 215, 2355–2377.

Martini-Stoica, H., Xu, Y., Ballabio, A., and Zheng, H. (2016) The Autophagy-Lysosomal Pathway in Neurodegeneration: A TFEB Perspective. *Trends Neurosci.*, 39, 221–234.

Matsui, H., Gavinio, R., and Takahashi, R. (2012) Medaka Fish Parkinson's Disease Model. *Exp. Neurobiol.*, 21, 94.

Mattson, M., Moehl, K., Ghena, N., Schamaedick, M., and Cheng, A. (2018) Intermittent metabolic switching, neuroplasticity and brain health. *Nat. Rev. Neurosci.*, 19, 63–80.

McCommis, K.S. and Baines, C.P. (2012) The Role of VDAC in Cell Death: Friend or Foe? *Biochim. Biophys. Acta*, 1818, 1444–1450.

McNaught, K.S.P. and Jenner, P. (2001) Proteasomal function is impaired in substantia nigra in Parkinson's disease. *Neurosci. Lett.*, 297, 191–194.

Medina, D.L., Fraldi, A., Bouche, V., Annunziata, F., Mansueto, G., Spampanato, C., Puri, C., Pignata, A., Martina, J.A., Sardiello, M., Palmieri, M., Polishchuk, R., Puertollano, R., and Ballabio, A. (2011) Transcriptional activation of lysosomal exocytosis promotes cellular clearance. *Dev. Cell*, 21, 421–430.

Medina, D.L., Di Paola, S., Peluso, I., Armani, A., De Stefani, D., Venditti, R., Montefusco, S., Scotto-Rosato, A., Prezioso, C., Forrester, A., Settembre, C., Wang, W., Gao, Q., Xu, H., Sandri, M., Rizzuto, R., De Matteis, M.A., and Ballabio, A. (2015) Lysosomal calcium signalling regulates autophagy through calcineurin and TFEB. *Nat. Cell Biol.*, 17, 288–299.

Meissner, W., Prunier, C., Guilloteau, D., Chalon, S., Gross, C.E., and Bezard, E. (2003) Time-Course of Nigrostriatal Degeneration in a Progressive MPTP-Lesioned Macaque Model of Parkinson's Disease. *Mol. Neurobiol.*, 28, 209–218.

Meka, D.P., Müller-Rischart, A.K., Nidadavolu, P., Mohammadi, B., Motori, E., Ponna, S.K., Aboutalebi, H., Bassal, M., Annamneedi, A., Finckh, B., Miesbauer, M., Rotermund, N.,

Lohr, C., Tatzelt, J., Winklhofer, K.F., and Kramer, E.R. (2015) Parkin cooperates with GDNF/RET signaling to prevent dopaminergic neuron degeneration. *J. Clin. Invest.*, 125, 1873–1885.

Melillo, R.M., Santoro, M., Ong, S.-H., Billaud, M., Fusco, A., Hadari, Y.R., Schlessinger, J., and Lax, I. (2001) Docking Protein FRS2 Links the Protein Tyrosine Kinase RET and Its Oncogenic Forms with the Mitogen-Activated Protein Kinase Signaling Cascade. *Mol. Cell. Biol.*, 21, 4177–4187.

Menezes, R., Tenreiro, S., Macedo, D., Santos, C., and Outeiro, T. (2015) From the baker to the bedside: yeast models of Parkinson's disease. *Microb. Cell*, 2, 262–279.

Meredith, G.E. and Rademacher, D.J. (2011) MPTP mouse models of Parkinson's disease: an update. *J. Parkinsons. Dis.*, 1, 19–33.

Meuer, K., Suppanz, I.E., Lingor, P., Planchamp, V., Göricke, B., Fichtner, L., Braus, G.H., Dietz, G.P.H., Jakobs, S., Bähr, M., and Weishaupt, J.H. (2007) Cyclin-dependent kinase 5 is an upstream regulator of mitochondrial fission during neuronal apoptosis. *Cell Death Differ.*, 14, 651–661.

Minakaki, G., Menges, S., Kittel, A., Emmanouilidou, E., Schaeffner, I., Barkovits, K., Bergmann, A., Rockenstein, E., Adame, A., Marxreiter, F., Mollenhauer, B., Galasko, D., Buzás, E., Schlötzer-Schrehardt, U., Marcus, K., Xiang, W., Lie, D., Vekrellis, K., Masliah, E., Winkler, J., and Kluchen, J. (2018) Autophagy inhibition promotes SNCA/alpha-synuclein release and transfer via extracellular vesicles with a hybrid autophagosome-exosome-like phenotype. *Autophagy*, 14, 98–119.

Mizushima, N., Yoshimori, T., and Ohsumi, Y. (2011) The Role of Atg Proteins in Autophagosome Formation. *Annu. Rev. Cell Dev. Biol.*, 27, 107–132.

Mochizuki, H., Goto, K., Mori, H., and Mizuno, Y. (1996) Histochemical detection of apoptosis in Parkinson's disease. *J. Neurol. Sci.*, 137, 120–123.

Mogi, M., Togari, A., Kondo, T., Mizuno, Y., Komure, O., Kuno, S., Ichinose, H., and Nagatsu, T. (1999) Brain-derived growth factor and nerve growth factor concentrations are decreased in the substantia nigra in Parkinson's disease. *Neurosci. Lett.*, 270, 45–48.

Mogi, M., Togari, A., Kondo, T., Mizuno, Y., Kogure, O., Kuno, S., Ichinose, H., and Nagatsu, T. (2001) Glial cell line-derived neurotrophic factor in the substantia nigra from control and parkinsonian brains. *Neurosci. Lett.*, 300, 179–181.

Moisoi, N., Klupsch, K., Fedele, V., East, P., Sharma, S., Renton, A., Plun-Favreau, H., Edwards, R.E., Teismann, P., Esposti, M.D., Morrison, A.D., Wood, N.W., Downward, J., and Martins, L.M. (2009) Mitochondrial dysfunction triggered by loss of HtrA2 results in the activation of a brain-specific transcriptional stress response. *Cell Death Differ.*, 16, 449–464.

Molinoff, P.B. and Axelrod, J. (1971) Biochemistry of catecholamines. *Annu. Rev.*, 40, 465–500.

Mor, D.E., Tsika, E., Mazzulli, J.R., Gould, N.S., Kim, H., Daniels, M.J., Doshi, S., Gupta, P., Grossman, J.L., Tan, V.X., Kalb, R.G., Caldwell, K.A., Caldwell, G.A., Wolfe, J.H., and Ischiropoulos, H. (2017) Dopamine induces soluble α-synuclein oligomers and nigrostriatal degeneration. *Nat. Neurosci.*, 20, 1560–1568.

Morrison, R.S., Kinoshita, Y., Johnson, M.D., Ghatan, S., Ho, J.T., and Garden, G. (2003) Neuronal Survival and Cell Death Signaling Pathways. *Mol. Cell. Biol. Neuroprotection CNS*, 513, 41–86.

Mosley, R.L., Hutter-Saunders, J.A., Stone, D.K., and Gendelman, H.E. (2012) Inflammation and adaptive immunity in Parkinson's disease. *Cold Spring Harb. Perspect. Med.*, 2, 1–17.

Mot, A.I., Liddell, J.R., White, A.R., and Crouch, P.J. (2016) Circumventing the Crabtree Effect: A method to induce lactate consumption and increase oxidative phosphorylation in cell culture. *Int. J. Biochem. Cell Biol.*, 79, 128–138.

Muñoz, P., Paris, I., Sanders, L.H., Greenamyre, J.T., and Segura-Aguilar, J. (2012) Overexpression of VMAT-2 and DT-diaphorase protects substantia nigra-derived cells against aminochrome neurotoxicity. *Biochim. Biophys. Acta - Mol. Basis Dis.*, 1822, 1125–1136.

Muthane, U., Ramsay, K.A., Jiang, H., Jackson-Lewis, V., Donaldson, D., Fernando, S., Ferreira, M., and Przedborski, S. (1994) Differences in Nigral Neuron Number and Sensitivity to 1-Methyl-4-phenyl-1,2,3,6-tetrahydropyridine in C57/bl and CD-1 Mice. *Exp. Neurol.*, 126, 195–204.

Nagatsu, T. and Sawada, M. (2009) L-dopa therapy for Parkinson's disease: Past, present, and future. *Park. Relat. Disord.*, 15, 3–8.

Napolitano, G. and Ballabio, A. (2016) TFEB at a glance. *J. Cell Sci.*, 129, 2475–2481.

Napolitano, G., Esposito, A., Choi, H., Matarese, M., Benedetti, V., Di Malta, C., Monfregola, J., Medina, D.L., Lippincott-Schwartz, J., and Ballabio, A. (2018) mTOR-dependent phosphorylation controls TFEB nuclear export. *Nat. Commun.*, 9, 3312.

Neuspiel, M., Zunino, R., Gangaraju, S., Rippstein, P., and McBride, H. (2005) Activated mitofusin 2 signals mitochondrial fusion, interferes with Bax activation, and reduces susceptibility to radical induced depolarization. *J. Biol. Chem.*, 280, 25060–25070.

Newhouse, K., Hsuan, S.L., Chang, S.H., Cai, B., Wang, Y., and Xia, Z. (2004) Rotenone-induced apoptosis is mediated by p38 and JNK MAP kinases in human dopaminergic SH-SY5Y cells. *Toxicol. Sci.*, 79, 137–146.

Nezich, C.L., Wang, C., Fogel, A.I., and Youle, R.J. (2015) MiT/TFE transcription factors are activated during mitophagy downstream of Parkin and Atg5. *J. Cell Biol.*, 210, 435–450.

Nicole, O., Ali, C., Docagne, F., Plawinski, L., MacKenzie, E.T., Vivien, D., and Buisson, A. (2001) Neuroprotection Mediated by Glial Cell Line-Derived Neurotrophic Factor: Involvement of a Reduction of NMDA-Induced Calcium Influx by the Mitogen-Activated Protein Kinase Pathway. *J. Neurosci.*, 21, 3024–3033.

O'Regan, G., Desouza, R.M., Balestrino, R., and Schapira, A.H. (2017) Glucocerebrosidase Mutations in Parkinson Disease. *J. Parkinsons. Dis.*, 7, 411–422.

Ohashi, Y., Tremel, S., and Williams, R.L. (2019) VPS34 complexes from a structural perspective. *J. Lipid Res.*, 60, 229–241.

Oiwa, Y., Yoshimura, R., Nakai, K., and Itakura, T. (2002) Dopaminergic neuroprotection and regeneration by neurturin assessed by using behavioral, biochemical and histochemical measurements in a model of progressive Parkinson's disease. *Brain Res.*, 947, 271–283.

Olanow, C.W., Bartus, R.T., Volpicelli-Daley, L.A., and Kordower, J.H. (2015) Trophic factors for Parkinson's disease: To live or let die. *Mov. Disord.*, 30, 1715–1724.

Oliveras-Salvá, M., Van Der Perren, A., Casadei, N., Stroobants, S., Nuber, S., D'Hooge, R., Van Den Haute, C., and Baekelandt, V. (2013) RAAV2/7 vector-mediated overexpression of alpha-synuclein in mouse substantia nigra induces protein aggregation and progressive dose-dependent neurodegeneration. *Mol. Neurodegener.*, 8, 1–14.

Ou, Y.H., Torres, M., Ram, R., Formstecher, E., Roland, C., Cheng, T., Brekken, R., Wurz, R., Tasker, A., Polverino, T., Tan, S.L., and White, M.A. (2011) TBK1 Directly Engages Akt/PKB Survival Signaling to Support Oncogenic Transformation. *Mol. Cell*, 41, 458–470.

Pabon, M., Bachstetter, A., Hudson, C., Gemma, C., and Bickford, P. (2011) CX3CL1 reduces neurotoxicity and microglial activation in a rat model of Parkinson's disease. *J. Neuroinflammation*, 8, 1–7.

Palacios, N., Gao, X., McCullough, M.L., Schwarzschild, M.A., Shah, R., Gapstur, S., and Ascherio, A. (2012) Caffeine and risk of Parkinson's disease in a large cohort of men and women. *Mov. Disord.*, 27, 1276–1282.

Palmieri, M., Impey, S., Kang, H., di Ronza, A., Pelz, C., Sardiello, M., and Ballabio, A. (2011) Characterization of the CLEAR network reveals an integrated control of cellular clearance pathways. *Hum. Mol. Genet.*, 20, 3852–3866.

Palmieri, M., Pal, R., Nelvagal, H.R., Lotfi, P., Stinnett, G.R., Seymour, M.L., Chaudhury, A., Bajaj, L., Bondar, V. V., Bremner, L., Saleem, U., Tse, D.Y., Sanagasetti, D., Wu, S.M., Neilson, J.R., Pereira, F.A., Pautler, R.G., Rodney, G.G., Cooper, J.D., and Sardiello, M. (2017) mTORC1-independent TFEB activation via Akt inhibition promotes cellular clearance in neurodegenerative storage diseases. *Nat. Commun.*, 8, 15793.

Pan, T., Kondo, S., Zhu, W., Xie, W., Jankovic, J., and Le, W. (2008) Neuroprotection of rapamycin in lactacystin-induced neurodegeneration via autophagy enhancement. *Neurobiol. Dis.*, 32, 16–25.

Panneton, W.M., Kumar, V.B., Gan, Q., Burke, W.J., and Galvin, J.E. (2010) The neurotoxicity of DOPAL: Behavioral and stereological evidence for its role in Parkinson disease pathogenesis. *PLoS One*, 5, 1–9.

Parain, K., Murer, M.G., Yan, Q., Faucheux, B., Agid, Y., Hirsch, E., and Raisman-Vozari, R. (1999) Reduced expression of brain-derived neurotrophic factor protein in Parkinson's disease substantia nigra. *Neuroreport*, 10, 557–561.

Park, J., Lee, S.B., Lee, S., Kim, Y., Song, S., Kim, S., Bae, E., Kim, J., Shong, M., Kim, J.M., and Chung, J. (2006) Mitochondrial dysfunction in Drosophila PINK1 mutants is complemented by parkin. *Nature*, 441, 1157–1161.

Parkinson Study Group PRECEPT Investigators (2007) Mixed Lineage Kinase Inhibitor Cep-1347 Fails To Delay Disability in Early Parkinson Disease. *Neurology*, 69, 1480–1490.

Parmar, N. and Tamanoi, F. (2010) Rheb G-proteins and the activation of mTORC1. *Enzymes*, 27, 39–56.

Patapoutian, A. and Reichardt, L.F. (2001) Trk receptors: mediators of neurotrophin action. *Curr. Opin. Neurobiol.*, 11, 272–280.

Patt, S. and Gerhard, L. (1993) A Golgi study of human locus coeruleus in normal brains and in Parkinson's disease. *Neuropathol. Appl. Neurobiol.*, 19, 519–523.

Pearce, RKB; Owen, A; Daniel, S; Jenner, P; Marsden, C. (1997) Alterations in the distribution of glutathione in the substantia nigra in Parkinson's disease. *J. Neural Transm.*, 104, 661–677.

Perera, R.M., Stoykova, S., Nicolay, B.N., Ross, K.N., Fitamant, J., Boukhali, M., Lengrand, J., Deshpande, V., Selig, M.K., Ferrone, C.R., Settleman, J., Stephanopoulos, G., Dyson, N.J., Zoncu, R., Ramaswamy, S., Haas, W., and Bardeesy, N. (2015) Transcriptional control of autophagy-lysosome function drives pancreatic cancer metabolism. *Nature*, 524, 361–365.

Parkinson, J. (1817) An essay on the shaking palsy. Whittingham and Rowland for Sherwood, Needly and Jones, London.

Perier, C., Tieu, K., Guegan, C., Caspersen, C., Jackson-Lewis, V., Carelli, V., Martinuzzi, A., Hirano, M., Przedborski, S., and Vila, M. (2005) Complex I deficiency primes Bax-dependent neuronal apoptosis through mitochondrial oxidative damage. *Proc. Natl. Acad. Sci.*, 102, 19126–19131.

Perier, C., Bové, J., Wu, D.-C., Dehay, B., Choi, D.-K., Jackson-Lewis, V., Rathke-Hartlieb, S., Bouillet, P., Strasser, A., Schulz, J.B., Przedborski, S., and Vila, M. (2007) Two molecular pathways initiate mitochondria-dependent dopaminergic neurodegeneration in experimental Parkinson's disease. *Proc. Natl. Acad. Sci.*, 104, 8161–8166.

Perier, C. and Vila, M. (2012) Mitochondrial biology and Parkinson's disease. *Cold Spring Harb. Perspect. Med.*, 2, 1–19.

Perier, C., Bové, J., and Vila, M. (2012) Mitochondria and Programmed Cell Death in Parkinson's Disease: Apoptosis and Beyond. *Antioxid. Redox Signal.*, 16, 883–895.

Petroske, E., Meredith, G.E., Callen, S., Totterdell, S., and Lau, Y.S. (2001) Mouse model of Parkinsonism: A comparison between subacute MPTP and chronic MPTP/probenecid treatment. *Neuroscience*, 106, 589–601.

Petrucelli, L., O'Farrell, C., Lockhart, P.J., Baptista, M., Kehoe, K., Vink, L., Choi, P., Wolozin, B., Farrer, M., Hardy, J., and Cookson, M.R. (2002) Parkin protects against the toxicity associated with mutant α-Synuclein: Proteasome dysfunction selectively affects catecholaminergic neurons. *Neuron*, 36, 1007–1019.

Pfanner, N., Warscheid, B., and Wiedemann, N. (2019) Mitochondrial proteins: from biogenesis to functional networks. *Nat. Rev. Mol. Cell Biol.*,.

Pham, A.H., Meng, S., Chu, Q.N., and Chan, D.C. (2012) Loss of Mfn2 results in progressive, retrograde degeneration of dopaminergic neurons in the nigrostriatal circuit. *Hum. Mol. Genet.*, 21, 4817–4826.

Piao, Y., Kim, H.G., Oh, M.S., and Pak, Y.K. (2012) Overexpression of TFAM, NRF-1 and myr-AKT protects the MPP +-induced mitochondrial dysfunctions in neuronal cells. *Biochim. Biophys. Acta - Gen. Subj.*, 1820, 577–585.

Piguet, F., Alves, S., and Cartier, N. (2017) Clinical Gene Therapy for Neurodegenerative Diseases: Past, Present, and Future. *Hum. Gene Ther.*, 28, 988–1003.

Pil Yun, S., Kim, D., Kim, S., Kim, S., Karuppagounder, S.S., Kwon, S.H., Lee, S., Kam, T.I., Lee, S., Ham, S., Park, J.H., Dawson, V.L., Dawson, T.M., Lee, Y., and Ko, H.S. (2018a) α-Synuclein accumulation and GBA deficiency due to L444P GBA mutation contributes to MPTP-induced parkinsonism. *Mol. Neurodegener.*, 13, 1–19.

Pil Yun, S., Kam, T.I., Panicker, N., Kim, S., Oh, Y., Park, J.S., Kwon, S.H., Park, Y.J., Karuppagounder, S.S., Park, H., Kim, S., Oh, N., Kim, N.A., Lee, S., Brahmachari, S., Mao, X., Lee, J.H., Kumar, M., An, D., Kang, S.U., Lee, Y., Lee, K.C., Na, D.H., Kim, D., Lee, S.H., Roschke, V. V., Liddelow, S.A., Mari, Z., Barres, B.A., Dawson, V.L., Lee, S., Dawson, T.M., and Ko, H.S. (2018b) Block of A1 astrocyte conversion by microglia is neuroprotective in models of Parkinson's disease. *Nat. Med.*, 24, 931–938.

Poewe, W. (2008) Non-motor symptoms of Parkinson disease. *Eur. J. Neurol.*, 15, 14–20.

Poewe, W., Antonini, A., Zijlmans, J.C., Burkhard, P.R., and Vingerhoets, F. (2010) Levodopa in the treatment of Parkinson's disease: an old drug still going strong. *Clin. Interv. Aging*, 5, 229–238.

Poewe, W., Seppi, K., Tanner, C., Halliday, G., Brundin, P., Volkmann, J., Schrag, A.-E., and Lang, A. (2017) Parkinson Disease. *Nat. Rev. Dis. Prim.*, 3, 1–21.

Pogenberg, V., Ögmundsdóttir, M.H., Bergsteinsdóttir, K., Schepsky, A., Phung, B., Deineko, V., Milewski, M., Steingrímsson, E., and Wilmanns, M. (2012) Restricted leucine zipper dimerization and specificity of DNA recognition of the melanocyte master regulator MITF. *Genes Dev.*, 26, 2647–2658.

Polito, V.A., Li, H., Martini-Stoica, H., Wang, B., Yang, L., Xu, Y., Swartzlander, D.B., Palmieri, M., di Ronza, A., Lee, V.M.-Y., Sardiello, M., Ballabio, A., and Zheng, H. (2014) Selective clearance of aberrant tau proteins and rescue of neurotoxicity by transcription factor EB. *EMBO Mol. Med.*, 6, 1142–1160.

Porras, G., Li, Q., and Bezard, E. (2012) Modeling Parkinson's disease in primates: The MPTP model. *Cold Spring Harb. Perspect. Med.*, 2, 1–10.

Pringsheim, T., Jette, N., Frolkis, A., and Steeves, T.D.L. (2014) The prevalence of Parkinson's disease: a systematic review and meta-analysis. *Mov. Disord.*, 29, 1583–1590.

Puertollano, R., Ferguson, S.M., Brugarolas, J., and Ballabio, A. (2018) The complex relationship between TFEB transcription factor phosphorylation and subcellular localization. *EMBO J.*, 37, e98804.

Pupyshev, A.B., Korolenko, T.A., Akopyan, A.A., Amstislavskaya, T.G., and Tikhonova, M.A. (2018) Suppression of autophagy in the brain of transgenic mice with overexpression of A53T-mutant α-synuclein as an early event at synucleinopathy progression. *Neurosci. Lett.*, 672, 140–144.

Quik, M. (2004) Smoking, nicotine and Parkinson's disease. *Trends Neurosci.*, 27, 561–568.

Quik, M., O'Leary, K., and Tanner, C. (2008) Nicotine and Parkinson's disease; implications for therapy. *Mov. Disord.*, 15, 1641–1652.

Ramonet, D., Perier, C., Recasens, A., Dehay, B., Bové, J., Costa, V., Scorrano, L., and Vila, M. (2013) Optic atrophy 1 mediates mitochondria remodeling and dopaminergic neurodegeneration linked to complex i deficiency. *Cell Death Differ.*, 20, 77–85.

Recasens, A. and Dehay, B. (2014) Alpha-synuclein spreading in Parkinson's disease. *Front. Neuroanat.*, 8, 1–9.

Recasens, A., Dehay, B., Bové, J., Carballo-Carbajal, I., Dovero, S., Pérez-Villalba, A., Fernagut, P.O., Blesa, J., Parent, A., Perier, C., Fariñas, I., Obeso, J.A., Bezard, E., and Vila, M. (2014) Lewy body extracts from Parkinson disease brains trigger α-synuclein pathology and neurodegeneration in mice and monkeys. *Ann. Neurol.*, 75, 351–362.

Rega, L.R., Polishchuk, E., Montefusco, S., Napolitano, G., Tozzi, G., Zhang, J., Bellomo, F., Taranta, A., Pastore, A., Polishchuk, R., Piemonte, F., Medina, D.L., Catz, S.D., Ballabio, A., and Emma, F. (2016) Activation of the transcription factor EB rescues lysosomal abnormalities in cystinotic kidney cells. *Kidney Int.*, 89, 862–873.

Rehli, M., Den Elzen, N., Cassady, A.I., Ostrowski, M.C., and Hume, D.A. (1999) Cloning and characterization of the murine genes for bHlH-ZIP transcription factors TFEC and TFEB reveal a common gene organization for all MiT subfamily members. *Genomics*, 56, 111–120.

Ren, X., Zhang, T., Gong, X., Hu, G., Ding, W., and Wang, X. (2013) AAV2-mediated striatum delivery of human CDNF prevents the deterioration of midbrain dopamine neurons in a 6-hydroxydopamine induced parkinsonian rat model. *Exp. Neurol.*, 248, 148–156.

Reshi, L., Wang, H.-V., Hui, C.-F., Su, Y.-C., and Hong, J.-R. (2017) *Anti-Apoptotic Genes Bcl-2 and Bcl-XL Overexpression Can Block Iridovirus Serine/Threonine Kinase-Induced Bax/Mitochondria-Mediated Cell Death in GF-1 Cells*, Fish and Shellfish Immunology. Elsevier Ltd.

Rey, N.L., George, S., and Brundin, P. (2016) Spreading the word: Precise animal models and validated methods are vital when evaluating prion-like behaviour of alpha-synuclein. *Neuropathol. Appl. Neurobiol.*, 42, 51–76.

Reyes-Corona, D., Vázquez-Hernández, N., Escobedo, L., Orozco-Barrios, C.E., Ayala-Davila, J., Moreno, M.G., Amaro-Lara, M.E., Flores-Martinez, Y.M., Espadas-Alvarez, A.J., Fernandez-Parrilla, M.A., Gonzalez-Barrios, J.A., Gutierrez-Castillo, M.E., González-Burgos, I., and Martinez-Fong, D. (2017) Neurturin overexpression in dopaminergic neurons induces presynaptic and postsynaptic structural changes in rats with chronic 6-hydroxydopamine lesion. *PLoS One*, 12, 1–28.

Richardson, J.R., Shalat, S.L., Buckley, B., Winnik, B., O'Suilleabhain, P., Diaz-Arrastia, R., Reisch, J., and German, D.C. (2009) Elevated serum pesticide levels and risk of Parkinson disease. *Arch. Neurol.*, 66, 870–875.

Ries, V., Henchcliffe, C., Kareva, T., Rzhetskaya, M., Bland, R., During, M.J., Kholodilov, N., and Burke, R.E. (2006) Oncoprotein Akt/PKB induces trophic effects in murine models of Parkinson's disease. *Proc. Natl. Acad. Sci.*, 103, 18757–18762.

Ries, V., Cheng, H.C., Baohan, A., Kareva, T., Oo, T.F., Rzhetskaya, M., Bland, R.J., During, M.J., Kholodilov, N., and Burke, R.E. (2009) Regulation of the postnatal development of dopamine neurons of the substantia nigra in vivo by Akt/protein kinase B. *J. Neurochem.*, 110, 23–33.

Ritov, V.B., Tverdislova, I.L., Avakyan, T.Y., Menshikova, E. V., Leikin, Y.N., Bratkovskaya, L.B., and Shimon, R.G. (1992) Alamethicin-induced pore formation in biological membranes. *Gen. Physiol. Biophys.*, 11, 49–58.

Rivera-Oliver, M; Díaz-Ríos, M. (2014) Using caffeine and other adenosine receptor antagonists and agonists as therapeutic tools against neurodegenerative diseases: A review. *Life Sci.*, 101, 1–9.

Robinet, C. and Pellerin, L. (2010) Brain-derived neurotrophic factor enhances the expression of the monocarboxylate transporter 2 through translational activation in mouse cultured cortical neurons. *J. Cereb. Blood Flow Metab.*, 30, 286–298.

Roczniak-Ferguson, A., Petit, C.S., Froehlich, F., Qian, S., Ky, J., Angarola, B., Walther, T.C., and Ferguson, S.M. (2012) The transcription factor TFEB links mTORC1 signaling to transcriptional control of lysosome homeostasis. *Sci. Signal.*, 5, ra42.

Rolland, S.G., Motori, E., Memar, N., Hench, J., Frank, S., Winklhofer, K.F., and Conradt, B. (2013) Impaired complex IV activity in response to loss of LRPPRC function can be compensated by mitochondrial hyperfusion. *Proc. Natl. Acad. Sci.*, 110, E2967–E2976.

Ron, D. and Walter, P. (2007) Signal integration in the endoplasmic reticulum unfolded protein response. *Nat. Rev. Mol. Cell Biol.*, 8, 519–529.

Rosenblad, C., Kirik, D., Devaux, B., Moffat, B., Phillips, H., and Björklund, A. (1999) Protection and regeneration of nigral dopaminergic neurons by neurturin or GDNF in a partial lesion model of Parkinson's disease after administration into the striatum. *Eur. J. …*, 11, 1554–1566.

Ross, G.W., Petrovitch, H., Abbott, R.D., Nelson, J., Markesbery, W., Davis, D., Hardman, J., Launer, L., Masaki, K., Tanner, C.M., and White, L.R. (2004) Parkinsonian signs and substantia nigra neuron density in decendents elders without PD. *Ann. Neurol.*, 56, 532–539.

Rostovtseva, T.K. and Bezrukov, S.M. (2008) VDAC regulation: Role of cytosolic proteins and mitochondrial lipids. *J. Bioenerg. Biomembr.*, 40, 163–170.

Roux, P., Shahbazian, D., Vu, H., Holz, M., Cohen, M., Taunton, J., Sonenberg, N., and Blenis, J. (2007) RAS/ERK Signaling Promotes Site-specific Ribosomal Protein S6 Phosphorylation via RSK and Stimulates Cap-dependent Translation. *J. Biol. Chem.*, 282, 14056–14064.

Rudow, G., O'Brien, R., Savonenko, A. V., Resnick, S.M., Zonderman, A.B., Pletnikova, O., Marsh, L., Dawson, T.M., Crain, B.J., West, M.J., and Troncoso, J.C. (2008) Morphometry of the human substantia nigra in ageing and Parkinson's disease. *Acta Neuropathol.*, 115, 461–470.

Rüegg, S., Baybis, M., Juul, H., Dichter, M., and Crino, P.B. (2007) Effects of rapamycin on gene expression, morphology, and electrophysiological properties of rat hippocampal neurons. *Epilepsy Res.*, 77, 85–92.

Rusmini, P., Cortese, K., Crippa, V., Cristofani, R., Cicardi, M.E., Ferrari, V., Vezzoli, G., Tedesco, B., Meroni, M., Messi, E., Piccolella, M., Galbiati, M., Garrè, M., Morelli, E., Vaccari, T., and Poletti, A. (2019) Trehalose induces autophagy via lysosomal-mediated TFEB activation in models of motoneuron degeneration. *Autophagy*, 15, 631–651.

Ruvinsky, I. and Meyuhas, O. (2006) Ribosomal protein S6 phosphorylation: from protein synthesis to cell size. *Trends Biochem. Sci.*, 31, 342–348.

Salama, M. and Arias-Carrión, O. (2011) Natural toxins implicated in the development of Parkinson's disease. *Ther. Adv. Neurol. Disord.*, 4, 361–373.

Salat, D. and Tolosa, E. (2013) Levodopa in the treatment of Parkinson's disease: current status and new developments. *J. Parkinsons. Dis.*, 3, 255–269.

Salinas, M., Martín, D., Alvarez, A., and Cuadrado, A. (2001) Akt1/PKBα protects PC12 cells against the Parkinsonism-inducing neurotoxin 1-methyl-4-phenylpyridinium and reduces the levels of oxygen-free radicals. *Mol. Cell. Neurosci.*, 17, 67–77.

Samie, M. and Cresswell, P. (2015) The transcription factor TFEB acts as a molecular switch that regulates exogenous antigen-presentation pathways. *Nat. Immunol.*, 16, 729–736.

Sancak, Y., Bar-Peled, L., Zoncu, R., Markhard, A.L., Nada, S., and Sabatini, D.M. (2010) Ragulator-rag complex targets mTORC1 to the lysosomal surface and is necessary for its activation by amino acids. *Cell*, 141, 290–303.

Saporito, M.S., Thomas, B.A., and Scott, R.W. (2000) MPTP activates c-Jun NH2-terminal kinase (JNK) and its upstream regulatory kinase MKK4 in nigrostriatal neurons in vivo. *J. Neurochem.*, 75, 1200–1208.

Sarbassov, D., Guertin, D., Ali, S., and Sabatini, D. (2005) Phosphorylation and Regulation of Akt/PKB by the Rictor-mTOR Complex. *Science (80-.).*, 307, 1098–1101.

Sardiello, M., Palmieri, M., di Ronza, A., Medina, D., Valenza, M., Gennarino, V., Di Malta, C., Donaudy, F., Embrione, V., Polishchuk, R., Banfi, S., Parenti, G., Cattaneo, E., and Ballabio, A. (2009) A Gene Network Regulating Lysosomal Biogenesis and Function. *Science (80-.).*, 325, 473–478.

Sauer, H., Rosenblad, C., and Bjorklund, A. (1995) Glial cell line-derived neurotrophic factor but not transforming growth factor beta 3 prevents delayed degeneration of nigral dopaminergic neurons following striatal 6-hydroxydopamine lesion. *Proc. Natl. Acad. Sci. U. S. A.*, 92, 8935–8939.

Saura, J., Parés, M., Bové, J., Pezzi, S., Alberch, J., Marin, C., Tolosa, E., and Martí, M.J. (2003) Intranigral infusion of interleukin-1β activates astrocytes and protects from subsequent 6-hydroxydopamine neurotoxicity. *J. Neurochem.*, 85, 651–661.

Saxton, R.A. and Sabatini, D.M. (2017) mTOR Signaling in Growth, Metabolism, and Disease. *Cell*, 168, 960–976.

Scarpulla, R.C., Vega, R.B., and Kelly, D.P. (2012) Transcriptional integration of mitochondrial biogenesis. *Trends Endocrinol. Metab.*, 23, 459–466.

Schapira, A.H.V., Cooper, J.M., Dexter, D., Clark, J.B., Jenner, P., and Marsden, C.D. (1990) Mitochondrial Complex I Deficiency in Parkinson's Disease. *J. Neurochem.*, 54, 823–827.

Schapira, A.H. and Jenner, P. (2011) Etiology and pathogenesis of Parkinson's disease. *Mov. Disord.*, 26, 1049–1055.

Schapira, A.H.V. (2015) Glucocerebrosidase and Parkinson disease: Recent advances. *Mol. Cell. Neurosci.*, 66, 37–42.

Schnabel, J. (2010) Secrets of the shaking palsy. *Nature*, 466, S2–S5.

Schneider, B., Zufferey, R., and Aebischer, P. (2008) Viral vectors, animal models and new therapies for Parkinson's disease. *Park. Relat. Disord.*, 14, 169–171.

Scrivo, A., Bourdenx, M., Pampliega, O., and Cuervo, A.M. (2018) Selective autophagy as a potential therapeutic target for neurodegenerative disorders. *Lancet Neurol.*, 17, 802–815.

Segura-Aguilar, J. and Paris, I. (2014) *Handbook of Neurotoxicity*, Handbook of Neurotoxicity.

Selvaraj, S., Sun, Y., Watt, J., Wang, S., Lei, S., Birnbaumer, L., and Singh, B. (2012) Neurotoxin-induced ER stress in mouse dopaminergic neurons involves downregulation of TRPC1 and inhibition of AKT/mTOR signaling. *J. Clin. Invest.*, 122, 1354–1367.

Seo, B., Yoon, S.H., and Do, J.T. (2018) Mitochondrial dynamics in stem cells and differentiation. *Int. J. Mol. Sci.*, 19.

Seppi, K., Ray Chaudhuri, K., Coelho, M., Fox, S.H., Katzenschlager, R., Perez Lloret, S., Weintraub, D., Sampaio, C., Chahine, L., Hametner, E.M., Heim, B., Lim, S.Y., Poewe, W., and Djamshidian-Tehrani, A. (2019) Update on treatments for nonmotor symptoms of Parkinson's disease—an evidence-based medicine review. *Mov. Disord.*, 34, 180–198.

Settembre, C., Di Malta, C., Polito, V.A., Garcia, M., Vetrini, F., Erdin, S., Erdin, S.U., Huynh, T., Medina, D., Colella, P., Sardiello, M., Rubinsztein, D.C., and Ballabio, A. (2011) TFEB Links Autophagy to Lysosomal Biogenesis. *Science*, 332, 1429–1433.

Settembre, C., Zoncu, R., Medina, D.L., Vetrini, F., Erdin, S., Erdin, S., Huynh, T., Ferron, M., Karsenty, G., Vellard, M.C., Facchinetti, V., Sabatini, D.M., and Ballabio, A. (2012) A lysosome-to-nucleus signalling mechanism senses and regulates the lysosome via mTOR and TFEB. *EMBO J.*, 31, 1095–1108.

Settembre, C., De Cegli, R., Mansueto, G., Saha, P.K., Vetrini, F., Visvikis, O., Huynh, T., Carissimo, A., Palmer, D., Jürgen Klisch, T., Wollenberg, A.C., Di Bernardo, D., Chan, L., Irazoqui, J.E., and Ballabio, A. (2013) TFEB controls cellular lipid metabolism through a starvation-induced autoregulatory loop. *Nat. Cell Biol.*, 15, 647–658.

Sha, Y., Rao, L., Settembre, C., Ballabio, A., and Eissa, N.T. (2017) STUB1 regulates TFEB-induced autophagy–lysosome pathway. *EMBO J.*, 36, e201796699.

Sherer, T.B., Betarbet, R., and Greenamyre, J.T. (2002) Environment, Mitochondria, and Parkinson's Disease. *Neuroscientist*, 8, 192–197.

Shimizu, S., Narita, M., and Tsujimoto, Y. (1999) Bcl-2 family proteins regulate the release of apoptogenic cytochrome. *Nature*, 66, 1–5.

Shin, J.H., Ko, H.S., Kang, H., Lee, Y., Lee, Y. Il, Pletinkova, O., Troconso, J.C., Dawson, V.L., and Dawson, T.M. (2011) PARIS (ZNF746) repression of PGC-1α contributes to neurodegeneration in parkinson's disease. *Cell*, 144, 689–702.

Shu, C., Sankaran, B., Chaton, C.T., Herr, A.B., Mishra, A., Peng, J., and Li, P. (2013) Structural insights into the functions of TBK1 in innate antimicrobial immunity. *Structure*, 21, 1137–1148.

Shulman, L.M. (2007) Gender Differences in Parkinson's Disease. *Gend. Med.*, 4, 8–18.

Shults, C., Kimber, T., and Martin, D. (1996) Intrastriatal injection of GDNF attenuates the effects of 6-hydroxydopamine. *Neuroreport*, 7, 627–631.

Silva, R.M., Ries, V., Oo, T.F., Yarygina, O., Jackson-Lewis, V., Ryu, E.J., Lu, P.D., Marciniak, S.J., Ron, D., Przedborski, S., Kholodilov, N., Greene, L.A., and Burke, R.E. (2005) CHOP/GADD153 is a mediator of apoptotic death in substantia nigra dopamine neurons in an in vivo neurotoxin model of parkinsonism. *J. Neurochem.*, 95, 974–986.

Smeyne, M., Jiao, Y., Shepherd, K.R., and Smeyne, R.J. (2005) Glia cell number modulates sensitivity to MPTP in mice. *Glia*, 52, 144–152.

Smith, W.W., Jiang, H., Pei, Z., Tanaka, Y., Morita, H., Sawa, A., Dawson, V.L., Dawson, T.M., and Ross, C.A. (2005) Endoplasmic reticulum stress and mitochondrial cell death pathways mediate A53T mutant alpha-synuclein-induced toxicity. *Hum. Mol. Genet.*, 14, 3801–3811.

Snyder, H., Mensah, K., Theisler, C., Lee, J., Matouschek, A., and Wolozin, B. (2003) Aggregated and Monomeric α-Synuclein Bind to the S6′ Proteasomal Protein and Inhibit Proteasomal Function. *J. Biol. Chem.*, 278, 11753–11759.

Song, J.X., Sun, Y.R., Peluso, I., Zeng, Y., Yu, X., Lu, J.H., Xu, Z., Wang, M.Z., Liu, L.F., Huang, Y.Y., Chen, L.L., Durairajan, S.S.K., Zhang, H.J.Q., Zhou, B., Zhang, H.J.Q., Lu, A., Ballabio, A., Medina, D.L., Guo, Z., and Li, M. (2016) A novel curcumin analog binds to and activates TFEB in vitro and in vivo independent of MTOR inhibition. *Autophagy*, 12, 1372–1389.

Song, H.L., Demirev, A.V., Kim, N.Y., Kim, D.H., and Yoon, S.Y. (2019) Ouabain activates transcription factor EB and exerts neuroprotection in models of Alzheimer's disease. *Mol. Cell. Neurosci.*, 95, 13–24.

Soria, F.N., Engeln, M., Martinez-Vicente, M., Glangetas, C., López-González, M.J., Dovero, S., Dehay, B., Normand, E., Vila, M., Favereaux, A., Georges, F., Lo Bianco, C., Bezard, E., and Fernagut, P.O. (2017) Glucocerebrosidase deficiency in dopaminergic neurons induces microglial activation without neurodegeneration. *Hum. Mol. Genet.*, 26, 2603–2615.

Spampanato, C., Feeney, E., Li, L., Cardone, M., Lim, J.A., Annunziata, F., Zare, H., Polishchuk, R., Puertollano, R., Parenti, G., Ballabio, A., and Raben, N. (2013) Transcription factor EB (TFEB) is a new therapeutic target for Pompe disease. *EMBO Mol. Med.*, 5, 691–706.

Spillantini, M.G., Crowther, R.A., Jakes, R., Hasegawa, M., and Goedert, M. (1998) a-Synuclein in filamentous inclusions of Lewy bodies from Parkinson's disease and dementia with Lewy bodies. *Proc. Natl. Acad. Sci.*, 95, 6469–6473.

Staal, R.G. and Sonsalla, P.K. (2000) Inhibition of brain vesicular monoamine transporter (VMAT2) enhances 1-methyl-4-phenylpyridinium neurotoxicity in vivo in rat striata. *J. Pharmacol. Exp. Ther.*, 293, 336–342.

Stefanis, L., Larsen, K.E., Rideout, H.J., Sulzer, D., and Greene, L.A. (2001) Expression of A53T mutant but not wild-type alpha-synuclein in PC12 cells induces alterations of the ubiquitin-dependent degradation system, loss of dopamine release, and autophagic cell death. *J. Neurosci.*, 21, 9549–9560.

Steingrímsson, E., Tessarollo, L., Reid, S.W., Jenkins, N.A., and Copeland, N.G. (1998) The bHLH-Zip transcription factor Tfeb is essential for placental vascularization. *Development*, 125, 4607–4616.

Steingrímsson, E., Copeland, N.G., and Jenkins, N.A. (2004) Melanocytes and the *Microphthalmia* Transcription Factor Network. *Annu. Rev. Genet.*, 38, 365–411.

Subramaniam, S.R. and Chesselet, M-F. (2013) Mitochondrial dysfunction and oxidative stress in Parkinson's disease. *Prog. Neurobiol.*, 106–107, 17–32.

Sugioka, R., Shimizu, S., and Tsujimoto, Y. (2004) Fzo1, a protein involved in mitochondrial fusion, inhibits apoptosis. *J. Biol. Chem.*, 279, 52726–52734.

Sunico, C.R., Nakamura, T., Rockenstein, E., Mante, M., Adame, A., Chan, S.F., Newmeyer, T.F., Masliah, E., Nakanishi, N., and Lipton, S.A. (2013) S-Nitrosylation of parkin as a novel regulator of p53-mediated neuronal cell death in sporadic Parkinson's disease. *Mol. Neurodegener.*, 8, 1.

Sweatt, J.D. (2001) The neuronal MAP kinase cascade: a biochemical signal integration system subserving synaptic plasticity and memory. *J. Neurochem.*, 76, 1–10.

Tai, Y.C., Chen, L., Huang, E.P., Liu, C., Yang, X.Y., Qiu, P.M., and Wang, H.J. (2014) Protective effect of alpha-synuclein knockdown on methamphetamine-induced neurotoxicity in dopaminergic neurons. *Neural Regen. Res.*, 9, 951–958.

Tain, L.S., Mortiboys, H., Tao, R.N., Ziviani, E., Bandmann, O., and Whitworth, A.J. (2009) Rapamycin activation of 4E-BP prevents parkinsonian dopaminergic neuron loss. *Nat. Neurosci.*, 12, 1129–1135.

Tambasco, N., Romoli, M., and Calabresi, P. (2018) Levodopa in Parkinson's Disease: Current Status and Future Developments. *Curr. Neuropharmacol.*, 16, 1239–1252.

Tan, E.K., Chai, A., Lum, S.Y., Shen, H., Tan, C., Teoh, M.L., Yih, Y., Wong, M.C., and Zhao, Y. (2003) Monoamine oxidase B polymorphism, cigarette smoking and risk of Parkinson's disease: A study in an Asian population. *Am. J. Med. Genet.*, 120B, 58–62.

Tanaka, Y., Engelender, S., Igarashi, S., Rao, R.K., Wanner, T., Tanzi, R.E., Sawa, A., L Dawson, V., Dawson, T.M., and Ross, C.A. (2001) Inducible expression of mutant alpha-synuclein decreases proteasome activity and increases sensitivity to mitochondria-dependent apoptosis. *Hum. Mol. Genet.*, 10, 919–926.

Tang, F.L., Liu, W., Hu, J.X., Erion, J.R., Ye, J., Mei, L., and Xiong, W.C. (2015) VPS35 Deficiency or Mutation Causes Dopaminergic Neuronal Loss by Impairing Mitochondrial Fusion and Function. *Cell Rep.*, 12, 1631–1643.

Tasaki, Y., Omura, T., Yamada, T., Ohkubo, T., Suno, M., Iida, S., Sakaguchi, T., Asari, M., Shimizu, K., and Matsubara, K. (2010) Meloxicam protects cell damage from 1-methyl-4-phenyl pyridinium toxicity via the phosphatidylinositol 3-kinase/Akt pathway in human dopaminergic neuroblastoma SH-SY5Y cells. *Brain Res.*, 1344, 25–33.

Tatton, N.A. and Kish, S.J. (1997) In situ detection of apoptotic nuclei in the substantia nigra compacta of 1-methyl-4-phenyl-1,2,3,6-tetrahydropyridine-treated mice using terminal deoxynucleotidyl transferase labelling and acridine orange staining. *Neuroscience*, 77, 1037–1048.

Tatton, N.A. (2000) Increased caspase 3 and Bax immunoreactivity accompany nuclear GAPDH translocation and neuronal apoptosis in Parkinson's disease. *Exp. Neurol.*, 166, 29–43.

Taymans, J.M., Nkiliza, A., and Chartier-Harlin, M.C. (2015) Deregulation of protein translation control, a potential game-changing hypothesis for Parkinson's disease pathogenesis. *Trends Mol. Med.*, 21, 466–472.

Thacker, E.L., O'Reilly, E.J., Weisskopf, M.G., Chen, H., Schwarzschild, M.A., McCullough, M.L., Calle, E.E., Thun, M.J., and Ascherio, A. (2007) Temporal relationship between cigarette smoking and risk of Parkinson disease. *Neurology*, 68, 764–768.

Thibaut, F., Faucheux, B.A., Marquez, J., Villares, J., Menard, J.F., Agid, Y., and Hirsch, E.C. (1995) Regional distribution of monoamine vesicular uptake sites in the mesencephalon of control subjects and patients with Parkinson's disease: a postmortem study using tritiated tetrabenazine. *Brain Res.*, 692, 233–243.

Thiels, E. and Klann, E. (2001) Extracellular Signal-Regulated Kinase, Synaptic Plasticity, and Memory. *Rev. Neurosci.*, 12, 327–345.

Thobois, S., Mertens, P., Guenot, M., Hermier, M., Mollion, H., Bouvard, M., Chazot, G., Broussolle, E., and Sindou, M. (2002) Subthalamic nucleus stimulation in Parkinson's disease: Clinical evaluation of 18 patients. *J. Neurol.*, 249, 529–534.

Thomas, B. and Beal, M. (2007) Parkinson's Disease. *Med. Clin. North Am.*, 16, 183–194.

Thoreen, C.C., Kang, S.A., Chang, J.W., Liu, Q., Zhang, J., Gao, Y., Reichling, L.J., Sim, T., Sabatini, D.M., and Gray, N.S. (2009) An ATP-competitive mammalian target of rapamycin inhibitor reveals rapamycin-resistant functions of mTORC1. *J. Biol. Chem.*, 284, 8023–8032.

Tieu, K. (2011) A guide to neurotoxic animal models of parkinson´s disease. *Cold Spring Harb. Perspect. Med.*, 1, 1–20.

Tomac, A., Lindqvist, E., Lin, L.F.H., ögren, S.O., Young, D., Hoffer, B.J., and Olson, L. (1995) Protection and repair of the nigrostriatal dopaminergic system by gdnf in vivo. *Nature*, 373, 335–339.

Tondera, D., Grandemange, S., Jourdain, A., Karbowski, M., Mattenberger, Y., Herzig, S., Da Cruz, S., Clerc, P., Raschke, I., Merkwirth, C., Ehses, S., Krause, F., Chan, D.C., Alexander, C., Bauer, C., Youle, R., Langer, T., and Martinou, J.C. (2009) SlP-2 is required for stress-induced mitochondrial hyperfusion. *EMBO J.*, 28, 1589–1600.

Tóth, G., Gardai, S.J., Zago, W., Bertoncini, C.W., Cremades, N., Roy, S.L., Tambe, M.A., Rochet, J.C., Galvagnion, C., Skibinski, G., Finkbeiner, S., Bova, M., Regnstrom, K., Chiou, S.S., Johnston, J., Callaway, K., Anderson, J.P., Jobling, M.F., Buell, A.K., Yednock, T.A., Knowles, T.P.J., Vendruscolo, M., Christodoulou, J., Dobson, C.M., Schenk, D., and McConlogue, L. (2014) Targeting the intrinsically disordered structural ensemble of a-synuclein by small molecules as a potential therapeutic strategy for Parkinson's disease. *PLoS One*, 9.

Toulorge, D., Schapira, A.H.V., and Hajj, R. (2016) Molecular changes in the postmortem parkinsonian brain. *J. Neurochem.*, 139, 27–58.

Trimmer, P.A., Smith, T.S., Jung, A.B., and Bennett, J.P. (1996) Dopamine neurons from transgenic mice with a knockout of the p53 gene resist MPTP neurotoxicity. *Neurodegeneration*, 5, 233–239.

Tsukahara, T., Takeda, M., and Shimohama, S. (1995) Effects of Brain-derived Neurotrophic Factor on 1-Methyl-4-phenyl-1,2,3,6-tetrahydropyridine- induced Parkinsonism in Monkeys Experimental Study. *Neurosurgery*, 37, 731–741.

Tsunemi, T., Ashe, T.D., Morrison, B.E., Soriano, K.R., Au, J., Roque, R.A.V., Lazarowski, E.R., Damian, V.A., Masliah, E., and La Spada, A.R. (2012) PGC-1a rescues Huntington's disease proteotoxicity by preventing oxidative stress and promoting TFEB function. *Sci. Transl. Med.*, 4.

Van der Bliek, A.M., Shen, Q., and Kawajiri, S. (2013) Mechanisms of mitochondrial fission and fusion. *Cold Spring Harb. Perspect. Biol.*, 5.

Vanle, B.C., Florang, V.R., Murry, D.J., Aguirre, A.L., and Doorn, J.A. (2017) Inactivation of glyceraldehyde-3-phosphate dehydrogenase by the dopamine metabolite, 3,4-dihydroxyphenylacetaldehyde. *Biochem. Biophys. Res. Commun.*, 492, 275–281.

Venderova, K; Park, D. (2012) Programmed cell death in Parkinson's disease. *Cold Spring Harb. Perspect. Med.*, 2, 1–24.

Vermilyea, S.C. and Emborg, M.E. (2015) α-Synuclein and nonhuman primate models of Parkinson's disease. *J. Neurosci. Methods*, 255, 38–51.

Vila, M., Jackson-lewis, V., Vukosavic, S., Djaldetti, R., Liberatore, G., Offen, D., Korsmeyer, S.J., and Przedborski, S. (2001) Bax ablation prevents dopaminergic neurodegeneration in the 1-methyl-4-phenyl-1,2,3,6-tetrahydropyridine mouse model of Parkinson's disease. *Proc. Natl. Acad. Sci. U. S. A.*, 98, 2837–2842.

Vila, M. and Przedborski, S. (2003) Targeting programmed cell death in neurodegenerative diseases. *Nat. Rev. Neurosci.*, 4, 365–375.

Vila, M., Ramonet, D., and Perier, C. (2008) Mitochondrial alterations in Parkinson's disease: New clues. *J. Neurochem.*, 107, 317–328.

Vingill, S., Brockelt, D., Lancelin, C., Tatenhorst, L., Dontcheva, G., Preisinger, C., Schwedhelm-Domeyer, N., Joseph, S., Mitkovski, M., Goebbels, S., Nave, K., Schulz, J.B., Marquardt, T., Lingor, P., and Stegmüller, J. (2016) Loss of FBXO7 (PARK15) results in reduced proteasome activity and models a parkinsonism-like phenotype in mice. *EMBO J.*, 35, 2008–2025.

Vingill, S., Connor-Robson, N., and Wade-Martins, R. (2018) Are rodent models of Parkinson's disease behaving as they should? *Behav. Brain Res.*, 352, 133–141.

Viswanath, V., Wu, Y., Boonplueang, R., Chen, S., Stevenson, F.F., Yantiri, F., Yang, L., Beal, M.F., and Andersen, J.K. (2001) Caspase-9 activation results in downstream caspase-8 activation and bid cleavage in 1-methyl-4-phenyl-1,2,3,6-tetrahydropyridine-induced Parkinson's disease. *J. Neurosci.*, 21, 9519–9528.

Vodicka, P., Chase, K., Iuliano, M., Tousley, A., Valentine, D.T., Sapp, E., Kegel-Gleason, K.B., Sena-Esteves, M., Aronin, N., and Difiglia, M. (2016) Autophagy Activation by Transcription Factor EB (TFEB) in Striatum of HD Q175/Q7 Mice. *J. Huntingtons. Dis.*, 5, 249–260.

Voutilainen, M.H., Bäck, S., Peränen, J., Lindholm, P., Raasmaja, A., Männistö, P.T., Saarma, M., and Tuominen, R.K. (2011) Chronic infusion of CDNF prevents 6-OHDA-induced deficits in a rat model of Parkinson's disease. *Exp. Neurol.*, 228, 99–108.

Wakabayashi, K., Tanji, K., Mori, F., and Takahashi, H. (2007) The Lewy body in Parkinson's disease: Molecules implicated in the formation and degradation of α-synuclein aggregates. *Neuropathology*, 27, 494–506.

Wang, X., Li, W., Parra, J.-L., Beugnet, A., and Proud, C.G. (2003) The C Terminus of Initiation Factor 4E-Binding Protein 1 Contains Multiple Regulatory Features That Influence Its Function and Phosphorylation. *Mol. Cell. Biol.*, 23, 1546–1557.

Wang, K., Huang, J., Xie, W., Huang, L., Zhong, C., and Chen, Z. (2016a) Beclin1 and HMGB1 ameliorate the aα-synuclein-mediated autophagy inhibition in PC12 cells. *Diagn. Pathol.*, 11, 1–10.

Wang, H., Wang, R., Carrera, I., Xu, S., and Lakshmana, M.K. (2016b) TFEB Overexpression in the P301S Model of Tauopathy Mitigates Increased PHF1 Levels and Lipofuscin Puncta and Rescues Memory Deficits. *eNeuro*, 3.

Wang, Y., Liu, F.T., Wang, Y.X., Guan, R.Y., Chen, C., Li, D.K., Bu, L.L., Song, J., Yang, Y.J., Dong, Y., Chen, Y., and Wang, J. (2018) Autophagic Modulation by Trehalose Reduces Accumulation of TDP-43 in a Cell Model of Amyotrophic Lateral Sclerosis via TFEB Activation. *Neurotox. Res.*, 34, 109–120.

Waskiewicz, A.J., Johnson, J.C., Penn, B., Mahalingam, M., Kimball, S.R., and Cooper, J.A. (1999) Phosphorylation of the Cap-Binding Protein Eukaryotic Translation Initiation Factor 4E by Protein Kinase Mnk1 In Vivo. *Mol. Cell. Biol.*, 19, 1871–1880.

Weiler, M., Blaes, J., Pusch, S., Sahm, F., Czabanka, M., Luger, S., Bunse, L., Solecki, G., Eichwald, V., Jugold, M., Hodecker, S., Osswald, M., Meisner, C., Hielscher, T., Rubmann, P., Pfenning, P.-N., Ronellenfitsch, M., Kempf, T., Schnolzer, M., Abdollahi, A., Lang, F., Bendszus, M., von Deimling, A., Winkler, F., Weller, M., Vajkoczy, P., Platten, M., and Wick, W. (2014) mTOR target NDRG1 confers MGMT-dependent resistance to alkylating chemotherapy. *Proc. Natl. Acad. Sci.*, 111, 409–414.

Weisthal, S., Keinan, N., Ben-Hail, D., Arif, T., and Shoshan-Barmatz, V. (2014) Ca2+-mediated regulation of VDAC1 expression levels is associated with cell death induction. *Biochim. Biophys. Acta - Mol. Cell Res.*, 1843, 2270–2281.

Westermann, B. (2012) Bioenergetic role of mitochondrial fusion and fission. *Biochim. Biophys. Acta - Bioenerg.*, 1817, 1833–1838.

Wiedemann, N. and Pfanner, N. (2017) Mitochondrial Machineries for Protein Import and Assembly. *Annu. Rev. Biochem.*, 86, 685–714.

Winkler, C., Sauer, H., Lee, C.S., and Björklund, A. (1996) Short-term GDNF treatment provides long-term rescue of lesioned nigral dopaminergic neurons in a rat model of Parkinson's disease. *J. Neurosci.*, 16, 7206–7215.

Winslow, A.R., Chen, C.W., Corrochano, S., Acevedo-Arozena, A., Gordon, D.E., Peden, A.A., Lichtenberg, M., Menzies, F.M., Ravikumar, B., Imarisio, S., Brown, S., O'Kane, C.J., and Rubinsztein, D.C. (2010) α-Synuclein impairs macroautophagy: Implications for Parkinson's disease. *J. Cell Biol.*, 190, 1023–1037.

Winter, J.N., Jefferson, L.S., and Kimball, S.R. (2011) ERK and Akt signaling pathways function through parallel mechanisms to promote mTORC1 signaling. *Am. J. Physiol. Physiol.*, 300, C1172–C1180.

Wurm, C.A., Neumann, D., Lauterbach, M.A., Harke, B., Egner, A., Hell, S.W., and Jakobs, S. (2011) Nanoscale distribution of mitochondrial import receptor Tom20 is adjusted to cellular conditions and exhibits an inner-cellular gradient. *Proc. Natl. Acad. Sci.*, 108, 13546–13551.

Xia, Z., Dickens, M., Raingeaud, J., Davis, R.J., Greenberg, M.E., and Raingeaud, J. (1995) Opposing Effects of MAP Kinases on Apoptosis. *Science (80-.).*, 270, 1326–1331.

Xiao, Q., Yan, P., Ma, X., Liu, H., Perez, R., Zhu, A., Gonzales, E., Burchett, J.M., Schuler, D.R., Cirrito, J.R., Diwan, A., and Lee, J.-M. (2014) Enhancing Astrocytic Lysosome Biogenesis Facilitates A Clearance and Attenuates Amyloid Plaque Pathogenesis. *J. Neurosci.*, 34, 9607–9620.

Xiao, Q., Yan, P., Ma, X., Liu, H., Perez, R., Zhu, A., Gonzales, E., Tripoli, D.L., Czerniewski, L., Ballabio, A., Cirrito, J.R., Diwan, A., and Lee, J.-M. (2015) Neuronal-Targeted TFEB Accelerates Lysosomal Degradation of APP, Reducing A Generation and Amyloid Plaque Pathogenesis. *J. Neurosci.*, 35, 12137–12151.

Xilouri, M., Vogiatzi, T., Vekrellis, K., Park, D., and Stefanis, L. (2009) Abberant α-synuclein confers toxicity to neurons in part through inhibition of chaperone-mediated autophagy. *PLoS One*, 4, 16–20.

Xing, J., Ginty, D., and Greenberg, M. (1996) Coupling of the RAS-MAPK Pathway to Gene Activation by RSK2 , a Growth Factor-Regulated CREB Kinase. *Science (80-.).*, 273, 959–963.

Xing, C. and Lo, E.H. (2017) Help-me signaling: Non-cell autonomous mechanisms of neuroprotection and neurorecovery. *Prog. Neurobiol.*, 152, 181–199.

Xiong, Y. and Yu, J. (2018) Modeling Parkinson's disease in Drosophila: What have we learned for dominant traits? *Front. Neurol.*, 9.

Xue, L., Murray, J.H., and Tolkovsky, A.M. (2000) The Ras/phosphatidylinositol 3-kinase and Ras/ERK pathways function as independent survival modules each of which inhibits a distinct apoptotic signaling pathway in sympathetic neurons. *J. Biol. Chem.*, 275, 8817–8824.

Yan, D., Zhang, Y., Liu, L., Shi, N., and Yan, H. (2018) Pesticide exposure and risk of Parkinson's disease: Dose-response meta-analysis of observational studies. *Regul. Toxicol. Pharmacol.*, 96, 57–63.

Yang, L., Matthews, R.T., Schulz, J.B., Klockgether, T., Liao, A.W., Martinou, J.-C., Penney, J.B., Hyman, B.T., and Beal, M.F. (1998) 1-Methyl-4-phenyl-1,2,3,6-tetrahydropyride Neurotoxicity Is Attenuated in Mice Overexpressing Bcl-2. *J. Neurosci.*, 18, 8145–8152.

Yang, Y., Nishimura, I., Imai, Y., Takahashi, R., and Lu, B. (2003) Parkin suppresses dopaminergic neuron-selective neurotoxicity induced by Pael-R in Drosophila. *Neuron*, 37, 911–924.

Yano, M., Kanazawa, M., Terada, K., Namchai, C., Yamaizumi, M., Hanson, B., Hoogenraad, N., and Mori, M. (1997) Visualization of mitochondrial protein import in cultured mammalian cells with green fluorescent protein and effects of overexpression of the human import receptor Tom20. *J. Biol. Chem.*, 272, 8459–8465.

Yano, H., Baranov, S. V., Baranova, O. V., Kim, J., Pan, Y., Yablonska, S., Carlisle, D.L., Ferrante, R.J., Kim, A.H., and Friedlander, R.M. (2014) Inhibition of mitochondrial protein import by mutant huntingtin. *Nat. Neurosci.*, 17, 822–831.

Yasuda, Y., Shimoda, T., Uno, K., Tateishi, N., Furuya, S., Yagi, K., Suzuki, K., and Fujita, S. (2008) The effects of MPTP on the activation of microglia/astrocytes and cytokine/chemokine levels in different mice strains. *J. Neuroimmunol.*, 204, 43–51.

Ye, B., Wang, Q., Hu, H., Shen, Y., Fan, C., Chen, P., Ma, Y., Wu, H., and Xiang, M. (2019) Restoring autophagic flux attenuates cochlear spiral ganglion neuron degeneration by promoting TFEB nuclear translocation via inhibiting MTOR. *Autophagy*, 00, 1–19.

Zaid, H., Abu-Hamad, S., Israelson, A., Nathan, I., and Shoshan-Barmatz, V. (2005) The voltage-dependent anion channel-1 modulates apoptotic cell death. *Cell Death Differ.*, 12, 751–760.

Zecca, L., Youdim, M.B.H., Riederer, P., Connor, J.R., and Crichton, R.R. (2004) Iron, brain ageing and neurodegenerative disorders. *Nat. Rev. Neurosci.*, 5, 863–873.

Zeng, X.S., Geng, W.S., Jia, J.J., Chen, L., and Zhang, P.P. (2018) Cellular and molecular basis of neurodegeneration in Parkinson disease. *Front. Aging Neurosci.*, 10, 1–16.

Zhang, J., Perry, G., Smith, M.A., Robertson, D., Olson, S.J., Graham, D.G., and Montine, T.J. (1999) Parkinson's disease is associated with oxidative damage to cytoplasmic DNA and RNA in substantia nigra neurons. *Am. J. Pathol.*, 154, 1423–1429.

Zhang, W. and Liu, H. (2002) MAPK signal pathways in the regulation of cell proliferation in mammalian cells. *Cell Res.*, 12, 9–18.

Zharikov, A.D., Cannon, J.R., Tapias, V., Bai, Q., Horowitz, M.P., Shah, V., El Ayadi, A., Hastings, T.G., Greenamyre, J.T., and Burton, E.A. (2015) ShRNA targeting α-synuclein prevents neurodegeneration in a Parkinson's disease model. *J. Clin. Invest.*, 125, 2721–2735.

Zhou, Z.D. and Tan, E.K. (2016) Potential Pathophysiological Crosstalk between Parkin and FBXO7 Signalling Pathways. *Electron. J. Biol.*, 12, 428–431.

Zhu, J.H., Kulich, S.M., Oury, T.D., and Chu, C.T. (2002) Cytoplasmic aggregates of phosphorylated extracellular signal-regulated protein kinases in lewy body diseases. *Am. J. Pathol.*, 161, 2087–2098.

Zhu, J.H., Guo, F., Shelburne, J., Watkins, S., and Chu, C.T. (2003) Localization of phosphorylated ERK/MAP kinases to mitochondria and autophagosomes in Lewy body diseases. *Brain Pathol.*, 13, 473–481.

Zolotukhin, S., Byrne, B.J., Mason, E., Zolotukhin, I., Potter, M., Chesnut, K., Summerford, C., Samulski, R.J., and Muzyczka, N. (1999) Recombinant adeno-associated virus purification using novel methods improves infectious titer and yield. *Gene Ther.*, 6, 973–985.

Zondler, L., Kostka, M., Garidel, P., Heinzelmann, U., Hengerer, B., Mayer, B., Weishaupt, J.H., Gillardon, F., and Danzer, K.M. (2017) Proteasome impairment by alpha-synuclein. *PLoS One*, 12, e0184040.

Zorzano, A. and Claret, M. (2015) Implications of mitochondrial dynamics on neurodegeneration and on hypothalamic dysfunction. *Front. Aging Neurosci.*, 7, 1–17.

Züchner, S., Mersiyanova, I. V., Muglia, M., Bissar-Tadmouri, N., Rochelle, J., Dadali, E.L., Zappia, M., Nelis, E., Patitucci, A., Senderek, J., Parman, Y., Evgrafov, O., De Jonghe, P., Takahashi, Y., Tsuji, S., Pericak-Vance, M.A., Quattrone, A., Battologlu, E., Polyakov, A. V., Timmerman, V., Schröder, J.M., and Vance, J.M. (2004) Mutations in the mitochondrial GTPase mitofusin 2 cause Charcot-Marie-Tooth neuropathy type 2A. *Nat. Genet.*, 36, 449–451.

Zuddas, A., Fascetti, F., Corsini, G.U., and Piccardi, M. (1994) In Brown Norway Rats, MPP+ is accumulated in the nigrostriatal dopaminergic terminals but it is not neurotoxic: a model of natural resistance to MPTP toxicity. *Exp. Neurol.*, 127, 54–61.

ANNEX I

Annex I

Scientific articles belonging to my PhD thesis:

Overexpression of TFEB drives a pleiotropic neurotrophic effect and prevents Parkinson's disease-related neurodegeneration

Torra A, Parent A, Cuadros T, Rodríguez-Galván B, Ruiz-Bronchal E, Ballabio A, Bortolozzi A, Vila M*, Bové J*. *co-corresponding authors

Molecular Therapy, 2018 Jun 6;26(6):1552-1567

DOI: https://doi.org/10.1016/j.ymthe.2018.02.022

TFEB overexpression induces mitochondrial fusion and prevents Parkinson's disease mitochondria-mediated cell death (In prep)

Torra A, Galiano-Landeira J, Pariente C, Ballabio A, Vila M*, Bové J*. *co-corresponding authors

Participation in other published articles:

Brain tyrosinase overexpression implicates age-dependent neuromelanin production in Parkinson's disease pathogenesis

Carballo-Carbajal I*, Laguna A*, Romero-Giménez J, Cuadros T, Bové J, Martínez-Vicente M, Parent A, González-Sepúlveda M, Peñuelas N, **Torra A**, Rodríguez-Galván B, Ballabio A, Hasegawa T, Bortolozzi A, Gelpí E, Vila M. *equally contributed

Nature Communications, 2019 Mar 7;10(1):973

DOI: https://doi.org/10.1038/s41467-019-08858-y

ANNEX II

Annex II

Participation in congresses as a first and presenting author:

Transcription Factor EB overexpression drives a neurotrophic effect that neuroprotects and neurorestores dopaminergic neurons in a mouse Parkinson's disease model. -POSTER-

Torra A, Galiano-Landeira J, Parent A, Cuadros T, Rodríguez-Galván B, Ruiz-Bronchal E, Bortolozzi A, Vila M, Bové J.

XI Symposium of Experimental Neurobiology, Catalan Society of Biology (SCB), Barcelona, Spain, 2018.

Transcription Factor EB overexpression drives a neurotrophic effect that neuroprotects and neurorestores dopaminergic neurons in a mouse Parkinson's disease model. -POSTER-

Torra A, Parent A, Cuadros T, Rodríguez-Galván B, Ruiz-Bronchal E, Bortolozzi A, Vila M, Bové J.

11th Federation of European Neuroscience Societies (FENS) Forum of Neuroscience, Berlin, Germany, 2018.

Activation of Transcription Factor EB as a neuroprotective strategy for Parkinson's disease. -ORAL PRESENTATION-

Torra A, Galiano-Landeira J, Parent A, Cuadros T, Rodríguez-Galván B, Ruiz-Bronchal E, Bortolozzi A, Vila M, Bové J.

II Congress of Biology, Catalan Society of Biology (SCB), Barcelona, Spain, 2018.

Transcription Factor EB neurotrophic and pro-survival effects prevent neurodegeneration in the MPTP mouse model of Parkinson's disease. -POSTER-

Torra A, Rodríguez-Galván B, Ruiz-Bronchal E, Bortolozzi A, Vila M, Bové J.

46th Congress of the Society for Neuroscience (SfN), San Diego, USA, 2016.

Transcription Factor EB activation as a neuroprotective strategy in Parkinson's disease. -ORAL PRESENTATION-

Torra A, Rodríguez-Galván B, Vila M, Bové J.

V Scientific Conference, Neurosciences Institute (INc) – Autonomous University of Barcelona (UAB), Bellaterra, Spain, 2016.

Transcription Factor EB overexpression in substantia nigra dopaminergic neurons triggers cell growth and renders neuroprotection in the MPTP Parkinson's disease mouse model. -POSTER-

Torra A, Rodríguez-Galván B, Vila M, Bové J.

16th National Congress of the Spanish Society for Neuroscience (SENC), Granada, Spain, 2015.

Overexpression of Transcription Factor EB prevents dopaminergic cell death in the MPTP mouse model of Parkinson's disease. -POSTER-

Torra A, Rodríguez-Galván B, Parent A, Cuadros T, Vila M, Bové J.

IX Symposium of Experimental Neurobiology, Catalan Society of Biology (SCB), Barcelona, Spain, 2014.

Participation in other studies presented in congresses:

Age-dependent intracellular neuromelanin production in humanized rats triggers Parkinson's disease pathology. -POSTER-

Carballo-Carbajal I*, Laguna A*, Romero-Giménez J, Cuadros T, Bové J, Martínez-Vicente M, Parent A, González-Sepúlveda M, Peñuelas N, **Torra A**, Rodríguez-Galván B, Ballabio A, Hasegawa T, Bortolozzi A, Gelpí E, Vila M. *equally contributed

14th International Conference AD/PD™, Lisbon, Portugal, 2019.

Role of neuromelanin in Parkinson's disease. -ORAL PRESENTATION-

Carballo-Carbajal I*, Laguna A*, Romero-Giménez J, Bové J, Cuadros T, Martínez-Vicente M, **Torra A**, Parent A, Rodríguez-Galván B, González-Sepúlveda M, Peñuelas N, Ballabio A, Hasegawa T, Bortolozzi A, Gelpí E, Vila M. *equally contributed

XI Symposium of Experimental Neurobiology, Catalan Society of Biology (SCB), Barcelona, Spain, 2018.

Adaptive immune response mediated by cytotoxic T lymphocytes is an early and progressive event in Parkinson's disease. -POSTER-

Galiano-Landeira J, **Torra A**, Pariente C, Vila M, Bové J.

XI Symposium of Experimental Neurobiology, Catalan Society of Biology (SCB), Barcelona, Spain, 2018.

Adaptive immune system in Parkinson's disease: the latent foe. -ORAL PRESENTATION-

Galiano-Landeira J, **Torra A**, Barranco A, Melià M, Vila M, Bové J.

VI Scientific Conference, Neurosciences Institute (INc) – Autonomous University of Barcelona (UAB), Sant Feliu de Guíxols, Spain, 2018.